

COLOR ENGINEERING OF π -CONJUGATED DONOR-ACCEPTOR SYSTEMS:
THE ROLE OF DONOR AND ACCEPTOR UNITS ON THE NEUTRAL STATE
COLOR

A THESIS SUBMITTED TO
THE GRADUATE SCHOOL OF NATURAL AND APPLIED SCIENCES
OF
MIDDLE EAST TECHNICAL UNIVERSITY

BY

MERVE İÇLİ ÖZKUT

IN PARTIAL FULFILLMENT OF THE REQUIREMENTS
FOR
THE DEGREE OF DOCTOR OF PHILOSOPHY
IN
CHEMISTRY

JULY 2011

Approval of the thesis:

**COLOR ENGINEERING OF π -CONJUGATED DONOR-ACCEPTOR SYSTEMS:
THE ROLE OF DONOR AND ACCEPTOR UNITS ON THE NEUTRAL STATE
COLOR**

Submitted by **MERVE İÇLİ ÖZKUT** in partial fulfillment of the requirements for the degree of **Doctor of Philosophy in Chemistry Department, Middle East Technical University** by,

Prof. Dr. Canan Özgen
Dean, Graduate School of **Natural and Applied Sciences**

Prof. Dr. İlker Özkan
Head of Department, **Chemistry**

Prof. Dr. Ahmet M. Önal
Supervisor, **Chemistry Dept., METU**

Assoc. Prof. Dr. Atilla Cihaner
Co-Supervisor, **Chem. Eng. and Appl. Chem., Atılım Uni.**

Examining Committee Members:

Prof. Dr. Teoman Tinçer
Chemistry Dept., METU

Prof. Dr. Ahmet M. Önal
Chemistry Dept., METU

Assist. Prof. Dr. Ali Çırpan
Chemistry Dept., METU

Assis. Prof. Dr. Fatih Algı
Chemistry Dept., COMU

Assis. Prof. Dr. H. Emrah Ünalın
Metallurgical and Mater. Eng., METU

Date: 20.07.2011

I hereby declare that all information in this document has been obtained and presented in accordance with academic rules and ethical conduct. I also declare that, as required by these rules and conduct, I have fully cited and referenced all materials and results that are not original to this work.

Name, Last name: Merve İÇLİ ÖZKUT

Signature :

ABSTRACT

COLOR ENGINEERING OF π -CONJUGATED DONOR-ACCEPTOR SYSTEMS: THE ROLE OF DONOR AND ACCEPTOR UNITS ON THE NEUTRAL STATE COLOR

İçli Özkut, Merve

Ph.D., Department of Chemistry

Supervisor: Prof. Dr. Ahmet M. Önal

Co-supervisor: Assoc. Prof. Dr. Atilla Cihaner

July 2011, 179 pages

Design of a monomer is a viable route for adjusting the properties of its corresponding polymer. The main goal of this study is to design and synthesize novel soluble polymers having various colors of color palette and amenable for use in electrochromic device applications. In designing the monomers, the factors affecting the properties of the polymers are also considered. For this purpose, each part of the monomers is chosen properly for each desirable properties and the effect of them is investigated separately. Thus, this study is based on the investigation of the effect of three major parts on the polymer properties: Donor groups, acceptor groups and the length of alkyl chain. For this aim, nine D-A-D type monomers, **TSeT**, **ESeE**, **PSeP-C₁₀**, **PSP-C₁₀**, **PNP-C₁₀**, **POP-C₁₀**, **PSeP-C₄**, **PSP-C₄** and **PSP-C₆**, and their corresponding polymers, **P(TSeT)**, **P(ESeE)**, **P(PSeP-C₁₀)**, **P(PSP-C₁₀)**, **P(PNP-**

C₁₀), **P(POP-C₁₀)**, **P(PSeP-C₄)**, **P(PSP-C₄)** and **P(PSP-C₆)**, based on thiophene, 3,4-ethylenedioxythiophene (EDOT), and 3,3-dialkyl-3,4-dihydro-2H-thieno[3,4-b]-[1,4]dioxepine (ProDOT-C_n) as D units and 2,1,3-benzoselenadiazole, 2,1,3-benzothiadiazole, 2-decyl-2H-benzo[d][1,2,3]triazole, and 2,1,3-benzooxadiazole as A units were synthesized. The obtained polymers have somewhat low band gap between 1.13 eV and 1.80 eV, they show electrochromic behaviors. Among them **P(POP-C₁₀)**, **P(PSP-C₁₀)** and **P(PSP-C₆)** have cyan color which is one leg of CMY (Cyan-Magenta-Yellow) color spaces. Since there have been scant studies on cyan colored polymers in the literature, these polymers are so precious. Via copolymerization of **PNP-C₁₀** and **PSeP-C₁₀**, the first electrochemically synthesized neutral state black polymer was obtained.

Keywords: D-A-D approach, electrochromic polymers, 3,4-alkylenedioxythiophene, benzotriazole, benzoselenadiazole, benzothiadiazole, benzooxadiazole, soluble polymers, CMY, RGB.

ÖZ

π -KONJÜGE DONÖR-AKSEPTÖR SİSTEMLERDE RENK AYARLANMASI: NÖTRAL HALDEKİ RENK ÜZERİNE DONÖR VE AKSEPTÖR GRUPLARIN ETKİSİ

İçli Özkut, Merve

Doktora, Kimya Bölümü

Tez Yöneticisi: Prof. Dr. Ahmet M. Önal

Ortak Tez Yöneticisi: Doç. Dr. Atilla Cihaner

Temmuz 2011, 179 sayfa

Polimerin özelliklerini ayarlayabilmek için öncelikle monomerin yapısının tasarlanması önemlidir. Bu çalışmada temel amaç, birçok farklı renkte, çözünürlük özelliğine sahip ve elektrokromik cihaz uygulamalarında kullanılacak polimerler sentezlemektir. Monomer yapıları tasarlanırken, polimerlerin özelliklerini etkileyecek faktörler de göz önünde bulundurulmuştur. Bu amaçla, monomerlerin herbir birimi istenenen herbir özellik için özenle seçilmiş ve herbir birimin etkisi ayrı ayrı incelenmiştir. Bu nedenle, bu çalışma üç ana bölümden oluşmaktadır: Donör gruplarının, akseptör gruplarının ve alkil zincirlerinin polimerin özellikleri üzerine etkisi. Tüm bu hedeflerin ışığında, tiyofen, 3,4-etilendioksitiyofen (EDOT), 3,3-dialkil-3,4-dihidro-2H-tiyeno[3,4-b]-[1,4]dioksefin (ProDOT-C_n) gruplarını D birimi olarak; 2,1,3-benzoselenadiazol, 2,1,3-benzothiadiazol, 2-decyl-2H-benzo[d][1,2,3]triazol ve 2,1,3-oksadiazol gruplarını A birim olarak içeren, dokuz adet D-A-D tipi monomer, **TSeT**, **ESeE**, **PSeP-C₁₀**, **PSP-C₁₀**, **PNP-C₁₀**, **POP-C₁₀**,

PSeP-C₄, **PSP-C₄** ve **PSP-C₆**, ve bunların polimerleri, **P(TSeT)**, **P(ESeE)**, **P(PSeP-C₁₀)**, **P(PSP-C₁₀)**, **P(PNP-C₁₀)**, **P(POP-C₁₀)**, **P(PSeP-C₄)**, **P(PSP-C₄)** ve **P(PSP-C₆)**, sentezlenmiştir. Elde edilen polimerlerin 1.13 eV ile 1.80 eV arasında deęişen, oldukça düşük bant aralıklarına sahip oldukları ve elektrokromik özellikleri olduęu görüldü. Bu polimerler arasında **P(POP-C₁₀)**, **P(PSP-C₁₀)** ve **P(PSP-C₆)**'nın CMY (Cyan-Cam Göbeęi, Magenta-Mor, Yellow-Sarı) renk sisteminin bir elemanı olan cam göbeęi rengine sahip oldukları görüldü. Literatürde cam göbeęi renkli polimerlerin sayısının az olması sebebiyle, bu polimerler oldukça değerlidir. **PNP-C₁₀** ve **PSeP-C₁₀**'un kopolimerizasyonu ile ilk defa elektrokimyasal yöntemle sentezlenen nötral halinde siyah renkli polimer elde edilmiştir.

Anahtar Kelimeler: D-A-D yaklaşımı, elektrokromik polimerler, 3,4-alkilendioksitiyofen, benzotriazol, benzoselenadiazol, benzotiyadiazol, benzooksadiazol, çözünür polimer, CMY, RGB.

*To my family,
especially to my spouse Onur Özkut...*

ACKNOWLEDGMENTS

I express my gratitude to my supervisor Prof. Dr. Ahmet M. Önal and my co-supervisor Assoc. Prof. Dr. Atilla Cihaner, since they believe that, this is not only an advisor-student relationship, but also a master and apprentice relationship. I would like to express my sincere thanks for their guidance, support, encouragement and patience.

I would like to thank Asist. Prof. Dr. Fatih Algı since the synthesis of the acceptor units had been done by his group, and also thanks for his comments during the monomer synthesis part of this thesis.

I would like to thank Asist. Prof. Dr. Seha Tirkeş for the conductivity measurements of the polymers.

I would like to thank also my labmates Nurdan Atılgan and Demet Asil, all my labmates from B-24 lab for their friendships during this study. I should also thank to my junior friends Samed Atak, Jetmire Mersini and Özden Çelikkilek, since my energy was enlarged by their energies during my studies. Special thanks come for Özden Çelikkilek, because synthesis of two monomers in this study had been done with her invaluable involvement.

I wish to thank Yasin Arslan for his help during the writing of the my thesis.

Grateful thanks go to my family; my mother Nazife İçli and my sister Rukiye Bıyık for their endless support and love during every step of my life.

Precious thanks to my spouse, Onur Özkut, without his support, understanding and encouragement, I could not achieve this thesis study.

I would like to thank my friends; Tuğba Nur Aslan, Fuat Aslan, Baki Doruker, Nilay Kaynar Arslan, Oğuz Arslan from whom I had stolen time from our meeting during the preparation of my thesis. Thank you so much for their kind friendships.

I also wish to thank all my colleagues in Chemistry Department of METU.

I would like to thank to TÜBİTAK for supplying financial support during my PhD on BS work.

I would like to extend my deepest thanks to Van Yüzüncü Yıl University for supporting me to complete my PhD in the Chemistry Department of METU.

TABLE OF CONTENTS

ABSTRACT.....	iv
ÖZ	vi
ACKNOWLEDGMENTS	ix
TABLE OF CONTENTS	xi
LIST OF FIGURES	xv
LIST OF SCHEMES.....	xxiii
LIST OF TABLES	xxiv
ABBREVIATIONS	xxvi
CHAPTERS	
1. INTRODUCTION	1
1.1. A Brief Introduction to Conducting Polymers	1
1.2. Band Gap Theory	2
1.3. Electrochromism	9
1.3.1. Electrochromic Contrast	11
1.3.2. Switching Time.....	12
1.3.3. Coloration Efficiency.....	13
1.4. Processable Conjugated Polymers.....	14
1.5. Polymerization Techniques	15
1.5.1. Electrochemical Polymerization	15
1.5.1.1. Solvent	17
1.5.1.2. Supporting Electrolyte	19

1.5.2. Chemical Polymerization.....	20
1.6. Aim of This Study	21
2. EXPERIMENTAL	24
2.1. Materials	24
2.1.1. Monomer Synthesis	24
2.1.2. Polymer Synthesis and Analysis.....	25
2.2. Instrumentation.....	26
2.3. Synthesis.....	27
2.3.1. Monomer Synthesis	27
2.3.1.1. Synthesis of the “Hat” Parts.....	28
2.3.1.1.1. Synthesis of Diethyl 2,2-dialkylmalonate (1-3)	29
2.3.1.1.2. 2,2-Didecylpropane-1,3-diol (4-6)	29
2.3.1.2. Synthesis of the Donor Units.....	31
2.3.1.2.1. 3,3-Dialkyl-3,4-dihydro-2H-thieno[3,4-b][1,4]dioxepine (7-9)	32
2.3.1.3. Synthesis of the Acceptor Units.....	33
2.3.1.3.1. 4,7-dibromobenzo[c][1,2,5]oxadiazole, 4,7-dibromobenzo[c]	
[1,2,5] thiadiazole and 4,7-dibromobenzo[c][1,2,5]selenadiazole (10-12).	33
2.3.1.4. Integrating Donor and Acceptor Parts.....	35
2.3.1.4.1. Stannylating of Donor Parts	36
2.3.2. Polymer Synthesis and Analysis.....	40
2.3.2.1. Electrochemical Synthesis of the Polymers and Their Analysis.....	41
2.3.2.2. Chemical Synthesis of the Polymers.....	42

3. RESULTS AND DISCUSSION	43
3.1. Structural Design of the Monomer	43
3.1.1. Band Gap Tuning	43
3.1.2. Color Tuning	44
3.2. Examining the Effect of Different Groups	47
3.2.1. Effect of Donor Groups	49
3.2.1.1. Cyclic Voltammogram of the Monomers	49
3.2.1.2. Electrochemical Polymerization and Properties of the Polymers	51
3.2.1.3. Spectroelectrochemical and Switching Behaviors of the Polymers....	56
3.2.1.4. Properties of the Polymers	65
3.2.1.5. Stability of the Polymers	71
3.2.2. Effect of Acceptor Groups	74
3.2.2.1. Cyclic Voltammograms of the Monomers	75
3.2.2.2. Electrochemical Polymerization and Properties of the Polymers	77
3.2.1.1. Spectroelectrochemical and Switching Behaviors of Polymers	82
3.2.2.3. Optical Properties of the Polymers	91
3.2.2.4. Properties of the Polymers	96
3.2.2.5. Stability of the Polymers	97
3.2.2.6. Colorimetric Measurements of the Polymers.....	100
3.2.3. Effect of Alkyl Chain Length.....	102
3.2.3.1. Cyclic Voltammograms of the Monomers	104

3.2.3.2. Electrochemical Polymerization and Properties of the Polymers	106
3.2.3.1. Spectroelectrochemical and Switching Behaviors of the Polymers.	114
3.2.3.4. Properties of the Polymers	121
3.2.3.1. Stability of the Polymers.....	122
3.2.4. Investigation of the Properties of the Polymers	124
3.2.4.1. Conductivity Measurements	124
3.2.4.1. ESR Measurements.....	124
3.2.5. Application of the Polymers to Color Mixing Theory (CMT).....	128
3.2.6. Synthesis of Neutral State Black Electrochromic Copolymer	132
3.2.7. Application of the Obtained Polymers as an Electrochromic Devices	140
4. CONCLUSIONS.....	146
REFERENCES.....	149
APPENDICES	
A: FTIR SPECTRA OF MONOMERS	155
B: NMR SPECTRA OF MONOMERS	162
VITA	179

LIST OF FIGURES

FIGURES

Figure 1.1. Energy transitions of doped and undoped conducting polymers.....	2
Figure 1.2. Representation of polaron and bipolaron in polythiophene.....	3
Figure 1.3. The band gap evolution from polyacetylene to poly(EDOT-Pyr) [40].	4
Figure 1. 4. (a) Calculation of the band gap from CV measurement and (b) Calculation of band gap from DPV measurement [41].	6
Figure 1. 5. Calculation of band gap from SPEL measurement [41].	7
Figure 1. 6. Estimated optical behavior of D-A-D type monomer's polymer [47].	8
Figure 1.7. Chronoabsorptometry experiment for a polymer monitored at specified wavelength.	12
Figure 1.8. Representation of an electrochemical cell used for electrochemical polymerization and/ or analysis.	17
Figure 2.1. Reaction system for the experiments done under inert atmosphere.	31
Figure 3.1. Spray-cast films on ITO/glass illustrating the subtractive color mixing concept as applied using electrochromic polymers. (a) The red-yellow-blue primaries where their overlaps create green, orange, and purple; and (b) the cyan-yellow-magenta primaries where their primaries create blue, red, and green [50].	45
Figure 3.2. Cyclic voltammograms of TSeT, ESeE, and PSeP-C ₁₀ in 0.1 M TBAH/DCM at 100 mV/s.	50
Figure 3.3. Electropolymerization of 1.5x10 ⁻³ M (a) TSeT, and (b) ESeE in 0.1 M TBAH-DCM and (c) PSeP-C ₁₀ in 0.1 M TBAH-DCM/ ACN (2/3-v/v) at 100 mV/s by potential scanning to give P(TSeT), P(ESeE), and P(PSeP-C ₁₀), respectively.	52
Figure 3.4. (a) CV of P(TSeT) film at different scan rates: (a) 20, (b) 40, (c) 60, (d) 80, (e) 100, (f) 120, (g) 140, (h) 160, (i) 180, (j) 200 mV/s. (b) Relationship of anodic (i _{p,a}) and cathodic current (i _{p,c}) peaks as a function of scan rate in 0.1 M TBAH/ DCM for P(TSeT) film during p-doping.	53

Figure 3.5. (a) CV of n- and p-doped P(ESeE) film at different scan rates: (a) 50, (b) 100, (c) 150, (d) 200, (e) 250 and (f) 300 mV/s, and relationship of anodic ($i_{p,a}$) and cathodic peak currents ($i_{p,c}$) as a function of scan rate for (b) p-doped and (c) n-doped P(ESeE) film in 0.1 M TBAH and DCM.	54
Figure 3.6. (a) CV of p-doped P(PSeP-C ₁₀) 0.1 TBAH/ACN at a scan rate of a) 40, b) 60, c) 80, d) 100, e) 120, f) 140, g) 160, h) 180, and i) 200 mV/s. (b) Relationship of anodic ($i_{p,a}$) and cathodic current ($i_{p,c}$) peaks as a function of scan rate for p-doped P(PSeP-C ₁₀) film in 0.1 M TBAH/ DCM.	54
Figure 3.7. Electronic absorption spectra of (a) P(TSeT) (from 0.00 to 1.20 V), (b) P(ESeE) (from -1.0 V to 1.0 V), and (c) P(PSeP-C ₁₀) (from -0.1 V to 1.1 V) on ITO in 0.1 M TBAH/ACN at various applied potentials.....	57
Figure 3.8. Chronoabsorptometry experiments for P(TSeT) on ITO in 0.1 M TBAH/DCM (During these procedures, polymer was switched between 0.0 V and 1.2 V).	58
Figure 3.9. Chronoabsorptometry experiments for P(ESeE) on ITO in 0.1 M TBAH/DCM (During these procedure, polymer was switched between -1.0 V and 1.0 V).	60
Figure 3.10. Spectroelectrochemical behavior of the P(ESeE) on ITO in 0.1 M TBAH/ DCM at various applied potentials between -1.85 V and -1.0 V. Insets: The colors of the polymer in its neutral and oxidized states.	61
Figure 3. 11. Chronoabsorptometry experiments for P(PSeP-C ₁₀) on ITO in 0.1 M TBAH/ ACN while the polymer was switched between -0.1 V and 1.1 V.	63
Figure 3. 12. Energy band diagram of the polymers P(TSeT), P(ESeE), and P(PSeP-C ₁₀).	64
Figure 3.13. Emission spectra and the colors of TSeT (excited at 480 nm) and P(TSeT) (excited at 560 nm) in DMSO.....	66
Figure 3.14. (a) Electrochemically coated P(PSeP-C ₁₀) on ITO, (b) dissolving electrochemically syththesized P(PSeP-C ₁₀) on ITO in chloroform (c) spray coating of chemically obtained P(PSeP-C ₁₀) after dissolving in chloroform.	67
Figure 3.15. Electronic absorption spectrum of chemically synthesized P(PSeP-C ₁₀) (from 0.3 V to 1.0 V) which was dip coated on ITO in 0.1 M TBAH/ACN. Inset:	

Cyclic voltammograms of chemically synthesized P(PSeP-C ₁₀) coated on ITO in 0.1 TBAH/ACN at a scan rate of 100 mV/s.	68
Figure 3.16. Chronoabsorptometry experiments for chemically polymerized P(PSeP-C ₁₀) coated on ITO in 0.1 M TBAH/ ACN while the polymer was switched between 0.0-1.0 V.	69
Figure 3.17. Chemically synthesized P(PSeP-C ₁₀) dissolved in DCM (a) p-doped with 10 ⁻³ M SbCl ₅ solution, (b) dedoped with 10 ⁻² M N ₂ H ₅ OH solution.	71
Figure 3.18. Stability test for (a) P(TSeT) , (b) P(ESeE), (c) P(PSeP-C ₁₀) films in 0.1 M TBAH/DCM at a scan rate of 100 mV s ⁻¹ under ambient conditions by cyclic voltammetry as a function of the number of cycles: A: 1, B: 500, C: 1000, D: 2000 cycles; Q _a : Anodic charge stored, i _{pa} : Anodic peak current, i _{pc} : Cathodic peak current.	73
Figure 3.19. Electronic absorption spectra of P(PSeP-C ₁₀) (from -0.1 V to 1.1 V) on ITO in 0.1 M TBAH/ACN at various applied potentials after prolonged standing at ambient conditions.	74
Figure 3. 20. Cyclic voltammograms of PSeP-C ₁₀ , PSP-C ₁₀ , PNP-C ₁₀ and POP-C ₁₀ in 0.1 M TBAH/DCM at 100mV/s.	76
Figure 3. 21. Electropolymerization of 1.5x10 ⁻³ M (a) POP-C ₁₀ , (b) PSP-C ₁₀ and (c) PNP-C ₁₀ in 0.1 M TBAH-DCM/ACN (2/3-v/v) at 100 mV/s by potential scanning to give P(POP-C ₁₀), P(PSP-C ₁₀), and P(PNP-C ₁₀), respectively.	78
Figure 3.22. (a) Cyclic voltammograms of p-doped P(POP-C ₁₀) in 0.1 TBAH/ACN at a scan rate between 20 mV/s and 200 mV/s with 20 mV/s increments. Relationship of (b) first anodic (i _{p,a}) and (b) second anodic current (i _{p,a}) peaks as a function of scan rate for p-doped P(POP-C ₁₀) film in 0.1 M TBAH/DCM.	79
Figure 3.23. (a) Cyclic voltammograms of p-doped P(PSP-C ₁₀) in 0.1 TBAH/ACN at a scan rate between 40 mV/s and 200 mV/s with 20 mV/s increments. (b) Relationship of anodic (i _{p,a}) peaks as a function of scan rate for p-doped P(PSP-C ₁₀) film in 0.1 M TBAH/DCM.	80
Figure 3.24. (a) Cyclic voltammograms of p-doped P(PNP-C ₁₀) in 0.1 TBAH/ACN at a scan rate between 40 mV/s and 200 mV/s with 20 mV/s increments. (b) Relationship of anodic (i _{p,a}) peaks as a function of scan rate for p-doped P(PNP-C ₁₀) film in 0.1 M TBAH/DCM.	80

Figure 3.25. CV of n-doped P(POP-C ₁₀) in 0.1 TBAH/ACN at a scan rate 60 mV/s.	81
Figure 3.26. Electronic absorption spectra of (a) P(POP-C ₁₀) (from 0.00 to 1.20 V), (b) P(PSP-C ₁₀) (from -0.50 V to 1.20 V), and (c) P(PNP-C ₁₀) (from 0.00 V to 1.00 V) on ITO in 0.1 M TBAH/ACN at various applied potentials.	84
Figure 3.27. Chronoabsorptometry experiments for P(POP-C ₁₀) on ITO in 0.1 M TBAH/ ACN while the polymer was switched between 1.2 V and 0.0 V.....	87
Figure 3.28. Chronoabsorptometry experiments for P(PSP-C ₁₀) on ITO in 0.1 M TBAH/ ACN while the polymer was switched between 1.2 V and -0.5 V.	88
Figure 3.29. Chronoabsorptometry experiments for P(PNP-C ₁₀) on ITO in 0.1 M TBAH/ACN during the polymer was switched between 1.0 V and 0.0 V.	89
Figure 3.30. Energy band diagram of the polymers P(PSeP-C ₁₀), P(PSP-C ₁₀), P(POP- C ₁₀) and P(PNP-C ₁₀).	90
Figure 3.31. Electronic absorption spectrum of chemically synthesized (a) P(POP- C ₁₀) (from 0.0 V to 1.2 V), (b) P(PSP-C ₁₀) (from 0.0 V to 1.2 V), and (c) P(PNP- C ₁₀) (from 0.0 V to 1.2 V) which was spray/ dip coated on ITO in 0.1 M TBAH/ACN. Insets: Cyclic voltammograms of chemically synthesized P(POP- C ₁₀), P(PSP-C ₁₀) and P(PNP-C ₁₀) coated on ITO in 0.1 TBAH/ACN at a scan rate of 100 mV/s.	92
Figure 3.32. Chronoabsorptometry experiments for chemically polymerized P(PSP- C ₁₀) coated on ITO in 0.1 M TBAH/ ACN while the polymer was switched between 0.0-1.2 V.	94
Figure 3.33. Chronoabsorptometry experiments for chemically polymerized P(PNP- C ₁₀) coated on ITO in 0.1 M TBAH/ ACN while the polymer was switched between 0.0-1.2 V.	95
Figure 3.34. Changes in optical absorption spectra of chemically obtained (a) P(POP- C ₁₀) and (b) P(PSP-C ₁₀) in DCM solution after addition of 10 μ L (for each spectrum) 10 ⁻³ M SbCl ₅ M and 10 ⁻² M N ₂ H ₅ OH.	97
Figure 3. 35. Stability test for (a) P(POP-C ₁₀), (b) P(PSP-C ₁₀), (c) P(PNP-C ₁₀) films in 0.1 M TBAH/DCM at a scan rate of 100 mV s ⁻¹ under ambient conditions by cyclic voltammetry as a function of the number of cycles: A: 1, B: 500, C: 1000,	

D: 2000 cycles; Q_a : Anodic charge stored, i_{pa} : Anodic peak current, i_{pc} : Cathodic peak current.....	99
Figure 3.36. The colors of the solutions of 10^{-6} M (a) PNP- C_{10} , (b) POP- C_{10} , (b) PSP- C_{10} , (b) PSeP- C_{10} in DCM.	100
Figure 3.37. Distribution of P(PSeP- C_{10}), P(PSP- C_{10}), P(POP- C_{10}) and P(PNP- C_{10}) polymers' color in their neutral states on the spectrum of visible region.	101
Figure 3.38. $L^*a^*b^*$ values of the P(PSeP- C_{10}), P(PSP- C_{10}), P(POP- C_{10}) and P(PNP- C_{10}) in their neutral (0) and oxidized state (+).....	102
Figure 3.39. Cyclic voltammograms of PSP- C_{10} , PSP- C_6 and PSP- C_4 in 0.1 M TBAH/ DCM at 100 mV/s.....	105
Figure 3.40. Cyclic voltammograms of PSeP- C_{10} and PSeP- C_4 in 0.1 M TBAH/DCM at 100mV/s.....	106
Figure 3.41. Electropolymerization of (a) 3.0×10^{-3} M PSP- C_6 (b) 5.0×10^{-3} M PSP- C_4 and (c) 16.0×10^{-3} M in 0.1 M TBAH-DCM/ACN (5:95-v/v) at a scan rate of 100 mV/s by potential scanning to give P(PSP- C_6), P(PSP- C_4) and P(PSeP- C_4), respectively.....	107
Figure 3.42. (a) Cyclic voltammograms of p-doped P(PSP- C_6) in 0.1M TBAH/ACN at a scan rate of (a-j) 20-200 mVs^{-1} with 20 mVs^{-1} increments. (b) Relationship of anodic ($i_{p,a}$) peaks as a function of scan rate for p-doped P(PSP- C_6) film in 0.1 M TBAH/DCM.....	110
Figure 3.43. (a) Cyclic voltammograms of p-doped P(PSP- C_4) in 0.1M TBAH/ACN at a scan rate of (a-i) 40-200 mVs^{-1} with 20 mVs^{-1} increments. (b) Relationship of anodic ($i_{p,a}$) peaks as a function of scan rate for p-doped P(PSP- C_4) film in 0.1 M TBAH/DCM.....	110
Figure 3.44. (a) Cyclic voltammograms of p-doped P(PSeP- C_4) in 0.1M TBAH/ACN at a scan rate of (a-i) 40-200 mVs^{-1} with 20 mVs^{-1} increments. (b) Relationship of anodic ($i_{p,a}$) peaks as a function of scan rate for p-doped P(PSeP- C_4) film in 0.1 M TBAH/DCM.....	111
Figure 3.45. Cyclic voltammograms of P(PSP- C_{10}), P(PSP- C_6) and P(PSP- C_4) in 0.1 M TBAH/ACN electrolyte solution at a scan rate of 100 mV/s vs. Ag/AgCl..	112
Figure 3.46. Cyclic voltammograms of P(PSeP- C_{10}) and P(PSeP- C_4) in 0.1 M TBAH/ACN electrolyte solution at a scan rate of 100 mV/s vs. Ag/AgCl.	113

Figure 3.47. Optical absorption spectra of (a) P(PSP-C ₆), (b) P(PSP-C ₄) and (c) P(PSeP-C ₄) on ITO in 0.1 M TBAH/ACN at various applied potentials.	115
Figure 3.48. Optical absorption spectra of (a) P(PSP-C ₆) (from 0 V to -1.60 V), (b) P(PSP-C ₄) (from 0 V to -1.55 V) and (c) P(PSeP-C ₄) on ITO in 0.1 M TBAH/ACN at various applied potentials. Inset: Colors of (a) P(PSP-C ₆), (b) P(PSP-C ₄) and (c) P(PSeP-C ₄) during cathodic scan.	117
Figure 3.49. Chronoabsorptometry experiments for P(PSP-C ₆) on ITO in 0.1 M TBAH/ ACN while the polymer was switched between -0.1 V and 1.1 V.	118
Figure 3.50. Chronoabsorptometry experiments for P(PSP-C ₄) on ITO in 0.1 M TBAH/ ACN while the polymer was switched between -0.1 V and 1.15 V. ...	119
Figure 3.51. Chronoabsorptometry experiments for P(PSeP-C ₄) on ITO in 0.1 M TBAH/ ACN while the polymer was switched between 0.0 V and 1.1 V.	120
Figure 3.52. Changes in optical absorption spectra of chemically obtained P(PSP-C ₆) in DCM solution after the addition of 10 μ L (for each spectrum) 5x10 ⁻⁴ M SbCl ₅ and 10 ⁻² M N ₂ H ₅ OH. Inset: Colors of P(PSP-C ₆) in DCM solution addition of SbCl ₅ and N ₂ H ₄ OH.	122
Figure 3.53. Stability test for (a) P(PSP-C ₆), (b) P(PSP-C ₄), (c) P(PSeP-C ₄) films in 0.1 M TBAH/DCM at a scan rate of 100 mV s ⁻¹ under ambient conditions by cyclic voltammetry as a function of the number of cycles: A: 1, B: 500, C: 1000, D: 2000 cycles; Q _a : Anodic charge stored, i _{pa} : Anodic peak current, i _{pc} : Cathodic peak current.	123
Figure 3.54. ESR spectrum results of P(PSP-C ₁₀) via addition of 10 ⁻⁸ M SbCl ₅ and 10 ⁻⁵ M N ₂ H ₄ OH dissolved in DCM.	125
Figure 3.55. Mass spectrum of chemically synthesized P(PSP-C ₁₀) (experimental notes: M _n = 7652.24; M _w = 8991.42; M _z = 10221.84; HI= 1.18).	126
Figure 3.56. Distrubution plots of chemically synthesized P(PSP-C ₆) (experimental notes: M _n = 10098; M _w = 61256; M _z = 276446; HI= 6.06).	127
Figure 3. 57. Distrubution plots of chemically synthesized P(POP-C ₁₀) (experimental notes: M _n = 2817; M _w = 5867; M _z = 11030; HI= 2.08).	127
Figure 3.58. Representation of CMY and RGB color spaces from the polymer solutions in CHCl ₃	128

- Figure 3.59. Obtaining blue color according to CMT: Absorption spectrum of cyan colored P(POP-C₁₀), magenta colored P(TOT)* and their mixures having blue color (*P(TOT) polymer contains thiophene as a donor unit and benzo[c][1,2,5]oxadiazole as acceptor unit like P(POP-C₁₀)). Inset: Picture of the polymers and their mixture in CHCl₃, and their $L^*a^*b^*$ values..... 129
- Figure 3.60. Obtaining green color according to CMT: Absorption spectrum of cyan colored P(POP-C₁₀), yellow colored P(PPyP-C₁₀)* and their mixures having green color (*P(PPyP-C₁₀) polymer contains ProDOT-C₁₀ as a donor unit like P(POP-C₁₀) and pyrene as acceptor unit. Inset: Picture of the polymers and their mixture in CHCl₃, and their $L^*a^*b^*$ values..... 130
- Figure 3. 61. Obtaining red color according to CMT: Absorption spectrum of yellow colored P(PPyP-C₁₀) and magenta colored P(TOT) and their mixures having red color. Inset: Picture of the polymers and their mixture in CHCl₃, and their $L^*a^*b^*$ values..... 131
- Figure 3.62. Obtaining black color according to CMT: Absorption spectrum of cyan colored P(POP-C₁₀), magenta colored P(TOT), yellow colored P(PPyP-C₁₀) and their mixures having black color. Inset: Picture of the polymers and their mixture in CHCl₃, and $L^*a^*b^*$ values..... 132
- Figure 3.63. Electronic absorption spectra of P(PSeP-C₁₀) and P(PNP-C₁₀) in their neutral states in 0.1 M TBAH dissolved in ACN and the colors of the polymers in different redox states..... 134
- Figure 3.64. CV during the repeated scan electropolymerization of a mixture of PSeP-C₁₀ and PNP-C₁₀ with 1:4 monomer feed ratio to give P(PSeP-C₁₀-co-PNP-C₁₀) in 0.1 M TBAH/DCM-ACN (3/2-v/v) at a scan rate of 100 mV/s, Pt disk working electrode, and (b) scan rate dependence of the P(PSeP-C₁₀-co-PNP-C₁₀) film in 0.1 M TBAH/ACN at different scan rates (mV/s): (a) 50; (b) 75; (c) 100; (d) 125; (e) 150; (f) 175; and (g) 200..... 135
- Figure 3.65. P(PSeP-C₁₀-co- PNP-C₁₀) film on ITO glass slide and P(PSeP-C₁₀-co-PNP-C₁₀) in DCM..... 136
- Figure 3.66. (a) Relationship of anodic (i_a), cathodic (i_c) peak currents and the charge (Q_a)/discharge (Q_c) variations of P(PSeP-C₁₀-co- PNP-C₁₀) as a function of number of cycles and (b) Cyclic voltammetry stability of P(PSeP-C₁₀-co- PNP-

<p>C_{10}) film at a scan rates of 200 mV/s between 0.0 V and 1.1 V in 0.1 M TBAH/ACN. Number of cycle: (a) 1; (b) 1000; (c) 2000; (d) 3000; and (e) 4000.</p>	137
<p>Figure 3.67. Electronic absorption spectra of the P(PSeP-C_{10}-co- PNP-C_{10}) film coated on ITO electrode at various applied potentials between 0.0 V and +1.2 V in 0.1 TBAH/ACN, and the colors of the P(PSeP-C_{10}-co- PNP-C_{10}) in different redox states.</p>	138
<p>Figure 3.68. Chronoabsorptometry experiment at 522 nm for P(PSeP-C_{10}-co- PNP-C_{10}) film on ITO electrode in 0.1 M TBAH/ACN while the polymer was switched between -0.1 V and 1.0 V (vs Ag wire) with a switching time of 10 s, 5 s, 3 s and 2 s.</p>	139
<p>Figure 3.69. Schematic representation of an electrochromic device.</p>	140
<p>Figure 3.70. CV of (a) P(PSeP-C_{10})- P(POP-C_{10}) (from -1.0 V to +1.5 V), (b) P(PSeP-C_{10})-PEDOT (from -0.4 V to +1.0 V), (c) P(PSeP-C_{10})- P(PNP-C_{10}) (from -0.6 V to +0.9 V) and (d) P(PSP-C_{10})-PEDOT (from -0.6 V to +1.7 V) devices at 75 mVs⁻¹.</p>	141
<p>Figure 3.71. Spectroelectrochemical behavior of (a) P(PSeP-C_{10})- P(POP-C_{10}) (from -1.0 V to +1.5 V), (b) P(PSeP-C_{10})-PEDOT (from -0.4 V to +1.0 V), (c) P(PSeP-C_{10})- P(PNP-C_{10}) (from -0.6 V to +0.9 V) and (d) P(PSP-C_{10})-PEDOT (from -0.6 V to +1.7 V) devices. Inset: Pictures of device in two color states and $L^*a^*b^*$ values of these states.</p>	142

LIST OF SCHEMES

SCHEMES

Scheme 1.1. Some examples of soluble polymers.	14
Scheme 1.2. D-A-D groups containing polymers, P(TSeT), P(ESeE), P(PSeP-C ₁₀), P(PSP-C ₁₀), P(PNP-C ₁₀), P(POP-C ₁₀), P(PSeP-C ₄), P(PSP-C ₄) and P(PSP-C ₆).23	
Scheme 2.1. Structure of monomers, TSeT, ESeE, PSeP-C ₁₀ , PSP-C ₁₀ , PNP-C ₁₀ , POP-C ₁₀ , PSeP-C ₄ , PSP-C ₄ and PSP-C ₆	28
Scheme 2.2. Synthesis of the “hat” part.	28
Scheme 2.3. Synthesis of the donor groups.	31
Scheme 2.4. Synthesis of the acceptor groups.	33
Scheme 2.5. Synthesis of 4,7-dibromo-2-decyl-2H-benzo[d][1,2,3]triazole.	34
Scheme 2.6. Stannylating of thiophene, EDOT, and ProDOT-C _n molecules.	36
Scheme 2.7. Reaction scheme of polymer synthesis.	40
Scheme 3.1. The design of the monomers according to desired properties.	44
Scheme 3.2. Categorizing the monomers according to used functional groups to be examined.	48
Scheme 3.3. Monomers that are used for the investigation of donor groups’ effect.	49
Scheme 3.4. Monomers that are used for the investigation of the acceptor groups’ effect.	75
Scheme 3.5. Monomers that are used for the investigation of alkyl chain length effect.	103

LIST OF TABLES

TABLES

Table 1.1. Properties of some commonly known electrochromic polymers [49].	10
Table 1.2. Working range of some commonly known solvents [49].	18
Table 3.1. Electrochemical and optical data for TSeT, ESeE, and PSeP-C ₁₀ and their corresponding polymers, P(TSeT), P(ESeE), and P(PSeP-C ₁₀).	55
Table 3.2. Optical and switching time data of electrochemically synthesized polymers P(TSeT), P(ESeE), P(PSeP-C ₁₀), and PEDOT.	62
Table 3.3. Electrochemically determined HOMO, LUMO and E _g values of polymers, P(TSeT), P(ESeE), and P(PSeP-C ₁₀).	65
Table 3.4. Optical and switching time data of chemically synthesized P(PSeP-C ₁₀), P(PSP-C ₁₀), and P(PNP-C ₁₀). The given CE value is the best one at a given wavelength.	70
Table 3.5. Electrochemical and optical data for PSeP-C ₁₀ , PSP-C ₁₀ , PNP-C ₁₀ , and POP-C ₁₀ , and their corresponding polymers, P(PSeP-C ₁₀), P(PSP-C ₁₀), P(PNP-C ₁₀), and P(POP-C ₁₀).	83
Table 3.6. Optical and switching time data of electrochemically synthesized polymers P(PSeP-C ₁₀), P(POP-C ₁₀), P(PSP-C ₁₀), P(PNP-C ₁₀) and their analogues. The given CE value is the best one at a given wavelength.* P(ESE) is poly(4-(2,3-dihydrothieno[3,4-b][1,4]dioxin-5-yl)-7-(2,3-dihydrothieno[3,4-b][1,4]dioxin-7-yl)benzo[c][1,2,5]thiadiazole) and P(ENE) is poly-4,7-bis(2,3-dihydrothieno[3,4-b][1,4]dioxin-5-yl)-2-dodecyl-2H-benzo [1,2,3] triazole [76, 80].	86
Table 3.7. Electrochemically determined HOMO, LUMO and E _g values of polymers, P(PSeP-C ₁₀), P(PSP-C ₁₀), P(PNP-C ₁₀), and P(POP-C ₁₀).	90
Table 3.8. Colorimetric data for PSP-C _n (n=4 and 6) and PSeP-C ₄	108
Table 3.9. Electrochemical and optical data for PSP-C ₁₀ , PSeP-C ₄ , PSP-C ₄ and PSP-C ₆ , and their corresponding polymers, P(PSP-C ₁₀), P(PSeP-C ₄), P(PSP-C ₄) and P(PSP-C ₆).	109
Table 3.10. Electrochemically determined HOMO, LUMO and E _g values for P(PSP-C ₆), P(PSP-C ₄) and P(PSeP-C ₄).	113

Table 3.11. Optical and switching time data of electrochemically synthesized polymers P(TSeT), P(ESeE) and P(PSeP-C ₁₀), PEDOT and their analogues. The given CE value is the best one at a given wavelength.....	121
Table 3.12. Optical and switching time data of P(PSeP-C ₁₀)- P(POP-C ₁₀), P(PSeP-C ₁₀)-PEDOT, P(PSeP-C ₁₀)- P(PNP-C ₁₀) and P(PSP-C ₁₀)-PEDOT devices.	144
Table 3.13. Electrochemical and optical stability of P(PSeP-C ₁₀)- P(POP-C ₁₀), P(PSeP-C ₁₀)-PEDOT, P(PSeP-C ₁₀)- P(PNP-C ₁₀) and P(PSP-C ₁₀)-PEDOT devices.	145

ABBREVIATIONS

E_g	Band Gap
VB	Valance Band
CB	Conduction Band
CV	Cyclic Voltammetry
DPV	Differential Pulse Voltammetry
SPEL	Spectroelectrochemistry
ITO	Indium Tin Oxide
WE	Working Electrode
CE	Counter Electrode
RE	Reference Electrode
t	Time
% T	Percent Transmittance
Δ%T	Percentage Transmittance Change
a.u.	Absorbance Unit
ACN	Acetonitrile
DCM	Dichloromethane
THF	Tetrahydrofuran
DMSO	Dimethylsulfoxide
TBAH	Tetrabutylammonium Hexafluorophosphate
ProDOT	3,4-propylenedioxythiophene

PEDOT	Poly(3,4-ethylenedioxythiophene)
D	Donor
A	Acceptor
D-A-D	Donor-Acceptor-Donor
RGB	Red-Green-Blue
CMY	Cyan-Magenta-Yellow
PEC	Polymeric Electrochromic
HOMO	Highest Occupied Molecular Orbital
LUMO	Lowest Unoccupied Molecular Orbital
CE	Coloration Efficiency
ESR	Electron Spin Resonance
ProDOT-Decyl₂	3,3-Didecyl-3,4-dihydro-2H-thieno[3,4-b][1,4]dioxepine
ProDOT-C_n	3,3-Alkyl-3,4-dihydro-2H-thieno[3,4-b][1,4]dioxepine
MALDI-TOF Mass Spectrometer	Matrix-Assisted Laser Desorption/Ionization Time-of-Flight
GPC	Gel Permeation Chromatography
M_n	Number Average Molecular Weight
M_w	Weight Average Molecular Weight
M_z	z-average Molecular Weight
HI	Heterogeneity Index
CMT	Color Mixing Theory
PCBM	[6,6]-phenyl-C ₆₁ -butyric acid methyl ester

CHAPTER 1

INTRODUCTION

1.1. A Brief Introduction to Conducting Polymers

The fundamentals of the chemistry started to form with the studies of the alchemists up to the Middle Ages: Finding “ab-1 hayat”, the liquid giving immortality to who drinks it, and “ab-1 zer”, the liquid turning any material to gold just pouring it. Actually, alchemists were not able to find such kind of liquids, however, their pioneering works paved the way of inception of the chemistry. Like this, each advanced materials just a single step of a stairs can be amenable for the future technological applications. This means like alchemists, chemists have also some dreams to improve the life of the mankind.

Among these dreams, polymers have a great role due to their greater impact on the modern technological life of today. Up to 1920, there was no idea about the polymers. Since Staudinger had introduced concept of the macromolecules [1-3], myriad of studies were started to be done by chemists.

After the accidental discovery of the doped polyacetylene, which was awarded the Nobel Prize in Chemistry in 2000, the first conducting polymer, in 1970s [4,5], the new research area was born: Conducting polymers. These materials have attracted considerable attention over the last three decades since they found a variety of advanced technological applications in the fields of light-emitting diodes [6-9], photovoltaics [10-14], transistors [15-18] and molecular electronics [19-21] owing to their low cost, compatibility and tunable intrinsic properties (electronic, optical, conductivity, and stability) offered by the structural design of the starting materials

[22-24]. In particular, they have been envisioned as one of the most favored electrochromes in devices [25,26], optical displays [27], smart windows [28,29], mirrors [30,31] and camouflage materials [32,33] because of their promising advantages when compared to the earliest inorganic electrochromes [34-49]: e.g., ease of processing over the large surfaces via spin coating, spraying and printing methods, high optical contrast ratio, multicolors with the same material, high redox stability and long cycle life with low response time. For that reason, significant efforts have been devoted to the design and synthesis of polymeric electrochromics (PECs) based on organic π -conjugated materials.

1.2. Band Gap Theory

The energy difference between the valance band (VB) and the conduction band (CB) is called as the band gap (E_g) (**Figure 1. 1**). Conducting polymers are semiconductors having band gap lower than 3 eV whereas metals have band gap as zero and that of insulators is higher than 3 eV.

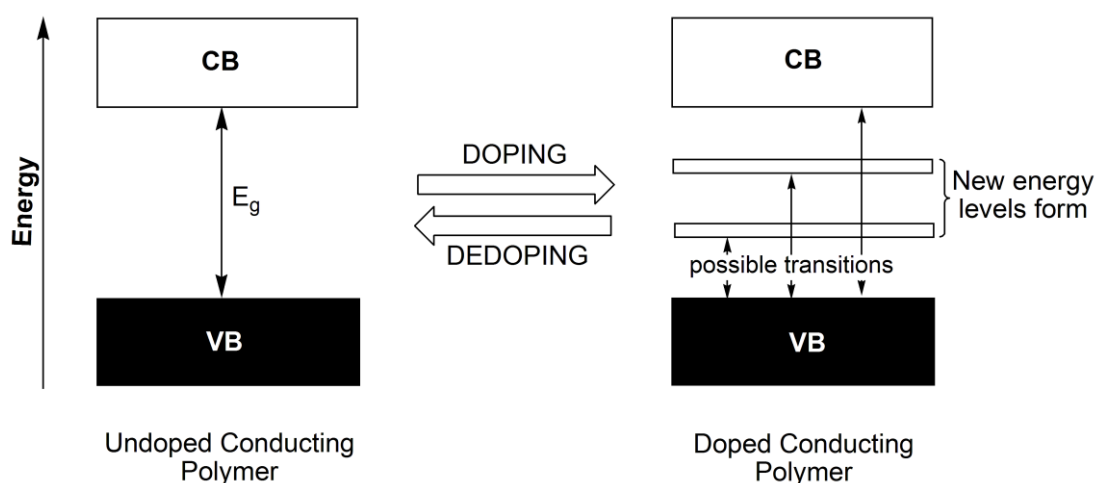


Figure 1.1. Energy transitions of doped and undoped conducting polymers.

For conjugated polymers, upon doping via oxidation or reduction, which produces new energy levels (Figure 1. 1), charges (polarons and bipolarons) are formed (Figure 1. 2) on the polymer backbone and these charges increase the tendency of the polymer as a conductive material.

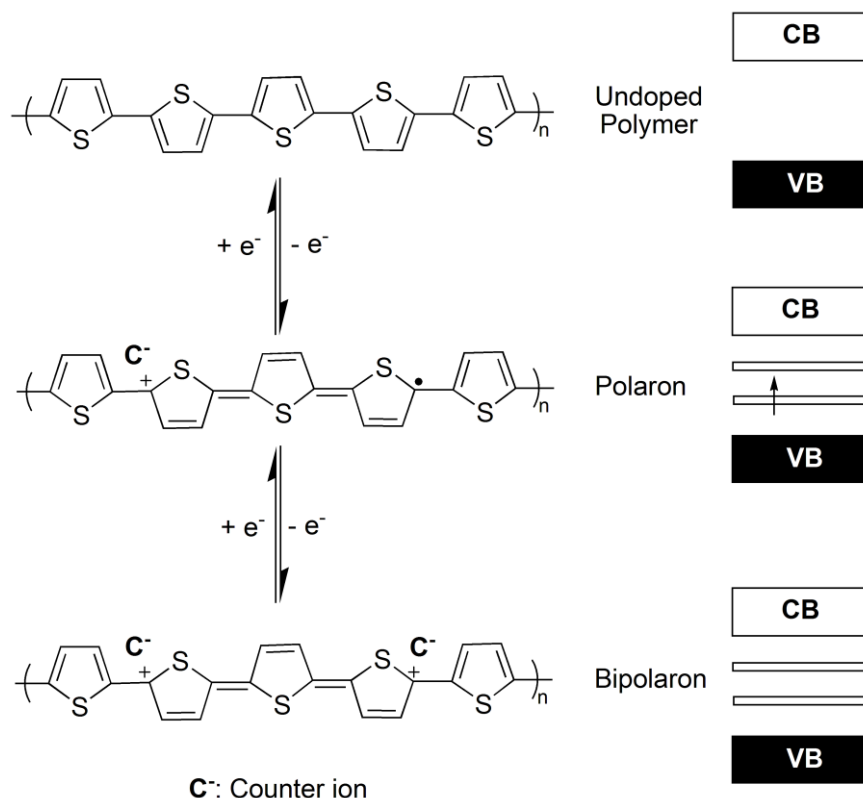


Figure 1.2. Representation of polaron and bipolaron in polythiophene and their states in the band gap.

In **Figure 1. 3**, the evolution of the band gap starting from polyacetylene to poly(2-(2,3-dihydrothieno[3,4-b][1,4]dioxin-5-yl)pyridine (poly(EDOT-Pyr)) is depicted [40].

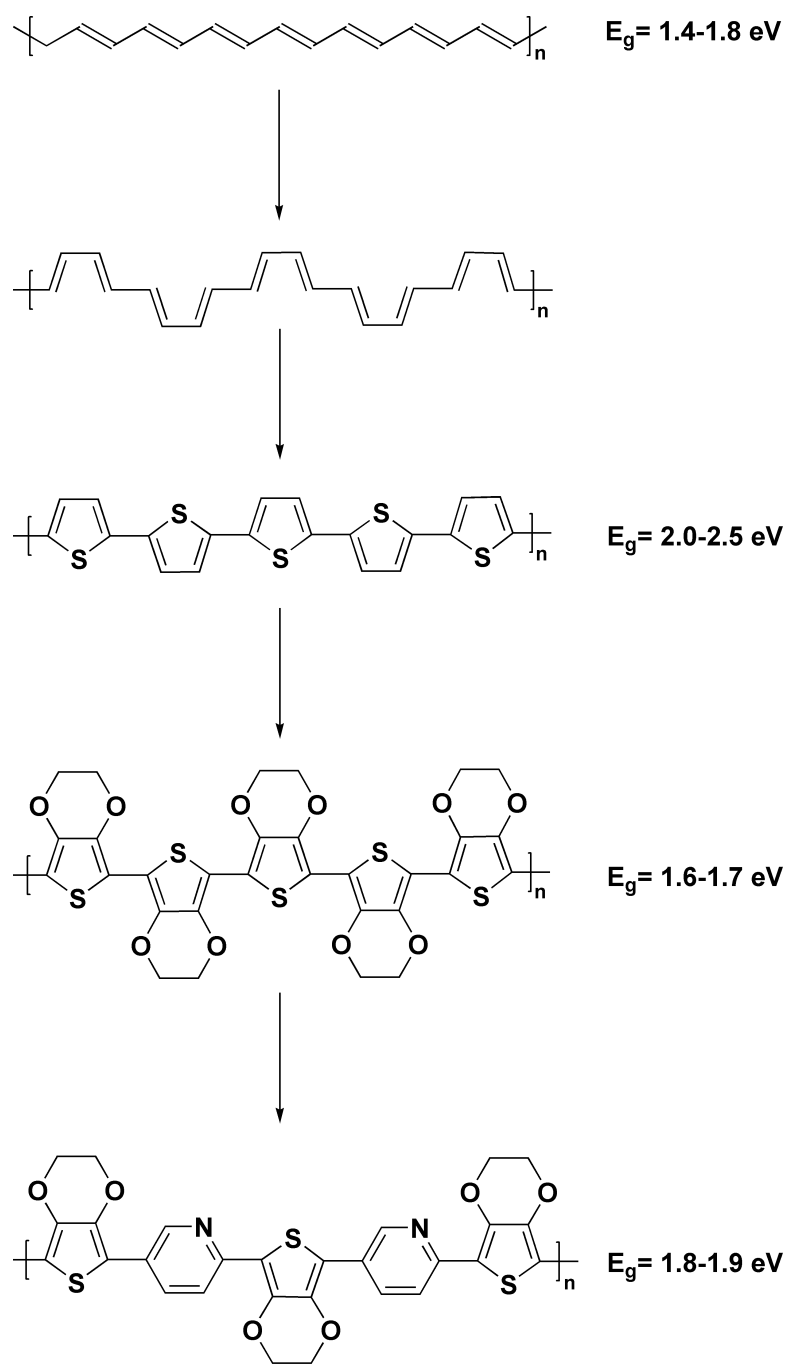


Figure 1.3. The band gap evolution from polyacetylene to poly(EDOT-Pyr) [40].

The band gap of the conjugated polymer can be calculated using the data obtained by several ways: cyclic voltammetry (CV), differential pulse voltammetry (DPV), and

spectroelectrochemical analysis (SPEL). For the determination of the band gap utilizing the data from CV and DPV measurements, the polymer film must have both n- and p-doping properties, on the other hand, n-doping is not essential for the determination of E_g from SPEL data. For the calculation via CV and DPV, the difference between the oxidation onset of p-doping and the reduction onset of n-doping is taken (**Figure 1. 4 (a)** and **(b)**). Among these two methods, DPV is more precise than CV since capacitive currents have fewer effects on the measurement in DPV, that is, the voltage is given to the system via pulse not continuously so just the difference between each steps is taken in this method.

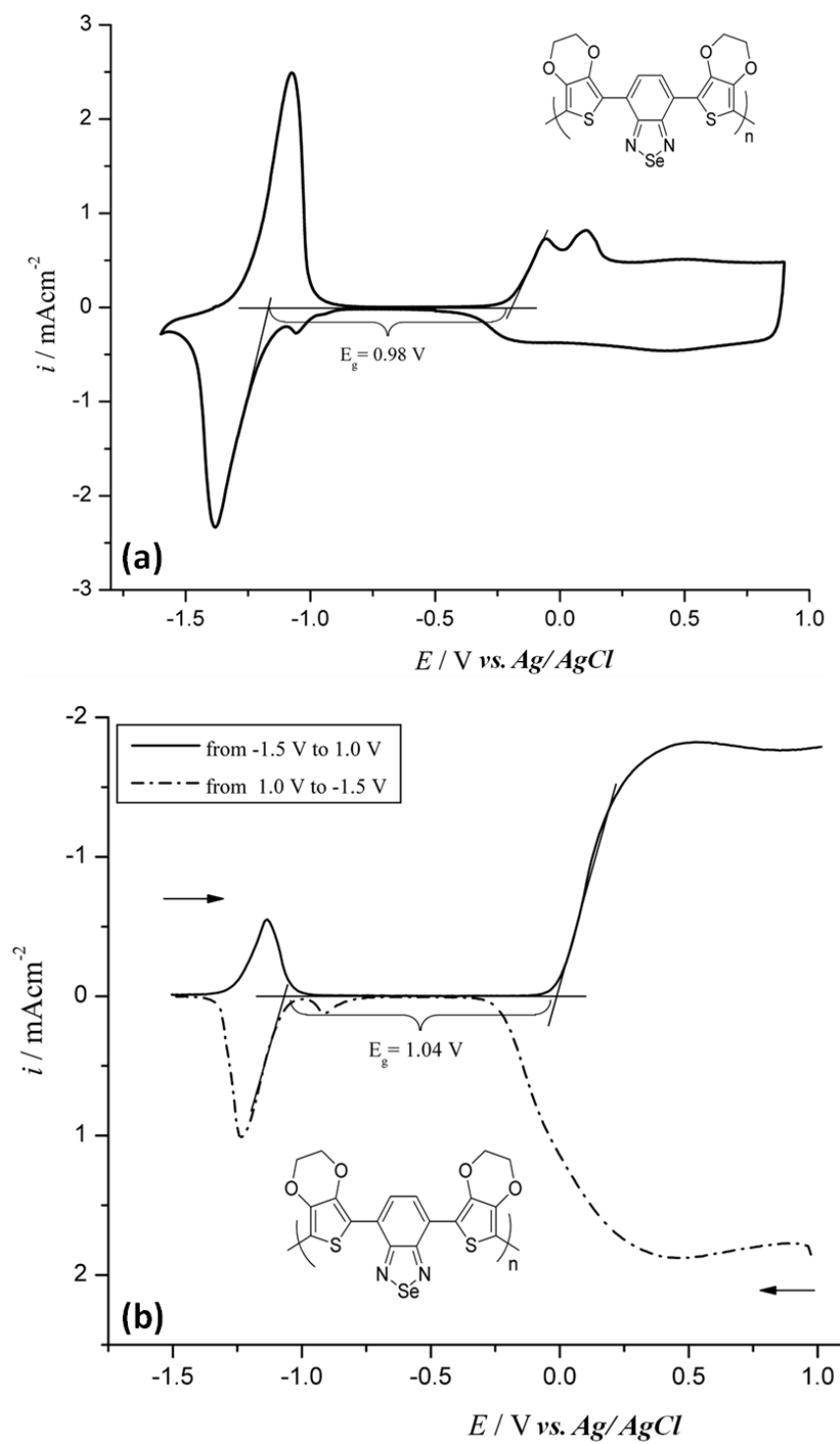


Figure 1. 4. Calculation of the band gap from (a) CV measurement and (b) DPV measurement [41].

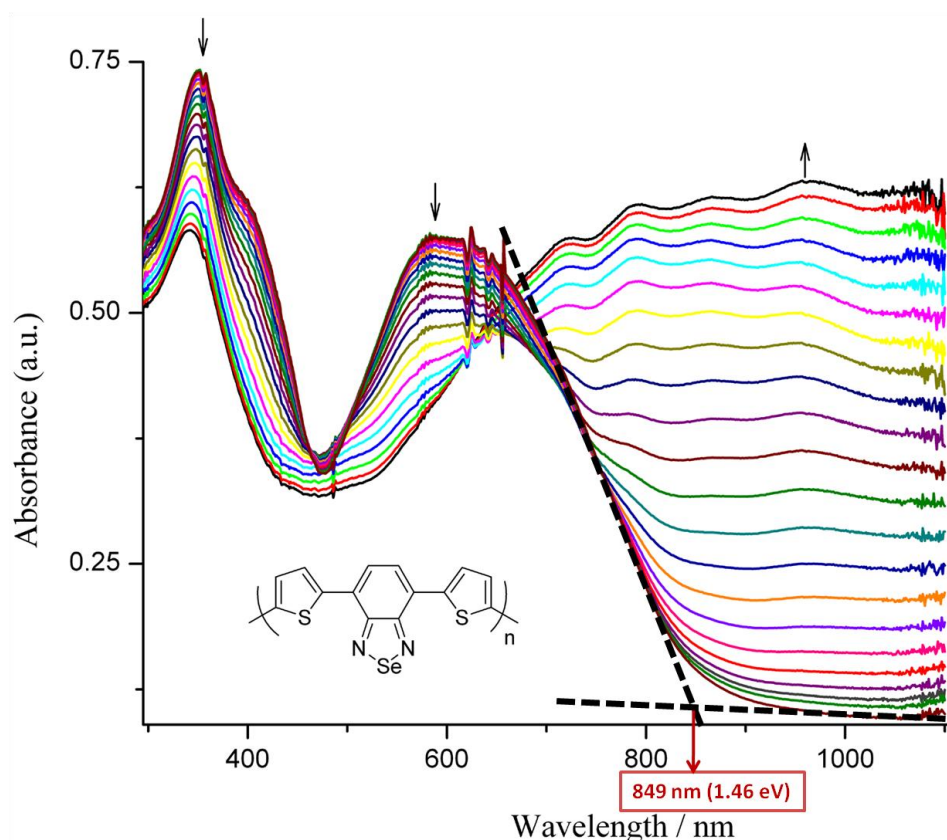


Figure 1. 5. Calculation of band gap from SPEL measurement [41].

SPEL, on the other hand, is one of the most extensively used method to calculate E_g of the conjugated polymers. E_g is calculated from the onset of the π - π^* transition of the polymer film in its neutral state (**Figure 1. 5**). For poly(4,7-di-2,3-dihydrothieno [3,4-b][1,4] dioxin-5-yl-2,1,3-benzoselenadiazole) E_g value was found to be as 0.98 eV (**Figure 1. 4 (a)**), 1.04 eV (**Figure 1. 4(b)**), and 1.05 eV by CV, DPV, and SPEL, respectively [41]. The close values obtained from DPV and SPEL data indicate that these techniques are more compatible with each other.

Tuning of the band gap is significantly important for the conducting polymers to be used in the industrial and technological applications since according to the application areas, the desired E_g values are differing. For instance, for organic solar cell applications, polymer should have band gap lower than 1.8 eV to utilize solar energy efficiently. For that reason, many theories have been developed in order to

tune the band gap of conjugated polymers: Bond-length alternation, creating highly planar systems, aromaticity effect, and donor-acceptor (D-A) effect [40,42-45]. Among these, the most effective and extensively used one is the D-A approach. Via this approach, tuning the band gap can be achieved by choosing a D molecule having desired oxidation potential and an A molecule with desired reduction potential and then combining these groups across the polymer chain in 1:2 A:D ratio. Instance of this approach can be seen in **Figure 1. 6**, by coupling D and A groups, energy levels can be tuned and the bang gap of obtained D-A type polymer is lower than those of both pristine D and A groups containing polymers. This process is called as “band gap compression” [46,47].

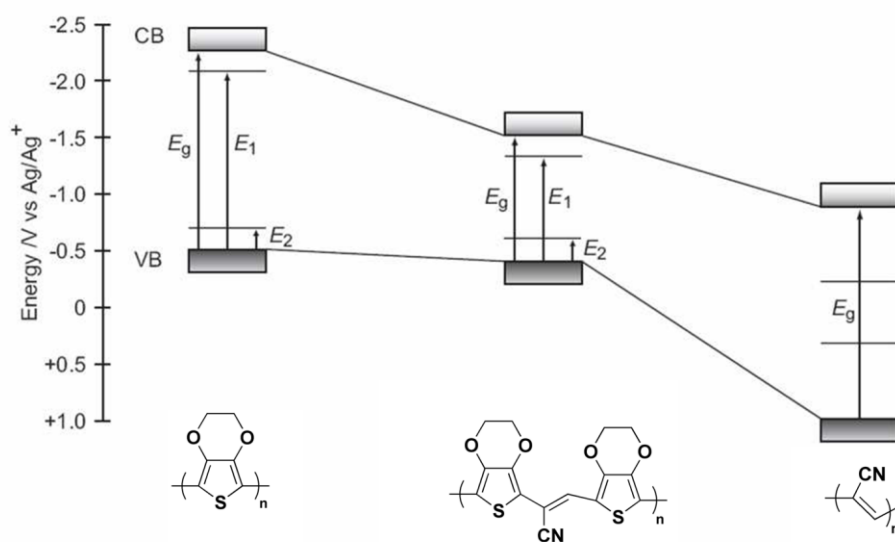


Figure 1. 6. Estimated optical behavior of D-A-D type monomer’s polymer [47].

1.3. Electrochromism

In its general meaning, chromism is a reversible alteration in the color of a material because of an external source such as temperature, external voltage, absorption of light, and solvent [48]. In electrochromism, this color change occurs via an external voltage.

Electrochromism's meaning is not just a color change during voltage switching. It means also change in the transmission of material via an external voltage pulse. Therefore, it occurs not only in the visible region, but also in the microwave, ultraviolet, and infrared regions and this makes the materials amenable for different applications.

Inorganic oxides (such as tungsten oxide), inorganic complexes (such as Prussian Blue), and viologens are commonly known electrochromic materials and conjugated polymers are also electrochromics which have been intensively studied since they have many priorities over former ones such as processability, color tunability, multiple colors with a single material, high redox stability, and fast switching time [22]. In **Table 1.1**, color changes and cycle life times of some commonly known polymers are given. A polymer to be used as a display material should possess following properties [49]:

- The color change should be observable.
- The color change has to be uniform along the whole electrochromic device and fast enough according to application area.
- Electrochromic device should be switched between redox state(s) several times (approximately 10^6 times).
- It should be robust and nontoxic.

Table 1.1. Properties of some commonly known electrochromic polymers [49].

Polymer	Color Change	Applied Voltage (V)	Cycle Life Time
Polyaniline	Yellow to green	2	$\sim 10^3$
Polythiophene	Red to blue	2	$\sim 10^3$
Polypyrrole	Yellow to blue-black	1.5	$\sim 10^3$
Polyisothianaphthalene	Blue to light yellow	-	$\sim 10^3$

In order to adjust the color of the polymer, many strategies can be used such as adding D and A units to the structure, adding functional groups to the structure and/or achieving copolymerization [22].

Since everyone's concept of color is different, that is, color concept is a few subjective, a more scientific method, colorimetry, was used to define the color in electrochromism. In colorimetry, three components are measured; hue (dominant wavelength or chromatic color), saturation (chroma, intensity, or purity), and brightness (lightness or luminance). There are two color spaces developed by CIE (The Commission Internationale de l'Eclairage- International Commission on Illumination) used for the determination of the colorimetric results of color of species: xy chromatography diagram developed in 1931 used for the measurement of hue (x), saturation (y), and luminance (Y). Another color space specified by CIE in 1976 is $L^*a^*b^*$ color space and this is most widely used. In this color space, L^* is the parameter of the lightness (it is between 0 and 100, that is, between black and white). Where as, a^* is the parameter of the red-green balance (it is between positive and negative values, that is, depending on the sign it is responsible for hues between red and green), b^* is the parameter of yellow-blue balance (it is between positive and negative values, that is, depending on the sign it is responsible for hues between yellow and blue) [50].

In the literature generally electrochromic materials are cathodically colored such as poly(3,4-ethylenedioxythiophene) (PEDOT), that is, they are colored in their neutral states and bleached in their oxidized states. However, some of them are anodically colored such as poly(2-(2,3-dihydro-6,8-dimethyl-[1,4]dioxepino[2,3-c]pyrrol-7(2H)-yl)ethanol) (hydroxyl-substituted PProDOP), or both anodically and cathodically colored. Some contains multiple colors at different redox states, e.g., viologen and anthraquinone functionalized polythiophenes [51].

The quality of electrochromic conjugated polymers depends on several parameters such as electrochromic contrast, switching time and coloration efficiency [52]. However, these parameters depend on the thickness and morphology of the obtained polymer film and the optimum value should be given with the declared thickness. These parameters are measured via *in situ* SPEL analysis called as chronoabsorptometry. Typical measurements are done like this: Polymer film is coated on the surface of indium tin oxide (ITO) coated glass slide. Background is taken with monomer-free electrolyte solution containing ITO inside it. After that polymer coated ITO is immersed inside the quartz cell. While redox potentials are given by the potentiostat modified with three-electrode system, data are collected between 300 nm and 1100 nm ($1\text{eV} = 1240\text{ nm}$) [22] in each 0.5 seconds via UV-Vis spectrometer. During the cathodic scan in order to eliminate the degradative effect of oxygen, the system is argon degassed.

1.3.1. Electrochromic Contrast

Transmittance difference between the redox states of a polymer at a specified wavelength is called as electrochromic contrast. As mentioned before, it is a substantial property of an EC polymer and measured by chronoabsorptometry at constant λ_{max} value(s) while the potential is switched between oxidized and neutral states. It can be calculated by extracting the percent transmittance of bleached state and that of colored state (Equation 1-2) (**Figure 1. 7**).

$$\Delta\% T = (\% T_{\text{bleached}}) - (\% T_{\text{colored}}) \quad (\text{Equation 1-2})$$

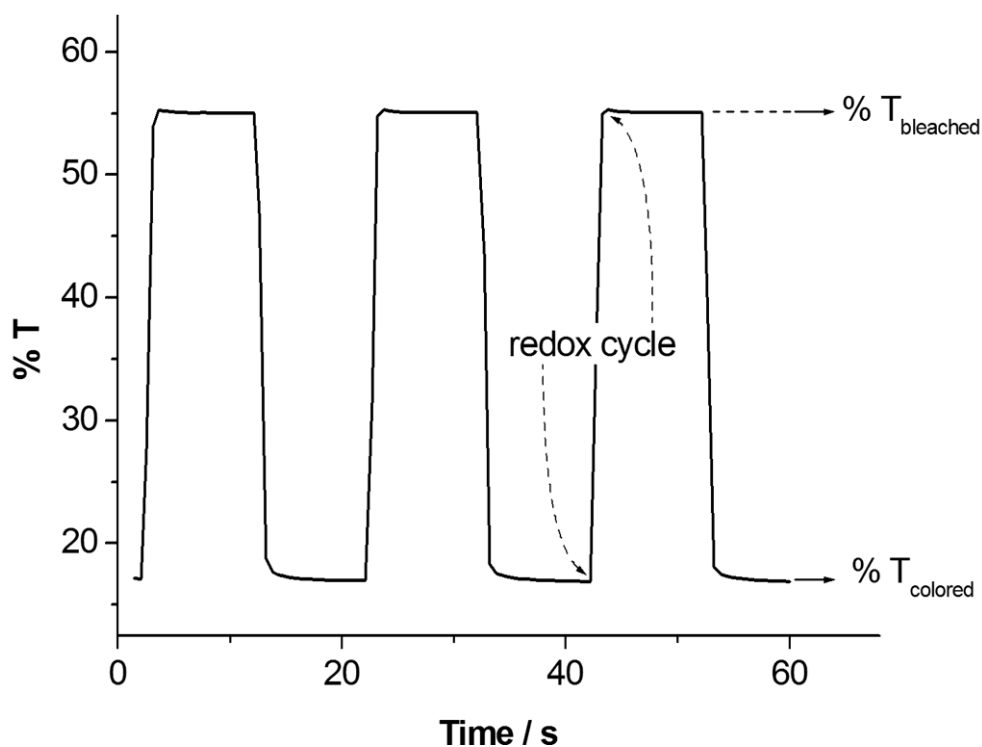


Figure 1.7. Chronoabsorptometry experiment for a polymer monitored at specified wavelength.

1.3.2. Switching Time

Switching time (response time) is the time required for an EC polymer to change its color during the redox process. Desired response time of an EC polymer depends on its application area. For instance, it could be around minutes for the smart windows whereas for electrochromic displays it should be in sub-seconds. Since the human eye can perceive 95 % of the full contrast, calculations are done according to this.

1.3.3. Coloration Efficiency

Coloration efficiency is the parameter of optical density while polymer is doped and dedoped. Generally it is assigned as η and has cm^2/C unit. It is calculated with tandem chronocoulometry / chronoabsorptometry measurements. In order to calculate coloration efficiency, firstly optical density (ΔOD) should be calculated (Equation 1-3).

$$\Delta \text{OD} = \log (T_{\text{bleached}} / T_{\text{colored}}) \quad (\text{Equation 1-3})$$

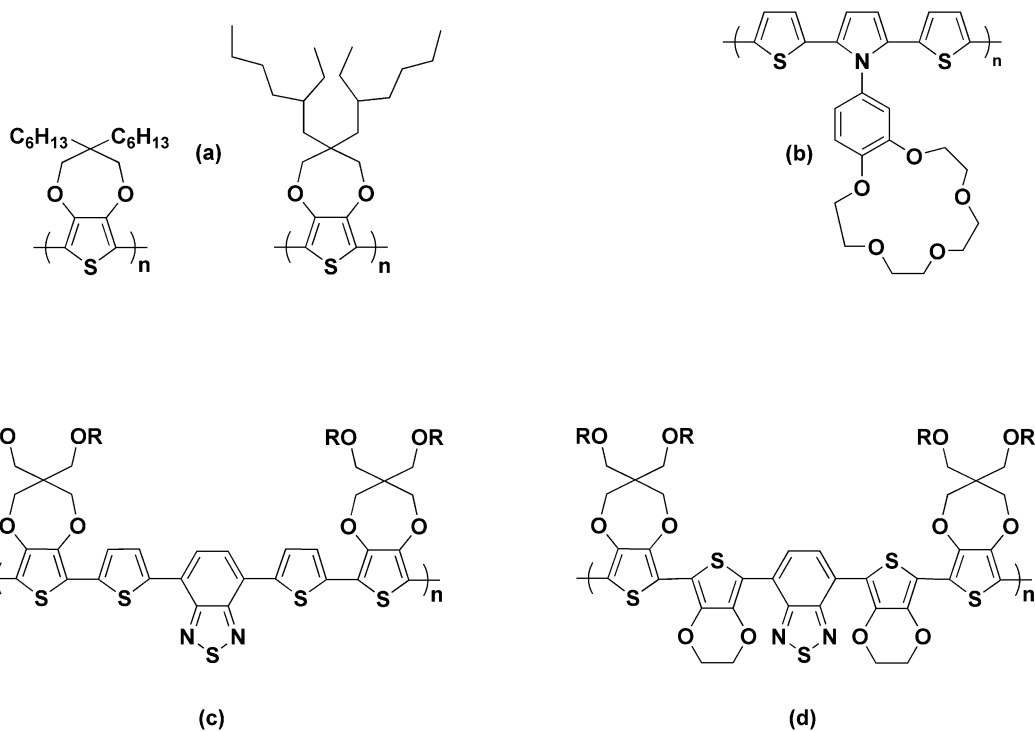
$$\eta = \Delta \text{OD} / Q \quad (\text{Equation 1-4})$$

In the **Equation 1-4**, Q is the density of injected or ejected charge during the redox process and it should be in C cm^{-2} unit.

The handicap in the calculation of coloration efficiency, η , utilizing the data evaluated from tandem chronocoulometry / chronoabsorptometry measurement, is the change in the value of η . To avoid this handicap, more recently, a new method has been introduced, in which Faradaic charge is extracted from the total charge passing through during the redox process. It is found that most of the polymers have higher η values when their coloration efficiencies are evaluated using this recently introduced method [51,53,54].

1.4. Processable Conjugated Polymers

The pursuit of producing soluble conducting polymers is recently one of the main aims of the scientists since they can be processable and so their application to the technological and industrial areas is easier and cheaper when compared to inorganic counterparts of these materials. To carry out this goal many viable strategies are developed: Addition of alkyl chains (**Scheme 1. 1-(a)**) [55], crown ether groups (**Scheme 1. 1-(b)**) [56], alkoxy chains ((**Scheme 1. 1-(c)** and **(d)**) [57] and ionic groups (for water solubility) [58].



Scheme 1.1. Some examples of soluble polymers.

1.5. Polymerization Techniques

Polymerization can be achieved by chemical or electrochemical means depending on the main intention. For example, electrochemical polymerization method is useful when the main goal is to obtain high quality polymer since the oxidation potential can be controlled. Also, thickness of the polymer film can be adjusted via determining the number of cycles or counting the number of Coulombs (in mC) passing during the polymerization. Moreover, small amounts of monomer can be enough to synthesize the desired polymer via electrochemical polymerization whereas chemical polymerization requires more. On the other hand, chemical polymerization is more convenient way if the large amounts of compound are required [59].

1.5.1. Electrochemical Polymerization

In electrochemical polymerization, the first step is electrochemical oxidation or reduction of the monomer which is followed by a chemical step. Polymerization can be achieved via repetitive cycling in the desired potential range (CV) or applying constant potential (controlled potential coulometry). Latter one is more amenable way since the amount of the charge used during the polymerization is known, which can be correlated to the thickness of the polymer film.

Electrochemical polymerization is achieved in an electrochemical cell and the main difference between a classical electrochemical cell and the cell used for electrochemical polymerization and/ or analysis is the number of electrode used in these systems. Generally, since the main aim is measuring the potential differences, in a classical electrochemical cell two electrodes are used: Working and reference electrode or two working electrodes systems. However, during the electrochemical polymerization and/ or analysis three electrodes are used: Working electrode (WE), counter (auxiliary) electrode (CE) and reference electrode (RE) (**Figure 1. 8**). During

the measurement while the voltage differences arranged and monitored between working and reference electrodes, the current between working and counter electrodes is measured.

Type of the working electrode is determined according to the monomer type, aim of the study, polymer stability on the electrode surface, etc. For example, for the corrosion studies generally a steel electrode is used, for SPEL analysis of polymers ITO is chosen since it is transparent. Glassy carbon, gold (Au) and platinum (Pt) electrodes are preferred due to their inert characteristics around the working range. Choice of counter electrode again depends on the study, generally Pt electrode is chosen. The most important point here is that the surface area of the counter electrode should be larger than that of working electrode in order to eliminate mass transfer via migration on the working electrode.

Ag wire, Ag/AgCl and standard calomel electrodes (SCE) are frequently used reference electrodes. As an internal reference, 10 mM ferrocene solution is also used.

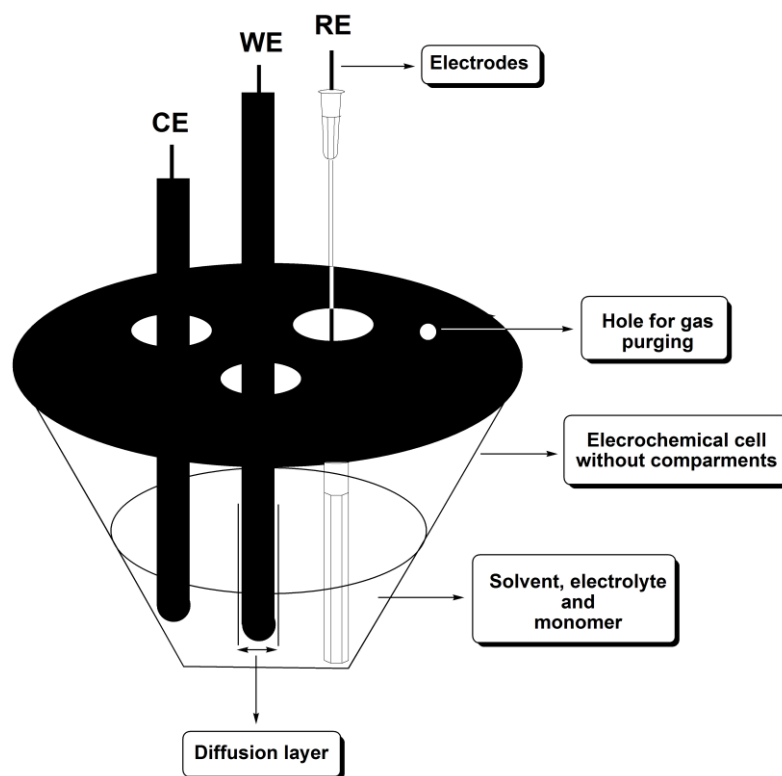


Figure 1.8. Representation of an electrochemical cell used for electrochemical polymerization and/ or analysis.

Prudent selection of the electrolytic medium, solvent and supporting electrolyte, is essential for the electrochemical polymerization (**Figure 1. 8**).

1.5.1.1. Solvent

First of all, solvent should dissolve monomer, but it should not dissolve the polymer deposited on the surface of working electrode. In some cases, these two properties cannot be obtained at the same time, therefore, solvent mixtures are used in order to attain both of them. Because of its high dielectric constant ($\epsilon = 37$) and wide potential range (**Table 1. 2**), acetonitrile (ACN) is one of the most frequently used solvent. The most widely used other solvents are water, dimethyl formamide ($\epsilon =$

37), dichloromethane (DCM) ($\epsilon = 9$), tetrahydrofuran ($\epsilon = 7$), nitrobenzene, ethanol, nitro methane, benzonitrile ($\epsilon = 25$), and propylene carbonate ($\epsilon = 64$). Among them ACN and DCM are used as mixtures frequently. Also, the presence of water in the organic solvent is favorable in some cases such as in the polymerization of pyrrole, on contrast, sometimes unfavorable for instance during the polymerization of polythiophene [49].

Working range, i.e. potential window, of the solvent is another parameter to be considered during the selection of the solvent. Potential ranges of some commonly used solvents are given in **Table 1.2**, actually these ranges depend also on the reference electrode, working electrode and supporting electrolyte used; in this table SCE, Pt, and tetra-n-butyl ammonium perchlorate are used, respectively [49]. Moreover, purity of the solvent and dryness affect the redox window of the solvent. In order to eliminate undesirable reactions in the working range of solvent further purification methods, such as distillation on CaH_2 , are carried out.

Table 1.2. Working range of some commonly known solvents [49].

Solvent	Approximate Working Range (V) vs. SCE
Acetonitrile (ACN)	+2.7 to -3.2
N,N-Dimethyl formamide (DMF)	+2.0 to -1.8
Propylene carbonate (PC)	+2.0 to -2.0
Dichloromethane (DCM)	+1.8 to -1.7
Water	+1.1 to -0.8

Before starting electrochemical analysis and/ or electrochemical polymerization a background analysis should be done for monomer free electrolytic solution during which maximum current density should not exceed $1\mu\text{Acm}^{-2}$ in the working range [46].

1.5.1.2. Supporting Electrolyte

In order to coat the polymer film on the surface of the electrode, monomers should come across around 3-8 Å of the working electrode, this range is called as diffusion layer (**Figure 1. 8**). Monomers reach to diffusion layer via mass transfer occurring in three ways: Diffusion, migration and convection due to concentration gradient, potential gradient and stirring, respectively.

Actually, according to Randles-Sevcik Equation (Equation 1-5), during the voltametric analysis and/ or electrochemical polymerization, process should occur by diffusion control. In order to eliminate convection, mixing is avoided. Also, migration can be ruled out via adding supporting electrolyte.

$$i_p = kn^{3/2}AC(VD)^{1/2} \quad \text{(Equation 1-5)}$$

i_p : Peak current

k : Constant

n : Number of electrons transfers (generally 1)

A : Electrode area in cm^2

C : Concentration in mol/ mL

V : Scan rate in V/ s

D : Diffusion coefficient in cm^2/s

Supporting electrolytes are not only used for the elimination of migration, but also has a work as counter ion during the doping processes. Tetrabutylammonium hexafluorophosphate (TBAH), tetrabutylammonium tetrafluoroborate (TBABF₄),

lithium perchlorate (LiClO_4), potassium chloride (KCl), and potassium nitrate (KNO_3) are commonly used electrolytes.

It is observed that the type of the counter ion, e.g. size of the ion, affects the growth rate of the polymer film on the electrode surface. It also affects the morphology of the polymer formed; that is, it is experimentally proven that BF_4^- or ClO_4^- containing polyanilines have more compact structure than Cl^- or NO_3^- containing ones [59].

1.5.2. Chemical Polymerization

Chemical polymerization can be achieved via oxidative polymerization or transition-metal mediated polymerization. For the second one, myriad of mechanism can be considered such as Still Cross-Coupling, Suzuki Cross-Coupling, Yamamoto Cross-Coupling, Kumada Cross-Coupling, Rieke Cross-Coupling, McCullough Cross-Coupling and Grignard Metathesis. Each of them has some advantages, for instance, by Still Cross-Coupling reaction highly low band gap, e.g. 0.7 eV, conjugated polymers could be obtained, and Suzuki Cross-Coupling method generally used for synthesis of water soluble polymers and polyelectrolytes [52].

Mechanism of the oxidative chemical polymerization is almost the same as that of electrochemical one. In both of them, polymerization starts by the formation of radical cations, just the initiators are different: chemical oxidant or voltage. Actually, electrochemical polymerization is the more controllable one.

Iron (III) chloride (FeCl_3) [57], ammonium persulfate ($(\text{NH}_4)_2\text{S}_2\text{O}_8$) [60, 61] and antimony pentafluoride (SbF_5) [52] are the examples of common oxidants used in chemical polymerization. Among them $(\text{NH}_4)_2\text{S}_2\text{O}_8$ is water soluble oxidant, so it can be amenable for monomers which are soluble in water.

1.6. Aim of This Study

As mentioned before, design of the monomer is a viable route for adjusting the properties of a polymer. In this study, the main goal is to design and synthesize novel soluble polymers having various colors of color palette and amenable in electrochromic device applications. In designing the monomers, the factors affecting the properties of the polymers were also considered. For this purpose, each part of the monomers is chosen properly for each desirable properties and the effect of each part is investigated separately. Thus, this study is based on the investigation of the effect of three major parts:

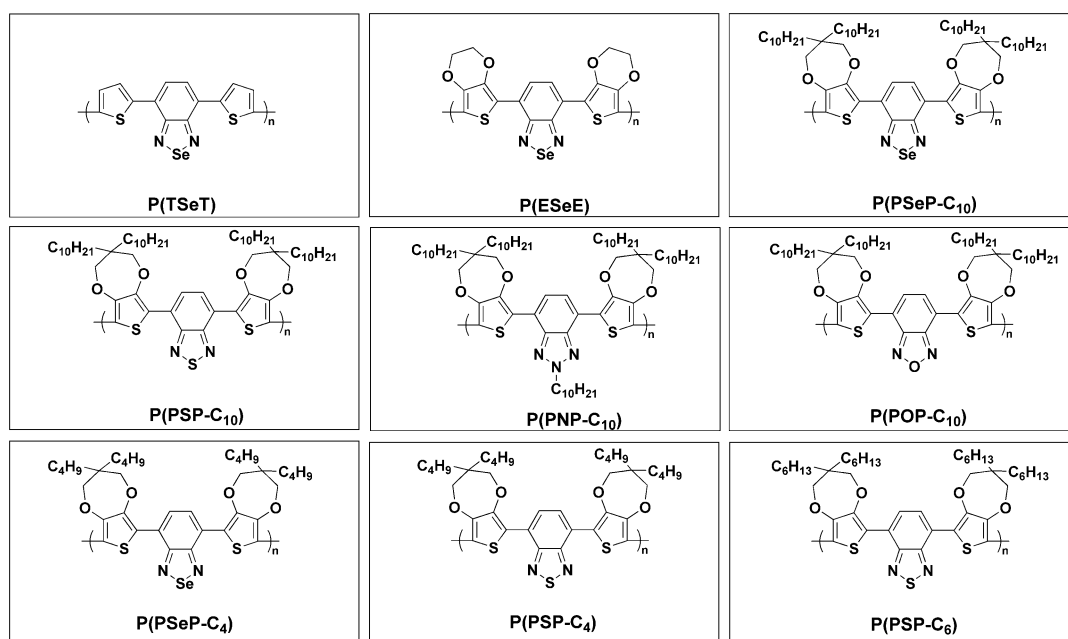
Effect of donor groups: Three donor groups are used for this aim; thiophene, 3,4-ethylenedioxythiophene and dialkyl substituted 3,4-propylenedioxythiophene.

Effect of acceptor groups: For this purpose, four different acceptor units are examined; benzo[c][1,2,5]oxadiazole, benzo[c][1,2,5]thiadiazole, benzo[c][1,2,5]selenadiazole, and 2-decyl-2H-benzo[d][1,2,3]triazole.

Effect of alkyl chain length: Effect of decyl, hexyl, and butyl groups on monomers and polymers properties is monitored.

For this aim nine D-A-D type monomers, **TSeT** (4,7-di(thiophen-2-yl)benzo[c][1,2,5]selenadiazole), **ESeE** (4-(2,3-dihydrothieno[3,4-b][1,4]dioxin-5-yl)-7-(2,3-dihydrothieno[3,4-b][1,4]dioxin-7-yl)benzo[c][1,2,5]selenadiazole), **PSeP-C₁₀** (4-(3,3-didecyl-3,4-dihydro-2H-thieno[3,4-b][1,4]dioxepin-6-yl)-7-(3,3-didecyl-3,4-dihydro-2H-thieno[3,4-b][1,4]dioxepin-8-yl)benzo[c][1,2,5]selenadiazole), **PSP-C₁₀** (4-(3,3-didecyl-3,4-dihydro-2H-thieno[3,4-b][1,4]dioxepin-6-yl)-7-(3,3-didecyl-3,4-dihydro-2H-thieno[3,4-b][1,4]dioxepin-8-yl)benzo[c][1,2,5]thiadiazole), **PNP-C₁₀** (2-decyl-4-(3,3-didecyl-3,4-dihydro-2H-thieno[3,4-b][1,4]dioxepin-6-yl)-7-(3,3-didecyl-3,4-dihydro-2H-thieno[3,4-b][1,4]dioxepin-8-yl)-2H-benzo[d][1,2,3]triazole), **POP-C₁₀** (4-(3,3-

didecyl-3,4-dihydro-2H-thieno[3,4-b][1,4]dioxepin-6-yl)-7-(3,3-didecyl-3,4-dihydro-2H-thieno[3,4-b][1,4]dioxepin-8-yl)benzo[c][1,2,5]oxadiazole), **PSeP-C₄** (4-(3,3-dibutyl-3,4-dihydro-2H-thieno[3,4-b][1,4]dioxepin-6-yl)-7-(3,3-dibutyl-3,4-dihydro-2H-thieno[3,4-b][1,4]dioxepin-8-yl)benzo[c][1,2,5]selenadiazole), **PSP-C₄** (4-(3,3-dibutyl-3,4-dihydro-2H-thieno[3,4-b][1,4]dioxepin-6-yl)-7-(3,3-dibutyl-3,4-dihydro-2H-thieno[3,4-b][1,4]dioxepin-8-yl)benzo[c][1,2,5]thiadiazole) and **PSP-C₆** (4-(3,3-dihexyl-3,4-dihydro-2H-thieno[3,4-b][1,4]dioxepin-6-yl)-7-(3,3-dihexyl-3,4-dihydro-2H-thieno[3,4-b][1,4]dioxepin-8-yl)benzo[c][1,2,5]thiadiazole), and their corresponding polymers, **P(TSeT)** (poly(4,7-di(thiophen-2-yl)benzo[c][1,2,5]selenadiazole)), **P(ESeE)** (poly(4-(2,3-dihydrothieno[3,4-b][1,4]dioxin-5-yl)-7-(2,3-dihydrothieno[3,4-b][1,4]dioxin-7-yl)benzo[c][1,2,5]selenadiazole)), **P(PSeP-C₁₀)** (poly(4-(3,3-didecyl-3,4-dihydro-2H-thieno[3,4-b][1,4]dioxepin-6-yl)-7-(3,3-didecyl-3,4-dihydro-2H-thieno[3,4-b][1,4]dioxepin-8-yl)benzo[c][1,2,5]selenadiazole)), **P(PSP-C₁₀)** (poly(4-(3,3-didecyl-3,4-dihydro-2H-thieno[3,4-b][1,4]dioxepin-6-yl)-7-(3,3-didecyl-3,4-dihydro-2H-thieno[3,4-b][1,4]dioxepin-8-yl)benzo[c][1,2,5]thiadiazole)), **P(PNP-C₁₀)** (poly((2-decyl-4-(3,3-didecyl-3,4-dihydro-2H-thieno[3,4-b][1,4]dioxepin-6-yl)-7-(3,3-didecyl-3,4-dihydro-2H-thieno[3,4-b][1,4]dioxepin-8-yl)-2H-benzo[d][1,2,3]triazole)), **P(POP-C₁₀)** (poly(4-(3,3-didecyl-3,4-dihydro-2H-thieno[3,4-b][1,4]dioxepin-6-yl)-7-(3,3-didecyl-3,4-dihydro-2H-thieno[3,4-b][1,4]dioxepin-8-yl)benzo[c][1,2,5]oxadiazole)), **P(PSeP-C₄)** (poly(4-(3,3-dibutyl-3,4-dihydro-2H-thieno[3,4-b][1,4]dioxepin-6-yl)-7-(3,3-dibutyl-3,4-dihydro-2H-thieno[3,4-b][1,4]dioxepin-8-yl)benzo[c][1,2,5]selenadiazole)), **P(PSP-C₄)** (poly(4-(3,3-dibutyl-3,4-dihydro-2H-thieno[3,4-b][1,4]dioxepin-6-yl)-7-(3,3-dibutyl-3,4-dihydro-2H-thieno[3,4-b][1,4]dioxepin-8-yl)benzo[c][1,2,5]thiadiazole)) and **P(PSP-C₆)** (poly((4-(3,3-dihexyl-3,4-dihydro-2H-thieno[3,4-b][1,4]dioxepin-6-yl)-7-(3,3-dihexyl-3,4-dihydro-2H-thieno[3,4-b][1,4]dioxepin-8-yl)benzo[c][1,2,5]thiadiazole)) (**Scheme 1.2**), based on thiophene, 3,4-ethylenedioxythiophene (EDOT), and 3,3-dialkyl-3,4-dihydro-2H-thieno[3,4-b]-[1,4]dioxepine (ProDOT-C_n) [62] as D units and 2,1,3-benzoselenadiazole, 2,1,3-benzothiadiazole, 2-decyl-2H-benzo[d][1,2,3]triazole, and 2,1,3-oxadiazole as A units are synthesized.



Scheme 1.2. D-A-D groups containing polymers, **P(TSeT)**, **P(ESeE)**, **P(PSeP-C₁₀)**, **P(PSP-C₁₀)**, **P(PNP-C₁₀)**, **P(POP-C₁₀)**, **P(PSeP-C₄)**, **P(PSP-C₄)** and **P(PSP-C₆)**.

CHAPTER 2

EXPERIMENTAL

2.1. Materials

2.1.1. Monomer Synthesis

Tetrahydrofuran (THF) (J.T. Beaker) was refluxed with potassium and benzophenone up to the observation of the blue color and continued to reflux approximately 1 hour before distillation by simple distillation method. Ethanol and methanol were also refluxed with magnesium and iodine, and procedure was carried out as described in the Vogel's Text Book of Practical Organic Chemistry [63]. Toluene was refluxed with CaH_2 during 1 hour and then distilled over it. Hexane and ethyl acetate were distilled via simple distillation method.

Na metal, diethylmalonate (Aldrich, 99 %), 1-bromodecane (Aldrich, 98 %), 3,4-dimethoxythiophene (Aldrich, 97 %), LiAlH_4 (Acros, 95 %), *para*-toluenesulfonic acid monohydrate (PTSA) (Aldrich, 98%), *n*-butyllithium (*n*-BuLi) (Acros, 2.5 M in hexane), tributyltinchloride ($\text{Sn}(\text{Bu})_3\text{Cl}$) (Fluka, ≥ 95 %), dichlorobis(triphenylphosphine)palladium (II) ($\text{Pd}(\text{PPh}_3)_2\text{Cl}_2$) (Aldrich, ≥ 99 %), benzo[*c*][1,2,5]oxadiazole (Aldrich), 2,1,3-benzothiadiazole, 1,2,3-benzotriazole (Acros), Bromine (Br_2) (Acros, 99+ %), HBr, potassium-*tert*-butoxide (KO*Bu-t*), chloroform (Merck), dichloromethane (Merck), sulfuric acid (H_2SO_4) (Merck), silver sulfate (AgSO_4), anhydrous magnesium sulfate (MgSO_4) (Sigma-Aldrich, ≥ 97 %) were used without further purification methods.

For the purification of some compounds, thin layer chromatography (TLC) and column chromatography techniques were used. For this aim TLC aluminum sheets (Merck, 20x20, Silica gel 60 F₂₅₄) and silica gel (SiO₂) (Acros, 0.060-0.200 mm, 60 A) were used.

2.1.2. Polymer Synthesis and Analysis

For electrochemical synthesis and analysis, tetrabutylammonium hexafluorophosphate (TBAH) (Fluka, ≥98 %), the supporting electrolyte, was used without further purification. Acetonitrile (ACN) (Merck) and dichloromethane (DCM) (Merck) were refluxed on CaH₂ (Acros, ≥99 %) during one hour and then distilled over it via simple distillation method.

Polished platinum button electrode (electrode area: 0.02 cm²) and platinum wire were used as WE and CE, respectively. As well as a silver wire was used as a pseudoreference electrode (calibrated externally using 10 mM solution of ferrocene/ferrocenium couple) or Ag/AgCl in 1.0 M NaCl reference electrode. In endeavors to carry out SPEL analysis, indium tin oxide coated quartz glass slide (ITO, Delta Tech. 8-12 Ω, 0.7 cm - 5 cm) was used as WE as well as a platinum wire as CE and Ag wire as a pseudo-reference electrode.

For chemical synthesis, anhydrous iron (III) chloride (FeCl₃) (99 %, Avocado), nitromethane (Across, 99 %), chloroform (Sigma-Aldrich), methanol (J. T. Beaker) and hydrazinium hydroxide (N₂H₅OH) (Merck, about 80 %) were used without further purification.

For the application of the electrochromic devices from the polymers, gel electrolyte was prepared. For this aim 3: 70: 7: 20 (weight percentage) TBAH/ ACN/ PMMA (Polymethylmetacrylate)/ PC (Propylene Carbonate) were used. After PMMA was added in PC, TBAH dissolved in ACN was added to this mixture. This mixture was

heated by a heater to 70⁰C via mixing sometimes. This heating procedure was continued until all ACN was evaporated. This can be understood by observing a gel (a viscous transparent compound) after the mixture was cooled.

2.2. Instrumentation

Electroanalytical measurements were performed using a Gamry PCI4/300 potentiostat-galvanostat. The electro-optical spectra were monitored on a Hewlett-Packard 8453A diode array spectrometer. FTIR spectra were recorded on Nicolet 510 FT-IR with attenuated total reflectance. Photographs of the polymer films were taken by using Canon (PowerShot A75), (PowerShot SD780 IS) and Fujifilm (Finepix F80 EXR) digital cameras. Mass spectra were acquired on a Voyager-DE PRO MALDI-TOF mass spectrometer (Applied Biosystems, USA) equipped with a nitrogen UV-laser operating at 337 nm. Combustion analysis was performed using a LECO CHNS-932 analyzer. Spectra were recorded in linear modes with average of 100 shots. ¹H and ¹³C NMR analysis were done via Bruker Spectrospin Avance DPX-400 Spectrometer at 400 MHz and chemical shifts were given relative to tetramethylsilane as the internal standard. High resolution mass spectrometry analysis of the monomer was done via Water, Synapt HRMS instrument. GPC analysis of the polymer was carried out with Polymer Laboratories PL-GPC 220 instrument. Calorimetric measurements were recorded on Specord S 600 (standart illuminator D65, field of with 10⁰ observer), color space were given by (CIE) Luminance (L), hue (a) and intensity (b). Platinum cobalt DIN ISO 621, iodine DIN EN 1557 and Gardner DIN ISO 6430 are the references of calorimetric measurements. ESR measurements were performed at room temperature with a Bruker ELEX E580 spectrometer.

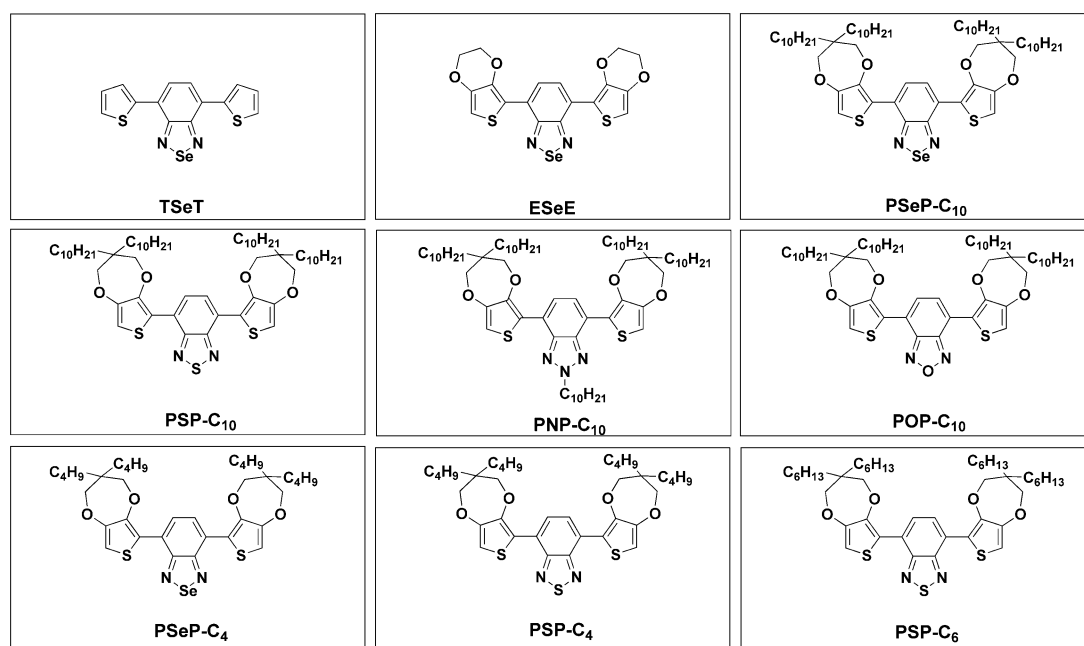
2.3. Synthesis

2.3.1. Monomer Synthesis

Herein nine monomers (**Scheme 2. 1**) and their corresponding polymers were discussed.

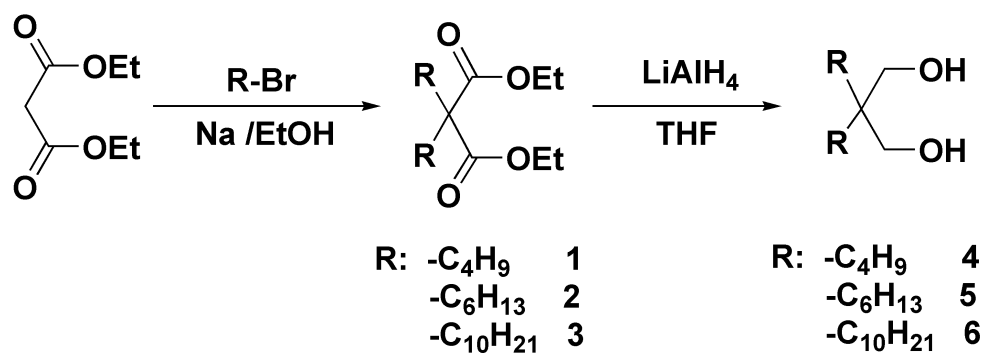
Synthesis of the monomers contains four major parts:

- Synthesis of the “hat” parts: *2,2-Didecylpropane-1,3-diol*; *2,2-Hexylpropane-1,3-diol* and *2,2-Butylpropane-1,3-diol*.
- Synthesis of the donor units: *3,3-Didecyl-3,4-dihydro-2H-thieno[3,4-b][1,4]dioxepine*; *3,3-Dihexyl-3,4-dihydro-2H-thieno[3,4-b][1,4]dioxepine* and *3,3-Dibutyl-3,4-dihydro-2H-thieno[3,4-b][1,4]dioxepine*.
- Synthesis of the acceptor units: *4,7-Dibromo-2,1,3-benzoselenadiazole*; *4,7-Dibromo-2,1,3-benzothiadiazole*; *4,7-Dibromo-2-decyl-2H-benzo[d][1,2,3]triazole* and *4,7-Dibromo-2,1,3-benzooxadiazole*.
- Integrating donor and acceptor parts.



Scheme 2.1. Structure of monomers, TSeT, ESeE, PSeP-C₁₀, PSP-C₁₀, PNP-C₁₀, POP-C₁₀, PSeP-C₄, PSP-C₄ and PSP-C₆.

2.3.1.1. Synthesis of the “Hat” Parts



Scheme 2.2. Synthesis of the “hat” part.

2.3.1.1.1. Synthesis of Diethyl 2,2-dialkylmalonate (1-3)

In a two-necked 250 mL round flask 216 mmol sodium and 120 mL ethyl alcohol were added. The mixture was stirred via a magnetic stirrer, until all sodium added was dissolved. After 66.7 mmol diethylmalonate were added to the solution, the reaction mixture heated to reflux. When the solution starts to reflux, 243.3 mmol 1-bromoalkane (-alkane: -butane, -hexane and -decane) were added with 30 mL ethyl alcohol to the reaction mixture (**Scheme 2. 2**). After refluxing the mixture for 6 days, the flask was cooled to room temperature, poured into cold water, and extracted with cold ether. The solvent was removed under vacuum. The obtained crude product was used for the next step without further purification [62]. ~95 % yield, transparent yellowish oily compounds.

1: ^1H NMR (400 MHz, CDCl_3 , δ , ppm): 4.12 (q, 4H); 1.8 (t, 4H, $J= 5.2$ Hz); 1.51-1.06 (br, 8H); 0.82 (t, 6H, $J= 7.4$ Hz); ^{13}C NMR (100 MHz, CDCl_3 , δ , ppm): 170.251; 59.106; 55.719; 50.293; 30.093; 24.367; 21.187; 12.320; 12.069.

2: ^1H NMR (400 MHz, CDCl_3 , δ , ppm): 4.18 (q, 4H); 1.89 (m, 4H); 1.41-1.00 (m, 16H); 0.88 (t, 6H, $J= 7.3$ Hz); ^{13}C NMR (100 MHz, CDCl_3 , δ , ppm): 171.68; 77.445; 77.125; 76.805; 60.899; 60.589; 57.337; 51.845; 31.382; 29.376; 22.384; 13.893.

3: ^1H NMR (400 MHz, CDCl_3 , δ , ppm): 4.11 (q, 4H); 1.79 (t, 4H, $J= 5.3$ Hz); 1.51-1.06 (br, 38H); 0.81 (t, 6H, $J= 7.2$ Hz); ^{13}C NMR (100 MHz, CDCl_3 , δ , ppm): 172.06; 126.12; 60.89; 57.54; 32.08; 31.90; 29.84; 29.61; 29.58; 29.54; 29.33; 26.22; 15.25; 14.11.

2.3.1.1.2. 2,2-Didecylpropane-1,3-diol (4-6)

In a two-necked 250 mL round flask 50 mmol LiAlH_4 and 100 mL THF were added under inert N_2 atmosphere (reaction system used in the synthesis is shown in **Figure**

2.1). After the dropwise addition of 28 mmol diethyl 2,2-dialkylmalonate (-alkyl: -butyl, -hexyl, -decyl), the reaction mixture was refluxed for 18 hours (**Scheme 2. 2**). The reaction mixture was cooled to room temperature, and 0.1 M aq. H₂SO₄ solution was added dropwise until the mixture color was turned from gray to white. Then, the obtained bulk was added to water, and extracted with diethyl ether. After solvent was removed under vacuum, the obtained product was used without further purification [62]. ~98 % yield, transparent pale yellow oily compounds.

4: ¹H NMR (400 MHz, CDCl₃, δ, ppm): 3.63 (s, 4H); 2.14 (s, br, 2H); 1.43-1.00 (m, 8H); 0.89 (t, 6H, *J* = 7.2 Hz); FTIR (ATR, cm⁻¹): 3338 (br); 2926; 2856; 1463; 1370; 1019; 890; 740.

5: ¹H NMR (400 MHz, CDCl₃, δ, ppm): 3.60 (s, 4H); 2.12 (s, br, 2H); 1.41-1.00 (m, 16H); 0.88 (t, 6H, *J* = 7.3 Hz); FTIR (ATR, cm⁻¹): 3347 (br); 2924; 2850; 1457; 1376; 1025; 898; 714.

6: ¹H NMR (400 MHz, CDCl₃, δ, ppm): 3.55 (s, 4H); 2.7 (br, 2H); 1.3 (br, 36H); 0.9 (t, 6H, *J* = 7.4 Hz); ¹³C NMR (100 MHz, CDCl₃, δ, ppm): 70.80; 69.46; 67.95; 66.03; 40.96; 31.91; 30.81; 30.60; 29.89; 29.80; 29.67; 29.63; 29.60; 29.56; 29.51; 29.34; 29.31; 27.24; 26.20; 25.59; 22.86; 22.67; 15.20; 14.08; FTIR (ATR, cm⁻¹): 3493 (br); 2926; 2844; 1457; 1375; 1118; 1041; 714.

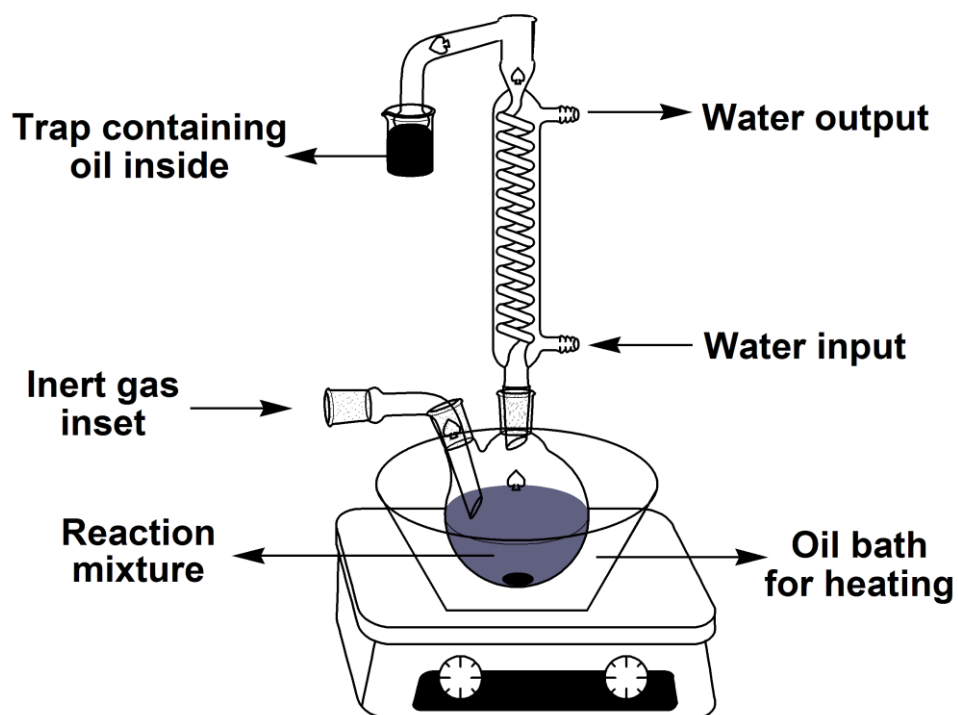
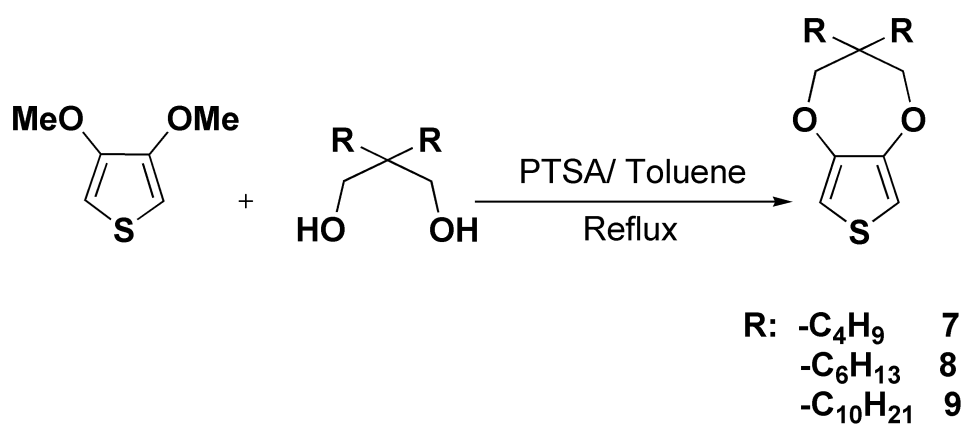


Figure 2.1. Reaction system for the experiments done under inert atmosphere.

2.3.1.2. Synthesis of the Donor Units



Scheme 2.3. Synthesis of the donor groups.

2.3.1.2.1. 3,3-Dialkyl-3,4-dihydro-2H-thieno[3,4-b][1,4]dioxepine (7-9)

6.9 mmol 3,4-dimethoxythiophene, 13.8 mmol 2,2-dialkylpropane-1,3-diol and 0.69 mmol p-toluenesulfonic acid monohydrate were dissolved (**Scheme 2. 3**) in the two-necked round flask as shown in **Figure 2.1**. After the reaction mixture was refluxed during 3 days under N₂ inert atmosphere, it was cooled to room temperature and washed with water. The crude mixture was chromatographed on silica gel by eluting with DCM: hexane (1:4, v/v) to give product as a yellow viscous liquid in 46 % yield.

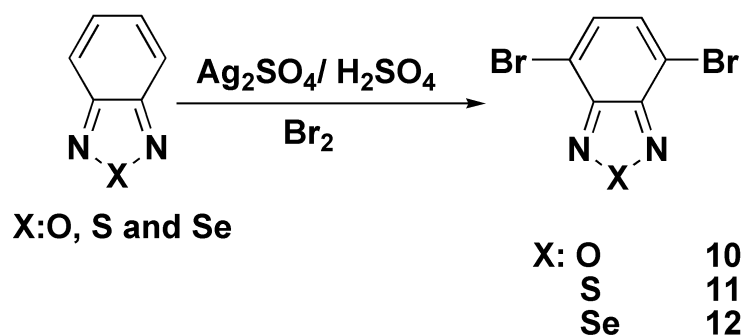
7: ¹H NMR (400 MHz, CDCl₃, δ, ppm): 6.40 (s, 2H, ArH); 3.85 (s, 4H); 1.38-1.26 (m, 12H); 0.90 (t, 6H, *J*= 6.83 Hz); ¹³C NMR (100 MHz, CDCl₃, δ, ppm): 149.74; 104.64; 43.67; 31.94; 29.67; 25.04; 14.11; FTIR (ATR, cm⁻¹): 2930; 2860; 1480; 1455; 1276; 1180; 1030; 852; 730.

8: ¹H NMR (400 MHz, CDCl₃, δ, ppm): 6.41 (s, 2H, ArH), 3.83 (s, 4H); 1.31-1.28 (m, 20H); 0.91 (t, 6H, *J*= 6.82 Hz); ¹³C NMR (100 MHz, CDCl₃, δ, ppm): 149.74; 104.63; 43.75; 31.89; 31.73; 30.14; 22.78; 22.64; 14.05; FTIR (ATR, cm⁻¹): 2926; 2850; 1480; 1452; 1376; 1182; 1124; 1025; 855; 767.

9: ¹H NMR (400 MHz, CDCl₃, δ, ppm): 6.35 (s, 2H); 3.76 (s, 4H); 1.23 (br, 36H); 0.7 (t, 6H, *J*= 6.83 Hz); ¹³C NMR (100 MHz, CDCl₃, δ, ppm): 149.75; 104.62; 77.32; 43.75; 31.90; 30.48; 29.63; 29.61; 29.53; 20.33; 22.81; 22.68; 14.10; FTIR (ATR, cm⁻¹): 2921; 2844; 1480; 1372; 1183; 1027; 848; 758; 719.

2.3.1.3. Synthesis of the Acceptor Units

2.3.1.3.1. 4,7-dibromobenzo[c][1,2,5]oxadiazole, 4,7-dibromobenzo[c][1,2,5]thiadiazole and 4,7-dibromobenzo[c][1,2,5]selenadiazole (10-12)



Scheme 2 4. Synthesis of the acceptor groups.

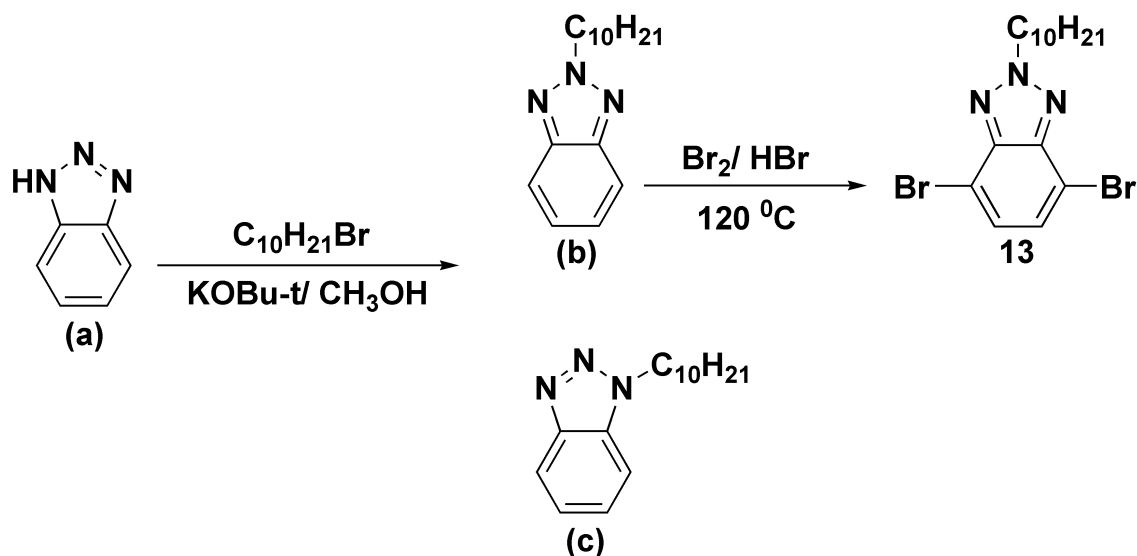
The mixture of 73.4 mmol 2,1,3-benzooxadiazole, 2,1,3-benzothiadiazole or 2,1,3-benzoselenadiazole with 73.4 mmol Ag_2SO_4 were prepared in 10 mL concentrated H_2SO_4 . 14.68 mmol Br_2 was added dropwise to this mixture and the mixture was mixed during 100 min. at room temperature (**Scheme 2. 4**). After removing the precipitated silver bromide, water-ice mixture was added to the reaction vessel. After the obtained product recrystallized in 250 mL ethyl acetate, the pure product is obtained [64,65].

10: ^1H NMR (400 MHz, CDCl_3 , δ , ppm): 7.5 (s, 2H); ^{13}C NMR (100 MHz, CDCl_3 , δ): 133.7; 106.6; 96.1. White solid.

11: ^1H NMR (400 MHz, CDCl_3 , δ , ppm): 7.75 (s, 2H); ^{13}C NMR (100 MHz, CDCl_3 , δ): 153.0; 132.4; 114. Yellow solid.

12: ^1H NMR (400 MHz, CDCl_3 , δ , ppm): 7.6 (s, 2H); ^{13}C NMR (100 MHz, CDCl_3 , δ): 149.5; 132.2; 103.5. Dark purplish-red solid.

2.3.1.3.2. 4,7-dibromo-2-decyl-2H-benzo[d][1,2,3]triazole (13)



Scheme 2.5. Synthesis of 4,7-dibromo-2-decyl-2H-benzo[d][1,2,3]triazole.

To a methanol solution of 1,2,3-benzotriazole (a) (4.0 g, 33.6 mmol), potassium *tert*-butoxide (5.6 g, 50.4 mmol) and 1-bromodecane (8.88 g, 50.4 mmol) was added, and the mixture was stirred under reflux for 12 h. After removal of the solvent by evaporation, the residue was diluted with water (200 mL) and extracted with CHCl_3 (3x100 mL). After evaporation of the solvent, the crude mixture was chromatographed on silica gel eluting with hexane- CHCl_3 (1:1, v/v) to give **b** (first fraction) and **c** (second fraction) (**Scheme 2.5**) as colorless oil in 1:1 ratio and a total yield of 90%.

2-decyl-2H-benzo[d][1,2,3]triazole (b): ^1H NMR (400 MHz, CDCl_3 , δ): 7.90-7.86 (m, 2H); 7.42-7.38 (m, 2H); 4.74 (t, $J=7.2$ Hz, 2H); 2.15-2.10 (m, 2H); 1.36-1.26 (m,

14H); 0.88 (t, J=7.1 Hz, 3H); ¹³C NMR (100 MHz, CDCl₃, δ): 144.2; 126.1; 117.9; 56.6; 31.9; 31.8; 30.0; 29.6; 29.4; 26.5; 26.1; 22.6; 14.1. Calcd for C₁₆H₂₅N₃: C 74.09; H 9.71; N 16.20; found: C 74.98; H 9.86; N 16.05.

1-decyl-1H-benzo[d][1,2,3]triazole (c): ¹H NMR (400 MHz, CDCl₃, δ): 8.07 (d, J=8.4 Hz, 1H); 7.55-7.47 (m, 2H); 7.39-7.35 (m, 1H); 4.64 (t, J=7.2 Hz, 2H); 2.05-1.98 (m, 2H); 1.42-1.24 (m, 14H); 0.88 (t, J=7.0 Hz, 3H); ¹³C NMR (100 MHz, CDCl₃, δ): 146.0; 132.9; 127.1; 123.7; 120.0; 109.3; 48.2; 31.8; 29.6; 29.4; 29.3; 29.2; 29.0; 26.7; 22.6; 14.0; Anal. Calcd for C₁₆H₂₅N₃: C 74.09; H 9.71; N 16.20; found: C 74.98; H 9.86; N 16.05.

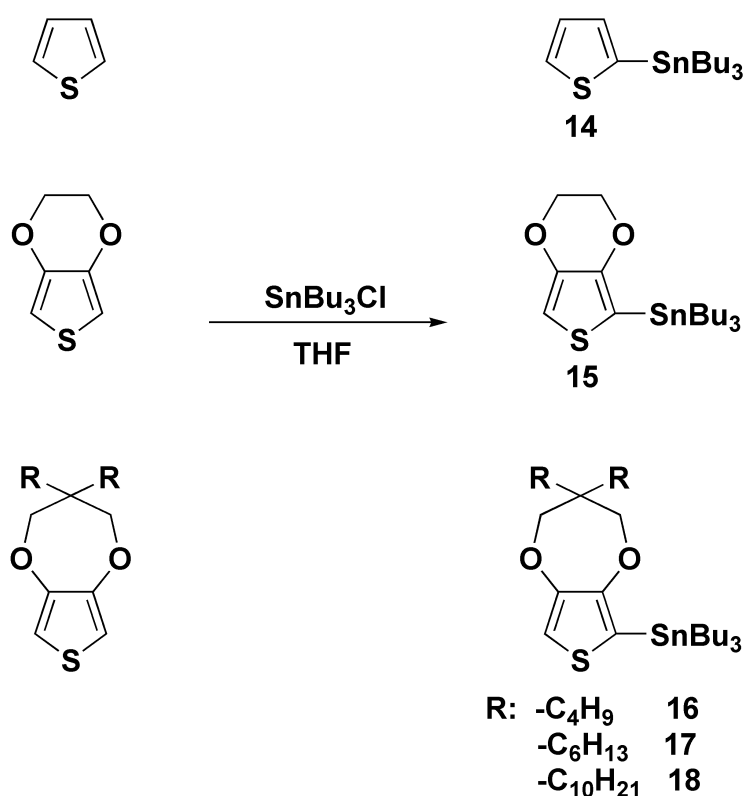
b (1.29 g, 5 mmol) and an aqueous HBr solution (5.8 M, 10 mL) were added to a flask, and the mixture was stirred for 1 h at 100 °C. Bromine (2.0 g, 12.5 mmol) was added, and the mixture was stirred for 12 h at 135 °C (**Scheme 2. 5**). After the mixture was cooled to room temperature, an aqueous solution of NaHCO₃ was added and the product was extracted with CHCl₃. The solvent was removed by evaporation, and the product was purified by column chromatography on a silica gel column by eluting with CH₂Cl₂ to afford **13** as yellow oil. Yield: 76%. ¹H NMR (400 MHz, CDCl₃, δ): 7.36 (s, 2H); 4.70 (t, J=7.5 Hz, 2H); 2.11-2.03 (m, 2H); 1.34-1.17 (m, 14H); 0.85 (t, J=6.9 Hz, 3H); ¹³C NMR (100 MHz, CDCl₃, δ): 147.4; 130.8; 110.8; 48.7; 32.1; 29.9; 29.7; 29.6; 29.4; 29.3; 26.9; 22.9; 14.3; FTIR (ATR, cm⁻¹): 2925; 2855; 1495; 1463; 1306; 1193; 1112; 949; 815; 720; 654; Anal. Calcd for C₁₆H₂₃N₃Br₂: C 46.06; H 5.56; N 10.07; found: C 46.01; H 5.59; N 10.04.

2.3.1.4. Integrating Donor and Acceptor Parts

To integrate donor and acceptor parts, that is, to synthesize the monomers, Stille coupling reaction was used. In this reaction, *trans*-dichloro-*bis*-triphenylphosphinepalladium (II) (Pd(PPh₃)₂Cl₂) was used as a catalyst to integrate

bromide containing acceptor units and stannylated donor units. For this aim, first of all, donor groups were stannylated according to literature [65].

2.3.1.4.1. Stannylating of Donor Parts



Scheme 2.6. Stannylating of thiophene, EDOT, and ProDOT-C_n molecules.

3.42 mmol thiophene; 3,4-ethylenedioxythiophene or 3,3-dialkyl-3,4-dihydro-2H-thieno[3,4-b][1,4]dioxepene was dissolved in 40 mL freshly distilled THF and system was purged with N₂ gas. After decreasing the reaction temperature to -78 °C, 3.59 mmol 2.5 M n-BuLi (in hexane) was added to the reaction solution dropwise and it was mixed during 30 min. at -78 °C. After this process, the reaction vessel was removed from low temperature bath, and it was further mixed at room

temperature for one hour, then temperature was decreased again to $-78\text{ }^{\circ}\text{C}$. At this low temperature, 3.42 mmol tributyltinchloride in 10 mL THF was added to the reaction mixture and mixed for an hour. Then, the solution was further mixed overnight at room temperature. In order to inactivate unreacted n-BuLi, small amount of water was added dropwise which is followed by concentrating the solution to 5 mL by evaporating THF under reduced pressure. 20 mL water was then added to the reaction mixture and extracted with DCM (**Scheme 2. 6**). The organic phase was dried over MgSO_4 and the solvent was removed under vacuum to yield dark yellow oily product (Yield= ~65 %).

16: ^1H NMR (400 MHz, CDCl_3 , δ , ppm): 6.59 (s, 2H); 3.78 (s,4H); 1.28 (br, 26H); 0.84 (t, 15H, $J= 6.83$ Hz).

17: ^1H NMR (400 MHz, CDCl_3 , δ , ppm): 6.66 (s, 2H); 3.84 (s,4H); 1.28 (br, 38H); 0.89 (t, 15H, $J= 6.82$ Hz).

18: ^1H NMR (400 MHz, CDCl_3 , δ , ppm): 6.65 (s, 2H); 3.85 (s,4H); 1.23 (br, 54H); 0.7 (t, 15H, $J= 6.82$ Hz).

2.3.1.4.1. Synthesis of TSeT, ESeE, PSeP-C₁₀, PSP-C₁₀, PNP-C₁₀, POP-C₁₀, PSeP-C₄, PSP-C₄ and PSP-C₆

To an argon degassed solution of **14/ 15/ 16/ 17** or **18** (0.334 mmol) and **10/ 11/ 12/ 13** or **14** (0.134 mmol) in dry toluene (15 mL), 18.8 mg $\text{Pd}(\text{PPh}_3)_2\text{Cl}_2$ (0.0268 mmol) was added and the mixture was heated under reflux overnight. After cooling to room temperature, the solvent was removed under reduced pressure. The crude mixture was chromatographed on silica gel by eluting with methanol: chloroform (4:1, v/v) to give monomers: **TSeT, ESeE, PSeP-C₁₀, PSP-C₁₀, PNP-C₁₀, POP-C₁₀, PSeP-C₄, PSP-C₄ and PSP-C₆**.

ESeE: Dark yellow solid. Yield: 65 %, mp>350 °C.

¹H NMR (400 MHz, DMSO-d₆, δ, ppm): 8.30 (s, 2H); 6.83 (s, 2H); 4.43 (t, J=2.68 Hz, 4H); 4.31 (t, J= 2.78 Hz, 4H); ¹³C NMR (100 MHz, CDCl₃, δ, ppm): 157.27; 141.86; 140.99; 126.12; 125.00; 113.26; 103.32; 65.51; 64.48, IR (KBr, cm⁻¹): 3097; 2928; 2873; 1476; 1450; 1370; 1167; 1056; 1005; 913; 839; 762; 618.

PSeP-C₁₀: Red, very viscous product. Yield: 35 %.

¹H NMR (400 MHz, CDCl₃, δ, ppm): 8.11 (s, 2H, Ar H); 6.57 (s, 2H, Ar); 3.96 (s, 4H); 3.87 (s, 4H); 1.40-1.35 (m, 8H); 1.30-1.20 (m, 64H); 0.83-0.77 (m, 12H); ¹³C NMR (100 MHz, CDCl₃, δ, ppm): 157.08; 148.45; 146.68; 127.01; 124.44; 116.50; 105.20; 78.08; 77.92; 42.48; 30.73; 30.60; 29.20; 28.34; 28.24; 28.03; 25.62; 21.57; 12.79; FTIR (ATR, cm⁻¹): 3115; 2920; 2853; 1478; 1377; 1259; 1168; 1028; 798; Anal. Calcd for C₆₀H₉₆N₂O₄S₂Se: C 68.47; H 9.19; N 2.66; S 6.09; found: C 68.45; H 9.21; N 2.58; S; 6.01.

PSP-C₁₀: Orange, very viscous product. Yield: 60 %.

¹H NMR (400 MHz, CDCl₃, δ, ppm): 8.20 (s, 2H); 6.56 (s, 2H); 3.96 (s, 4H); 3.87 (s, 4H); 1.56 (t, J= 7.1 Hz, 2H); 1.41-1.33 (m, 8H); 1.29-1.21 (m, 62H); 0.90-0.86 (m, 12H); ¹³C NMR (100 MHz, CDCl₃, δ, ppm): 151.6; 148.7; 146.8; 126.4; 123.2; 116.3; 105.1; 76.69; 76.54; 43.7; 30.9; 30.8; 29.4; 28.5; 28.4; 28.2; 21.7; 21.5; 13.0; FTIR (ATR, cm⁻¹): 2925; 2852; 1502; 1452; 1375; 1167; 1033; 855; 829; 804; 720; 633; Anal. Calcd for C₆₀H₉₆N₂O₄S₃: C 71.66; H 9.62; N 2.79; S 9.57; found: C 71.63; H 9.65; N 2.69; S 9.56.

PNP-C₁₀: Yellow, very viscous product. Yield: 40 %.

¹H NMR (400 MHz, CDCl₃, δ, ppm): 7.94 (s, 2H); 6.49 (s, 2H); 4.69 (t, J=7.2 Hz, 2H); 3.95 (s, 4H); 3.86 (s, 4H); 2.09 (t, J=7.2 Hz, 2H); 1.43-1.37 (m, 8H); 1.31-1.22 (m, 62H); 0.85-0.82 (m, 12H); ¹³C NMR (100 MHz, CDCl₃, δ, ppm): 150.3; 147.5; 142.4; 124.7; 122.0; 118.3; 105.1; 78.05; 77.97; 44.1; 44.0; 32.3; 30.8; 30.2; 29.8; 29.6; 29.5; 29.3; 23.2; 23.1; 14.3; FTIR (ATR, cm⁻¹): 2917; 2851; 1516; 1480; 1451; 1407; 1378; 1255; 1164; 1029; 833; 797; 727; 647; 611. Anal. Calcd for

$C_{70}H_{117}N_3O_4S_2$: C 74.48; H 10.45; N 3.72; S 5.68; found: C 74.44; H 10.47; N 3.69; S 5.66.

POP-C₁₀: 1H NMR (400 MHz, $CDCl_3$, δ , ppm): 7.98 (s, 2H); 6.55 (s, 2H); 3.98 (s, 4H); 3.86 (s, 4H); 1.36–1.2 (m, 62 H); 0.80 (t, $J= 6.82$ Hz, 12H); ^{13}C NMR (100 MHz, $CDCl_3$, δ , ppm): 150.01; 148.35; 147.94; 128.251; 119.96; 116.16; 106.70; 77.65; 77.56; 40.80; 32.05; 31.90; 30.51; 29.66; 29.57; 29.36; 22.88; 22.70; 14.13; FTIR (ATR, cm^{-1}): 2920; 2850; 1509; 1481; 1369; 1182; 1024; 855; 690.

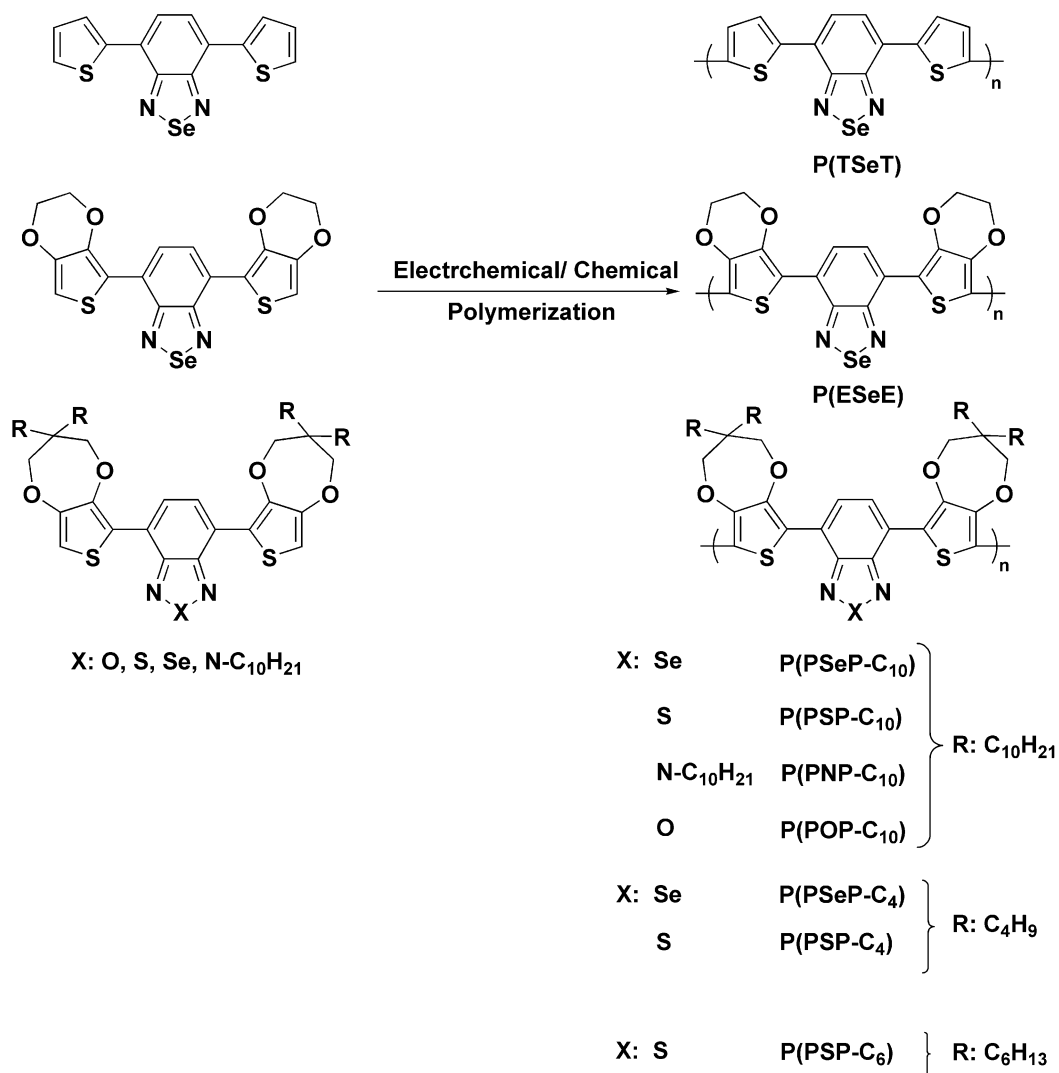
PSeP-C₄: 1H NMR (400 MHz, $CDCl_3$, δ , ppm): 8.12 (s, 2H); 6.57 (s, 2H); 3.97 (s, 4H); 3.93 (s, 4H); 1.38–1.04 (m, 30 H); 0.87 (t, $J= 7.2$ Hz, 6H); ^{13}C NMR (100 MHz, $CDCl_3$, δ , ppm): 158.37; 149.75; 147.97; 129.03; 127.98; 117.81; 106.52; 77.62; 77.76; 41.91; 31.70; 25.10; 23.57; 14.04; FTIR (ATR, cm^{-1}): 3115; 2921; 2853; 1479; 1377; 1259; 1169; 1028; 797.

PSP-C₄: 1H NMR (400 MHz, $CDCl_3$, δ , ppm): 8.28 (s, 2H); 6.63 (s, 2H); 4.03 (s, 4H); 3.94 (s, 4H); 1.35–1.26 (m, 30H); 0.91 (t, $J= 7.07$ Hz, 6H); ^{13}C NMR (100 MHz, $CDCl_3$, δ , ppm): 150.92; 148.08; 146.16; 136.04; 127.23; 122.536; 115.68; 76.76; 76.33; 41.91; 29.97; 25.13; 23.30; 12.25; FTIR (ATR, cm^{-1}): 2918; 2851; 1516; 1480; 1451; 1407; 1378; 1256; 1164; 1029; 833; 797; 727; 647; 612.

PSP-C₆: 1H NMR (400 MHz, $CDCl_3$, δ , ppm): 8.28 (s, 2H); 6.64 (s, 2H); 4.04(s, 4H); 3.95 (s, 4H); 1.31 (m, 40H); 0.91 (m, 12H); ^{13}C NMR (100 MHz, $CDCl_3$, δ , ppm): 152.2; 149.38; 147.46; 127.09; 123.81; 116.93; 105.7; 43.31; 31.27; 29.68; 22.36; 22.18; 13.61; FTIR (ATR, cm^{-1}): 2934; 2856; 1500; 1372; 1174; 1045; 840; 719.

2.3.2. Polymer Synthesis and Analysis

In this study, all polymers were synthesized electrochemically, in the case of soluble ones chemical polymerization was also used to obtain polymers in larger quantities (Scheme 2. 7).



Scheme 2.7. Reaction scheme of polymer synthesis.

2.3.2.1. Electrochemical Synthesis of the Polymers and Their Analysis

Repetitive cycling or constant potential electrolysis was used to obtain the polymer films. Electro-optical properties were investigated by using an ITO as working electrode. In order to equilibrate the redox behavior of the polymer film, that is, to break-in the film, and to obtain reproducible results, the coated polymer films were switched between their neutral and oxidized states several times before electroanalytical and optical studies.

Since monomers **PSeP-C₁₀**, **PSP-C₁₀**, **PNP-C₁₀**, **POP-C₁₀**, **PSeP-C₄**, **PSP-C₄** and **PSP-C₆** (Scheme 2.1) are not soluble in ACN and **P(PSeP-C₁₀)**, **P(PSP-C₁₀)**, **P(PNP-C₁₀)**, **P(POP-C₁₀)**, **P(PSeP-C₄)**, **P(PSP-C₄)** and **P(PSP-C₆)** (Scheme 2.1) are soluble in dichloromethane DCM, solution containing 0.1 M TBAH and 1.5×10^{-3} M monomer prepared in a mixture of DCM and ACN for electrochemical synthesis. As a monomer-free electrolytic solution 0.1 M TBAH was prepared in ACN. For the electrochemical polymerization of **TSeT** and **ESeE**, DCM containing 0.1 M TBAH was used as solvent. **TSeT** and **ESeE** concentrations were 1.0×10^{-3} M and 1.5×10^{-3} M, respectively.

Electrolytic solution was purged with Ar gas to eliminate the degradative effect of O₂, especially during the cathodic scan. Electrochemical cell used in the polymer synthesis or analysis is shown in **Figure 1.8**.

Note that all of the polymers' stability tests were carried out under air atmosphere and the system was not sealed (sealing would further increase the long-term stability of the material upon switching and/or cycling) in order to show both operational stability and environmental robustness under ambient conditions.

2.3.2.2. Chemical Synthesis of the Polymers

Monomers, **PSeP-C₁₀**, **PSP-C₁₀**, **PNP-C₁₀**, **POP-C₁₀** and **PSP-C₆** were also polymerized using a chemical oxidant. For this purpose 0.64 mmol of monomer was dissolved in chloroform (45 mL). A solution of anhydrous FeCl₃ (444 mg, 2.74 mmol, 5 equiv) in nitromethane was added dropwise over a period of 45 min. to the stirred monomer solution at room temperature (the bright red/ orange/ yellow/ orange/ orange colors of monomer solutions turned progressively dark blue or green with addition of oxidizing agent). The mixture was stirred 48 h at room temperature and the polymer was precipitated by pouring the solution into methanol (300 mL). The precipitate was filtered, redissolved in chloroform (300 mL), and stirred for 6 h with hydrazine monohydrate (6 mL). After evaporation, the concentrate (dark blue or green) was precipitated into methanol (300 mL), the precipitate was filtered through a Soxhlet thimble and purified via Soxhlet extraction for 48 h with methanol. The polymer was extracted with chloroform and concentrated by evaporation. Then, the polymer was precipitated in methanol (300 mL) and collected as a black solid (yield = 82% for **P(PSeP-C₁₀)**, 84% for **P(PSP-C₁₀)**, 86% for **P(PNP-C₁₀)**, 75 % for **P(POP-C₁₀)**, and 50 % for **P(PSP-C₆)**).

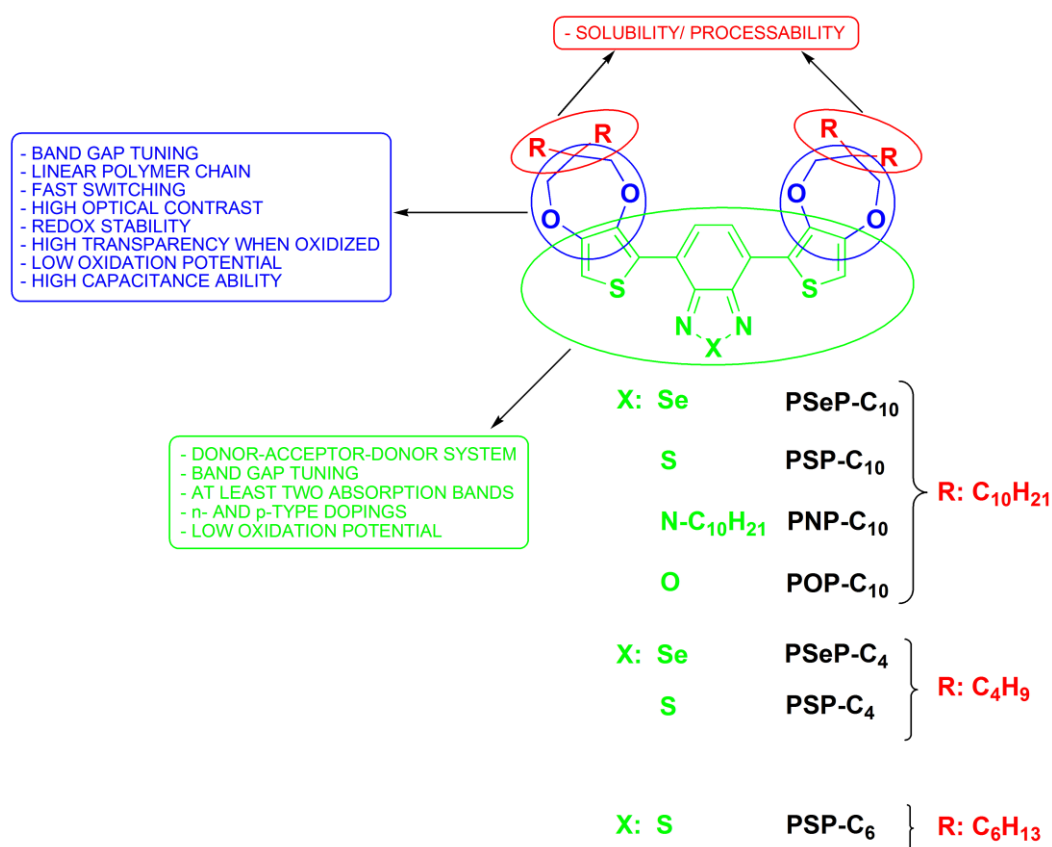
CHAPTER 3

RESULTS AND DISCUSSION

3.1. Structural Design of the Monomer

3.1.1. Band Gap Tuning

In this study, the aim was to synthesize processable conjugated polymers with low band gap and high transmittance. In order to obtain low band gap polymers three different donor groups, 3,4-propylenedioxythiophene (ProDOT), 3,4-ethylenedioxythiophene (EDOT) and thiophene were used (**Scheme 1. 2**). ProDOT containing polymers have less compact structure than EDOT containing ones [22], which would not only facilitate the ion flux during doping/dedoping process but also would impart lower transmittance values as compared to the EDOT containing polymers. Also, adding functional group(s) to enhance the solubility is more facile for ProDOT groups (**Scheme 3. 1**).



Scheme 3.1. The design of the monomers according to desired properties.

3.1.2. Color Tuning

Most of the PECs exhibit either red or blue colors in their neutral states, and the third leg (green) of the primary additive colors (red, green, and blue constitute the primary additive RGB color-space, whereas cyan, magenta, and yellow constitute the CMY primary subtractive color-space) (**Figure 1. 9**) has remained elusive for a long time. The importance of the RGB and CMY colors is that via just mixing any two of these colors in the proper amount (for black three of them should be mixed), any color or any tunes of a color can be obtained in the visible spectrum, this is called as color mixing theory [66,67]. An illustration of color mixing concept, as shown in a recent report of Dyer and his co-workers [50], is given in **Figure 3.1**.

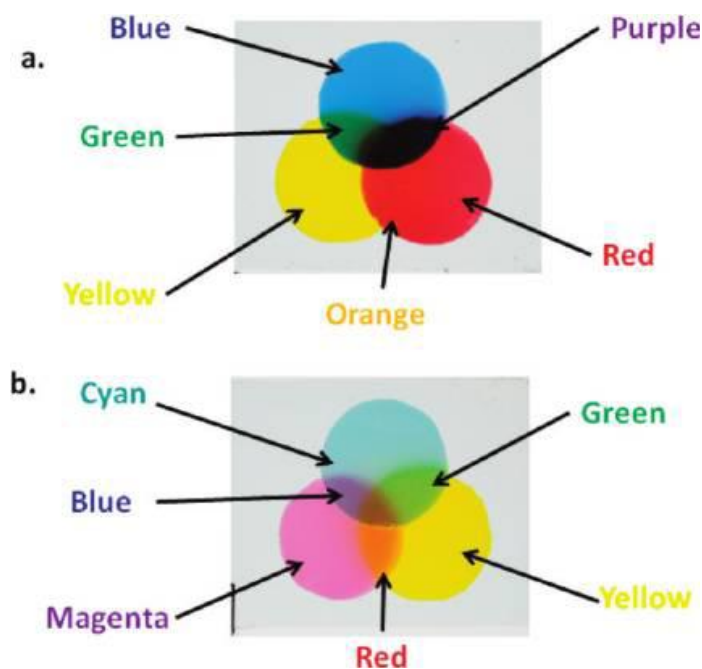


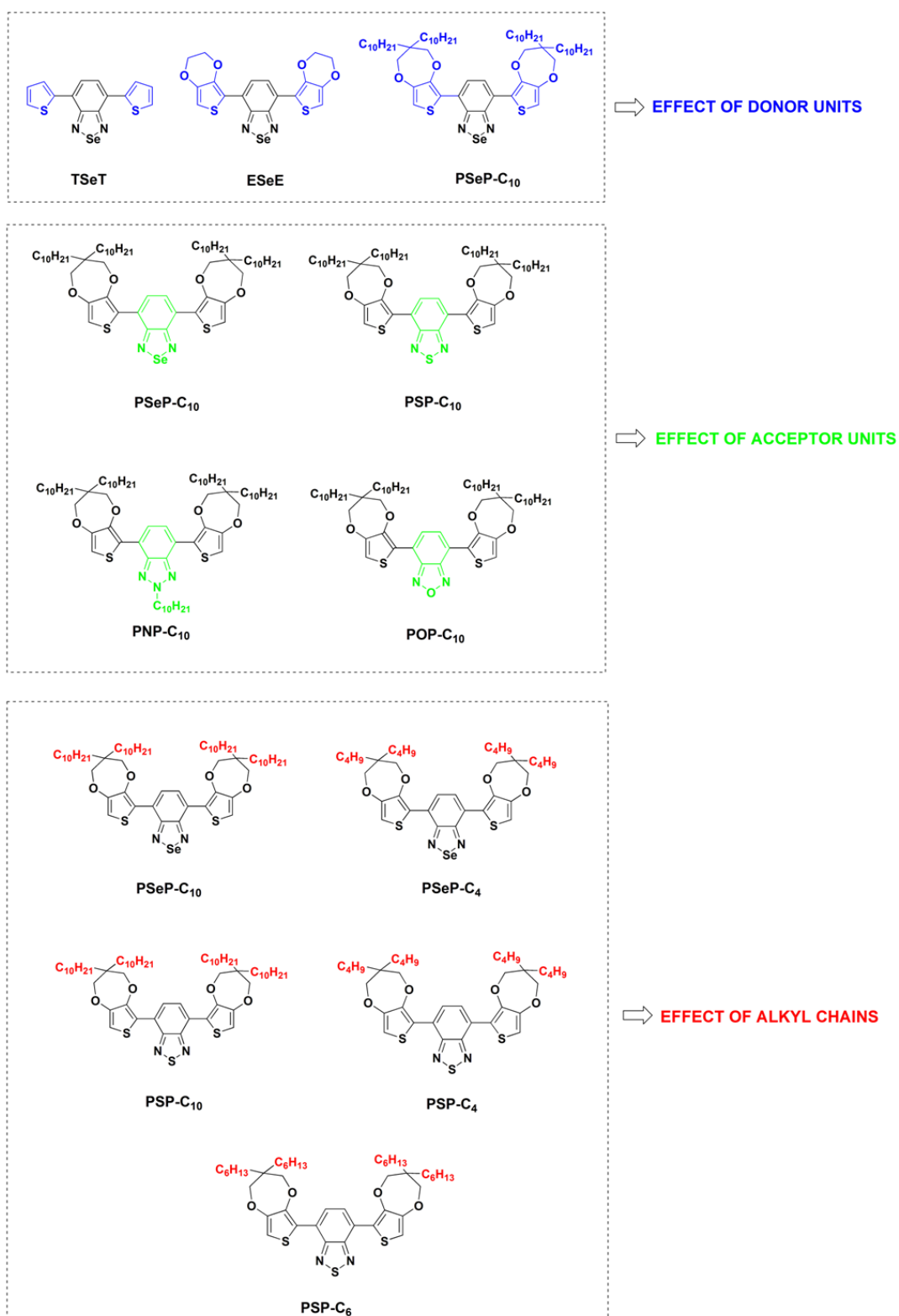
Figure 3.1. Spray-cast films on ITO/glass illustrating the subtractive color mixing concept as applied using electrochromic polymers. (a) The red-yellow-blue primaries where their overlaps create green, orange, and purple; and (b) the cyan-yellow-magenta primaries where their primaries create blue, red, and green [50].

The construction of PECs with a neutral state truly green and its tones possessed some major challenges due to the fact that the reflection of green color necessitated at least two absorption bands, which could deplete simultaneously during the redox processes, and it has been very difficult to control both of the absorption bands by the application of a voltage pulse. Fortunately, this puzzle has been solved by turning the spotlight on macromolecular conjugated systems based on alternating electron-rich (donor, D) and -poor (acceptor, A) units [68]. This D-A approach [69] not only allowed a fine-tuning of the band gap (E_g) of the as-prepared organic materials [70-73] but also provided access to a range of colors in the full visible spectrum, as exhaustively shown by both Reynolds' [51,57,74,75] and Toppare's [76-80]

laboratories. More recently, Cihaner and Algi reported the design and synthesis of novel D-A systems that could produce green color in the neutral state [41,81]. However, it is still a challenging task to attain the two complementary color-spaces (RGB and CMY) in the context of innovative high-performance display technologies. Considering the fact that a neutral state PEC should not only produce the green color but should also be solution-processable [57,82] for polymeric RGB applications in an industrial platform, attentions should be turned to processable variants of the D-A systems. For this purpose, in this study D-A approach utilizing D- and A- units of different electronic strength have been undertaken. This approach would give the opportunity to understand the effect of these units on both the neutral state color and the electrochromic performance of the corresponding D-A type polymers. It is important to note that only few reports have focused on systematic comparison of the structure-property relationship [22,75,83-85] in spite of the fact that much literature concerning the design of new systems for PECs exists. Furthermore, these newly designed D-A systems might hold promise for a processable blue to transparent PEC candidate which would also be highly valuable en route to the commercialization of PECs [80]. Although it is tempting to think that poly(3,4-ethylenedioxythiophene) (PEDOT), as an electrochrome, provides the color blue, it is unfortunate that this industrially important polymer is not solution processable. Very recently, a spray processable blue-to-highly transmissive switching polymer electrochromes were reported [86, 87]. On the other hand, a systematic approach would also help us to surmount the barricade for accessing either to cyan color [75] which is one of the primary subtractive colors of CMY color-space or to a neutral state black PEC [74] by electrochemical means, which are highly difficult to attain because of the complexity of designing such materials, so there have been scant studies on cyan colored polymers [75] in the literature.

3.2. Examining the Effect of Different Groups

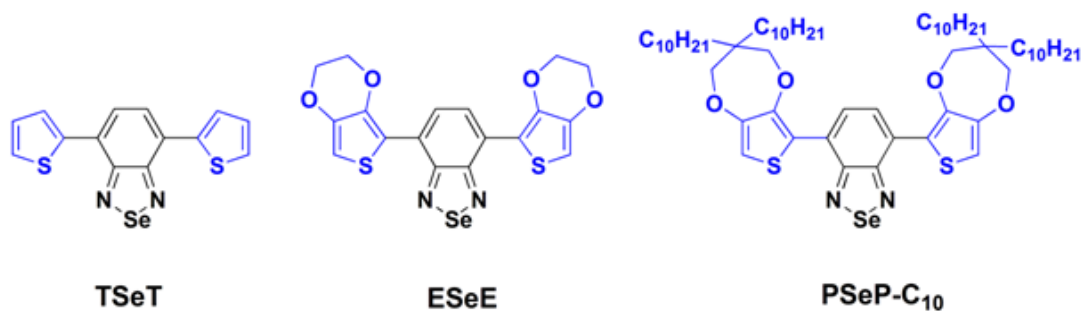
As mentioned before, in order to investigate the effect of different groups on the electrochemical, optical, electrochromic and solubility properties of the electrochromic polymers, three different donor, four different acceptor, and three different alkyl chain length containing monomers and their corresponding polymers were synthesized and their properties were investigated (**Scheme 3.2**) in this study.



Scheme 3.2. Categorizing the monomers according to used functional groups to be examined.

3.2.1. Effect of Donor Groups

In this part three monomers, **TSeT**, **ESeE**, and **PSeP-C₁₀**, (Scheme 3.3) and their corresponding polymers, **P(TSeT)**, **P(ESeE)**, and **P(PSeP-C₁₀)**, were investigated.



Scheme 3.3. Monomers that are used for the investigation of donor groups' effect.

3.2.1.1. Cyclic Voltammogram of the Monomers

The role of the D- units on the redox behaviour of 2,1,3-benzoselenadiazole based D-A systems, **TSeT**, **ESeE**, and **PSeP-C₁₀**, was investigated by cyclic voltammetry studies in 0.1 M TBAH dissolved in DCM. It was found that these systems exhibited ambipolar redox behaviors. During anodic scans, irreversible oxidation peaks were observed at ($E_{m,a}^{ox}$) 1.21 V, 0.84 V and 0.98 V (vs. Ag/AgCl) for **TSeT**, **ESeE**, and **PSeP-C₁₀**, respectively. As depicted in **Figure 3.2**, the voltammograms nicely reflected the electronic nature of the D units. **PSeP-C₁₀** had an oxidation potential of 0.98 V which is between those of **TSeT** and **ESeE** and this was attributed to higher electron density when compared to **TSeT**, whilst increased bridge size from ethylene to propylene caused a higher oxidation potential when compared to **ESeE**, respectively [22].

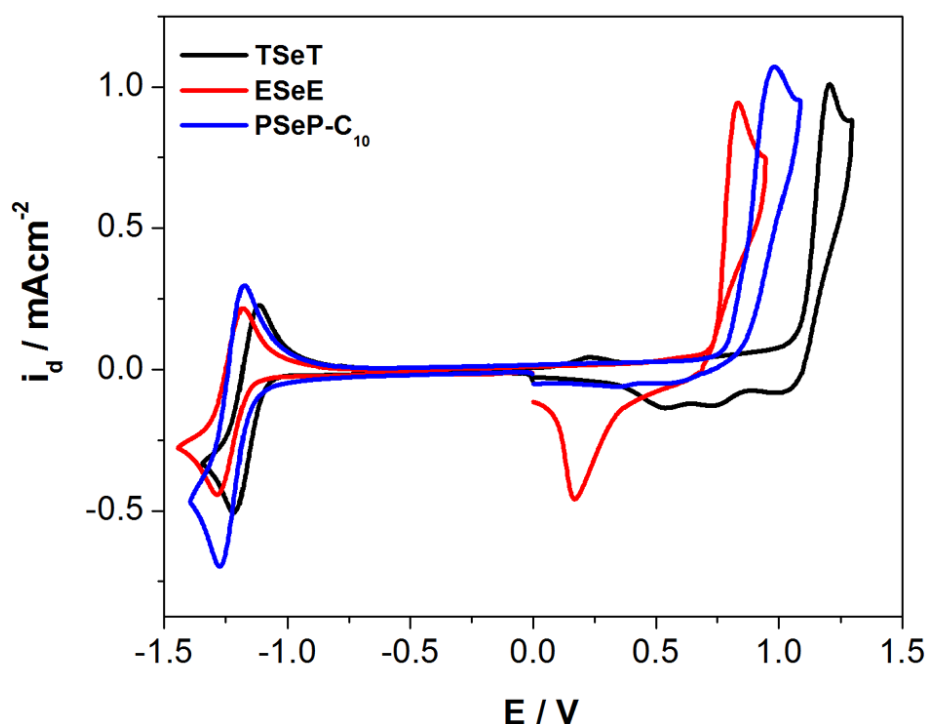


Figure 3.2. Cyclic voltammograms of **TSeT**, **ESeE**, and **PSeP-C₁₀** in 0.1 M TBAH/DCM at 100 mV/s.

On the other hand, during cathodic scans **TSeT**, **ESeE**, and **PSeP-C₁₀** have shown reversible reduction peaks due to the A part with half peak potentials ($E_{1/2}^{red}$) of -1.17 V, -1.22 V and -1.23 V (vs. Ag/AgCl), respectively. The observed somewhat higher negative peak potential for the formation of radical anions of **ESeE** and **PSeP-C₁₀** can be ascribed to higher electron density of the A- part as compared to **TSeT**. These results clearly suggested that the D- units in **TSeT**, **ESeE**, and **PSeP-C₁₀** have a key role to tune the redox behaviour and the interaction between HOMO and LUMO levels of the system.

3.2.1.2. Electrochemical Polymerization and Properties of the Polymers

After the determination of redox characteristics of **TSeT**, **ESeE**, and **PSeP-C₁₀**, the electropolymerization was carried out to get the corresponding polymers **P(TSeT)**, **P(ESeE)**, and **P(PSeP-C₁₀)**. Whereas polymerization of **TSeT** and **ESeE** were done in 0.1 M TBAH/ DCM electrolyte/ solvent couple, polymerization of **PSeP-C₁₀** was carried out in 0.1 M TBAH dissolved in a mixture of DCM and ACN solution (since the polymer, **P(PSeP-C₁₀)**, were highly soluble in DCM). During the electropolymerization, new reversible redox couples appeared after repetitive anodic scans, which clearly indicated the formation of electroactive polymer films on the electrode surface (**Figure 3.3**). Also, thickness of the polymer films increased, which was confirmed by intensified current value of the redox couples after each successive cycle.

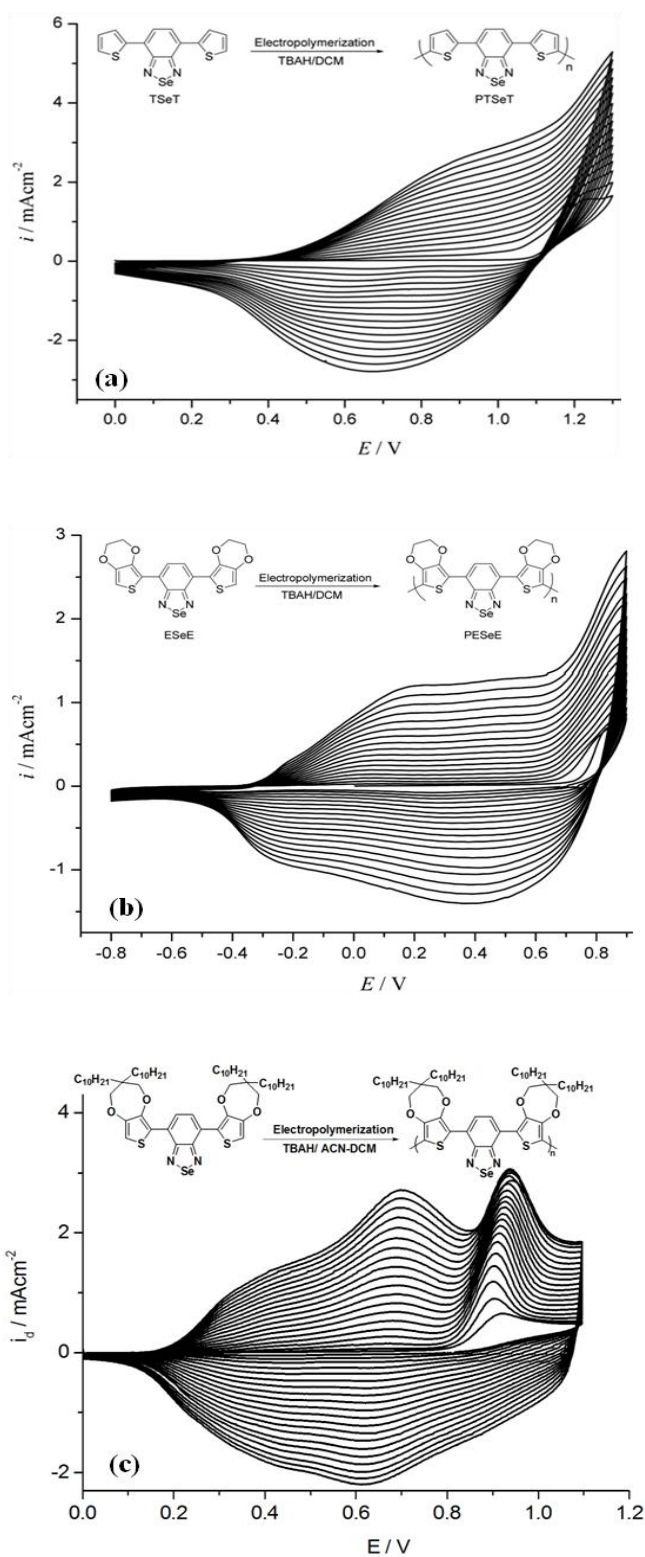


Figure 3.3. Electropolymerization of 1.5×10^{-3} M (a) **TSeT**, and (b) **ESeE** in 0.1 M TBAH-DCM and (c) **PSeP-C₁₀** in 0.1 M TBAH-DCM/ ACN (2/3-v/v) at 100 mV/s by potential scanning to give **P(TSeT)**, **P(ESeE)**, and **P(PSeP-C₁₀)**, respectively.

It was noteworthy that **TSeT** has blue-green, **ESeE** and **PSeP-C₁₀** have green colors in their neutral states. Thus, addition of electron rich EDOT and ProDOT units as D part instead of thiophene into the D-A system was amenable way to adjust the color of the neutral state polymer from blue-green to green by shifting the absorption bands of red and blue colors to longer wavelengths (see **Table 3.1**).

When **P(TSeT)**, **P(ESeE)**, and **P(PSeP-C₁₀)** were scanned anodically in monomer-free electrolyte solution containing 0.1 M TBAH/ACN, they exhibited well-defined reversible redox couples ($E_{p,1/2}^{ox} = 0.93$ V for **P(TSeT)**, $E_{p,1/2}^{ox} = -0.09$ V for **P(ESeE)**, $E_{p,1/2}^{ox} = 0.66$ V for **P(PSeP-C₁₀)**) which were consistent with the behaviors of the starting materials. A linear increase in the peak currents as a function of the scan rates confirmed well-adhered electroactive polymer films on the electrode surface as well as non-diffusional redox process (**Figure 3.4-3.6**).

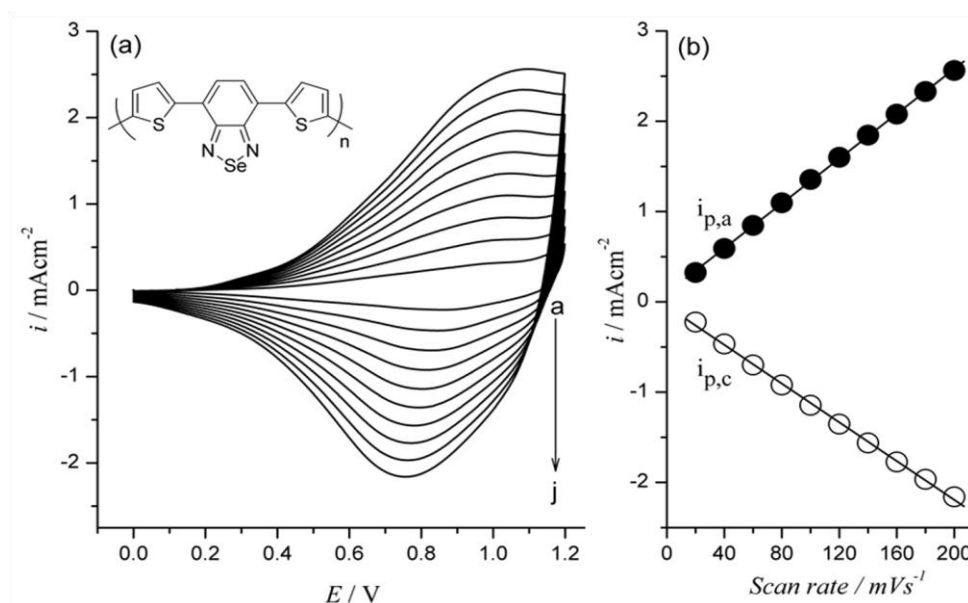


Figure 3.4. (a) CV of **P(TSeT)** film at different scan rates: (a) 20, (b) 40, (c) 60, (d) 80, (e) 100, (f) 120, (g) 140, (h) 160, (i) 180, (j) 200 mV/s. (b) Relationship of anodic ($i_{p,a}$) and cathodic current ($i_{p,c}$) peaks as a function of scan rate in 0.1 M TBAH/DCM for **P(TSeT)** film during p-doping.

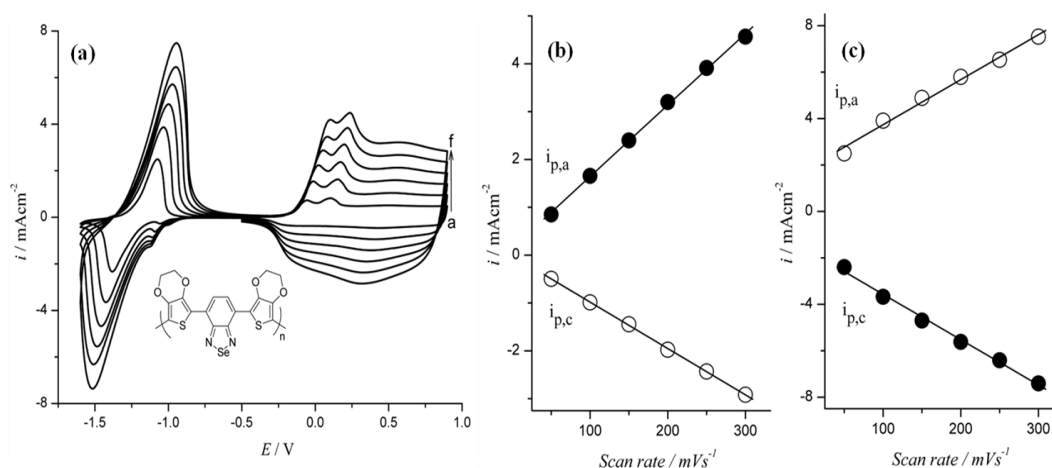


Figure 3.5. (a) CV of n- and p-doped **P(ESeE)** film at different scan rates: (a) 50, (b) 100, (c) 150, (d) 200, (e) 250 and (f) 300 mV/s, and relationship of anodic ($i_{p,a}$) and cathodic peak currents ($i_{p,c}$) as a function of scan rate for (b) p-doped and (c) n-doped **P(ESeE)** film in 0.1 M TBAH and DCM.

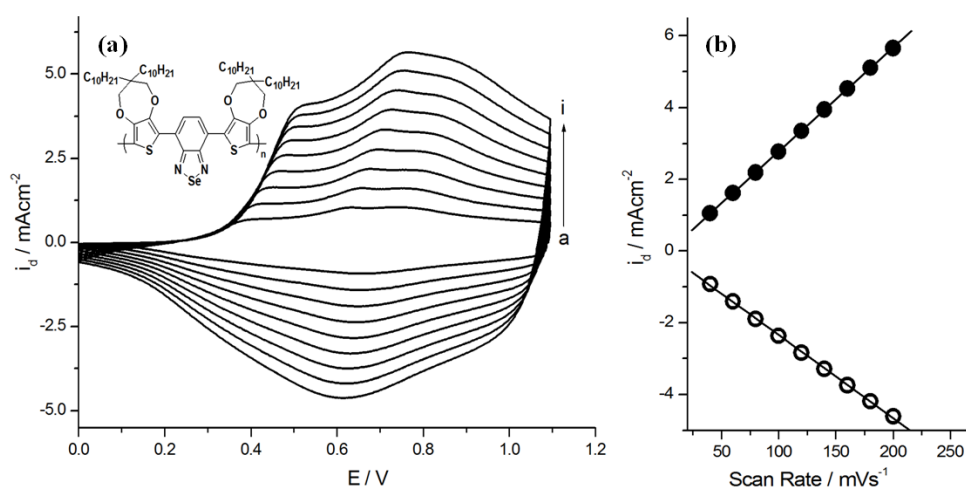
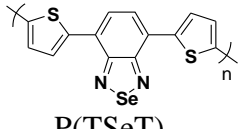


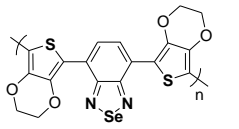


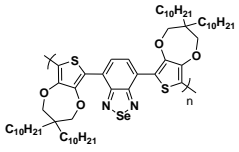




Figure 3.6. (a) CV of p-doped **P(PSeP-C₁₀)** 0.1 TBAH/ACN at a scan rate of a) 40, b) 60, c) 80, d) 100, e) 120, f) 140, g) 160, h) 180, and i) 200 mV/s. (b) Relationship of anodic ($i_{p,a}$) and cathodic current ($i_{p,c}$) peaks as a function of scan rate for p-doped **P(PSeP-C₁₀)** film in 0.1 M TBAH/ DCM.

Table 3.1. Electrochemical and optical data for **TSeT**, **ESeE**, and **PSeP-C₁₀** and their corresponding polymers, **P(TSeT)**, **P(ESeE)**, and **P(PSeP-C₁₀)**.

Polymer	$E_{m,a}^{ox}$	$E_{m,1/2}^{red}$	$E_{p,1/2}^{ox}$	$\lambda_{max,1}$	$\lambda_{max,2}$	$\lambda_{max,3}$	Neutral State	Oxidized State
 P(TSeT)	1.21	-1.17	0.93	350	600	-		
 P(ESeE)	0.84	-1.22	-0.09	343	448	796		
 P(PSeP-C₁₀)	0.98	-1.23	0.66	343	419	700		

The redox behaviors of **P(TSeT)**, **P(ESeE)**, and **P(PSeP-C₁₀)** were also examined during n-doping. Although **P(PSeP-C₁₀)** showed a slight activity indicating n-doping and **P(TSeT)** could not be n-doped, the **P(ESeE)** polymer film showed well-defined reversible n-doping process ($E_{p,1/2}^{red} = -1.24$ V). During n-doping process, it was observed that intensities of the anodic and cathodic peak currents were increasing linearly as a function of scan rate proving that redox process was non-diffusion-controlled (see **Figure 3.5**). Furthermore, the half wave potential of the **P(ESeE)** during n-doping has more negative value than that of its sulfur analogue, **P(ESE)** [76,88].

3.2.1.3. Spectroelectrochemical and Switching Behaviors of the Polymers

From the viewpoint of device and high performance display applications, spectroelectrochemical properties of the electrochromes should be manifested by using the changes in optical absorption spectra under voltage pulses. Therefore, UV-vis spectra of **P(TSeT)**, **P(ESeE)**, and **P(PSeP-C₁₀)** films which were electrodeposited on ITO glass slides were recorded *in situ* after neutralization.

It was observed that both A- and D- fragment of the D-A system significantly influenced the absorption spectra of the polymers. Upon oxidation, the intensity of the absorption bands started to decrease simultaneously with a concomitant increase in the near-IR region, indicating the formation of charge carriers. These changes in the absorption spectra were accompanied with color changes from blue-green to purple, green to sky blue and green to transparent (colorless) states for **P(TSeT)**, **P(ESeE)**, and **P(PSeP-C₁₀)**, respectively, during p-doping process (**Figure 3.7** and **Table 3.1**). The color change from one to a highly transmissive state, as in cases of **P(PSeP-C₁₀)**, is also a quite significant trait in RGB PECs and especially useful in display applications.

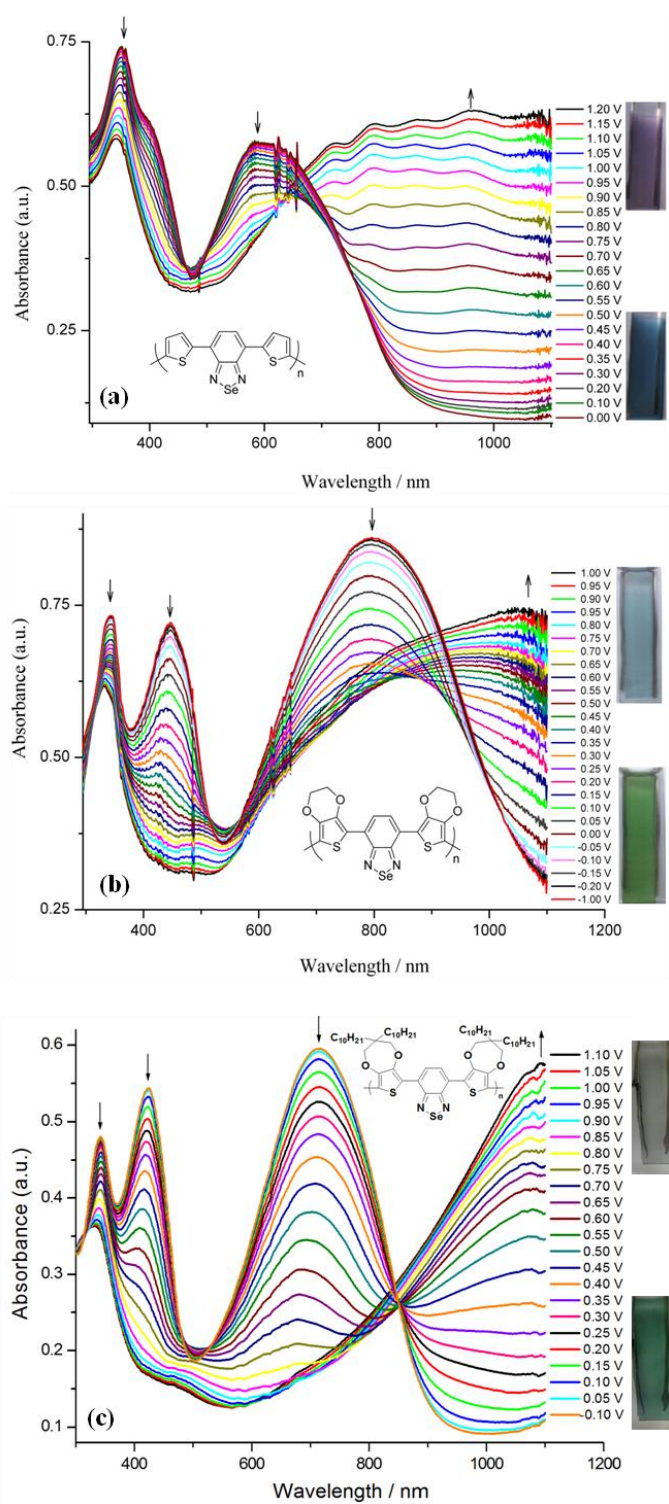


Figure 3.7. Electronic absorption spectra of (a) **P(TSeT)** (from 0.00 to 1.20 V), (b) **P(ESeE)** (from -1.0 V to 1.0 V), and (c) **P(PSeP-C₁₀)** (from -0.1 V to 1.1 V) on ITO in 0.1 M TBAH/ACN at various applied potentials.

During the oxidation process, the value of the absorption of the two π - π^* transition bands of **P(TSeT)** were declined simultaneously which is accompanied with the formation of a new absorption band around 962 nm due to the polaron formation. Upon further oxidation, the band around 350 nm decreased to the minimum intensity and the band at 600 nm completely disappeared (**Figure 3.7.-(a)**). The percentage transmittance changes ($\Delta\%T$) between the neutral and oxidized states (at 0.0 and 1.2 V, respectively) were calculated as 8% (at 350 nm), 12% (at 600 nm) in the visible region as well as 47.5% (at 962 nm) in the NIR region (**Figure 3.8**). CE of the **P(TSeT)** was calculated as 89 cm^2/C (at 600 nm; a switching time of 2.4 s) and 182 cm^2/C (at 962 nm; a switching time of 4.6 s).

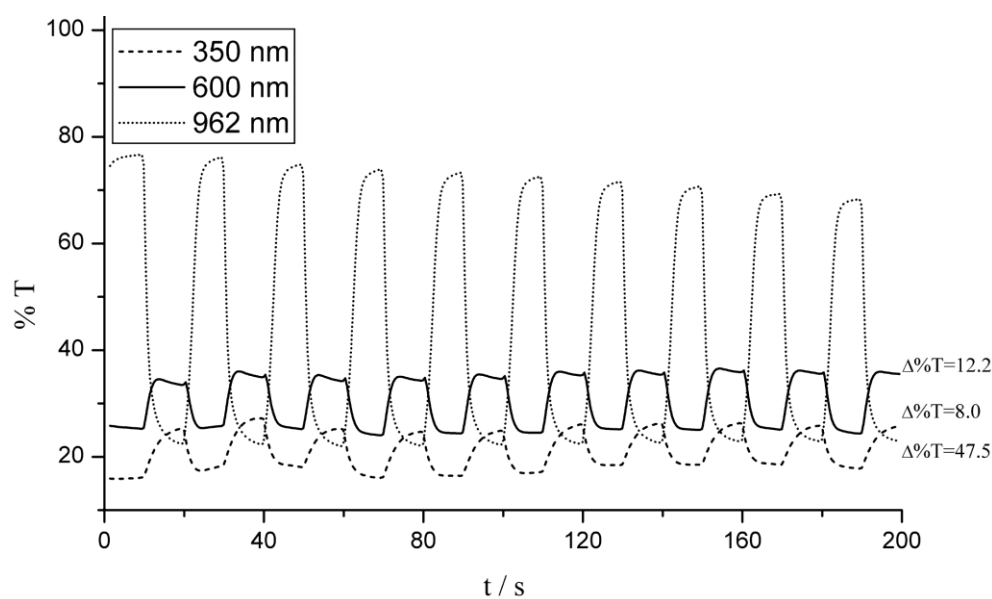


Figure 3.8. Chronoabsorptometry experiments for **P(TSeT)** on ITO in 0.1 M TBAH/DCM (During these procedures, polymer was switched between 0.0 V and 1.2 V).

P(ESeE) film has three well-defined absorption bands at 343 nm, 448 nm and 796 nm in its neutral state (**Figure 3.7.-(b)**). To our best knowledge, **P(ESeE)** is the first

example of a green polymer having three absorption bands in its neutral state. One of these bands absorb the red color (<500 nm) and the latter absorbs blue color (>700 nm) in the visible spectrum (**Table 3. 1**) maintaining the green color of the polymer. The brightness and hue of the green color are adjusted according to transmittance differences between maximum absorption bands and the deep valleys [68]. The **P(ESeE)** has two deep valleys at 378 nm and 542 nm and the calculated differences in transmittance were found to be 15 %, 9.9%, 9.3% for 378 nm and 28.3%, 23.6%, 23 %, for 542 nm. Even though, these values of **P(ESeE)** seem to be lower than that of its sulfur analogue, they are considerably enough to get the green color with various hue [76]. The band gaps (E_g) of **P(ESeE)** film was calculated as 1.13 eV from the onset of the low energy end of the π - π^* transition at 796 nm. It should be also noted that having green color in the neutral state together with sky blue oxidized state a quite important property in electrochromic displays and/or devices (**Figure 3.7.-(b)**).

At the beginning of the doping process, the intensities of three π - π^* transition bands of **P(ESeE)** declined simultaneously and a new absorption band started to form around 1000 nm showing the formation of polarons. Upon further doping, the bands at 448 and 796 nm disappeared completely and the absorption band at 343 nm reached the minimum intensity. The percentage transmittance changes values between the neutral and oxidized states were found to be 10.9% for 796 nm, 27.3% for 448 nm and 4.7% for 343 nm (**Figure 3.9**).

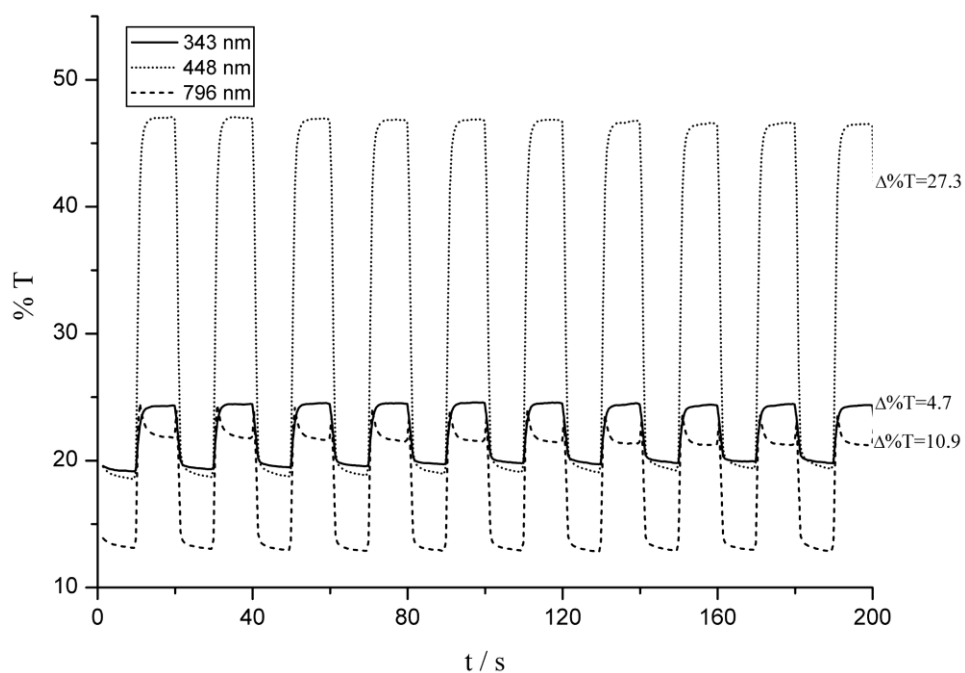


Figure 3.9. Chronoabsorptometry experiments for **P(ESeE)** on ITO in 0.1 M TBAH/DCM (During these procedure, polymer was switched between -1.0 V and 1.0 V).

The promising n-doping property of the **P(ESeE)** film observed with CV was also confirmed by the changes in the optical spectrum during the cathodic scan. During this scan, polymer's color changed from green to dark purple and the absorption bands started to decrease simultaneously and three new absorption bands began to form at 379 nm, 519 nm and beyond 1000 nm with a concomitant appearance of five isosbestic points (357 nm, 405 nm, 463 nm, 657 nm and 1024 nm). (**Figure 3.10**).

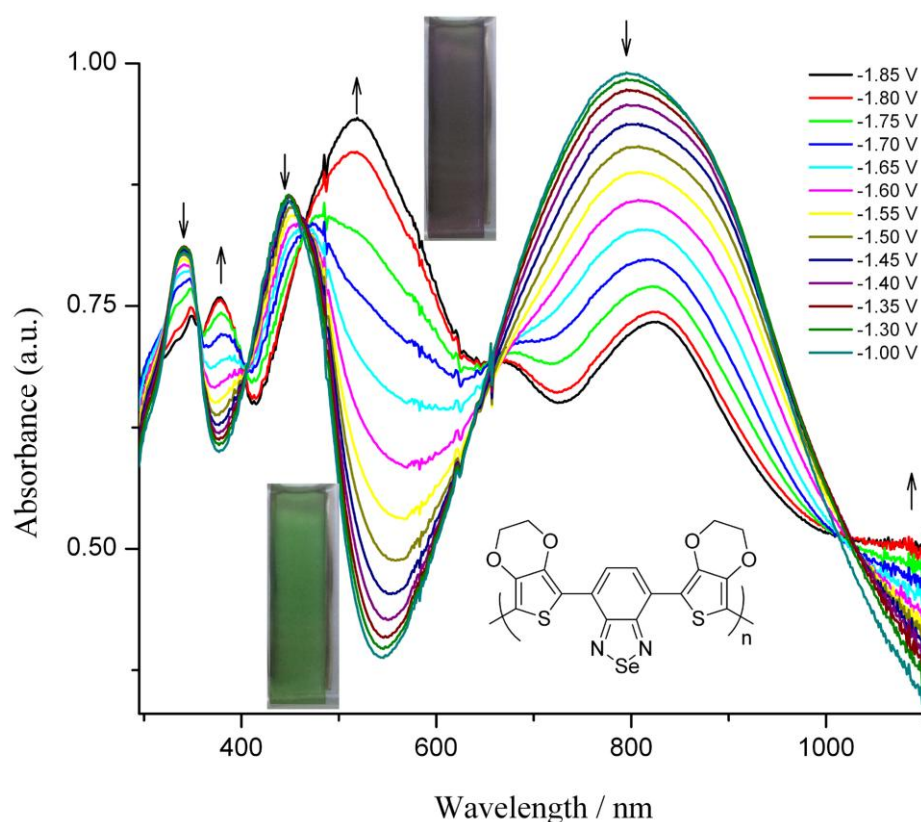


Figure 3.10. Spectroelectrochemical behavior of the **P(ESeE)** on ITO in 0.1 M TBAH/ DCM at various applied potentials between -1.85 V and -1.0 V. Insets: The colors of the polymer in its neutral and oxidized states.

P(PSeP-C₁₀) displayed higher CE value and lower response time (see **Table 3.2**) when compared to PEDOT [89,90]. For **P(PSeP-C₁₀)**, estimated differences in percentage transmittance of the bands (at 343 nm, 425 nm and 715 nm) with respect to the deep valleys were found to be 8.0 %, 12.3 %, 15.5 % for 343 nm and 32.4 %, 36.7 %, 39.9 % for 504 nm. These values were quite enough to get the green color with various hues as in case of **P(ESeE)**. $\Delta\%T$ between the neutral (at -0.1 V) and oxidized states (at 1.1 V) of **P(PSeP-C₁₀)** were found to be 11.2 % for 343 nm, 39.3 % for 425 nm, 40.3 % for 715 nm and 53.8 % for 1080 nm (**Figure 3.11**). The CE (at 95% of the full contrast) of the **P(PSeP-C₁₀)** film was found to be 45 cm²/C for 343 nm (a response time of 1.2 s), 147 cm²/C for 425 nm (a response time of 1.0 s) and

208 cm²/C for 715 nm (a response time of 0.6 s) during p-doping. Apparently, these values are both higher than those of **P(TSeT)** and **P(ESeE)** and even than that of PEDOT (183 cm²/C at 610 nm) [89,91].

Table 3.2. Optical and switching time data of electrochemically synthesized polymers **P(TSeT)**, **P(ESeE)**, **P(PSeP-C₁₀)**, and **PEDOT**.

Polymer	Wavelength (λ_{max}, nm)	Contrast %T	CE (cm²/C)	Switching time (t, s)
P(TSeT)	600	12.0	89	2.4
P(ESeE)	796	10.9	94	1.7
P(PSeP-C₁₀)	715	40.3	208	0.6
PEDOT	615	44.0	183	2.2

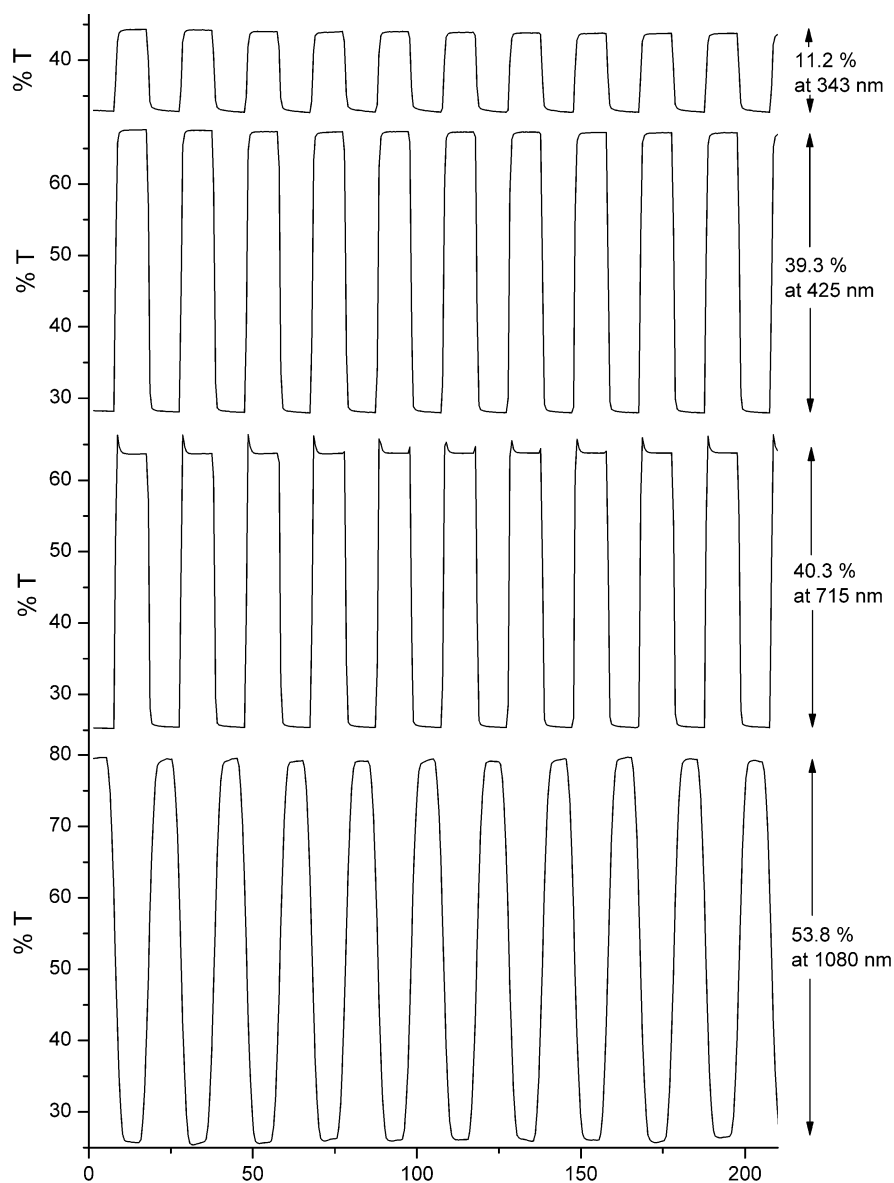


Figure 3. 11. Chronoabsorptometry experiments for **P(PSeP-C₁₀)** on ITO in 0.1 M TBAH/ ACN while the polymer was switched between -0.1 V and 1.1 V.

The band gaps (E_g) of **P(TSeT)**, **P(ESeE)**, and **P(PSeP-C₁₀)** were calculated from the onset of the low energy end of the π - π^* transitions to be 1.46 eV, 1.13 eV, and 1.37 eV, respectively (**Figure 3.7**, **Figure 3.12**, and **Table 3.3**). It can be easily

concluded that the smallest band gap can be obtained when EDOT units were attached as the D- part to any A- unit [76,80], probably due to the effective intramolecular charge transfer between the D- and the A- units (HOMO-LUMO interaction).

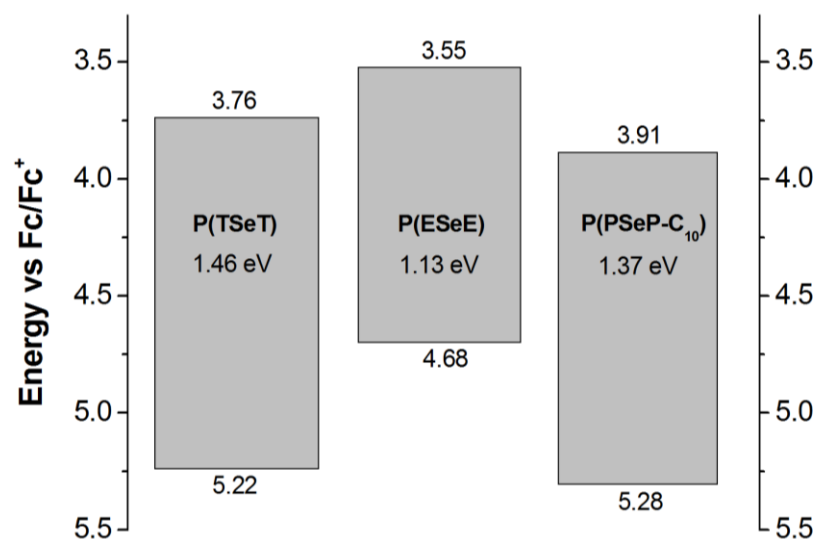


Figure 3. 12. Energy band diagram of the polymers **P(TSeT)**, **P(ESeE)**, and **P(PSeP-C₁₀)**.

Table 3.3. Electrochemically determined HOMO, LUMO and E_g values of polymers, **P(TSeT)**, **P(ESeE)**, and **P(PSeP-C₁₀)**.

Polymer	E_{ox} onset (V)	HOMO (eV)	LUMO (eV)	E_g optical (V)
P(TSeT)	0.42	5.22	3.76	1.46
P(ESeE)	-0.12	4.68	3.55	1.13
P(PSeP-C₁₀)	0.48	5.28	3.91	1.37

For the calculation of HOMO and LUMO levels: Oxidation potentials are reported vs. Fc/Fc^+ . The energy level of Fc/Fc^+ was taken as 4.8 eV below vacuum [91]. The oxidation onset potential of Fc/Fc^+ was measured as 0.36 V vs. $Ag/AgCl$. HOMO energy level was obtained from the onset potential of the oxidation at CV and LUMO energy level was calculated by the subtraction of the optical band gap from the HOMO level.

3.2.1.4. Properties of the Polymers

Although **P(TSeT)** was found to be soluble in N,N-dimethylformamide, it was found to be highly soluble in dimethylsulfoxide (DMSO), N-methyl-2-pyrrolidone in its oxidized state. Therefore, fluorescence properties of **P(TSeT)** and its monomer, **TSeT**, were investigated by recording their emission spectra in DMSO and the results are shown in **Figure 3.13**. As it is seen from the figure, **TSeT** exhibits an emission band at around 600 nm when excited at 560 nm. However, **P(TSeT)** emits at higher wavelength (at around 660 nm) corresponding to red light. This emission property makes **P(TSeT)** a promising candidate for the application of polymer-based photovoltaics [92].

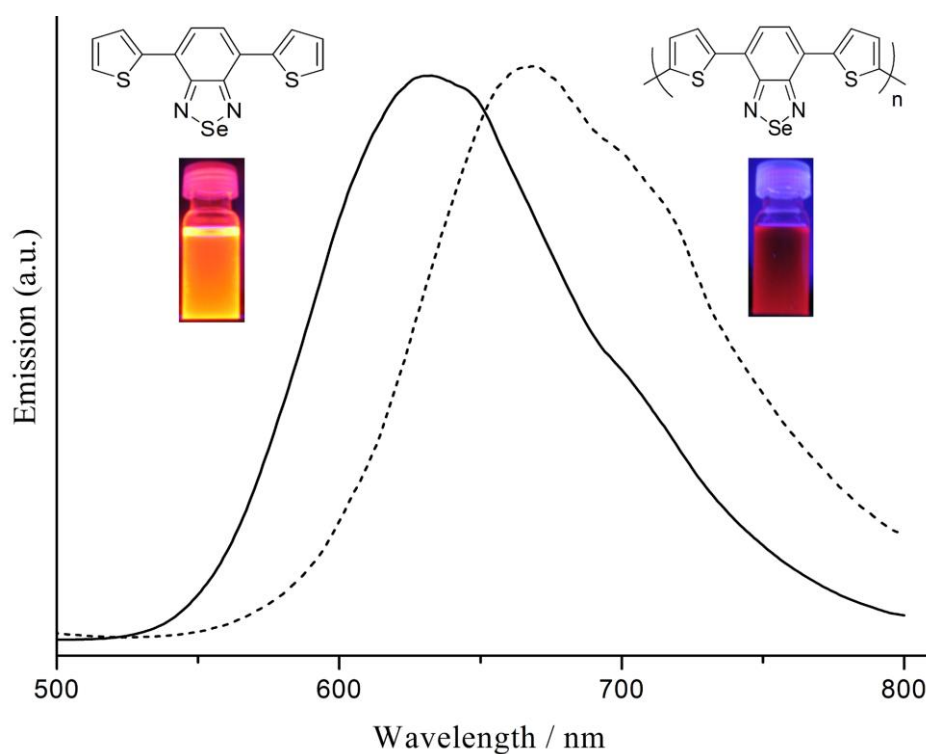


Figure 3.13. Emission spectra and the colors of **TSeT** (excited at 480 nm) and **P(TSeT)** (excited at 560 nm) in DMSO.

P(PSeP-C₁₀) was also soluble in organic solvents such as DCM and CHCl₃, whereas slightly soluble in toluene, which clearly suggested that it could easily be processed over surfaces via spin coating, spraying and printing techniques.

In order to prove the solution processability, **P(PSeP-C₁₀)**, which was obtained by chemical polymerization of **PSeP-C₁₀**, could be dip and/or spray coated on Pt disc electrode or ITO glass slide. The as-prepared **P(PSeP-C₁₀)**, which was dissolved in CHCl₃ (2 mg polymer/ 1 mL CHCl₃), was spray coated on ITO glass slide utilizing Aztek airbrush at 10 psi Ar (**Figure 3.14**) and it was found that **P(PSeP-C₁₀)** exhibited nearly the same characteristics (for CV, spectroelectrochemistry and chronoabsorptometry see **Figures 3.15** and **3.16**) when compared to that of the

electrochemically deposited **P(PSeP-C₁₀)**. Upon oxidation, the color of the chemically prepared **P(PSeP-C₁₀)** can be switched from green to colorless (transparent). The optical contrasts and switching of **P(PSeP-C₁₀)** were found to be 12 % and 1.4 s for 340 nm, 44 % and 1.3 s for 428 nm, 42 % and 1.0 s for 732 nm and 45 % and 1.98 s for 1000 nm, respectively (**Figure 3.16**).

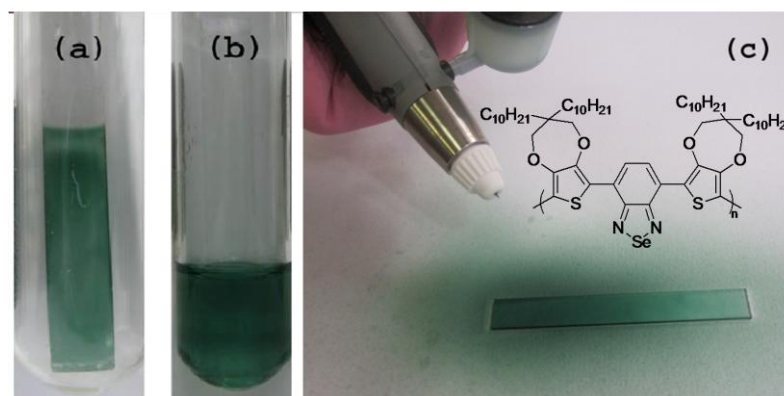


Figure 3.14. (a) Electrochemically coated **P(PSeP-C₁₀)** on ITO, (b) dissolving electrochemically synthesized **P(PSeP-C₁₀)** on ITO in chloroform (c) spray coating of chemically obtained **P(PSeP-C₁₀)** after dissolving in chloroform.

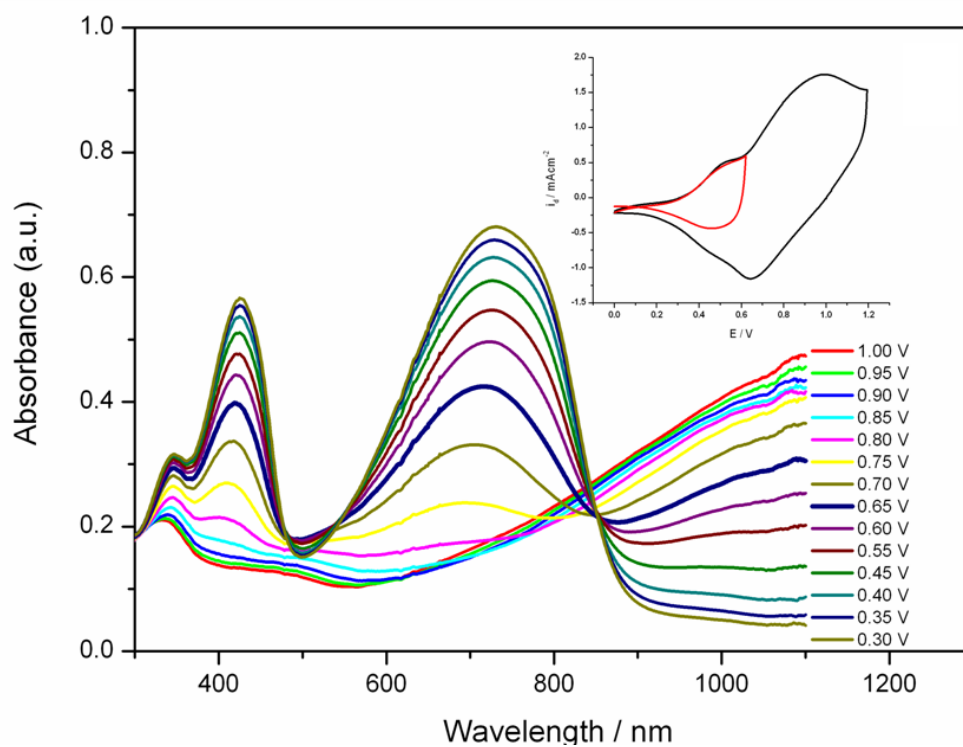


Figure 3.15. Electronic absorption spectrum of chemically synthesized **P(PSeP-C₁₀)** (from 0.3 V to 1.0 V) which was dip coated on ITO in 0.1 M TBAH/ACN. Inset: Cyclic voltammograms of chemically synthesized **P(PSeP-C₁₀)** coated on ITO in 0.1 TBAH/ACN at a scan rate of 100 mV/s.

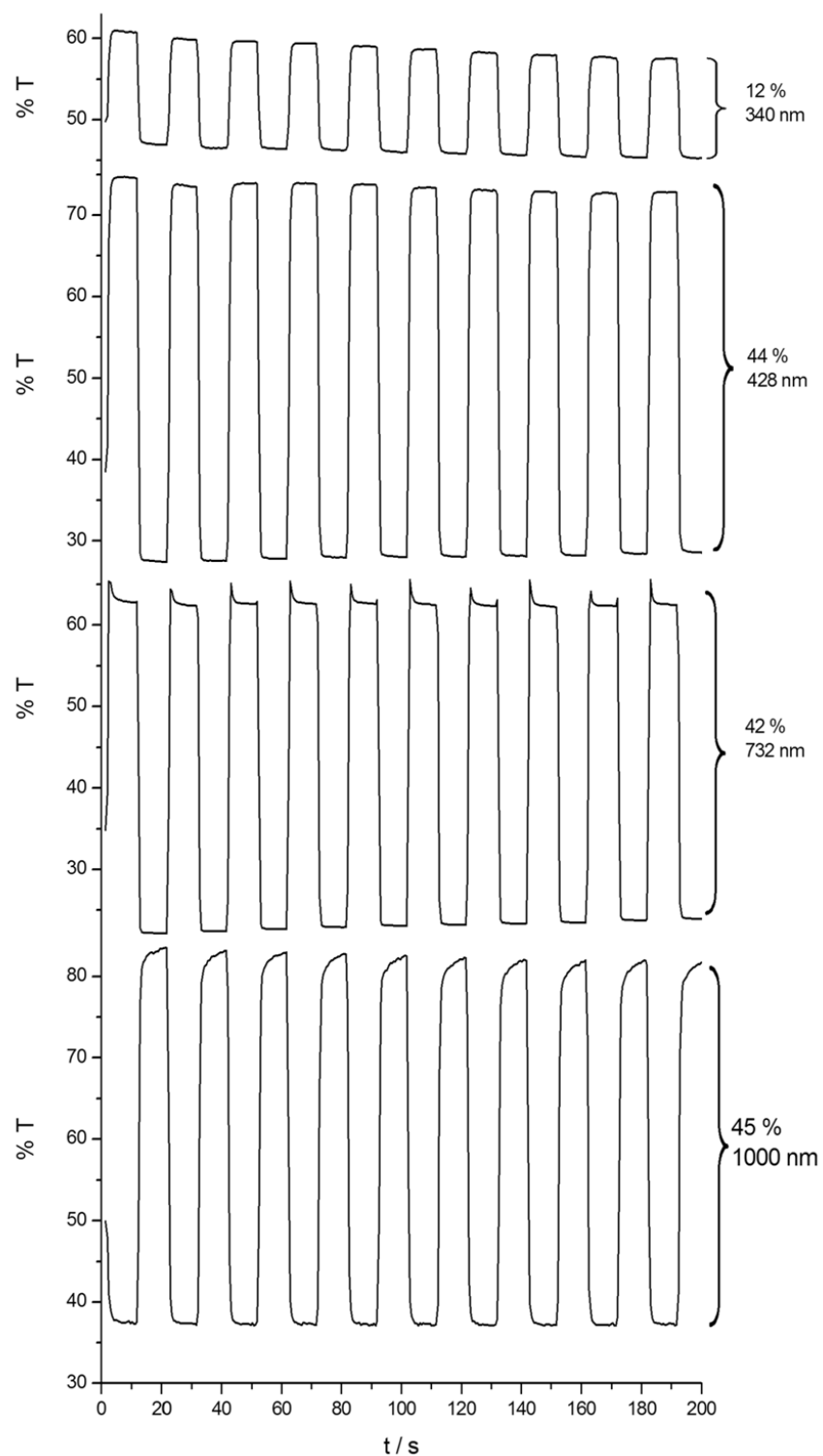


Figure 3.16. Chronoabsorptometry experiments for chemically polymerized **P(PSeP-C₁₀)** coated on ITO in 0.1 M TBAH/ ACN while the polymer was switched between 0.0-1.0 V.

Table 3.4. Optical and switching time data of chemically synthesized **P(PSeP-C₁₀)**, **P(PSP-C₁₀)**, and **P(PNP-C₁₀)**. The given CE value is the best one at a given wavelength.

Polymer	Wavelength (λ_{max}, nm)	Contrast %T	CE (cm^2/C)	Switching time (t, s)
P(PSeP-C₁₀)	732	42	220	1.0
P(PSP-C₁₀)	690	40	210	0.53
P(PNP-C₁₀)	560	19	240	1.3

Another procedure that was used to dope and dedope chemically obtained polymer is using solution of oxidizing and reducing agents such as SbCl_5 and $\text{N}_2\text{H}_5\text{OH}$. This procedure was used for **P(PSeP-C₁₀)**. For this aim, chemically obtained and neutralized **P(PSeP-C₁₀)** was dissolved in DCM. After that, for p-doping, 10^{-3} M SbCl_5 solution in DCM was added in 10 μL amounts (**Figure 3. 17 (a)**), and for neutralization, i.e., dedoping, 10^{-2} M $\text{N}_2\text{H}_5\text{OH}$ solution in DCM was added again in 10 μL amounts (**Figure 3. 17 (b)**). It was observed that the results obtained from chemical doping-dedoping procedure were almost the same with the electrochemical one (**Figure 3. 15**). Actually this doping-dedoping procedure was repeated many times (almost 30 times), there had been no observation of salt formation during repetitions, this should be because of the low concentration of oxidizing and reducing agents. This procedure should be useful for the determination of the mechanism of the doping and dedoping procedure taking place in the polymer structure using ESR (Electron Spin Resonance) method. It will be explained in detailed in part **3. 2. 4**.

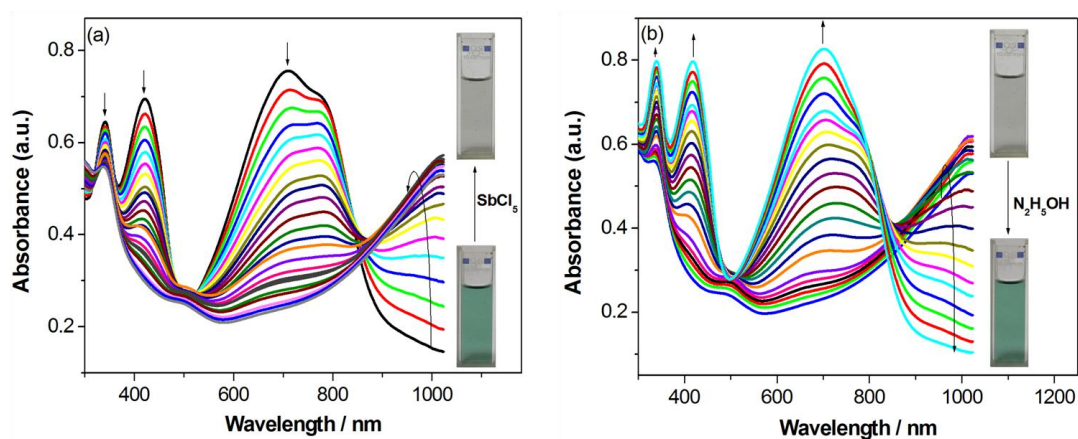


Figure 3.17. Chemically synthesized **P(PSeP-C₁₀)** dissolved in DCM (a) p-doped with 10^{-3} M SbCl_5 solution, (b) dedoped with 10^{-2} M $\text{N}_2\text{H}_5\text{OH}$ solution.

3.2.1.5. Stability of the Polymers

The long-term stability upon switching and/or cycling plays a key role on the electrochromic performance of the devices and smart windows. For that reason, the stability of **P(TSeT)**, **P(ESeE)** and **P(PSeP-C₁₀)**, which were deposited on Pt disk electrode, upon switching or cycling was elaborated by potential scanning between neutral and oxidized states. It was noted that the polymer films **P(TSeT)**, **P(ESeE)** and **P(PSeP-C₁₀)** exhibited excellent stability retaining at least 63%, 84% and 72% of the electroactivity even after 2000 cycles, respectively (see **Figure 3.18**). Note that the stability tests were carried out under air atmosphere and the devices were not sealed (sealing would further increase the long-term stability of these materials upon switching and/or cycling). The electrochemical stability and robustness of the systems suggested that the polymers were promising candidates for electrochromic devices and optical displays. In special case of **P(PSeP-C₁₀)**, for example, the response of the polymer film on ITO glass slide was almost the same as it was newly

prepared, even after prolonged standing at ambient conditions (e.g. two-months, and no further trial was done afterwards) (see **Figure 3.19**).

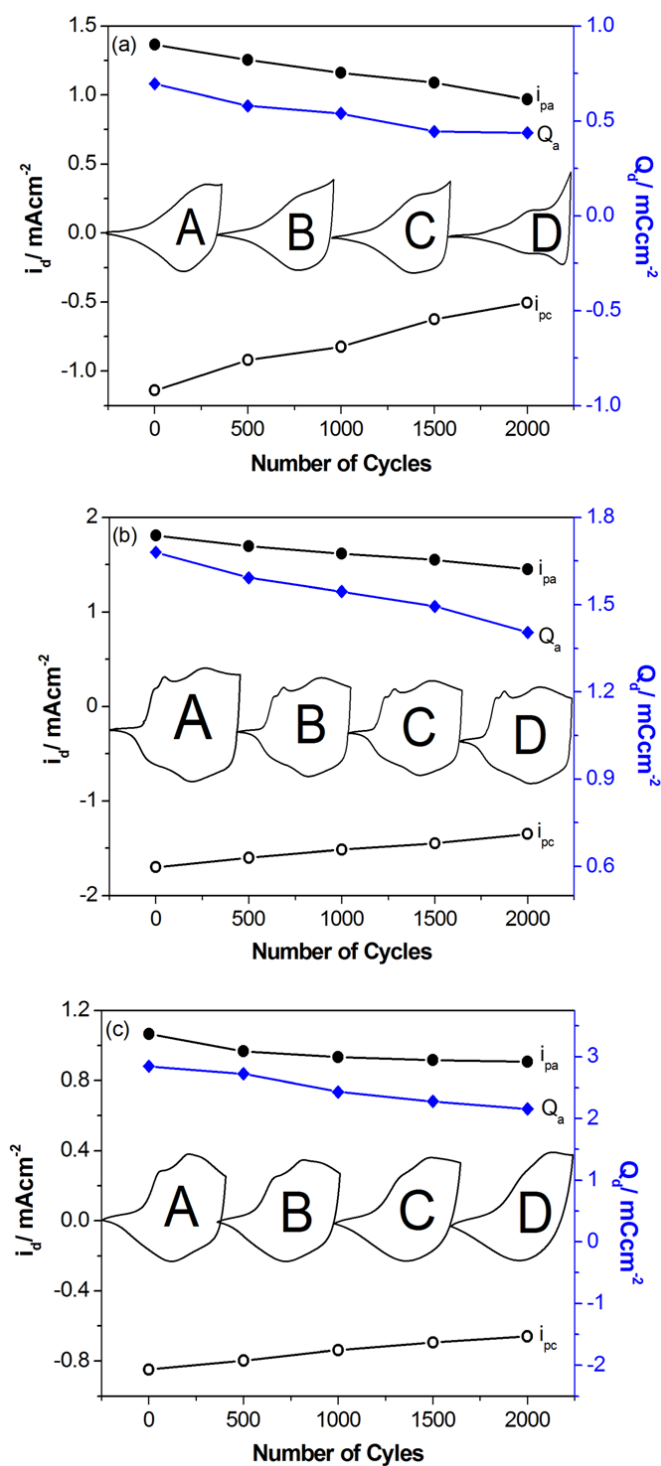


Figure 3.18. Stability test for (a) P(TSeT), (b) P(ESeE), (c) P(PSeP-C₁₀) films in 0.1 M TBAH/DCM at a scan rate of 100 mV s⁻¹ under ambient conditions by cyclic voltammetry as a function of the number of cycles: A: 1, B: 500, C: 1000, D: 2000 cycles; Q_a : Anodic charge stored, i_{pa} : Anodic peak current, i_{pc} : Cathodic peak current.

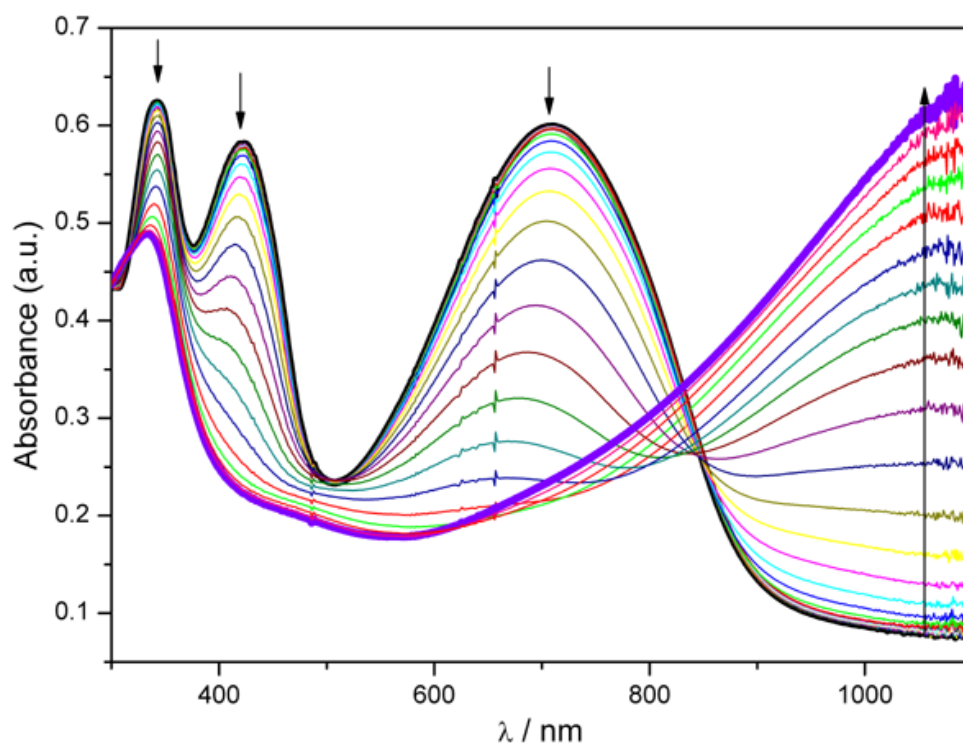
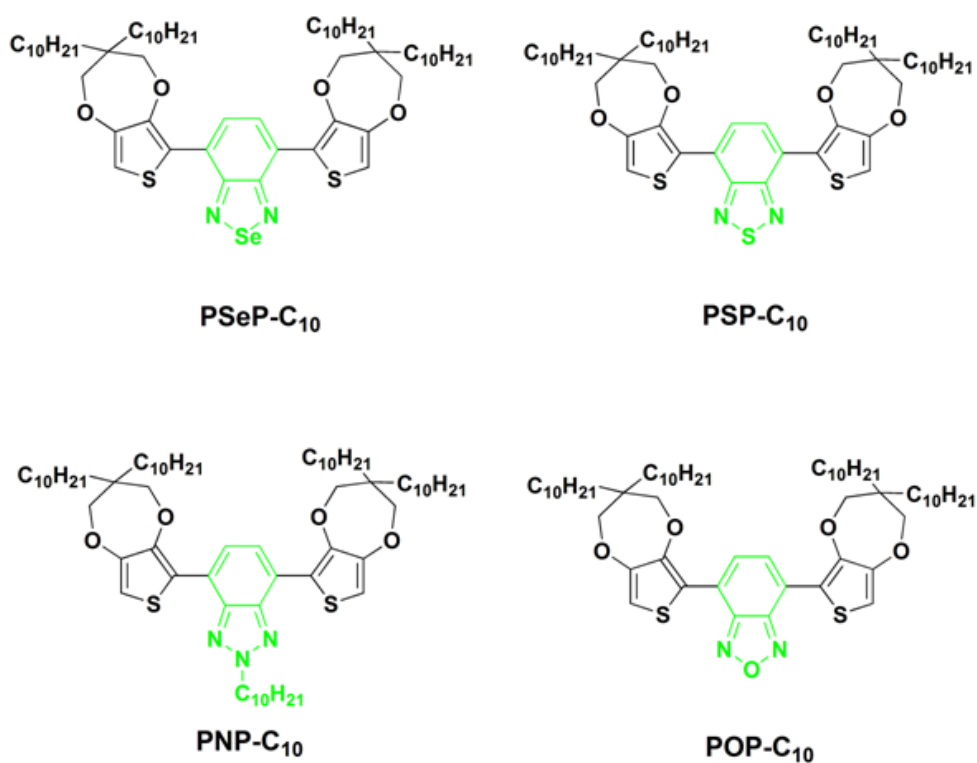


Figure 3.19. Electronic absorption spectra of **P(PSeP-C₁₀)** (from -0.1 V to 1.1 V) on ITO in 0.1 M TBAH/ACN at various applied potentials after prolonged standing at ambient conditions.

3.2.2. Effect of Acceptor Groups

In this part, four novel monomers, **PSeP-C₁₀**, **PSP-C₁₀**, **PNP-C₁₀** and **POP-C₁₀** (**Scheme 3.4**), and their corresponding polymers, **P(PSeP-C₁₀)**, **P(PSP-C₁₀)**, **P(PNP-C₁₀)** and **P(POP-C₁₀)** were investigated.



Scheme 3.4. Monomers that are used for the investigation of the acceptor groups' effect.

3.2.2.1. Cyclic Voltammograms of the Monomers

No appreciable change was observed in the oxidation values of **PSeP-C₁₀**, **PSP-C₁₀**, **PNP-C₁₀** and **POP-C₁₀** ($E_{m,a}^{ox} = \sim 1.0$ V) which is expected since the donor units of the monomers, ProDOT-C₁₀, are the same. (**Figure 3. 20**).

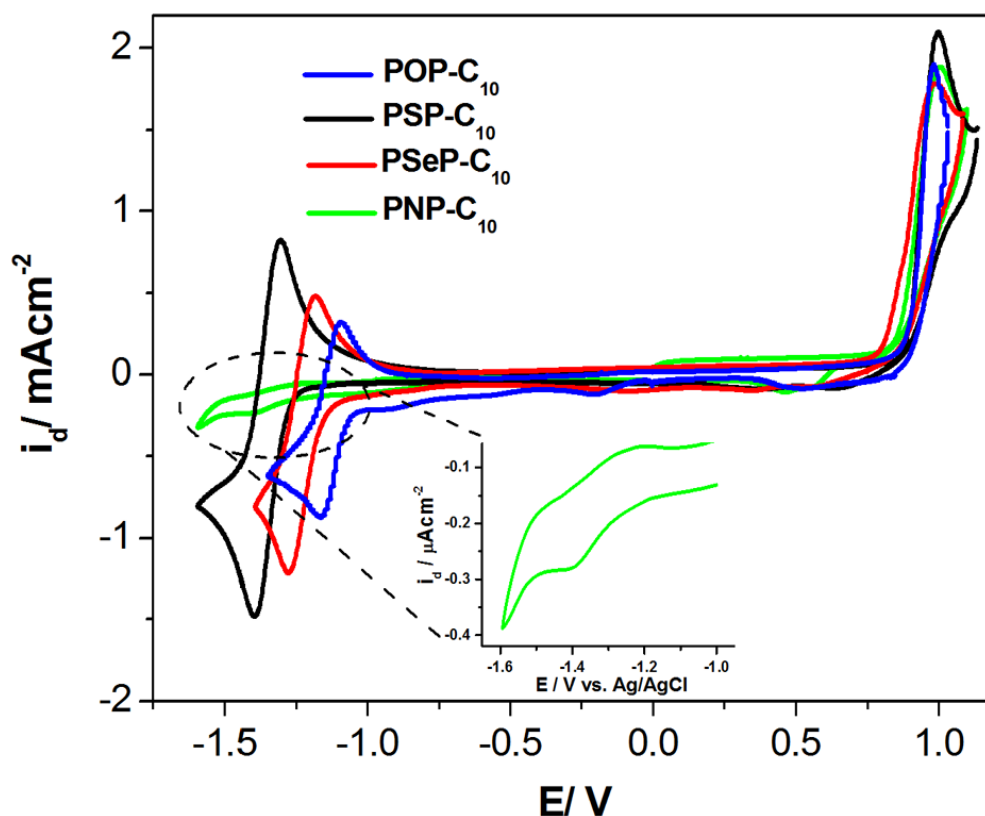


Figure 3. 20. Cyclic voltammograms of **PSeP-C₁₀**, **PSP-C₁₀**, **PNP-C₁₀** and **POP-C₁₀** in 0.1 M TBAH/DCM at 100mV/s.

As it was explained in **Part 3.1.1.**, when the reduction potentials of **TSeT** and **ESeE** (**Figure 3.1**) were compared with that of their sulfur containing analogues, **TST** [93,94] and **ESE** [76,88], **TST** ($E_{1/2}^{red} = -0.95$ V) and **ESE** ($E_{1/2}^{red} = -1.10$ V) have less negative reduction potentials than **TSeT** ($E_{1/2}^{red} = -1.17$ V) and **ESeE** ($E_{1/2}^{red} = -1.22$ V). In this case, monomers had similar trends with the electronic nature of the A units. That is, sulfur atom is more electronegative than selenium atom and so benzothiadiazole is better acceptor unit than benzoselenadiazole unit [41,88,93]. However, there has been an unexpected result observed during cathodic scans of **PSeP-C₁₀** and **PSP-C₁₀**, that is, **PSP-C₁₀** exhibited a higher reversible reduction peak with a half peak potential ($E_{1/2}^{red} = -1.36$) than **PSeP-C₁₀** ($E_{1/2}^{red} = -1.23$ V) (**Figure 3.**

20). That of **POP-C₁₀** is around -1.2 V, this is also lower than that of **PSeP-C₁₀**, therefore, the situation can not be explained with electronegativity or electronic nature of A unit. It is likely that the HOMO and LUMO energy levels, which determine the electrochemical behavior of the D-A systems, are affected in a different way in the case of an increasingly substituted D unit such as ProDOT-decyl₂ when compared to thiophene or EDOT [41].

On the other hand, an indistinct reversible reduction peak was observed at -1.31 V for **PNP-C₁₀**, this was probably arising from the presence of long alkyl chains in both D and A units of **PNP-C₁₀**, since it was evident that the reduction process clearly takes place when the similar A (benzotriazole) unit was linked with EDOT [80], thiophene [95] or selenophene [96] as the D units, which had no alkyl chains.

3.2.2.2. Electrochemical Polymerization and Properties of the Polymers

Like **PSeP-C₁₀**, electropolymerization of **POP-C₁₀**, **PSP-C₁₀** and **PNP-C₁₀** was carried out in a mixture of DCM and ACN solution containing 0.1 M TBAH. Formation of an electroactive polymer film on the electrode surface was proven by the new redox couples appearing after each repetitive cycles. As the number of the cycles was increased, the current density of these signals increased showing the increase in the thickness of the polymer film (**Figure 3. 21**).

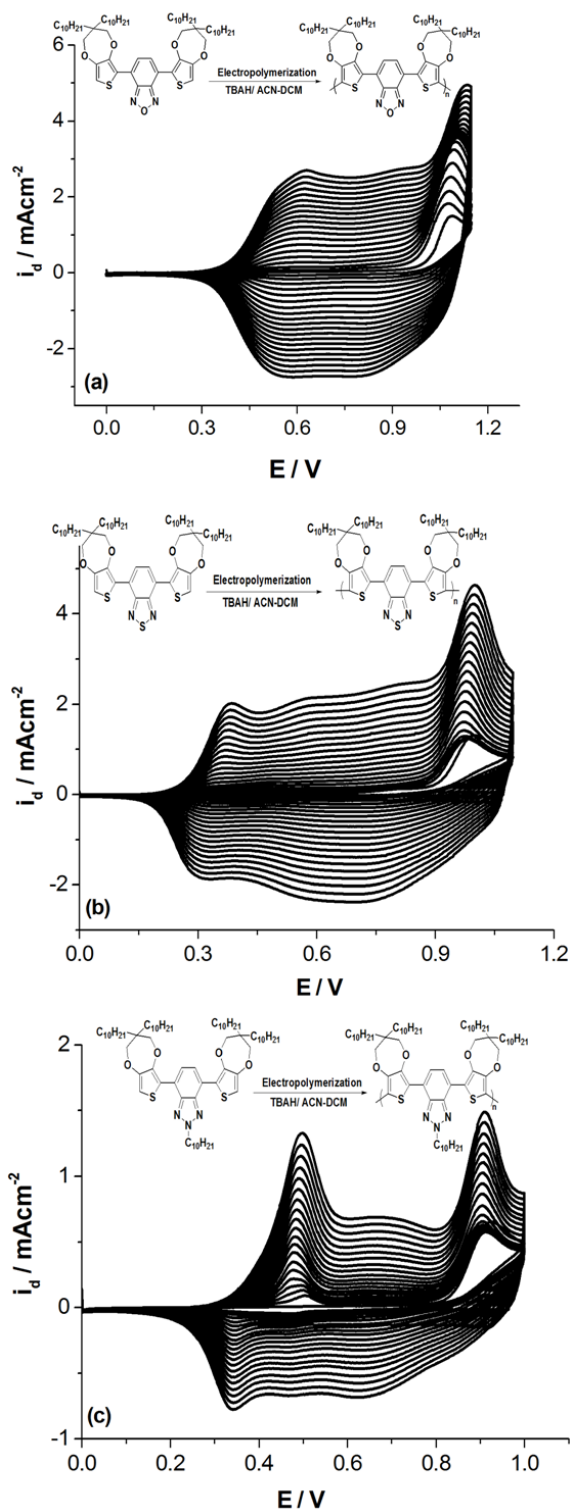


Figure 3. 21. Electropolymerization of 1.5×10^{-3} M (a) **POP-C₁₀**, (b) **PSP-C₁₀** and (c) **PNP-C₁₀** in 0.1 M TBAH-DCM/ACN (2/3-v/v) at 100 mV/s by potential scanning to give **P(POP-C₁₀)**, **P(PSP-C₁₀)**, and **P(PNP-C₁₀)**, respectively.

When **P(POP-C₁₀)**, **P(PSP-C₁₀)**, and **P(PNP-C₁₀)** were scanned anodically in monomer-free electrolyte solution containing 0.1 M TBAH/ACN, they exhibited well-defined reversible redox couples ($E_{p,1/2}^{ox} = 0.60$ V for **P(POP-C₁₀)**, $E_{p,1/2}^{ox} = 0.48$ V for **P(PSP-C₁₀)**, $E_{p,1/2}^{ox} = 0.60$ V for **P(PNP-C₁₀)**) which were consistent with the behaviors of the starting materials (see **Figure 3. 22-24**).

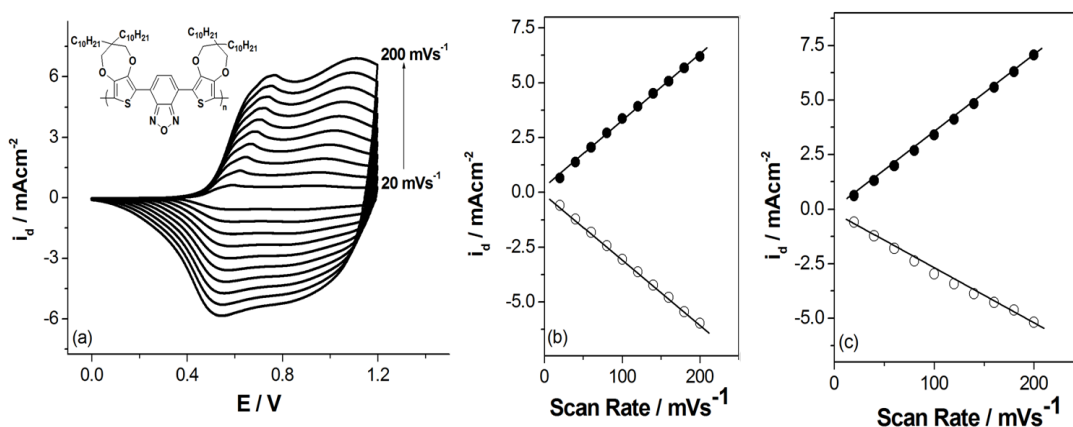


Figure 3.22. (a) Cyclic voltammograms of p-doped **P(POP-C₁₀)** in 0.1 TBAH/ACN at a scan rate between 20 mV/s and 200 mV/s with 20 mV/s increments. Relationship of (b) first anodic ($i_{p,a}$) and (c) second anodic current ($i_{p,a}$) peaks as a function of scan rate for p-doped **P(POP-C₁₀)** film in 0.1 M TBAH/DCM.

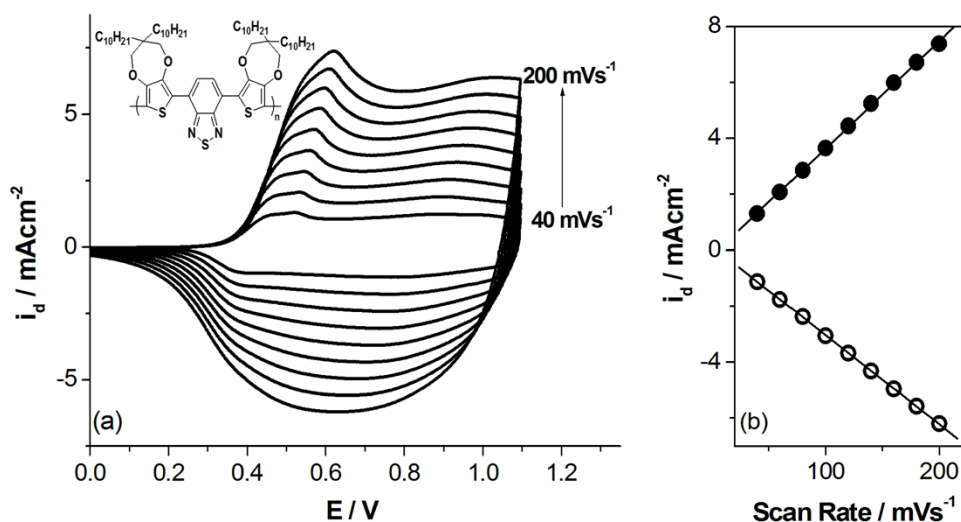


Figure 3.23. (a) Cyclic voltammograms of p-doped **P(PSP-C₁₀)** in 0.1 TBAH/ACN at a scan rate between 40 mV/s and 200 mV/s with 20 mV/s increments. (b) Relationship of anodic ($i_{p,a}$) peaks as a function of scan rate for p-doped **P(PSP-C₁₀)** film in 0.1 M TBAH/DCM.

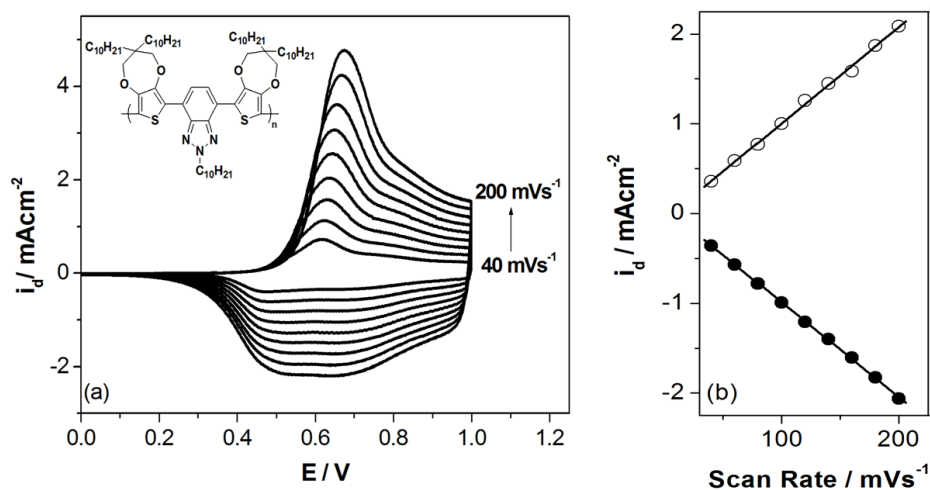


Figure 3.24. (a) Cyclic voltammograms of p-doped **P(PNP-C₁₀)** in 0.1 TBAH/ACN at a scan rate between 40 mV/s and 200 mV/s with 20 mV/s increments. (b) Relationship of anodic ($i_{p,a}$) peaks as a function of scan rate for p-doped **P(PNP-C₁₀)** film in 0.1 M TBAH/DCM.

A linear increase in the peak currents as a function of the scan rates confirmed well-adhered electroactive polymer films on the electrode surface as well as non-diffusional redox process (**Figure 3. 22-24**). Moreover, during cathodic scan of the **P(POP-C₁₀)**, it was observed that this polymer has n-doping property different from its counterparts, **P(PSP-C₁₀)**, **P(PSeP-C₁₀)**, and **P(PNP-C₁₀)** (**Figure 3. 25**). As it was previously explained, the reason behind not observing n-doping in these polymers is probably the steric effect of long alkyl chains in the polymer structure. When the attention is turned to the electronegativity values of N, O, S and Se (3.04, 3.44, 2.58 and 2.55, respectively), oxygen has the highest electronegativity value among the others. Thus, it can be concluded that the best acceptor groups between them is the *benzo[c][1,2,5]oxadiazole* due to the greater electronegativity of oxygen atom in the acceptor group and the electronegativity of heteroatom is more effective than the steric effect of the alkyl chains.

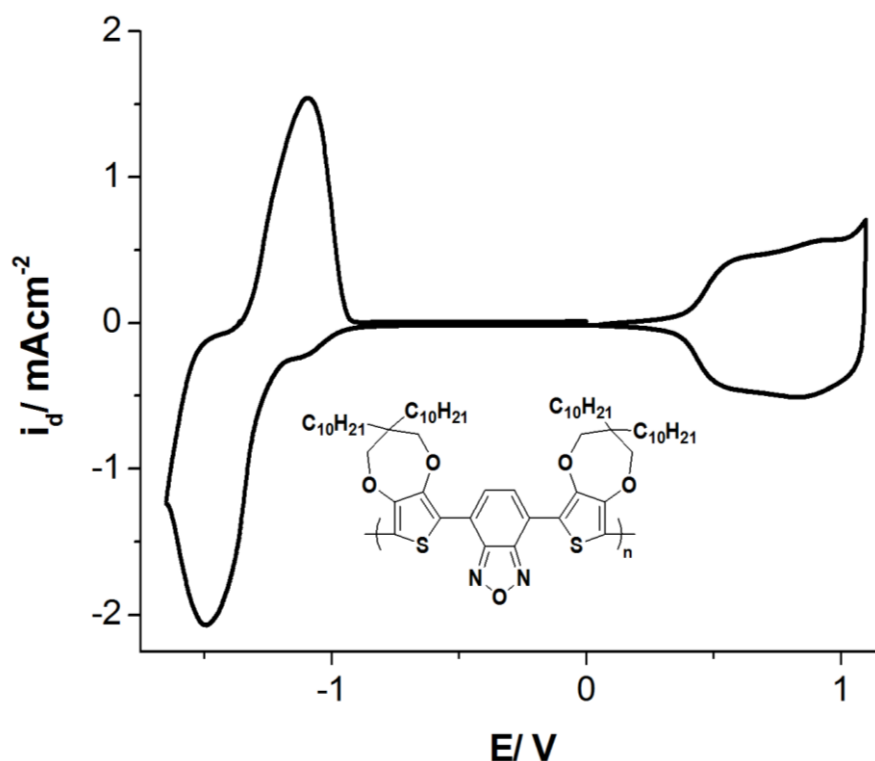
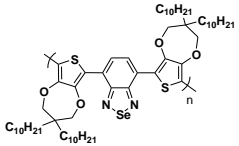


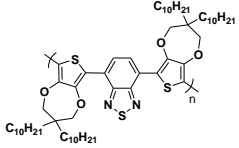


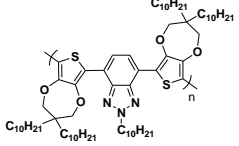


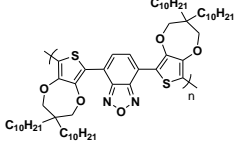




Figure 3.25. CV of n-doped **P(POP-C₁₀)** in 0.1 TBAH/ACN at a scan rate 60 mV/s.

3.2.1.1. Spectroelectrochemical and Switching Behaviors of Polymers

For **P(POP-C₁₀)**, **P(PSP-C₁₀)** and **P(PNP-C₁₀)** spectroelectrochemical behavior was also investigated. It is found that the heteroatom in the acceptor units influenced both the absorption spectrum and the color of the polymers (**Figure 3. 7 (c)**, **Figure 3.26** and **Table 3. 5**). The color of the polymers were changed from green to blue via changing the heteroatom in the acceptor part of the polymers. **P(POP-C₁₀)** and **P(PSP-C₁₀)** are cyan in the neutral state and transparent in the oxidized state. These soluble cyan colored polymers are very precious, since there has been scant attention on the cyan colored polymers [75] because synthesizing cyan colored polymer is not an easy task. This will be discussed in more detail in the colorimetric measurements part.

Table 3.5. Electrochemical and optical data for **PSeP-C₁₀**, **PSP-C₁₀**, **PNP-C₁₀**, and **POP-C₁₀**, and their corresponding polymers, **P(PSeP-C₁₀)**, **P(PSP-C₁₀)**, **P(PNP-C₁₀)**, and **P(POP-C₁₀)**.

Polymer	$E_{m,a}^{ox}$	$E_{m,1/2}^{red}$	$E_{p,1/2}^{ox}$	$\lambda_{max,1}$	$\lambda_{max,2}$	$\lambda_{max,3}$	Neutral State	Oxidized State
 P(PSeP-C₁₀)	0.98	-1.23	0.66	343	419	700		
 P(PSP-C₁₀)	1.00	-1.36	0.48	408	685	-		
 P(PNP-C₁₀)	1.02	-1.31	0.56	585	-	-		
 P(POP-C₁₀)	1.02	-1.20	0.60	400	697	-		

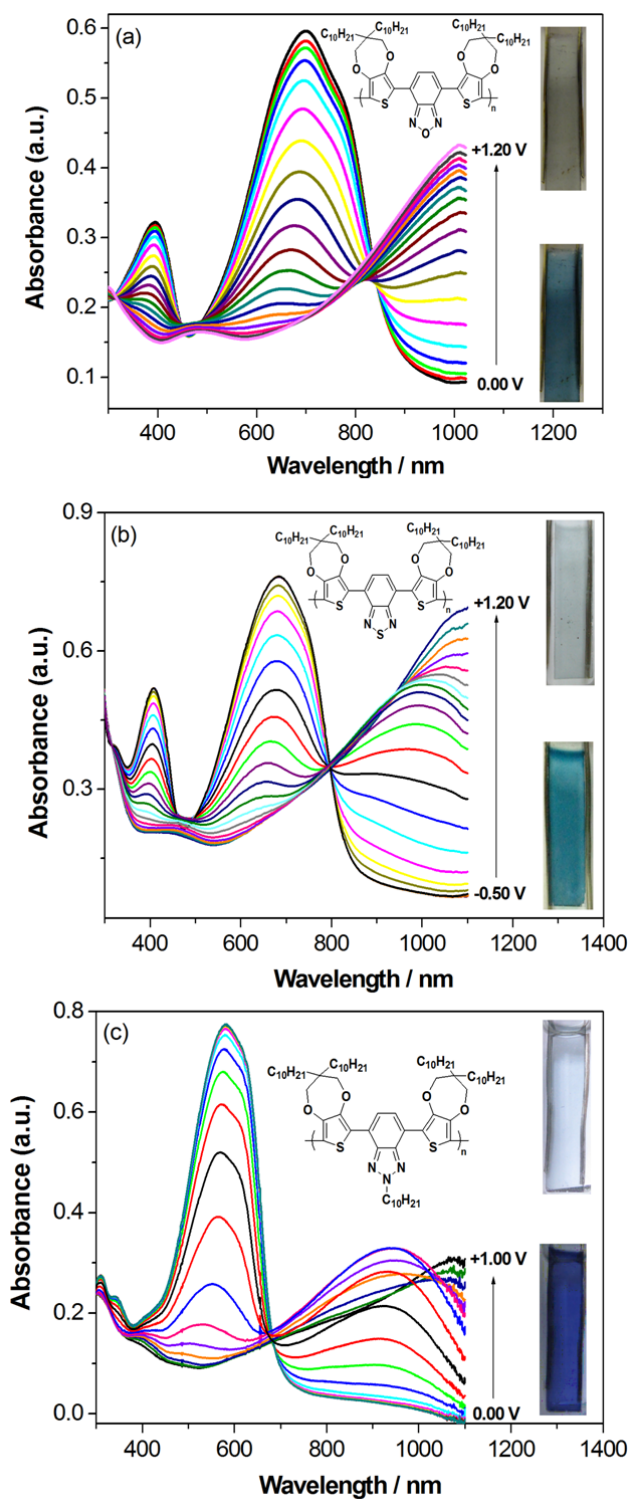


Figure 3.26. Electronic absorption spectra of (a) **P(POP-C₁₀)** (from 0.00 to 1.20 V), (b) **P(PSP-C₁₀)** (from -0.50 V to 1.20 V), and (c) **P(PNP-C₁₀)** (from 0.00 V to 1.00 V) on ITO in 0.1 M TBAH/ACN at various applied potentials.

The optical contrasts and CE values were found to be 38 % and 279 cm²/C at 697 nm with a 0.9 s response time for **P(POP-C₁₀)**, respectively. Another cyan colored polymer has 41.8 % optical contrast at 653 nm in the literature, however, there is not much information about other properties of the polymer, such as CE and switching time [75].

P(PSP-C₁₀) exhibited two well-defined absorption bands at 410 nm and 690 nm. Upon oxidation, while the color changed from cyan to colorless, the intensity of the absorption bands started to decrease simultaneously and a new band at 1000 nm formed due to the formation of charge carriers (**Figure 26(b)**). During this process, the optical contrasts and CE were found to be 51.4% and 230 cm²/C at 690 nm, and 32.8% and 147 cm²/C at 410 nm, respectively. Obviously, the optical contrast and CE values of **P(PSP-C₁₀)** were higher than those of its EDOT analogue (P(ESE)) (see ref. [76] and **Table 3.6**).

On the other hand, the CE (at 95% of the full contrast) and the response time of **P(PNP-C₁₀)** were found as 106 cm²/C and 2.2 s at 480 nm, respectively. CE and response times for **P(PNP-C₁₀)** were calculated as 273 cm²/C and 1.1 s, at 585 nm, respectively. The obtained results confirmed that the properties of **P(PNP-C₁₀)** is better than those of PEDOT and even those of its EDOT analogue, P(ENE) [80] in terms of both optical contrast and CE (**Table 3. 6**). Additionally, considering the fact that **P(PNP-C₁₀)** can easily be processed over surfaces, it is an excellent blue-to-colorless PEC candidate, which, to our best knowledge, exhibits the highest optical contrast and CE, when compared to PEDOT and/or P(ENE) [80] (see **Table 3. 6**).

Table 3.6. Optical and switching time data of electrochemically synthesized polymers **P(PSeP-C₁₀)**, **P(POP-C₁₀)**, **P(PSP-C₁₀)**, **P(PNP-C₁₀)** and their analogues. The given CE value is the best one at a given wavelength.* P(ESE) is poly(4-(2,3-dihydrothieno[3,4-b][1,4]dioxin-5-yl)-7-(2,3-dihydrothieno[3,4-b][1,4]dioxin-7-yl)benzo[c][1,2,5]thiadiazole) and P(ENE) is poly-4,7-bis(2,3-dihydrothieno[3,4-b][1,4]dioxin-5-yl)-2-dodecyl-2H-benzo [1,2,3] triazole [76, 80].

Polymer	Wavelength (λ_{\max}, nm)	Contrast %T	CE (cm²/C)	Switching time (t, s)
P(PSeP-C₁₀)	715	40.3	208	0.6
P(ESE)* [76]	755	23.0	130	0.4
P(POP-C₁₀)	697	38.0	279	0.9
P(PSP-C₁₀)	690	38.5	230	1.4
P(ENE)* [80]	618	53.0	211	1.1
P(PNP-C₁₀)	585	61.8	273	1.1

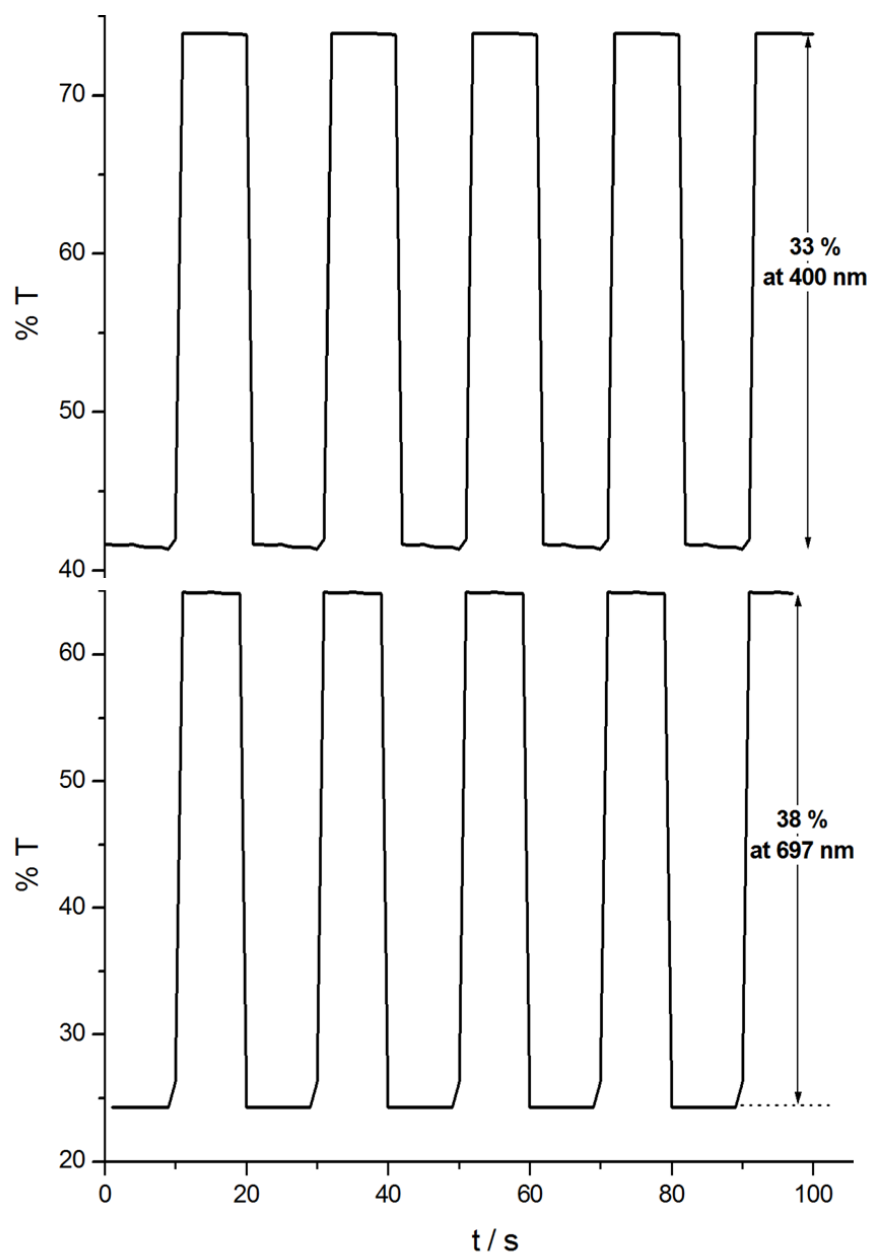


Figure 3.27. Chronoabsorptometry experiments for **P(POP-C₁₀)** on ITO in 0.1 M TBAH/ ACN while the polymer was switched between 1.2 V and 0.0 V.

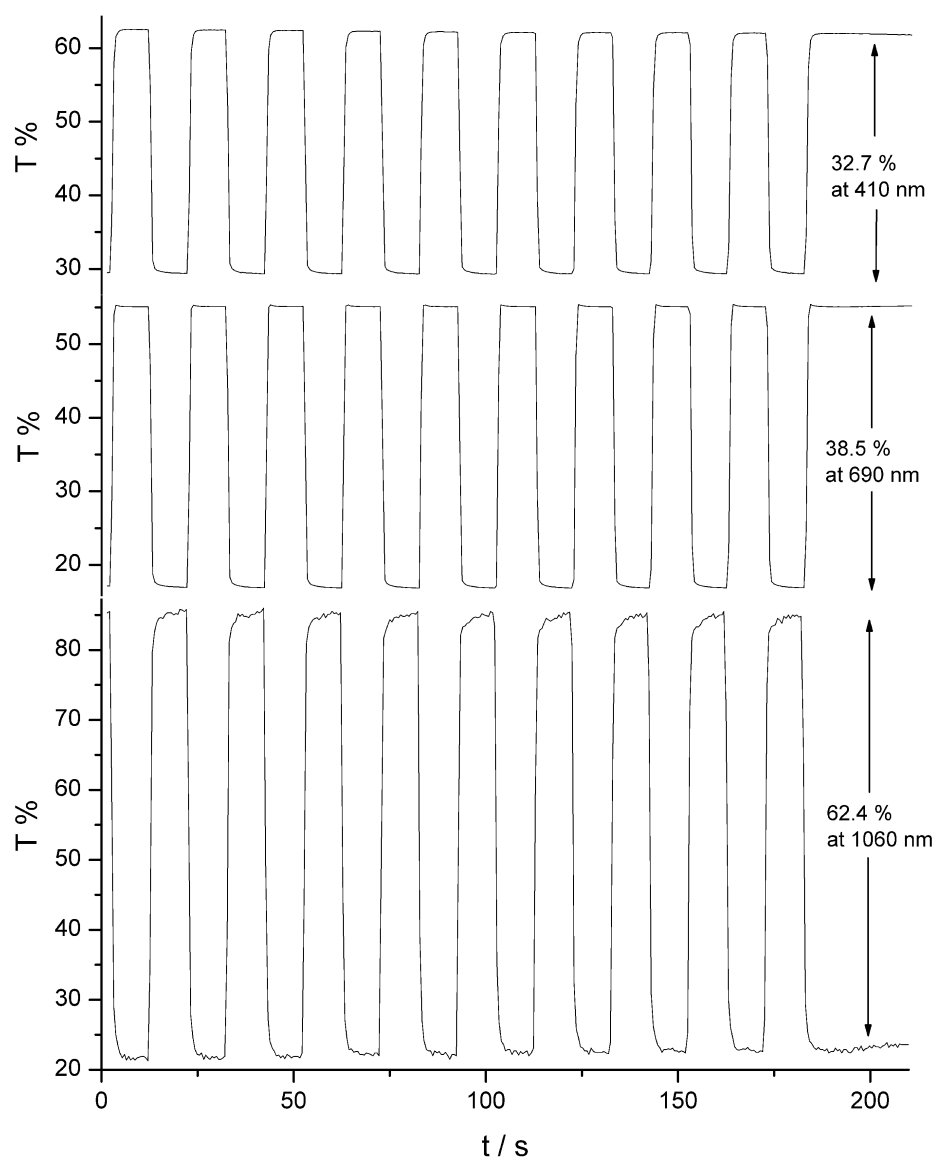


Figure 3.28. Chronoabsorptometry experiments for **P(PSP-C₁₀)** on ITO in 0.1 M TBAH/ ACN while the polymer was switched between 1.2 V and -0.5 V.

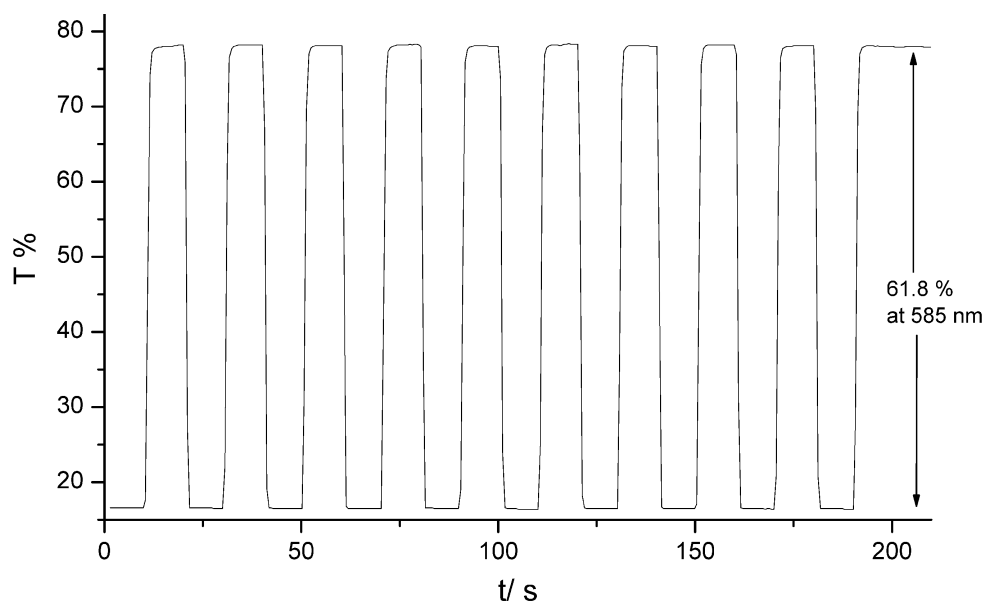


Figure 3.29. Chronoabsorptometry experiments for **P(PNP-C₁₀)** on ITO in 0.1 M TBAH/ACN during the polymer was switched between 1.0 V and 0.0 V.

In the situation of the **P(PNP-C₁₀)**, a soluble, that is, a processable polymer was obtained by integrating ProDOT-decyl₂ donor units to the polymer structure. It was also previously aimed to obtain a soluble polymer via alkylation of benzotriazole acceptor units with EDOT donor unit, however, it was not achieved [80].

The band gaps (E_g) of **P(PSeP-C₁₀)**, **P(PSP-C₁₀)**, **P(POP-C₁₀)** and **P(PNP-C₁₀)** were calculated from the onset of the low energy end of the π - π^* transitions to be 1.37 eV, 1.48 eV, 1.40 eV, and 1.80 eV, respectively. It was observed that, there has been no correlation between the electronegativity values of the heteroatoms on the acceptor units, that is, electron density of the A unit, and LUMO level of the obtained polymers (**Figure 3. 30** and **Table 3. 7**). It can be explained by the “band gap compression”(Figure 1. 6 and see ref. [47])

Table 3.7. Electrochemically determined HOMO, LUMO and E_g values of polymers, **P(PSeP-C₁₀)**, **P(PSP-C₁₀)**, **P(PNP-C₁₀)**, and **P(POP-C₁₀)**.

Polymer	E_{ox} onset (V)	HOMO (eV)	LUMO (eV)	E_g optical (V)
P(PSeP-C₁₀)	0.48	5.28	3.91	1.37
P(PSP-C₁₀)	0.33	5.13	3.63	1.48
P(PNP-C₁₀)	0.46	5.26	3.46	1.80
P(POP-C₁₀)	0.48	5.28	3.88	1.40

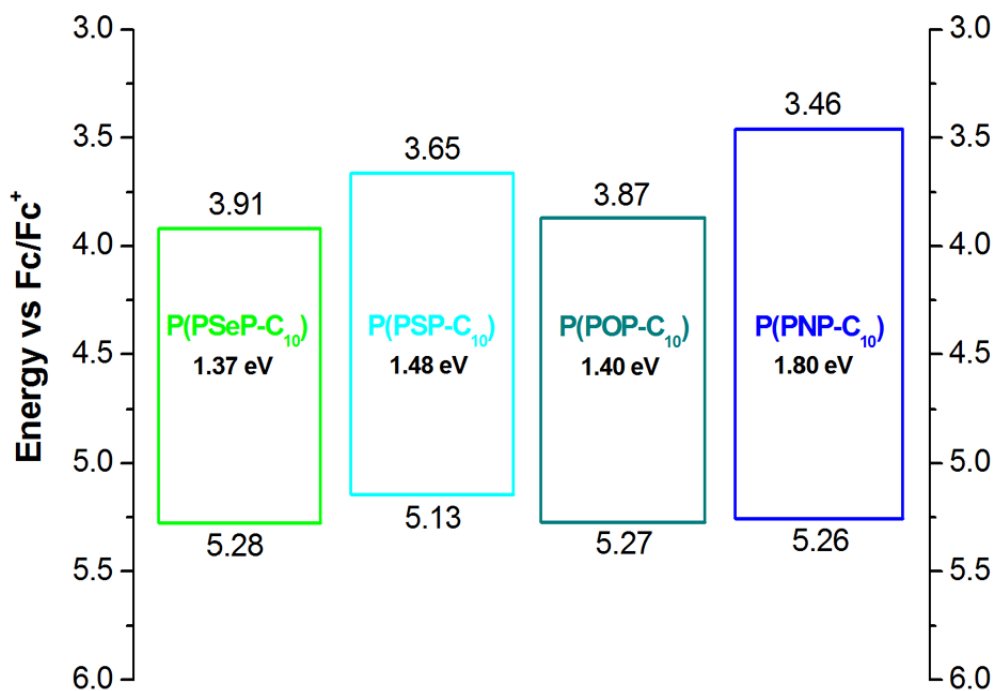


Figure 3.30. Energy band diagram of the polymers **P(PSeP-C₁₀)**, **P(PSP-C₁₀)**, **P(POP-C₁₀)** and **P(PNP-C₁₀)**.

3.2.2.3. Optical Properties of the Polymers

As in the case of **P(PSeP-C₁₀)**, also **P(PSP-C₁₀)**, **P(POP-C₁₀)** and **P(PNP-C₁₀)** are soluble in organic solvents such as DCM and CHCl₃, whereas slightly soluble in toluene. For that reason, all these polymers could easily be processed over surfaces via spin coating, spraying, dip coating and printing techniques.

Like **P(PSeP-C₁₀)**, **P(PSP-C₁₀)**, **P(POP-C₁₀)** and **P(PNP-C₁₀)** are also polymerized chemically in order to obtain the polymers in large quantities. After that, again the polymers were spray coated onto ITO with the same method. That is, 2 mg polymer was dissolved in 1 mL CHCl₃ and spray coated via Aztek airbrush at 10 psi Ar.

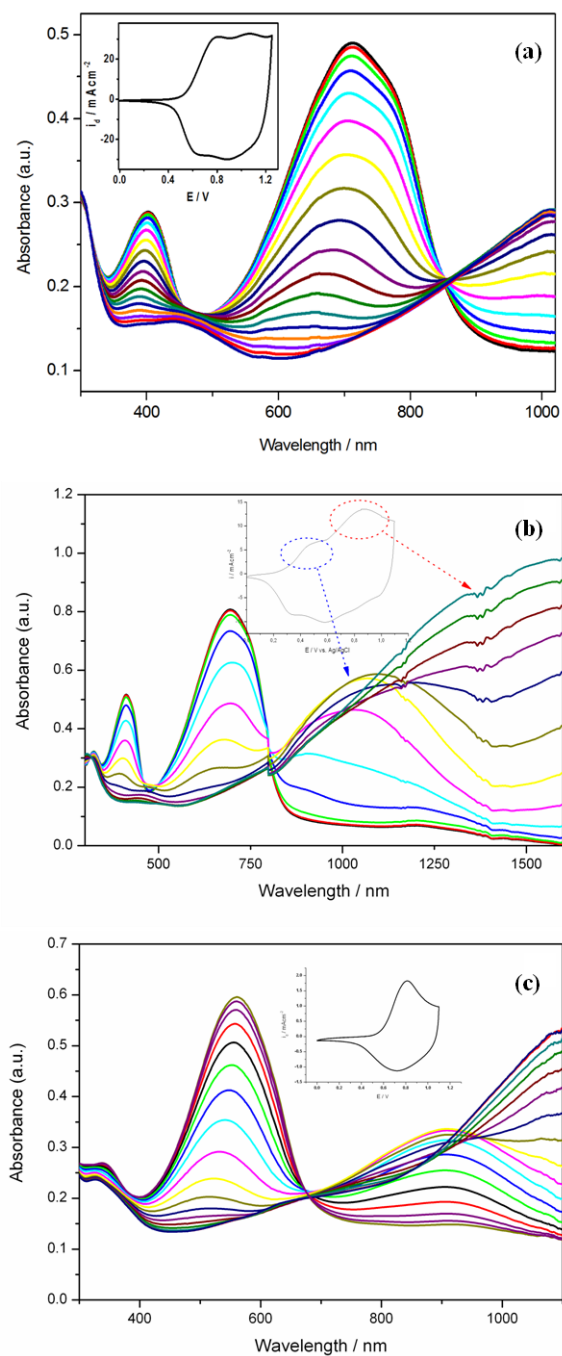


Figure 3.31. Electronic absorption spectrum of chemically synthesized (a) **P(POP-C₁₀)** (from 0.0 V to 1.2 V), (b) **P(PSP-C₁₀)** (from 0.0 V to 1.2 V), and (c) **P(PNP-C₁₀)** (from 0.0 V to 1.2 V) which was spray/ dip coated on ITO in 0.1 M TBAH/ACN. Insets: Cyclic voltammograms of chemically synthesized **P(POP-C₁₀)**, **P(PSP-C₁₀)** and **P(PNP-C₁₀)** coated on ITO in 0.1 TBAH/ACN at a scan rate of 100 mV/s.

The optical contrast and response time for **P(PSP-C₁₀)** were calculated as 34 % and 0.85 s at 410 nm and 40 % and 0.53 s at 690 nm, and 85 % and 0.65 s at 1700 nm, respectively. Those of **P(PNP-C₁₀)** were found as 5.5 % and 2 s at 330 nm, 43 % and 1.1 s at 560 nm, and 36 % and 7 s at 1000 nm, respectively (**Table 3. 4** and Figures **3. 32** and **3. 33**).

It was observed that **P(POP-C₁₀)** and **P(PSP-C₁₀)** exhibited nearly the same characteristics (similar CV and spectroelectrochemistry **Figure 3.31**) when compared to that of the electrochemically deposited **P(POP-C₁₀)** and **P(PSP-C₁₀)**, respectively. The color of the polymers were also the same with the electrochemically obtained ones, that is, the color of the **P(POP-C₁₀)** and **P(PSP-C₁₀)** were turned from cyan to transparent via oxidation. However, for **P(PNP-C₁₀)** a blue shift was observed around 25 nm when the method was turned from electrochemical polymerization to chemical polymerization, that is, the absorption band of the polymers shifted from 585 nm to 560 nm (see **Figure 3. 26 (c)**, **Figure 3. 31 (c)** and also **Table 3. 6** and **Table 3. 4**). Therefore, the obtained polymer's color was no more blue when the polymerization method is chemical polymerization, its color was magenta. This should be because of different chain length of the obtained polymers at different methods. Thus, via adjusting the chemical polymerization, the color, i.e., the optical properties of the polymer can be adjusted. However, no further studies had been done on this. Although it seems that this result, obtaining magenta colored polymer instead of a blue one, a disadvantage, actually it should be turned to an advantage. Since, there has been limited number of soluble polymers having magenta color in the literature [50].

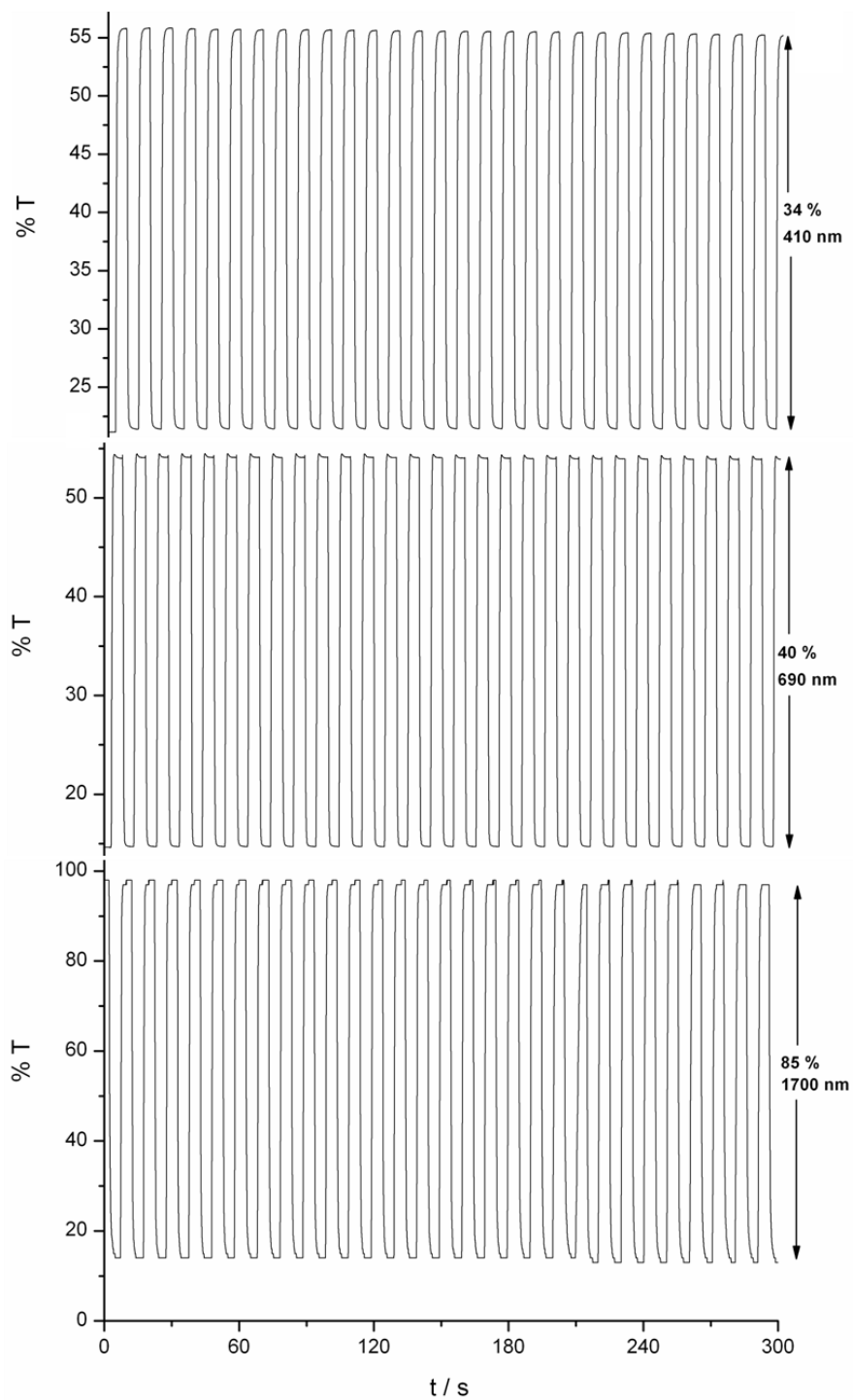


Figure 3.32. Chronoabsorptometry experiments for chemically polymerized **P(PSP-C₁₀)** coated on ITO in 0.1 M TBAH/ ACN while the polymer was switched between 0.0-1.2 V.

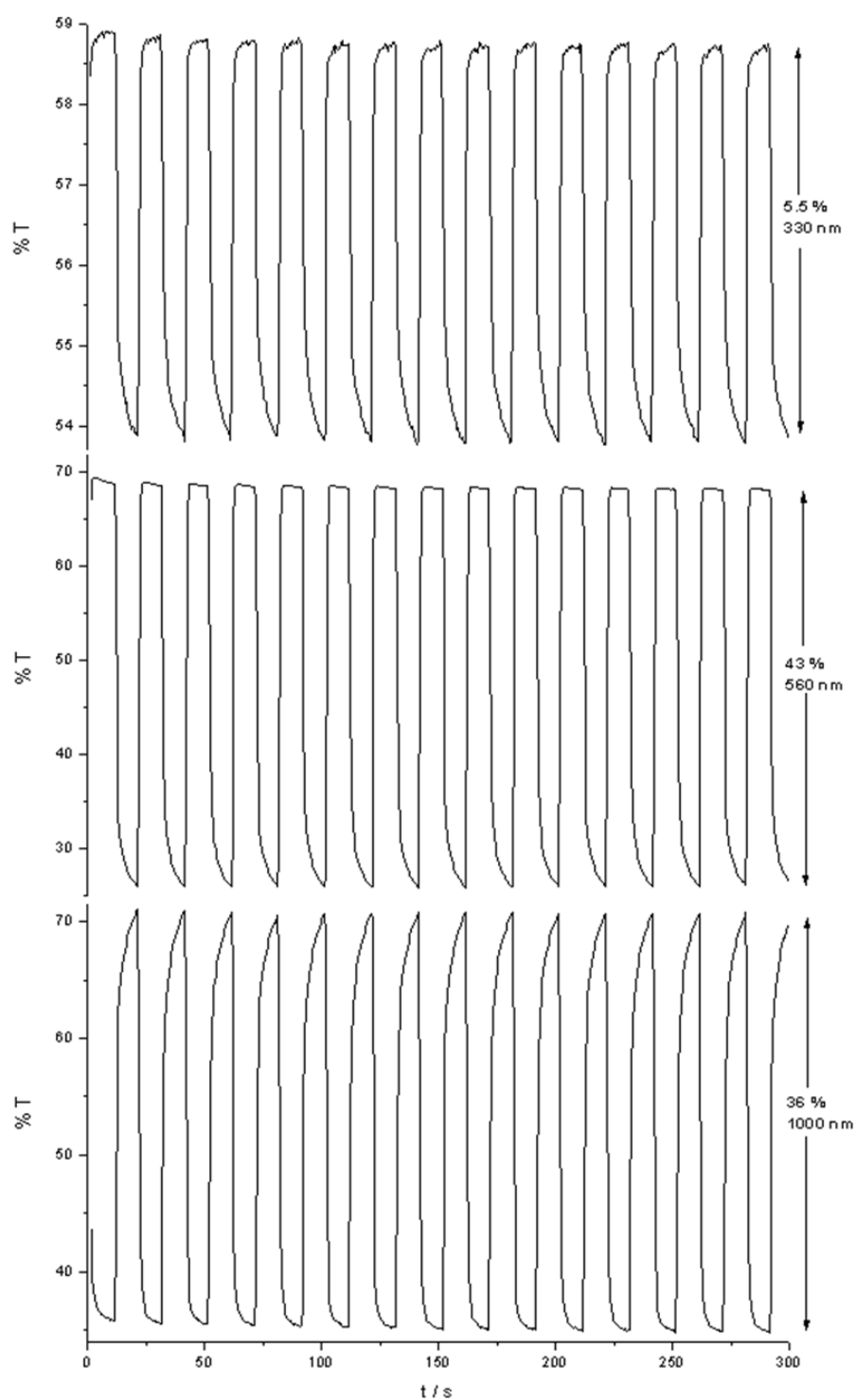


Figure 3.33. Chronoabsorptometry experiments for chemically polymerized **P(PNP-C₁₀)** coated on ITO in 0.1 M TBAH/ ACN while the polymer was switched between 0.0-1.2 V.

3.2.2.4. Properties of the Polymers

Like **P(PSeP-C₁₀)**, in endeavours to dope and dedope, chemically obtained **P(POP-C₁₀)** and **P(PSP-C₁₀)** again SbCl_5 and $\text{N}_2\text{H}_5\text{OH}$ were used. For this purpose, chemically obtained and neutralized **P(POP-C₁₀)** and **P(PSP-C₁₀)** were first dissolved in DCM and then p-doped by adding 10^{-3} M SbCl_5 solution in 10 μL portions (**Figure 3. 34 (a)** and **(c)**). For neutralization, i.e., dedoping, 10^{-2} M $\text{N}_2\text{H}_5\text{OH}$ solution in DCM was added again in 10 μL portions (**Figure 3. 34 (b)** and **(d)**). It was observed that the results obtained from chemical doping-dedoping procedure were almost same with the electrochemical ones (**Figure 3. 31 (a)** and **(b)**). As mentioned before, this procedure should be useful for the determination of the doping-dedoping process, i.e., the formation of the charge carriers. It will be discussed in detail in the polymer characterization part.

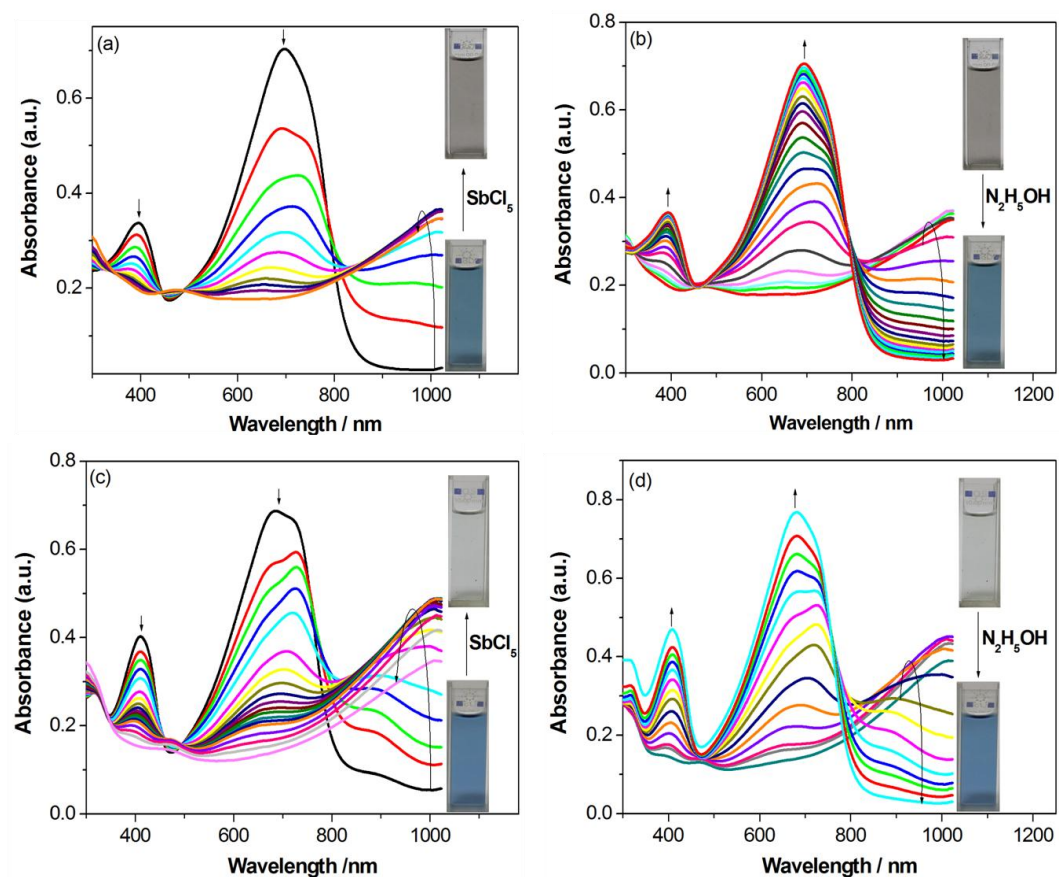


Figure 3.34. Changes in optical absorption spectra of chemically obtained (a) **P(POP-C₁₀)** and (b) **P(PSP-C₁₀)** in DCM solution after addition of 10 μ L (for each spectrum) 10^{-3} M SbCl_5 and 10^{-2} M $\text{N}_2\text{H}_5\text{OH}$.

3.2.2.5. Stability of the Polymers

Electrochemical stability of the polymers, **P(POP-C₁₀)**, **P(PSP-C₁₀)** and **P(PNP-C₁₀)** upon switching were investigated. During these investigations, whereas **P(PSP-C₁₀)** and **P(PNP-C₁₀)** were switched between the whole redox ranges, **P(POP-C₁₀)** was switched between in the range of first redox couple. Since the polymers show optical behavior in that range, it is not necessary to see second redox range. **P(POP-C₁₀)**,

P(PSP-C₁₀) and **P(PNP-C₁₀)** showed excellent stabilities: They retained 94 %, 72 % and 76 % of their electroactivity after 2000 switching, respectively (**Figure 3. 35**). When the results were compared with the thiophene containing D-A-D counter part of these polymers, i.e. **P(TSeT)**, (see **Figure 3. 18**) the stabilities of these polymers are rather higher than that of **P(TSeT)** (63 %). This proves the contribution of the ProDOT-C_n units to the stability.

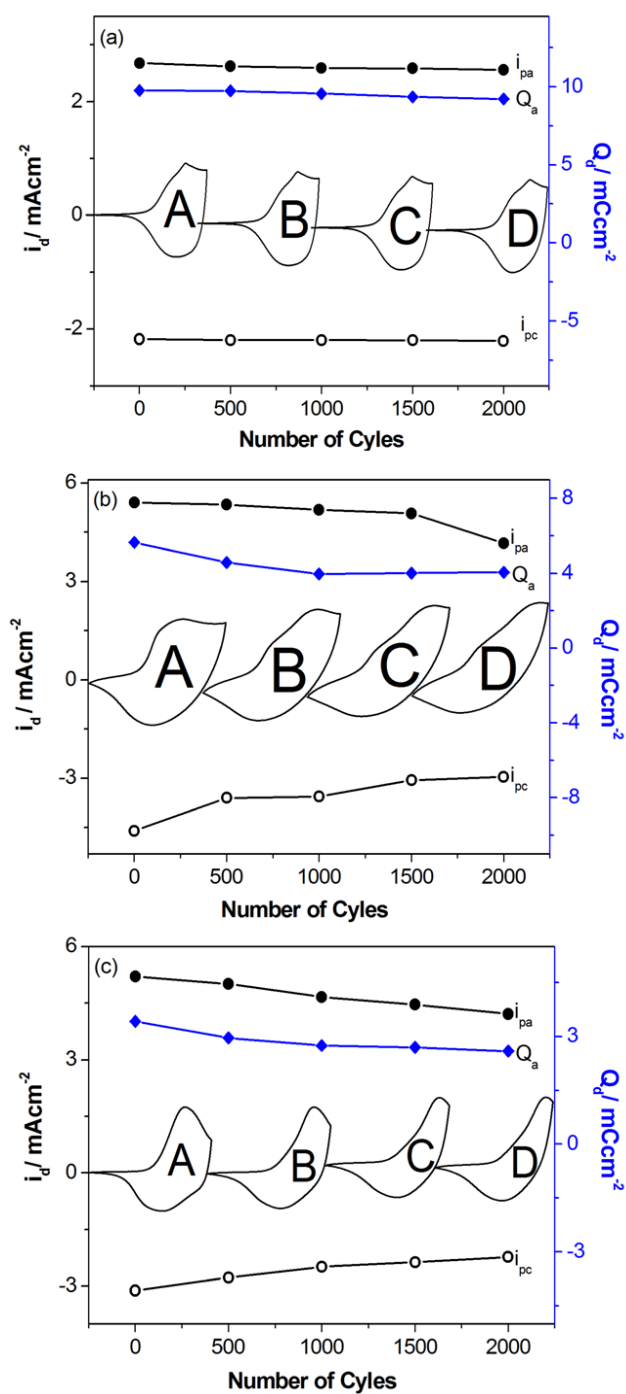


Figure 3. 35. Stability test for (a) **P(POP-C₁₀)**, (b) **P(PSP-C₁₀)**, (c) **P(PNP-C₁₀)** films in 0.1 M TBAH/DCM at a scan rate of 100 mV s^{-1} under ambient conditions by cyclic voltammetry as a function of the number of cycles: A: 1, B: 500, C: 1000, D: 2000 cycles; Q_a : Anodic charge stored, i_{pa} : Anodic peak current, i_{pc} : Cathodic peak current.

3.2.2.6. Colorimetric Measurements of the Polymers

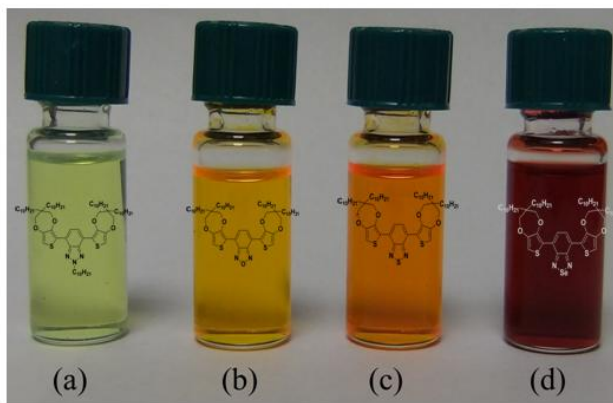


Figure 3.36. The colors of the solutions of 10^{-6} M (a) **PNP-C₁₀**, (b) **POP-C₁₀**, (b) **PSP-C₁₀**, (b) **PSeP-C₁₀** in DCM.

Since at the early stages of this study, the neutral state green polymer, **P(PSeP-C₁₀)**, and then the neutral state blue one, **P(PNP-C₁₀)** were obtained. After those results, the question here is that if it would be possible to obtain neutral state cyan colored polymer via changing the heteroatom of acceptor unit. **PSP-C₁₀** and **POP-C₁₀** were synthesized and polymerized for this purpose. In **Figure 3. 36**, the colors of the monomers **PSeP-C₁₀**, **PSP-C₁₀**, **POP-C₁₀** and **PNP-C₁₀** can be seen at the same concentration in DCM. It was observed that, as the heteroatom was changed from nitrogen to selenium, the color of the monomer was turned from yellow to red in a sequence. It was wondered that, also a sequence can be obtained for the polymers, that is, it is possible to obtain cyan colored polymer via just changing the heteroatom in the acceptor unit. Actually, the results were as expected: **P(PSeP-C₁₀)**, **P(PSP-C₁₀)**, **P(POP-C₁₀)** and **P(PNP-C₁₀)** have green, cyan, dark cyan and blue colors in the neutral state, respectively (**Figure 3. 37**) and they all are transparent in the oxidized state. As mentioned before, since everybody has different color concepts, a more scientific method was used to determine the color: Colorimetry. In **Figure 3. 37**, the colorimetric measurement results can be seen.

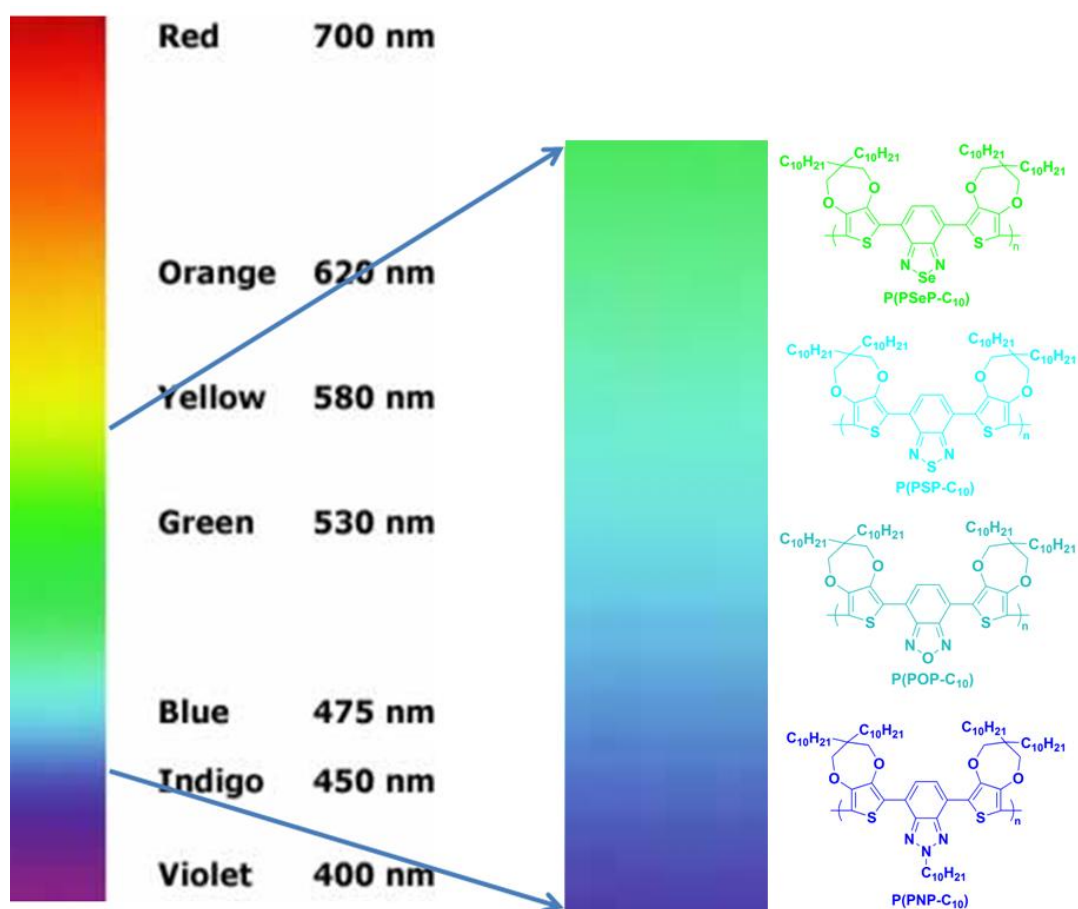


Figure 3.37. Distribution of **P(PSeP-C₁₀)**, **P(PSP-C₁₀)**, **P(POP-C₁₀)** and **P(PNP-C₁₀)** polymers' color in their neutral states on the spectrum of visible region.

Among these polymers, **P(PSeP-C₁₀)** has the least transparency, since it has higher hue than the others, that is, its a^* and b^* values are less closer to the zero. All polymers, **P(PSeP-C₁₀)**, **P(PSP-C₁₀)**, **P(POP-C₁₀)** and **P(PNP-C₁₀)**, have high transparency, since their L^* values are nearer to 100. Since, **P(PNP-C₁₀)** has a large negative b^* value, it has a deep blue color whereas larger a^* values for **P(PSeP-C₁₀)**, **P(PSP-C₁₀)**, **P(POP-C₁₀)** are account for the green, cyan and dark cyan (tunes of green) colors, respectively, since they have negative a^* values (**Figure 3. 38**).

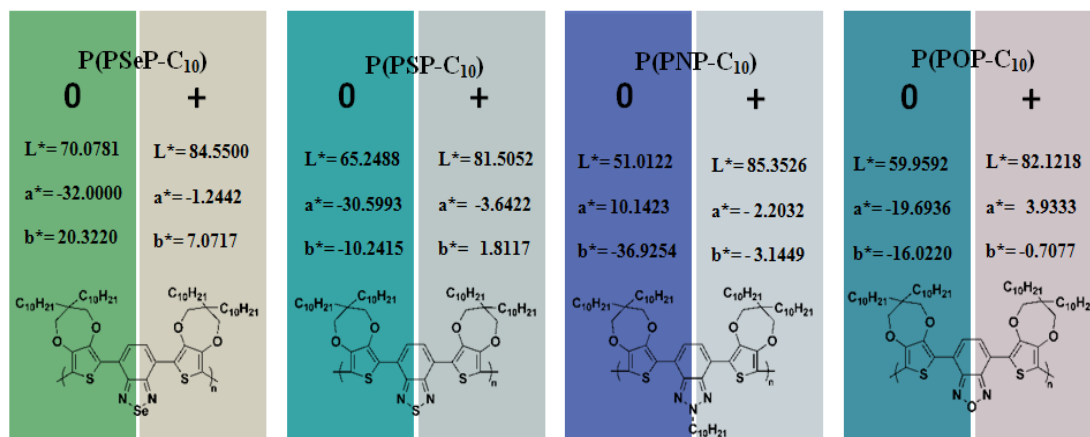
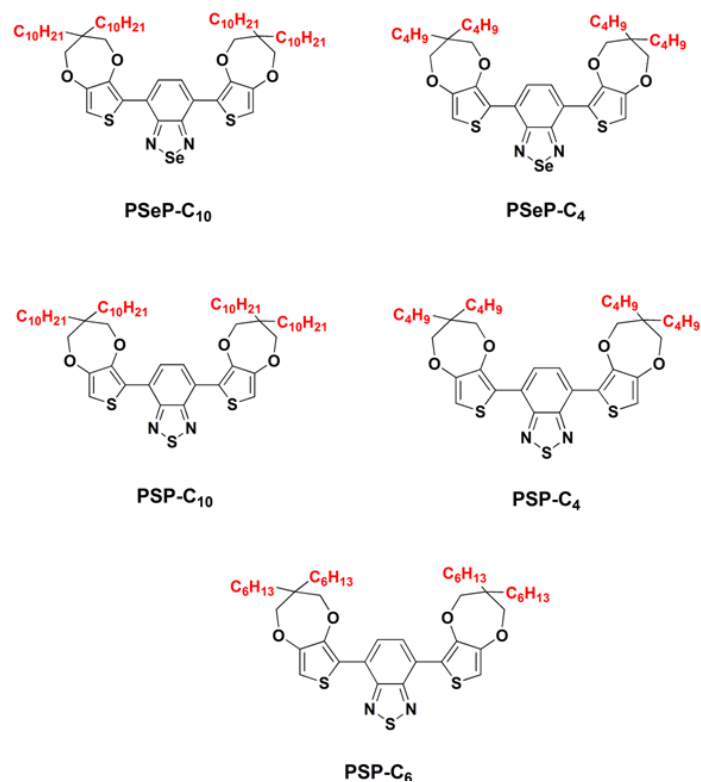


Figure 3.38. $L^*a^*b^*$ values of the **P(PSeP-C₁₀)**, **P(PSP-C₁₀)**, **P(POP-C₁₀)** and **P(PNP-C₁₀)** in their neutral (0) and oxidized state (+).

3.2.3. Effect of Alkyl Chain Length

In this part, in order to investigate the effect of the alkyl chain on the electrochemical and optical properties of a polymer, five new monomers, **PSeP-C₁₀**, **PSeP-C₄**, **PSP-C₁₀**, **PSP-C₄** and **PSP-C₆** (Scheme 3. 5), and their corresponding polymers, **P(PSeP-C₁₀)**, **P(PSeP-C₄)**, **P(PSP-C₁₀)**, **P(PSP-C₄)** and **P(PSP-C₆)** were synthesized and their electrochemical and optical properties were investigated.



Scheme 3.5. Monomers that are used for the investigation of alkyl chain length effect.

Much of the focus has been on the design and synthesis of p-type (hole transporting) organic π -conjugated materials, probably due to the fact that it is relatively easier to design electron-rich conjugated polymers (p-type) rather than electron-poor ones (n-type). Besides, n-type (electron transporting) materials have some serious drawbacks such as instability in air and poor solubility. However, the systems exhibiting both n- and p-type doping would be fascinating in terms of extending the colors available with a single material [41].

As it is explained up to here, the polymers obtained from **PNP-C₁₀**, **POP-C₁₀**, **PSP-C₁₀** and **PSeP-C₁₀**, that is **P(PNP-C₁₀)**, **P(POP-C₁₀)**, **P(PSP-C₁₀)** and **P(PSeP-C₁₀)**, were excellent processable high performance (high stability, high optical contrast, high coloration efficiency, and sub-second switching time) PEC candidates, which

had a specific band gap to reflect the blue, dark cyan, cyan and green colors, respectively. Interestingly, however, among these polymers only **P(POP-C₁₀)** showed n-doping property. The fact that n-doping process was observed with similar systems without any alkyl chains, such as thiophene [93,94], 3,4-ethylenedioxythiophene [76,88] or selenophene [97], has stimulated us to investigate the effect of the alkyl chain length of the D- units on the doping process (**Scheme 3.5**).

3.2.3.1. Cyclic Voltammograms of the Monomers

PSP-C₁₀, **PSP-C₆** and **PSP-C₄** exhibited one irreversible oxidation peak around 1.0 V arising from the D-unit with a reversible reduction peak at about -1.35 V due to benzothiadiazole unit (**Figure 3.39**). Furthermore, no appreciable shift in the peak potential values was observed. Among them, **PSP-C₆** exhibited somewhat less positive oxidation peak (0.95 V) and also less negative reduction (1.31 V), which was probably due to the conformation of the hexyl chains [99].

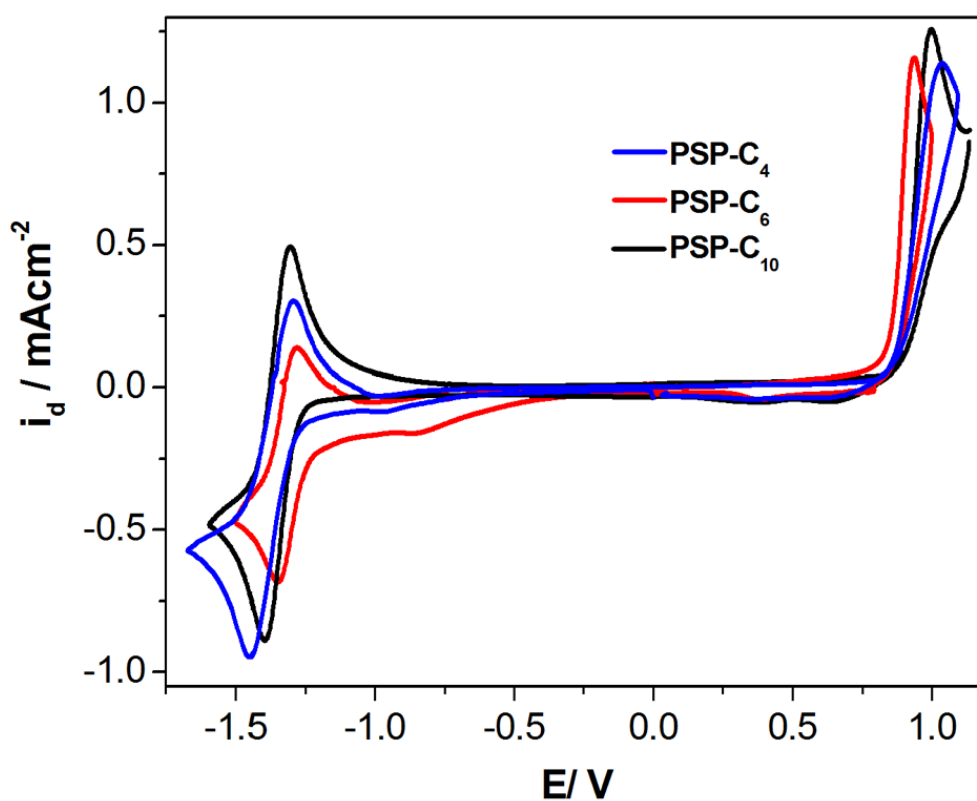


Figure 3.39. Cyclic voltammograms of **PSP-C₁₀**, **PSP-C₆** and **PSP-C₄** in 0.1 M TBAH/ DCM at 100 mV/s.

In order to confirm the results obtained from thiadiazole A unit containing monomers, **PSeP-C₁₀** and **PSeP-C₄** were also synthesized, and the same behavior was observed. Since the D- units are almost the same except the length of alky chain, there is no appreciable difference in the oxidation potential of the monomers. Similarly, their reduction potentials were also very close to each other since the A groups were the same (**Figure 3. 40**).

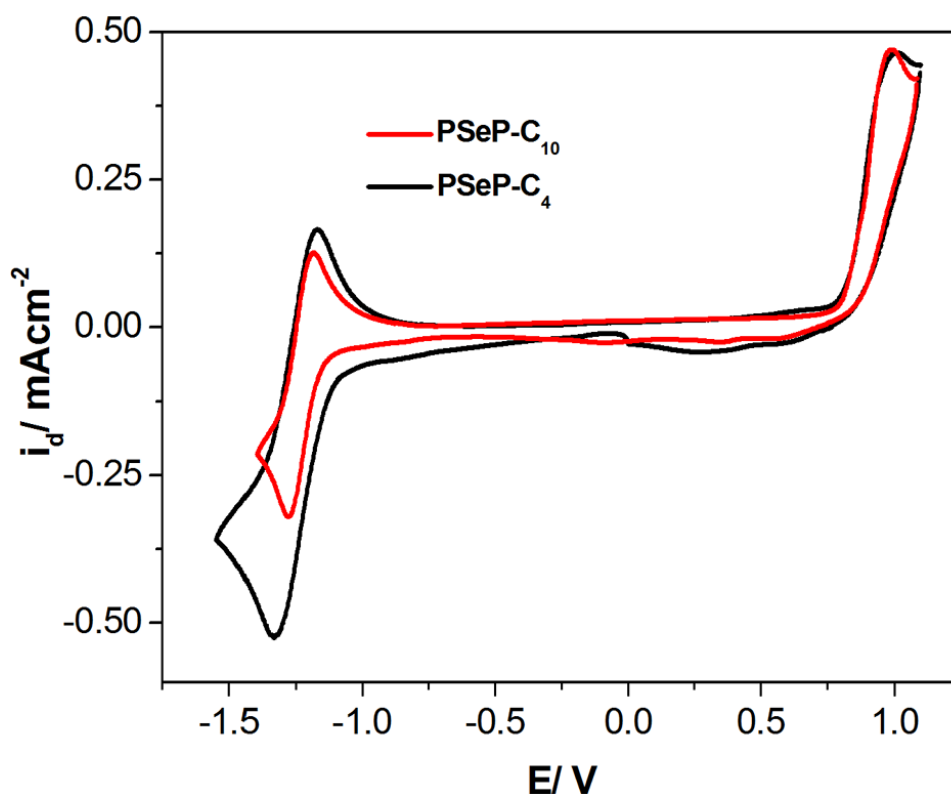


Figure 3.40. Cyclic voltammograms of **PSeP-C₁₀** and **PSeP-C₄** in 0.1 M TBAH/DCM at 100mV/s.

3.2.3.2. Electrochemical Polymerization and Properties of the Polymers

As in the situation of **PSP-C₁₀** and **PSeP-C₁₀**, electropolymerization of **PSP-C₆**, **PSP-C₄** and **PSeP-C₄** was carried out in a mixture of DCM and ACN solution containing in 0.1 M TBAH. During the repetitive scanning, a new reversible redox couple appeared which is characteristic signature of a conducting polymer film formation on the electrode surface (**Figure 3. 41**). Also, as expected from the formation of a conducting polymer film, after each successive scan, the current values of the redox couple were intensified, confirming the increasing polymer film thickness.

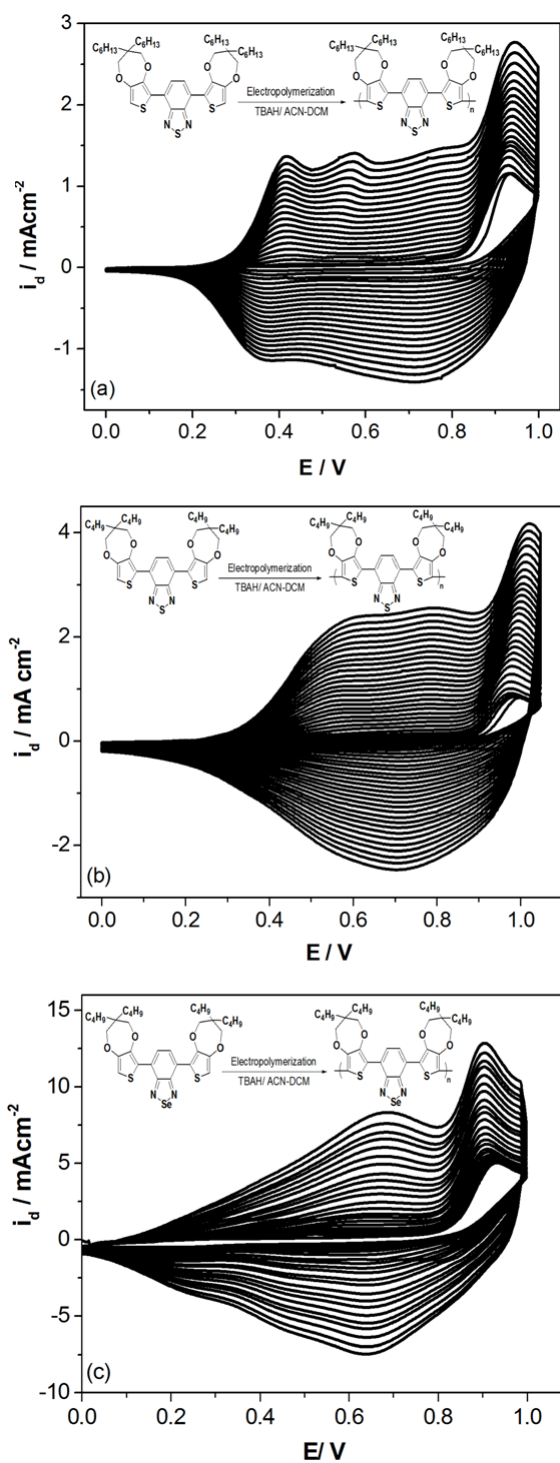
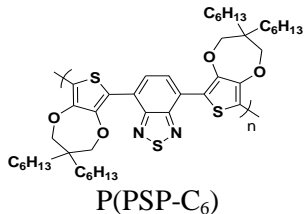

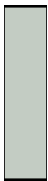
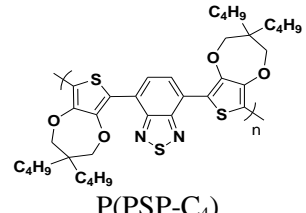


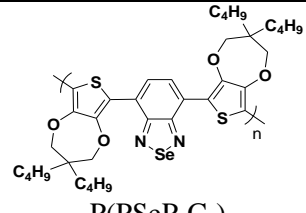




Figure 3.41. Electropolymerization of (a) 3.0×10^{-3} M PSP-C₆ (b) 5.0×10^{-3} M PSP-C₄ and (c) 16.0×10^{-3} M in 0.1 M TBAH-DCM/ACN (5:95-v/v) at a scan rate of 100 mV/s by potential scanning to give P(PSP-C₆), P(PSP-C₄) and P(PSeP-C₄), respectively.

Like **P(PSeP-C₁₀)**, **P(PSeP-C₄)** has green color in the neutral state. **P(PSP-C₁₀)**, **P(PSP-C₆)** and **P(PSP-C₄)** have cyan color (**Table 3. 8** and **Table 3. 9**). As expected, the length of the alkyl chain has no observable change on the color of the polymers.

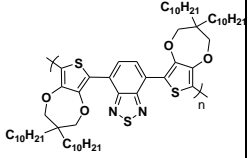


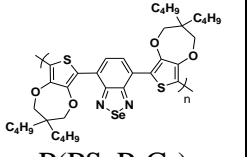


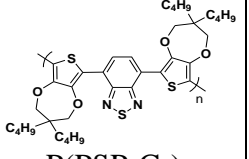


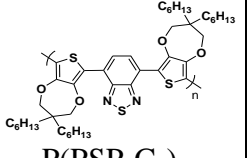


Table 3.8. Colorimetric data for **PSP-C_n** (n=4 and 6) and **PSeP-C₄**.

Polymers	Colorimetric results			Colors of Polymers	
		Neut.	Ox.	Neut.	Ox.
 P(PSP-C ₆)	L*	63.59	83.22		
	a*	-27.42	-3.55		
	b*	-12.00	1.99		
 P(PSP-C ₄)	L*	50.81	73.25		
	a*	-26.92	-4.05		
	b*	0.49	5.17		
 P(PSeP-C ₄)	L*	62.20	76.13		
	a*	-21.59	-3.71		
	b*	9.54	2.19		

Polymers were anodically scanned in a monomer-free electrolyte solution of 0.1 M TBAH/ACN. During the anodic scan of **P(PSP-C₆)**, **P(PSP-C₄)** and **P(PSeP-C₄)**, well-defined reversible redox couples ($E_{p,1/2}^{ox} = 0.40$ V for **P(PSP-C₆)**, $E_{p,1/2}^{ox} = 0.35$ V for **P(PSP-C₄)**, $E_{p,1/2}^{ox} = 0.70$ V for **P(PSeP-C₄)**) were observed like **PSP-C₁₀** and **PSeP-C₁₀** (**Figure 3. 42-44**). As in the case of the decyl containing counter parts (**P(PSP-C₁₀)** and **P(PSeP-C₁₀)**) of these polymers (**P(PSP-C₆)**, **P(PSP-C₄)** and **P(PSeP-C₄)**), Se atom containing polymers in the A parts have higher oxidation

potential than S containing ones (**Table 3.5** and **Table 3. 9**). A linear increase in the peak currents as a function of the scan rates confirmed well-adhered electroactive polymer films on the electrode surface as well as non-diffusional redox process (**Figure 3. 42-44**).

Table 3.9. Electrochemical and optical data for **PSP-C₁₀**, **PSeP-C₄**, **PSP-C₄** and **PSP-C₆**, and their corresponding polymers, **P(PSP-C₁₀)**, **P(PSeP-C₄)**, **P(PSP-C₄)** and **P(PSP-C₆)**.

Polymer	$E_{m,a}^{ox}$	$E_{m,1/2}^{red}$	$E_{p,1/2}^{ox}$	$\lambda_{max,1}$	$\lambda_{max,2}$	$\lambda_{max,3}$	Neutral State	Oxidized State
 P(PSP-C₁₀)	1.00	-1.36	0.48	408	685	-		
 P(PSeP-C₄)	0.99	-1.26	0.70	348	420	697		
 P(PSP-C₄)	1.03	-1.37	0.35	409	674	-		
 P(PSP-C₆)	0.95	-1.32	0.40	417	665	-		

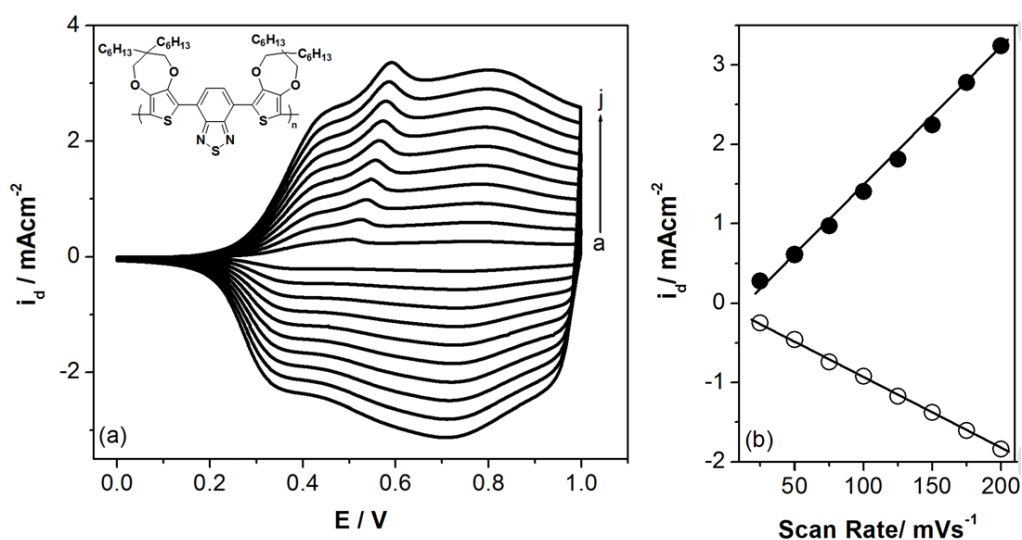


Figure 3.42. (a) Cyclic voltammograms of p-doped **P(PSP-C₆)** in 0.1M TBAH/ACN at a scan rate of (a-j) 20-200 mVs⁻¹ with 20 mVs⁻¹ increments. (b) Relationship of anodic (*i_{p,a}*) peaks as a function of scan rate for p-doped **P(PSP-C₆)** film in 0.1 M TBAH/DCM.

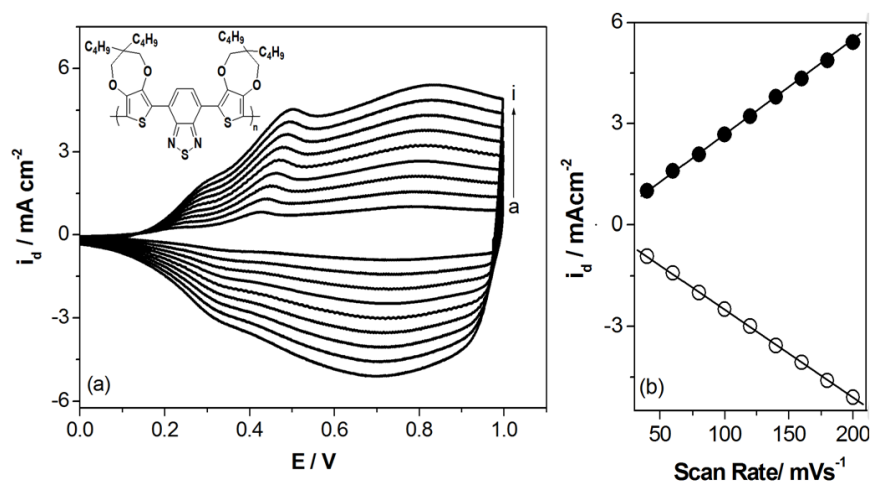


Figure 3.43. (a) Cyclic voltammograms of p-doped **P(PSP-C₄)** in 0.1M TBAH/ACN at a scan rate of (a-i) 40-200 mVs⁻¹ with 20 mVs⁻¹ increments. (b) Relationship of anodic (*i_{p,a}*) peaks as a function of scan rate for p-doped **P(PSP-C₄)** film in 0.1 M TBAH/DCM.

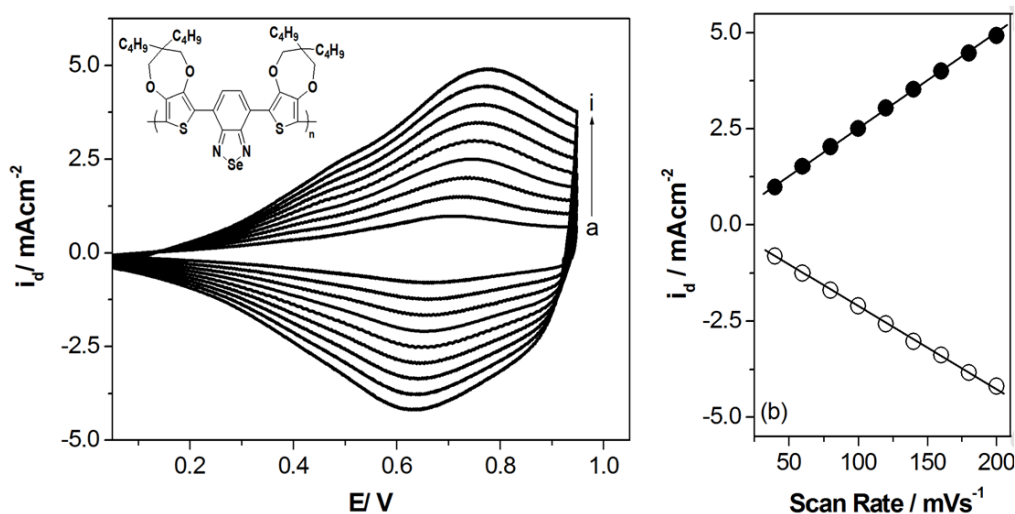


Figure 3.44. (a) Cyclic voltammograms of p-doped **P(PSeP-C₄)** in 0.1M TBAH/ACN at a scan rate of (a-i) 40-200 mVs⁻¹ with 20 mVs⁻¹ increments. (b) Relationship of anodic (*i_{p,a}*) peaks as a function of scan rate for p-doped **P(PSeP-C₄)** film in 0.1 M TBAH/DCM.

In order to represent the ability of n- doping of the polymer films, they were also scanned cathodically in a monomer-free electrolyte solution of 0.1 M TBAH/ACN. As mentioned previously, **P(PSP-C₁₀)** did not exhibit n-type doping process and **P(PSeP-C₁₀)** can hardly be n-dopable, but as shown in **Figure 3. 45-46**, the n-type doping capability can be imparted to the polymer films by decreasing alkyl chain length from decyl to hexyl and butyl. For example, **P(PSP-C₆)** not only exhibited an irreversible redox peak with a half wave potential of $E_{p,1/2}^{ox}=0.39$ V during anodic scan (p-doping) but also showed a reversible redox couple with a half wave potential of $E_{p,1/2}^{red} = -1.34$ V during cathodic scan (n-doping). n-type doping processes were also confirmed and supported by spectroelectrochemical studies as well as cyclic voltammetric measurements.

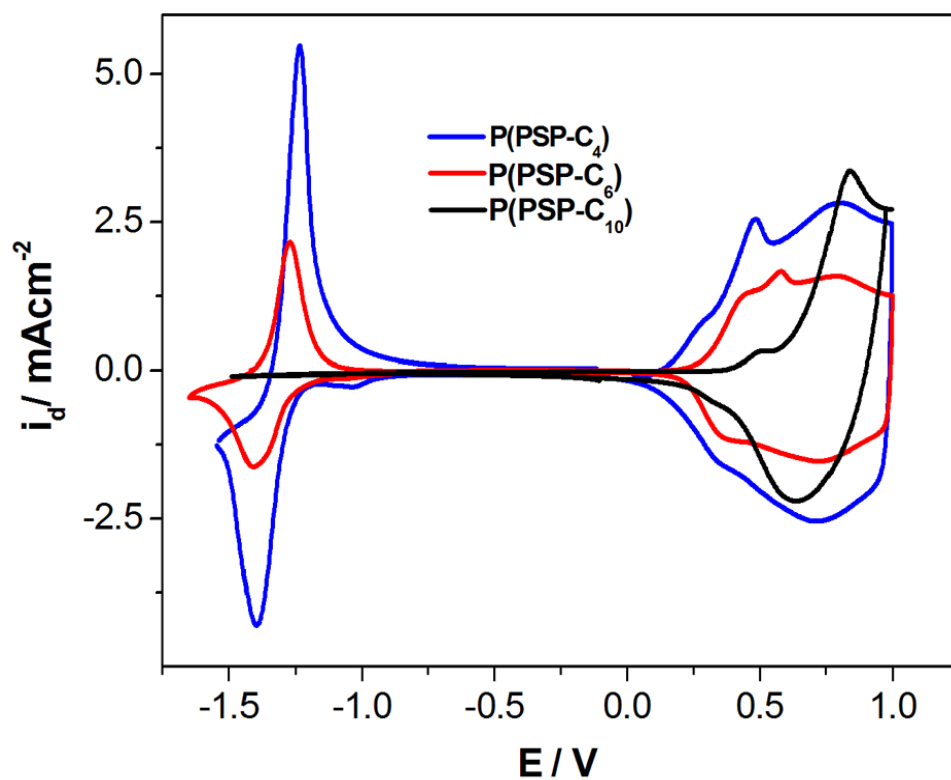


Figure 3.45. Cyclic voltammograms of **P(PSP-C₁₀)**, **P(PSP-C₆)** and **P(PSP-C₄)** in 0.1 M TBAH/ACN electrolyte solution at a scan rate of 100 mV/s vs. Ag/AgCl.

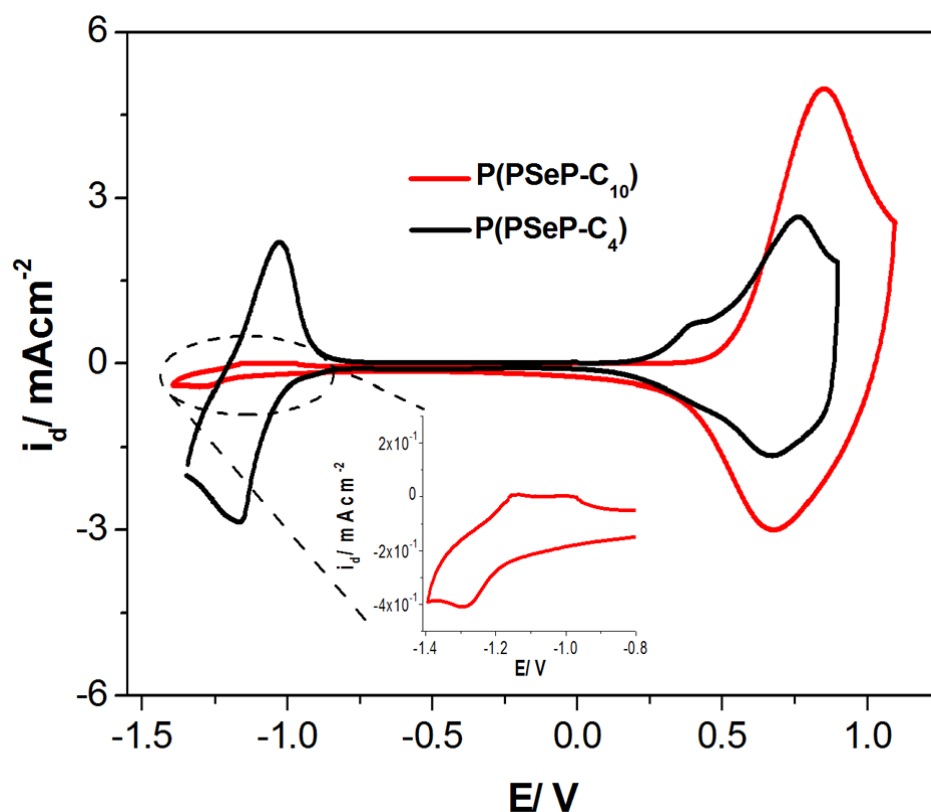


Figure 3.46. Cyclic voltammograms of **P(PSeP-C₁₀)** and **P(PSeP-C₄)** in 0.1 M TBAH/ACN electrolyte solution at a scan rate of 100 mV/s vs. Ag/AgCl.

Table 3.10. Electrochemically determined HOMO, LUMO and E_g values for **P(PSP-C₆)**, **P(PSP-C₄)** and **P(PSeP-C₄)**.

Polymer	E_{ox} onset (V)	HOMO (eV)	LUMO (eV)	E_g^{CV} (V)
P(PSP-C₆)	0.27	5.07	3.57	1.50
P(PSP-C₄)	0.22	5.02	3.58	1.44
P(PSeP-C₄)	0.20	5.00	3.78	1.22

Since the polymers **P(PSP-C₆)**, **P(PSP-C₄)** and **P(PSeP-C₄)** have n-doping properties, E_g of the polymers can also be calculated utilizing the data evaluated from CV measurements. It was found that, the band gap values (E_g^{SPEL}) of the polymers

calculated from the onset of π - π^* -transition band (**Table 3. 9**) were in well agreement with the band gaps (E_g^{CV}) calculated from cyclic voltammogram data (**Table 3. 10**).

3.2.3.1. Spectroelectrochemical and Switching Behaviors of the Polymers

The optical properties of these novel systems, **P(PSP-C₆)**, **P(PSP-C₄)** and **P(PSeP-C₄)**, were also analyzed.

During oxidation, π - π^* -transition bands started to decrease and a concomitant increase was observed at 1000 nm due to the formation of charges. For **P(PSP-C₆)** and **P(PSP-C₄)**, upon further oxidation, the absorption band at 410 nm diminished completely and the absorption band around 670 nm reached a minimum level due to the leg of the absorption band of the charge carriers. For **P(PSeP-C₄)**, upon oxidation, the bands at 348 nm, 420 nm and 697 nm reached a minimum level again because of the formation of the charge carriers (**Figure 3. 47**). During this process, **P(PSP-C₆)**, **P(PSP-C₄)** and **P(PSeP-C₄)** polymer films exhibited electrochromic behavior: switching from cyan, greenish-blue and green, respectively, in the neutral states to highly transmissive grey color when oxidized (see **Table 3.8-3.9**).

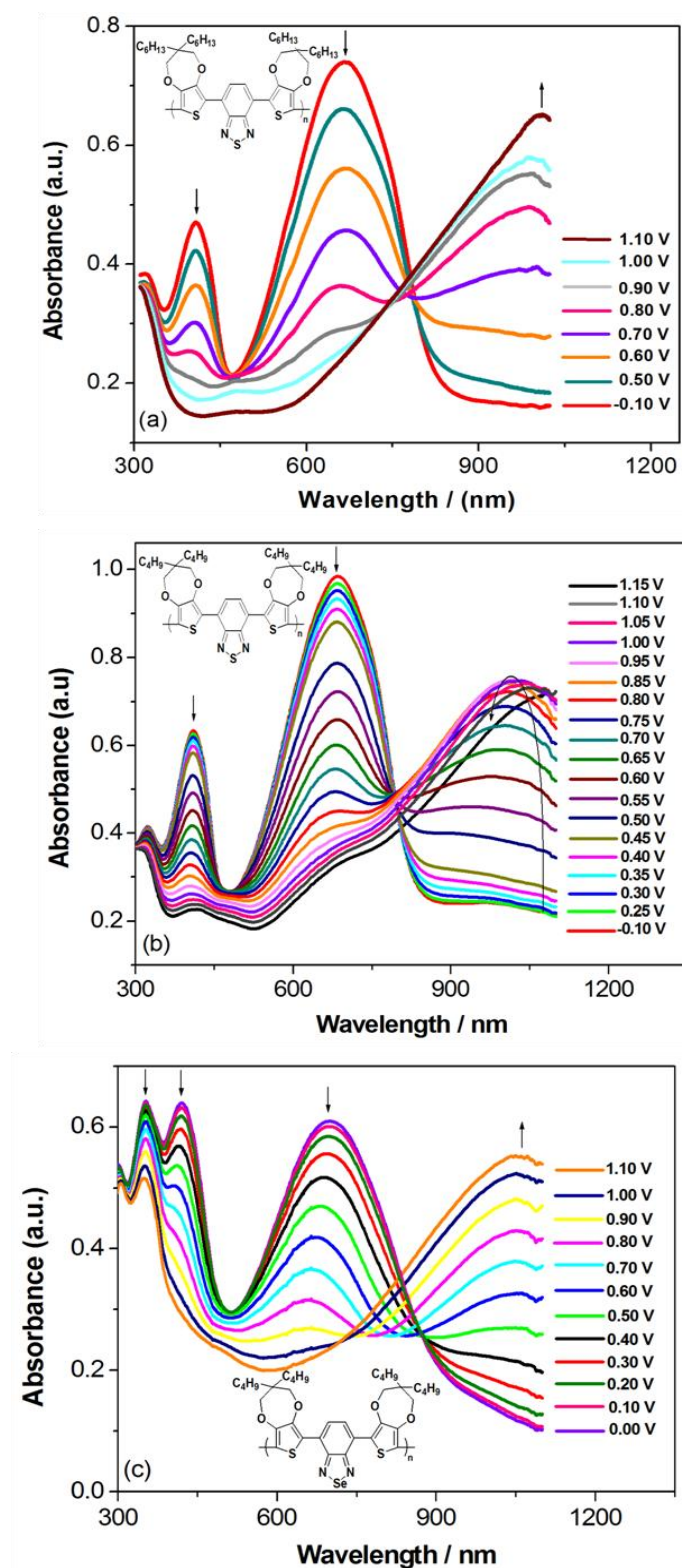


Figure 3.47. Optical absorption spectra of (a) P(PSP-C₆), (b) P(PSP-C₄) and (c) P(PSeP-C₄) on ITO in 0.1 M TBAH/ACN at various applied potentials.

In order to prove n-type doping of **P(PSP-C₆)**, **P(PSP-C₄)** and **P(PSeP-C₄)**, the polymer films were scanned cathodically and the changes in optical spectra were monitored by in-situ studies (**Figure 3. 48**). As in the case of p-type doping process, upon reduction, π - π^* -transition bands started to decrease and the formation of charge carriers was observed beyond 800 nm, which explicitly indicated the ability of n-type doping of the polymers. During this process, the colors of the **P(PSP-C₆)**, **P(PSP-C₄)** and **P(PSeP-C₄)** polymer films were turned from cyan to dark brown, blue-green to fish smoked and green to brown, respectively.

Among the three polymer films, **P(PSP-C₆)**, **P(PSP-C₄)** and **P(PSeP-C₄)**, only **P(PSP-C₆)** was both soluble and n-dopable. **P(PSP-C₁₀)** and **P(PSeP-C₁₀)**, on the other hand, were soluble but not n-dopable while **P(PSP-C₄)** and **P(PSeP-C₄)** were insoluble but n-dopable. **P(PSP-C₆)** was soluble in common organic solvents such as CH₂Cl₂, CHCl₃ and THF which clearly suggested that it could easily be processed over surfaces via spin coating, spraying, and printing techniques.

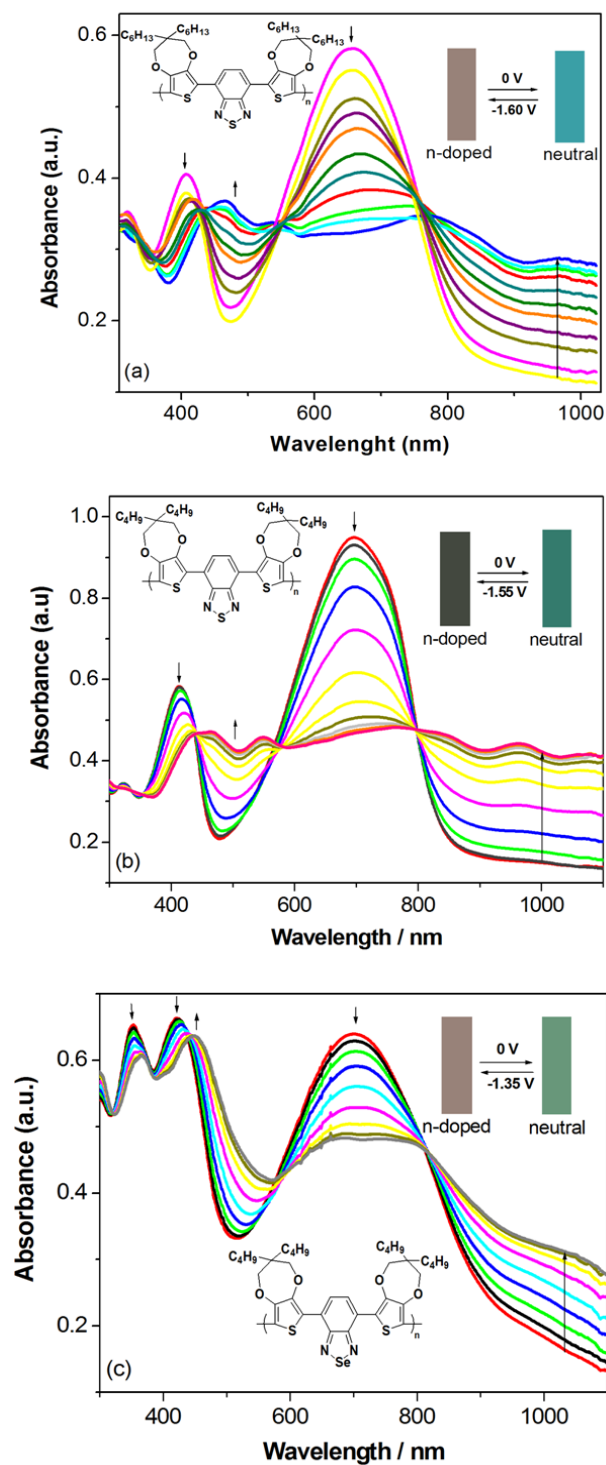


Figure 3.48. Optical absorption spectra of (a) **P(PSP-C₆)** (from 0 V to -1.60 V), (b) **P(PSP-C₄)** (from 0 V to -1.55 V) and (c) **P(PSeP-C₄)** on ITO in 0.1 M TBAH/ACN at various applied potentials. Inset: Colors of (a) **P(PSP-C₆)**, (b) **P(PSP-C₄)** and (c) **P(PSeP-C₄)** during cathodic scan.

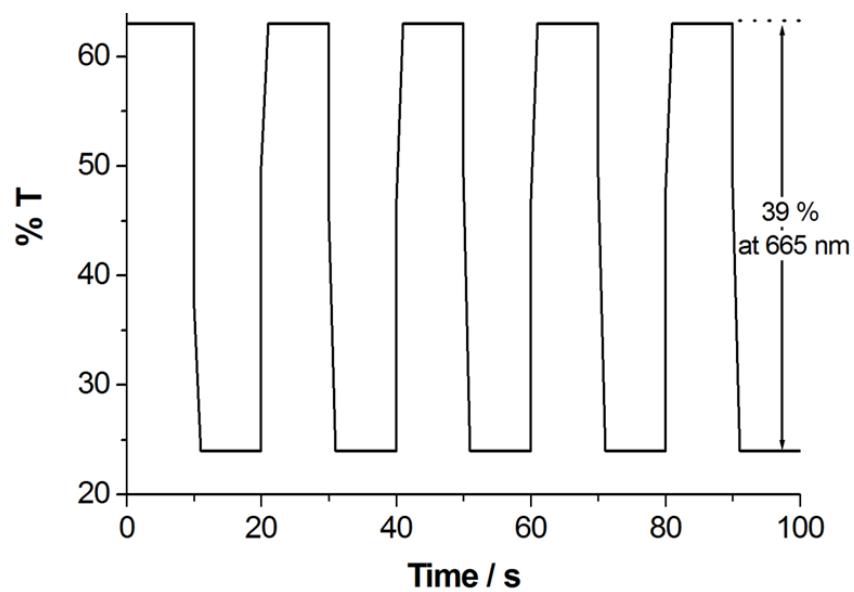


Figure 3.49. Chronoabsorptometry experiments for **P(PSP-C₆)** on ITO in 0.1 M TBAH/ ACN while the polymer was switched between -0.1 V and 1.1 V.

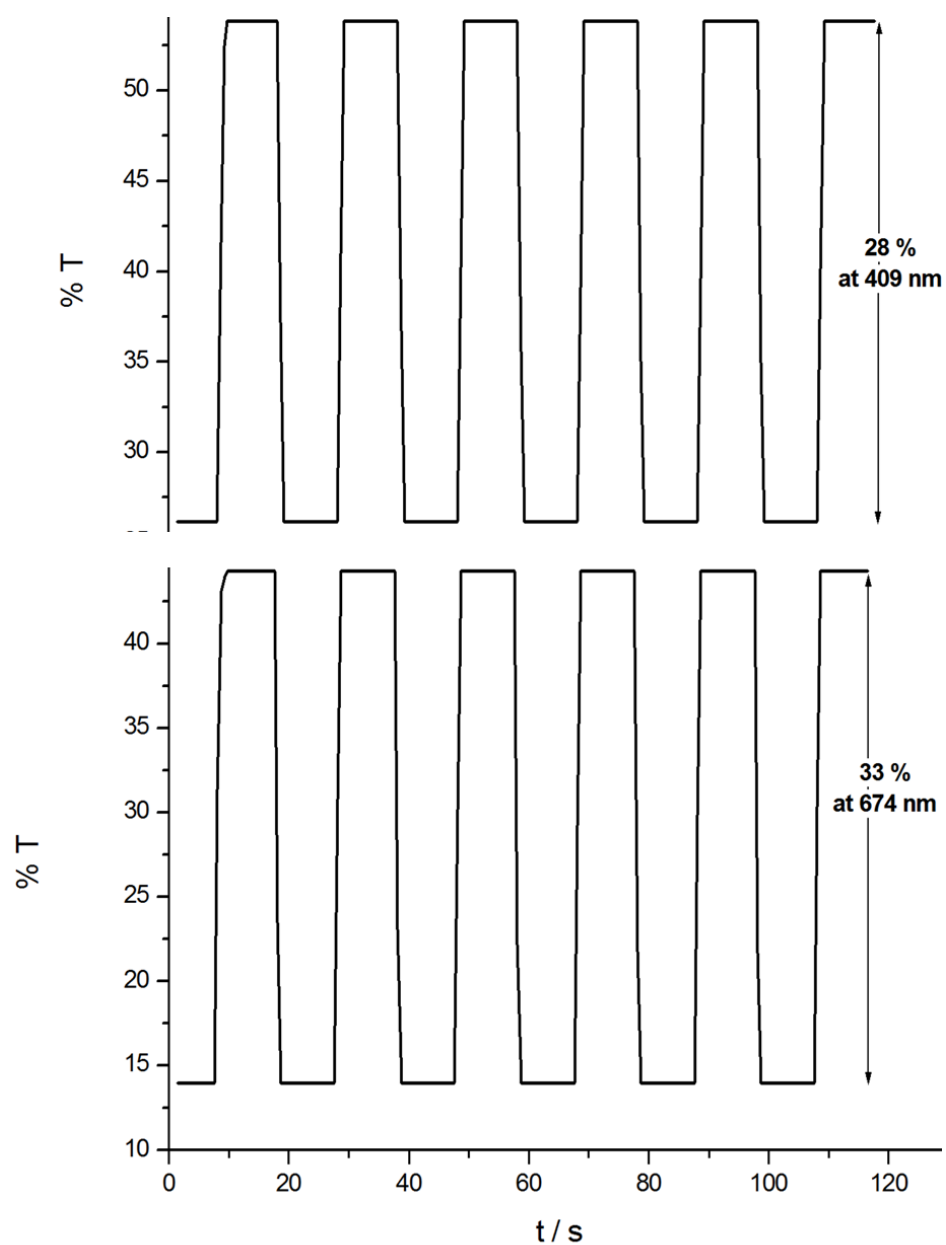


Figure 3.50. Chronoabsorptometry experiments for **P(PSP-C₄)** on ITO in 0.1 M TBAH/ ACN while the polymer was switched between -0.1 V and 1.15 V.

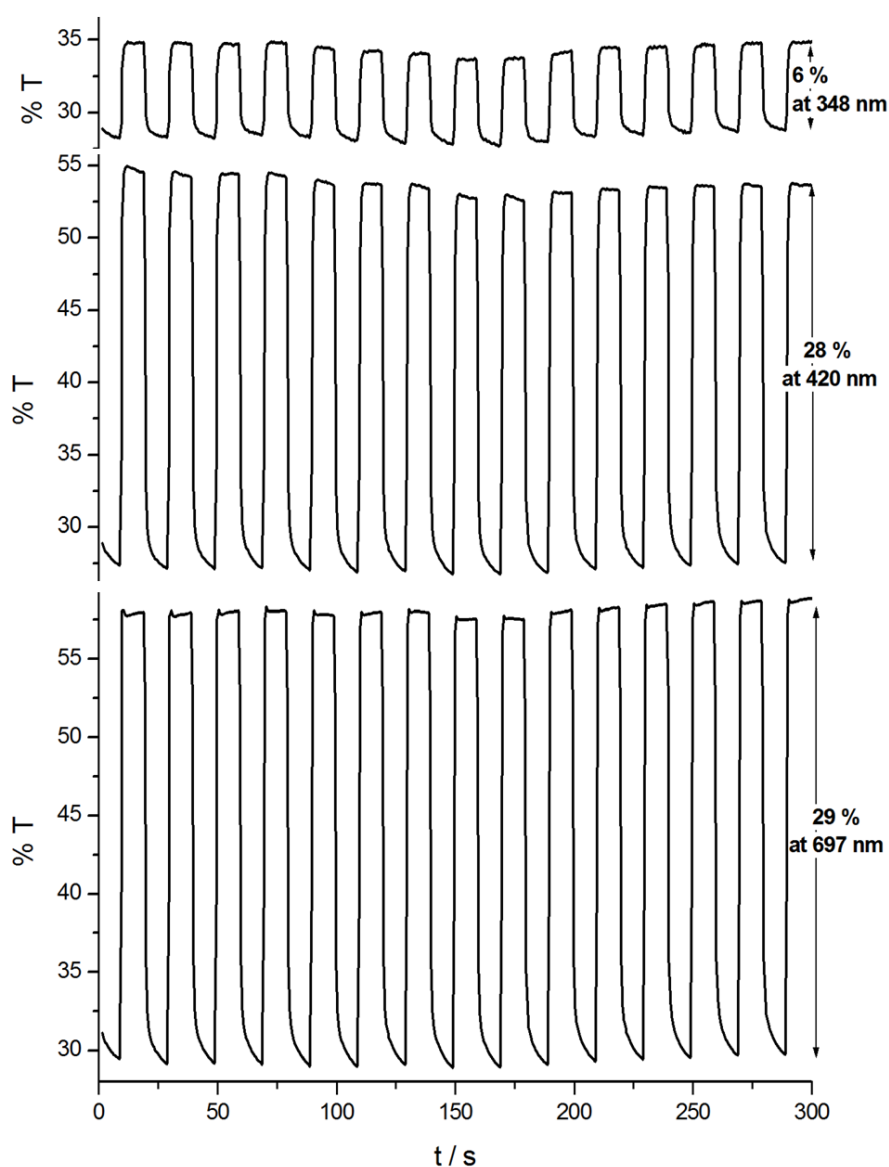


Figure 3.51. Chronoabsorptometry experiments for **P(PSeP-C₄)** on ITO in 0.1 M TBAH/ ACN while the polymer was switched between 0.0 V and 1.1 V.

While the optical contrast of **P(PSP-C₆)** was found to be 39 % at 665 nm with a response time of 0.95 s (95 % of full optical switching), the optical contrast and response time were calculated as 33 % and 0.7 s at 674 nm, respectively, for **P(PSP-**

C₄). Also, those of **P(PSeP-C₄)** were found to be 29.0 % and 1.1 s at 697 nm (see **Table 3. 11** and **Figures 3. 49-51**). It is important to note that the polymer films exhibited higher CEs than PEDOT (183 cm²/C) [89,91], one of the mostly used electrochromic materials for optical devices and displays. The calculated CE values are 202 cm²/C for **P(PSP-C₆)**, 235 cm²/C for **P(PSP-C₄)** and 295 cm²/C for **P(PSeP-C₄)** (**Table 3. 11**).

Table 3.11. Optical and switching time data of electrochemically synthesized polymers **P(TSeT)**, **P(ESeE)** and **P(PSeP-C₁₀)**, PEDOT and their analogues. The given CE value is the best one at a given wavelength.

Polymer	Wavelength (λ_{\max} , nm)	Contrast %T	CE (cm ² /C)	Switching time (t, s)
P(PSeP-C₁₀)	715	40.3	208	0.6
P(PSeP-C₄)	697	29.0	295	1.1
P(PSP-C₄)	674	33.0	235	0.7
P(PSP-C₆)	665	39.0	202	0.95

3.2.3.4. Properties of the Polymers

Since **P(PSP-C₆)** is found to be soluble in common organic solvents such as DCM, CHCl₃ and THF, it was also obtained via chemical polymerization. As described previously, the polymer was dissolved in DCM and doped and dedoped utilizing SbCl₅ and N₂H₅OH, respectively. It was observed that the results obtained from chemical doping-dedoping procedure (**Figure 3. 52**) was almost same with the electrochemical one (**Figure 3. 47 (a)**). As mentioned before, this procedure should be useful for the determination of the doping-dedoping process, i.e. the formation of the charge carriers. It will be explained in the polymer characterization part.

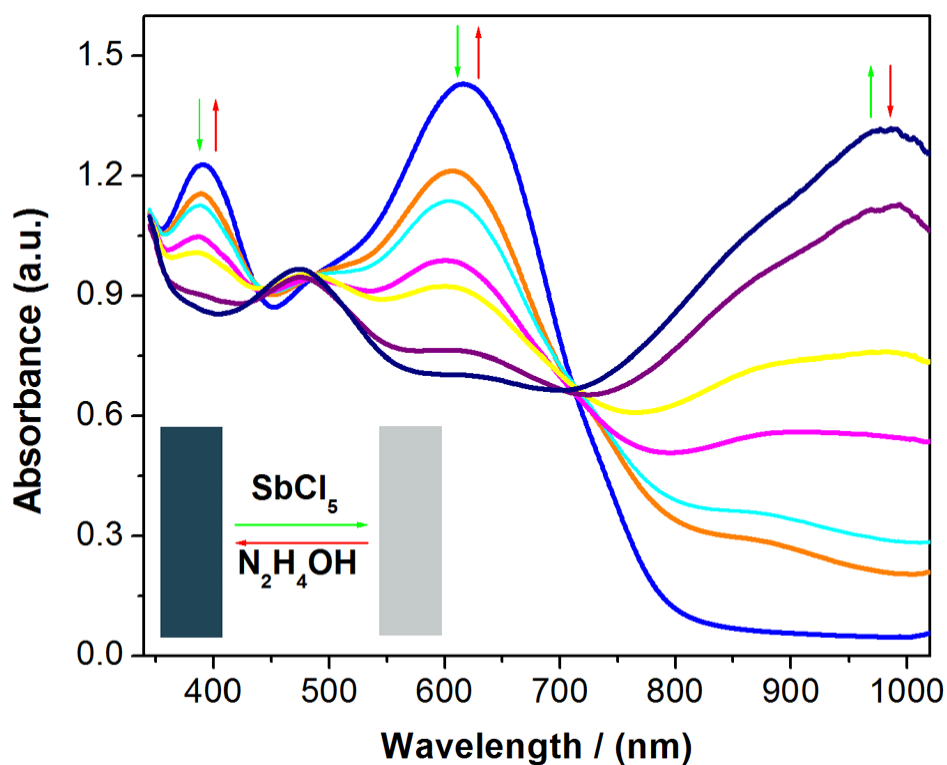


Figure 3.52. Changes in optical absorption spectra of chemically obtained **P(PSP-C₆)** in DCM solution after the addition of 10 μ L (for each spectrum) 5×10^{-4} M SbCl₅ and 10^{-2} M N₂H₅OH. Inset: Colors of **P(PSP-C₆)** in DCM solution addition of SbCl₅ and N₂H₄OH.

3.2.3.1. Stability of the Polymers

P(PSP-C₆), **P(PSP-C₄)** and **P(PSeP-C₄)** showed excellent stabilities, that is, they retained 94 %, 62 % and 57 % of their electroactivity after 2000 switching, respectively (**Figure 3. 53**). The results show that, among all of the polymers containing *benzo*[*c*][1,2,5]thiadiazole as an A part, **P(PSP-C₆)** is the most stable one.

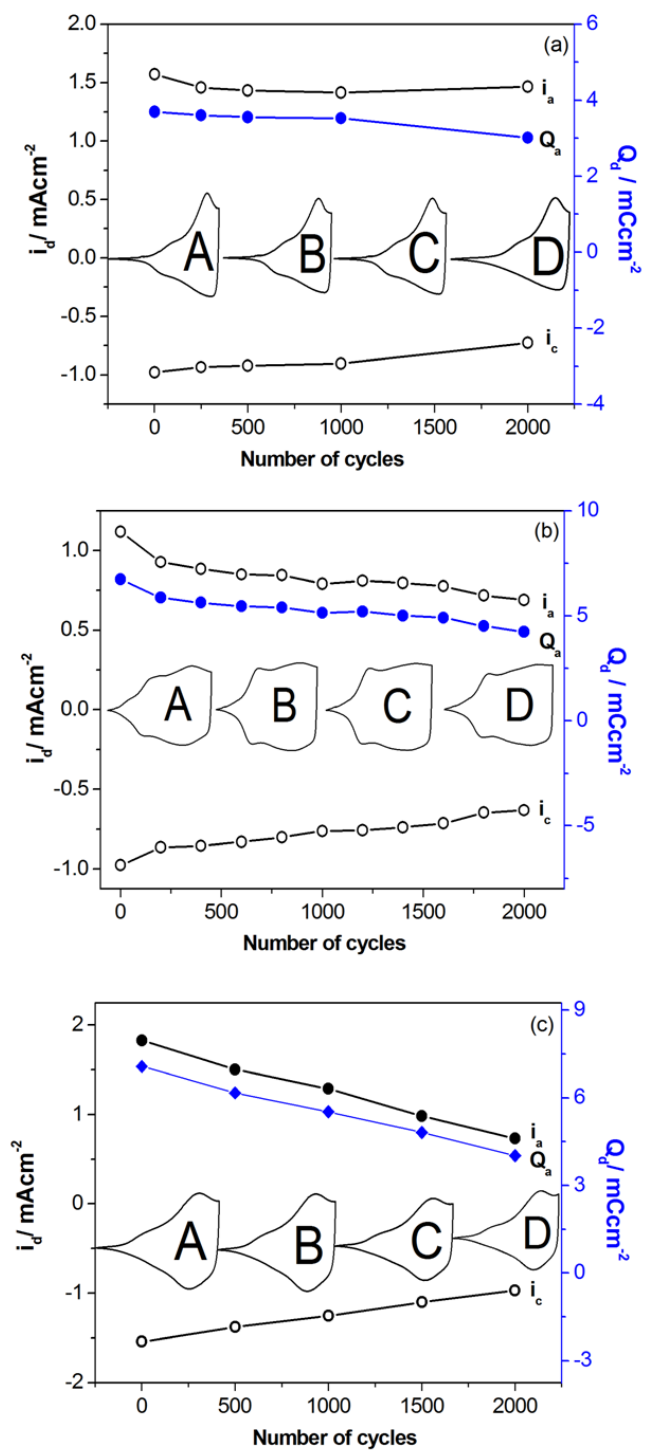


Figure 3.53. Stability test for (a) **P(PSP-C₆)**, (b) **P(PSP-C₄)**, (c) **P(PSeP-C₄)** films in 0.1 M TBAH/DCM at a scan rate of 100 mV s⁻¹ under ambient conditions by cyclic voltammetry as a function of the number of cycles: A: 1, B: 500, C: 1000, D: 2000 cycles; Q_a: Anodic charge stored, i_{pa}: Anodic peak current, i_{pc}: Cathodic peak current.

3.2.4. Investigation of the Properties of the Polymers

3.2.4.1. Conductivity Measurements

Since among all the polymers, **P(PSeP-C₁₀)** and **P(PSP-C₁₀)** were susceptible to be obtained as a film, their conductivities were measured via four probe method. For this aim, chemically obtained **P(PSeP-C₁₀)** and **P(PSP-C₁₀)** (without subjecting neutralization) were dissolved in CHCl₃ and kept under ambient conditions up to all solvent was evaporated. After the formation of the film was observed, obtained film was dried in an oven at 70⁰ C during 24 h.

The conductivity result obtained for **P(PSeP-C₁₀)** was 3.40x10⁻² Scm⁻¹ and that for **P(PSP-C₁₀)** was 4.48 x10⁻⁴ Scm⁻¹. Also, conductivity of **P(PSP-C₁₀)** was measured after doping with iodine, the result was found as 0.33 Scm⁻¹. Conductivities of the **P(PSeP-C₁₀)** and **P(PSP-C₁₀)** were low when compared that of poly(hexylthiophene) (1000 Scm⁻¹) . However, the conductivity of **P(PSP-C₁₀)** in iodine doped state was higher than that of polyselenophenes (0.28 Scm⁻¹) [100].

3.2.4.1. ESR Measurements

In endeavors to reveal the doping-dedoping mechanism of the obtained polymers, ESR measurement was carried out. For this aim, PPSP-C₁₀ was dissolved in DCM and then 10⁻⁸ M SbCl₅ solution in DCM was added drop wise. After addition of each drop, an ESR spectrum had been recorded. As it can be seen from **Figure 3. 54**, before addition of SbCl₅, that is the polymer was in its neutral state, no signal was observed. As SbCl₅ solution was added drop wise, a singlet with a g value very close to that of free electron and linewidth $\Delta H_{pp}=0.29$ mT value started to intensify, proving the formation of the polaron charge carriers. The intensifying singlet very asymmetric at start and almost asymmetric during the experiment indicating an increase

in the conductivity of polymer via doping process [101]. Upon further addition of SbCl_5 solution causes a decrease in the intensity of the singlet signal, corresponding to the formation of bipolaron. This procedure can be reversed by drop wise addition of 10^{-5} M $\text{N}_2\text{H}_4\text{OH}$ (Figure 3.54).

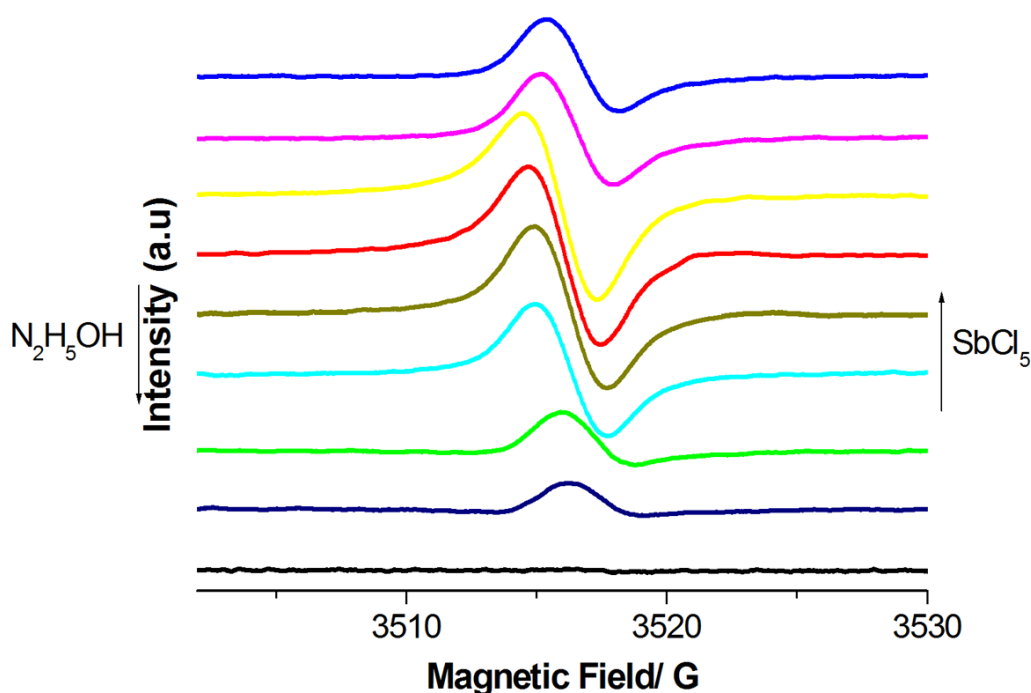


Figure 3.54. ESR spectrum results of **P(PSP-C₁₀)** via addition of 10^{-8} M SbCl_5 and 10^{-5} M $\text{N}_2\text{H}_4\text{OH}$ dissolved in DCM.

3.2.4.2. Molecular Weight Analysis

In order to determine the molecular weight of the obtained polymers, two methods were used: MALDI-TOF Analysis and GPC.

For the determination of the molecular weight of **P(PSP-C₁₀)** MALDI-TOF Analysis was used. It had a weight average molecular weight (M_w) of 8991 with a low polydispersity index of 1.18. This indicates that its chain lengths vary over a narrow

range of molecular masses (**Figure 3. 55**). Also, **P(PSP-C₁₀)** polymer had a minimum average number of 9 repeating units including 27 heterocyclic units. In order to determine molecular weight of **P(POP-C₁₀)** and **P(PSP-C₆)**, GPC measurements had been done. HPLC grade of THF was used as a solvent for this study. For **P(PSP-C₆)**, M_w value was found as 61756 with a very high polydispersity index of 6.06. It can be concluded that, **P(PSP-C₆)** had average number of 79 repeating units, i.e., 237 heterocyclic units (**Figure 3. 56**). The results for **P(POP-C₁₀)** was somewhat disappointing. That is, M_w value was found as 5867 with a low polydispersity index of 2.08. **P(POP-C₁₀)** had average number of 6 repeating units, that is, 18 heterocyclic units (**Figure 3. 57**). Maybe, repeating units can be increased via extending the polymerization time.

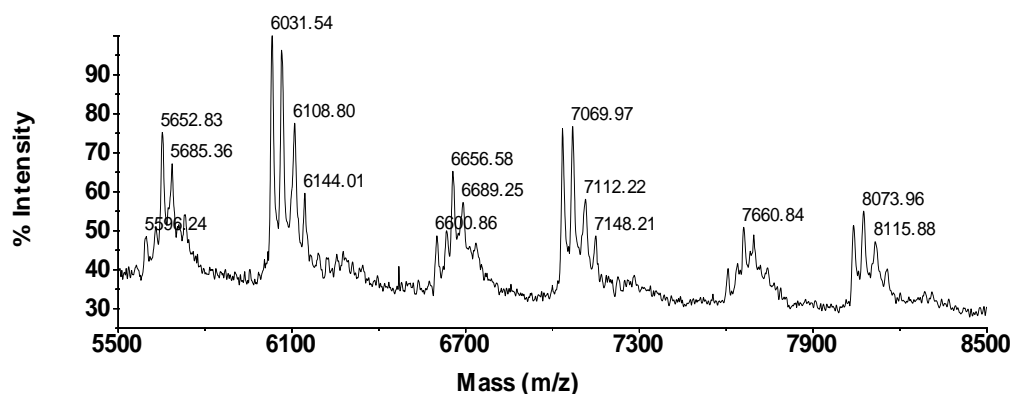


Figure 3.55. Mass spectrum of chemically synthesized **P(PSP-C₁₀)** (experimental notes: $M_n= 7652.24$; $M_w= 8991.42$; $M_z= 10221.84$; $HI= 1.18$).

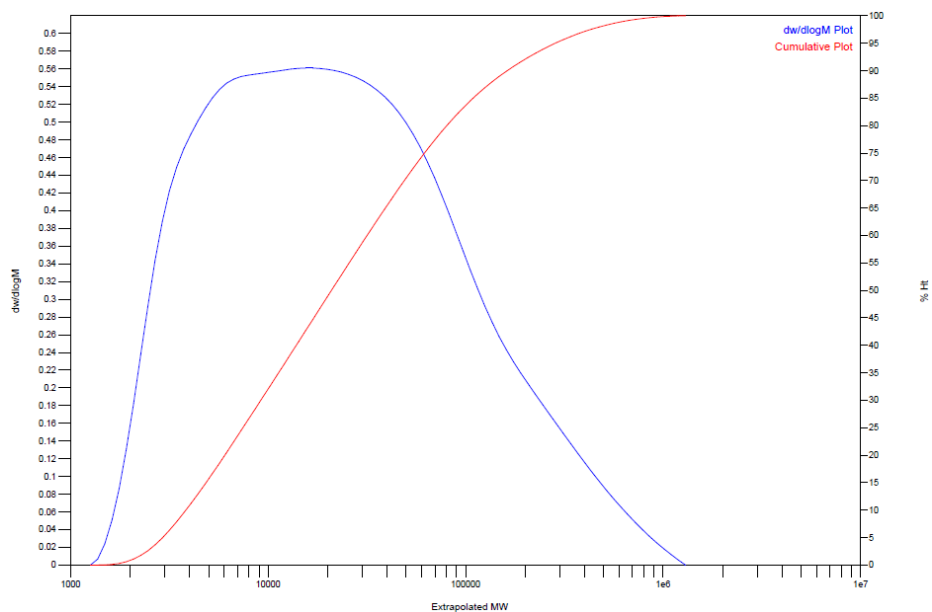


Figure 3.56. Distrubution plots of chemically synthesized **P(PSP-C₆)** (experimental notes: $M_n= 10098$; $M_w= 61256$; $M_z= 276446$; $HI= 6.06$).

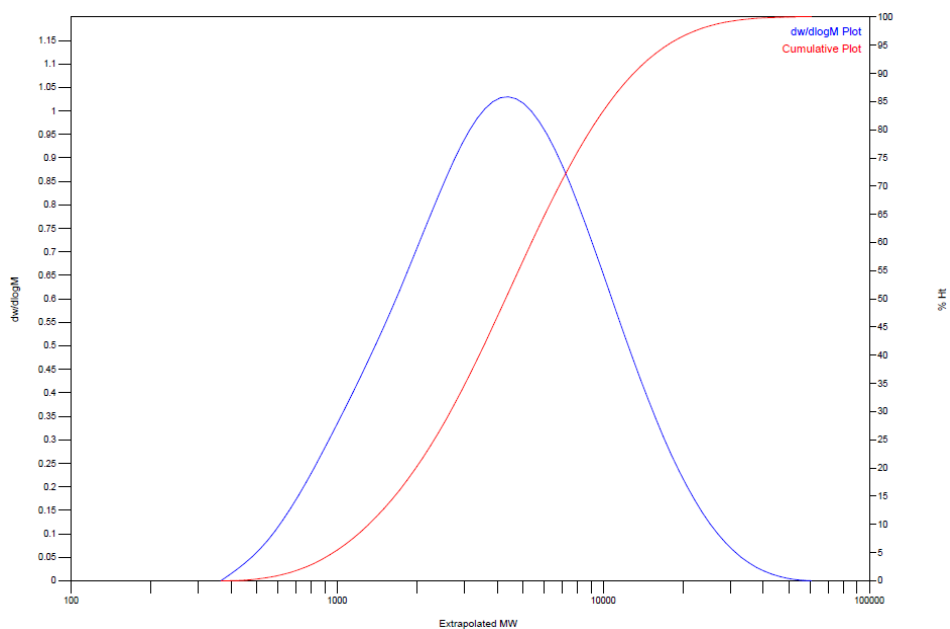


Figure 3. 57. Distrubution plots of chemically synthesized **P(POP-C₁₀)** (experimental notes: $M_n= 2817$; $M_w= 5867$; $M_z= 11030$; $HI= 2.08$).

3.2.5. Application of the Polymers to Color Mixing Theory (CMT)

In order to obtain any color in the visible spectrum, three subtractive colors, that is, red, green, blue (RGB) or cyan, magenta, yellow (CMY) colors and “key” black colors are needed. Since the polymers are non-emitting color systems, the theory of obtaining a tune of an EC polymer is just like the mixing theory of the paints. For example, via mixing cyan and magenta, blue can be obtained [50].

Among all polymers synthesized, **P(PSeP-C₁₀)**, **P(PSP-C₁₀)**, **P(PSP-C₆)** and **P(POP-C₁₀)** were very precious. Since they all were not only soluble, i.e. processable, but also they were the member of the CMY and RGB color spaces, that is, cyan colored **P(PSP-C₁₀)**, **P(PSP-C₆)** and **P(POP-C₁₀)** were the member of the CMY and **P(PSeP-C₁₀)** was the member of the RGB color spaces (**Figure 3. 58**).

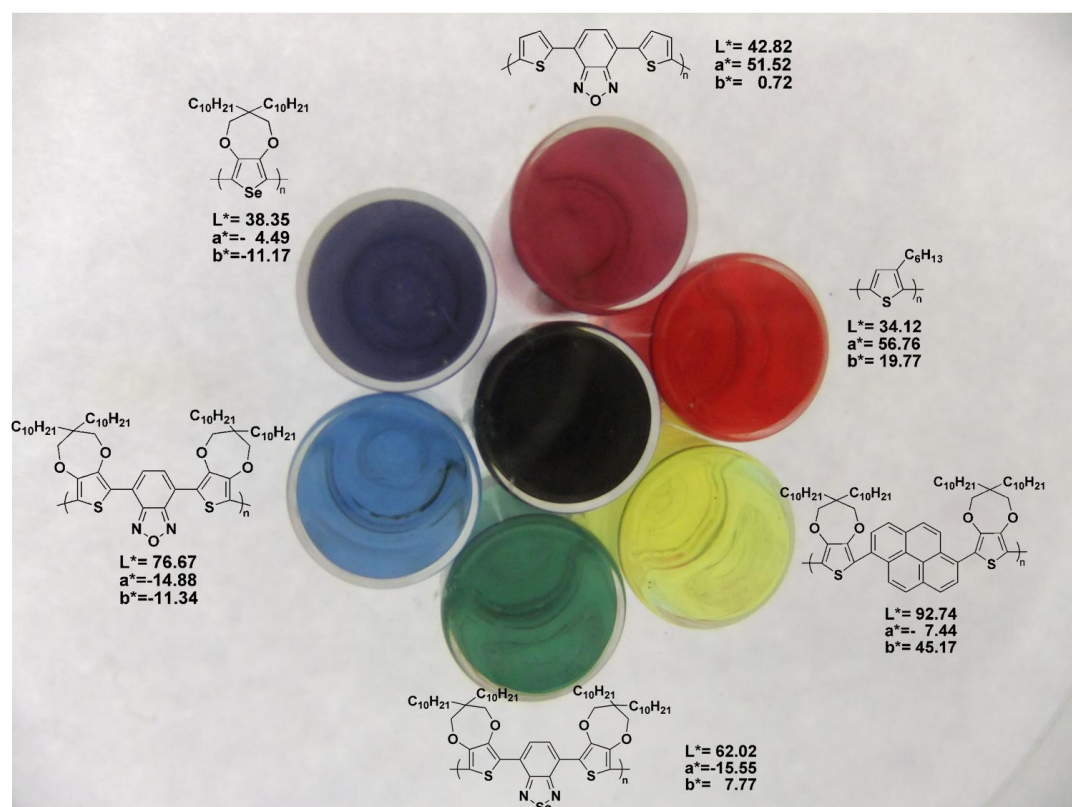


Figure 3.58. Representation of CMY and RGB color spaces from the polymer solutions in CHCl₃.

Figure 3.59-61 show how to obtain a third color via mixing two colors from CMY color spaces. **Figure 3.62** represents how to obtain black color by mixing all colors in the visible spectrum.

The explanation of the results is very reasonable for the CMT. For example, in order to obtain green color, at least two absorption bands were needed, that is, the polymer should absorb red and blue light (absorptions around 400 and 700 nm were needed) at the same time [57,79]. **P(POP-C₁₀)** showed two absorption bands at these wavelengths actually, however, the intensity of the band around 400 nm was not enough to obtain green color. Then, via mixing **P(POP-C₁₀)** polymer with a polymer absorbing the red region of visible spectrum, that is, a yellow polymer (in our cases this was **P(PPyP-C₁₀)**), green color was obtained (**Figure 3.60**).

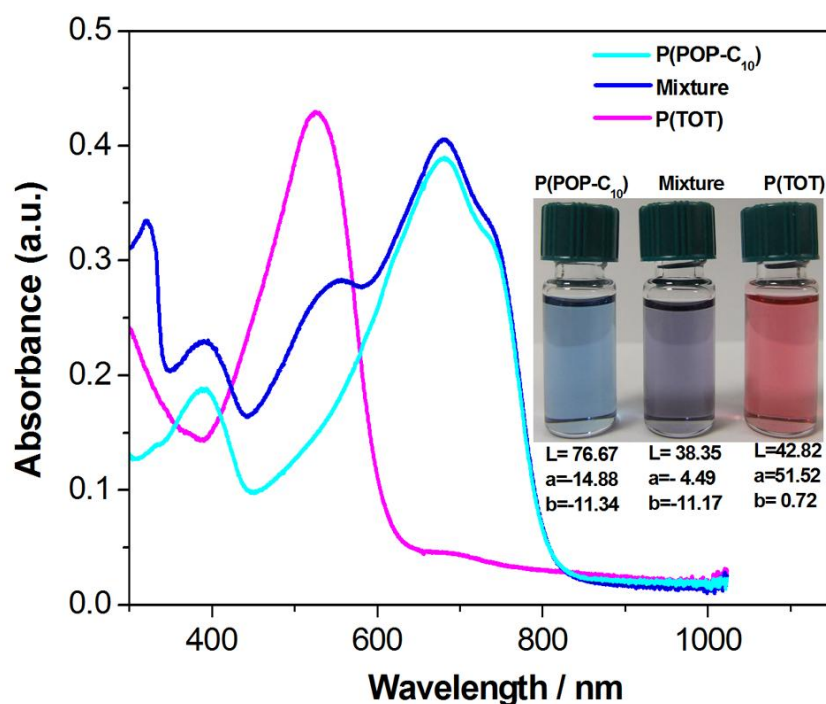


Figure 3.59. Obtaining blue color according to CMT: Absorption spectrum of cyan colored **P(POP-C₁₀)**, magenta colored **P(TOT)*** and their mixures having blue color (***P(TOT)** polymer contains thiophene as a donor unit and benzo[c][1,2,5]oxadiazole as acceptor unit like **P(POP-C₁₀)**). Inset: Picture of the polymers and their mixture in CHCl₃, and their *L*a*b** values.

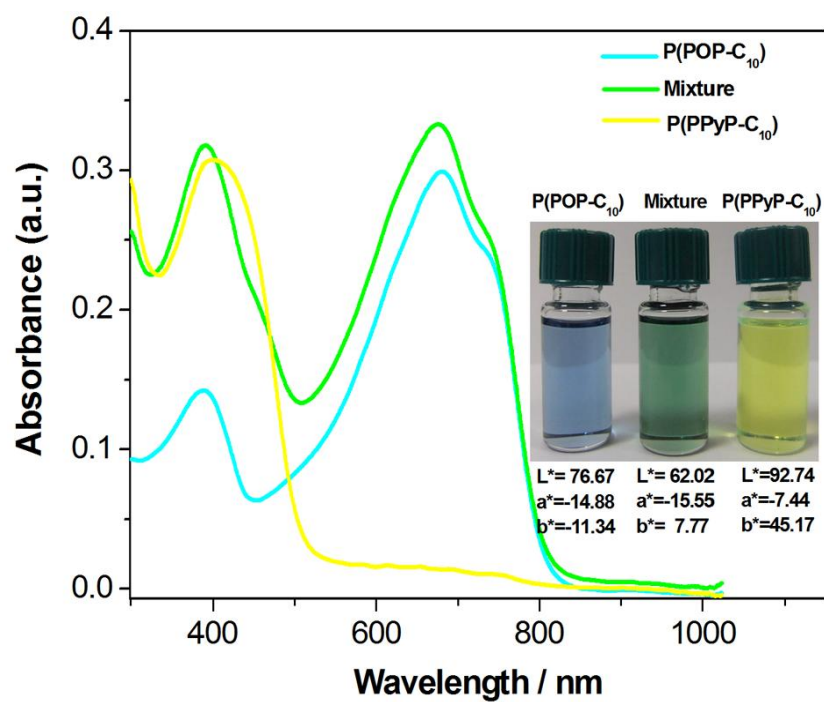


Figure 3.60. Obtaining green color according to CMT: Absorption spectrum of cyan colored **P(POP-C₁₀)**, yellow colored **P(PPyP-C₁₀)*** and their mixtures having green color (***P(PPyP-C₁₀)** polymer contains ProDOT-C₁₀ as a donor unit like **P(POP-C₁₀)**) and pyrene as acceptor unit. Inset: Picture of the polymers and their mixture in CHCl₃, and their $L^*a^*b^*$ values.

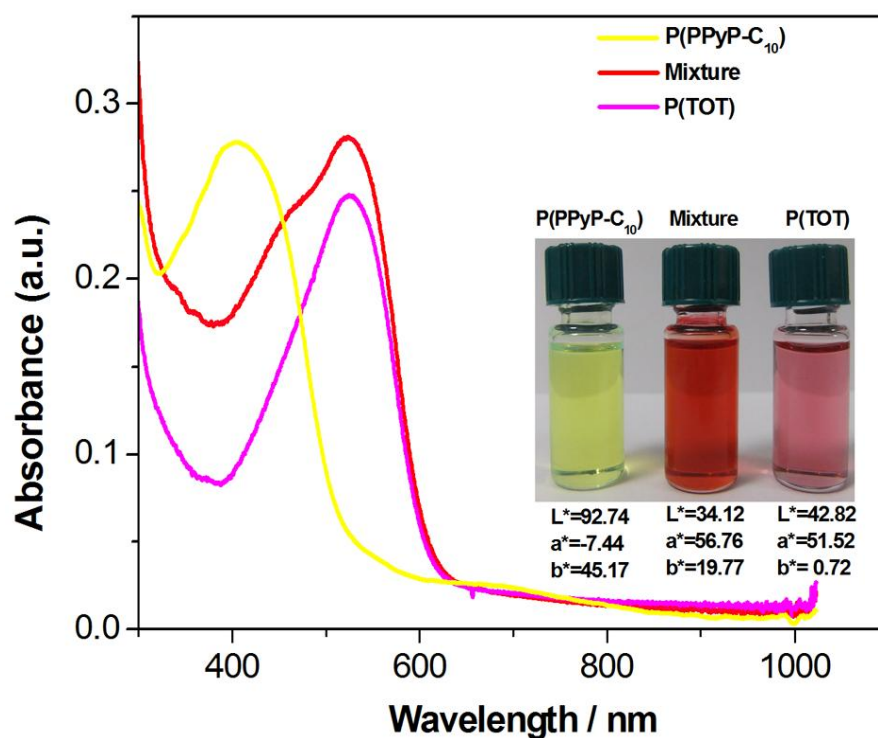


Figure 3. 61. Obtaining red color according to CMT: Absorption spectrum of yellow colored **P(PPyP-C₁₀)** and magenta colored **P(TOT)** and their mixtures having red color. Inset: Picture of the polymers and their mixture in CHCl_3 , and their $L^*a^*b^*$ values.

In order to obtain black color, the whole visible spectrum should be absorbed by the material. It is not an easy process to obtain such as this kind of compound. In literature, copolymerization had been applied to obtain black color ECs [74,102,103]. Actually, color mixing theory is a viable route to obtain black color. During this study, the black color was obtained via mixing cyan, magenta and yellow colors.

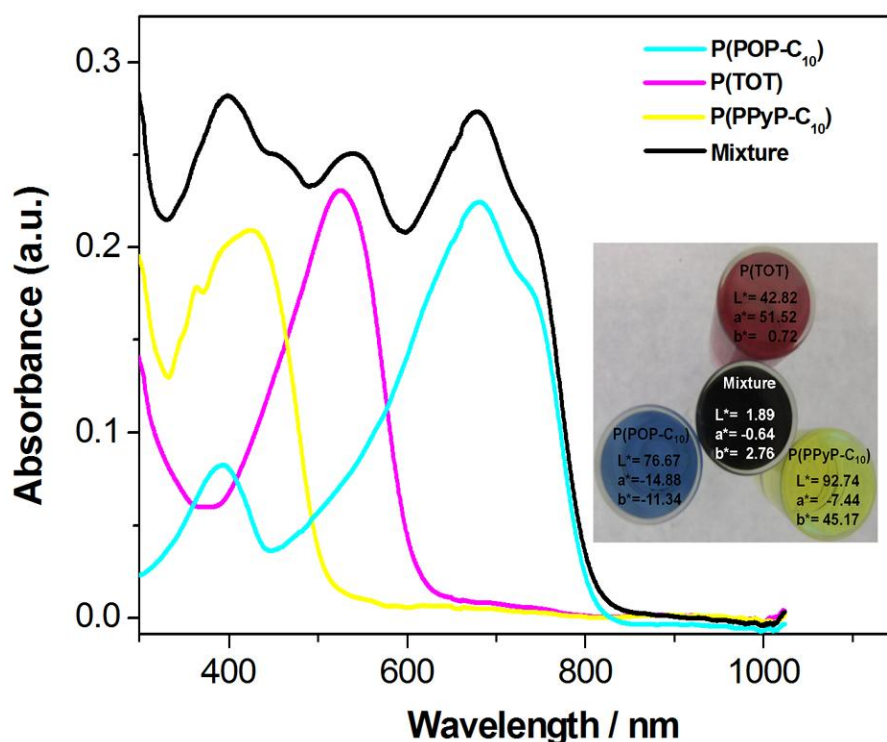


Figure 3.62. Obtaining black color according to CMT: Absorption spectrum of cyan colored **P(POP-C₁₀)**, magenta colored **P(TOT)**, yellow colored **P(PPyP-C₁₀)** and their mixtures having black color. Inset: Picture of the polymers and their mixture in CHCl_3 , and $L^*a^*b^*$ values.

3.2.6. Synthesis of Neutral State Black Electrochromic Copolymer

As mentioned before, according to color mixing theory, which claims that if two color stimuli are mixed, the resulting color will lie somewhere along a straight line connecting two points on the chromaticity diagram [68]. Although this claim is only valid through the emission of light, and the substances present color to the eye by reflection rather than the emission, the color space concept can also be applied to the chromophores (e.g., by mixing dyes of two colors to attain another color); since the observed color is a result of the way that the eye detects it, and is not a property of light. To date, significant efforts have been devoted to the design and synthesis of

novel PECs with saturated and tunable colors. In spite of the panoramic breadth of the colors of PECs, the construction of a neutral state black PEC by electrochemical means remains elusive due to the complexity of designing such material: broadband absorption covering the whole visible spectrum (400-800 nm) in the neutral state, extra requirement of distinct and low oxidation potentials for electropolymerization, simultaneous depletion of absorption bands upon doping and so forth. The first example of black PEC has emerged from Reynolds' laboratory [74] by using chemical copolymerization of an increasingly substituted donor-acceptor (D-A) system [69]. Therefore, it is a challenging task to access neutral state black polymer electrochemically in view of optoelectronic devices, displays (road signs, clocks and shop displays), windows shades along with many flexible and portable art and design applications [51, 104]. Furthermore, neutral state black polymers would also be highly valuable for solar cell applications [105]. As mentioned in the previous part that, via mixing cyan, magenta and yellow colored polymers, black color was obtained. Also, it can be obtained by mixing red, green and blue colored polymers. However, to apply this process at least three polymers were necessary. During this study, it was observed that, the sum of the electronic absorption spectra of **P(PSeP-C₁₀)** and **P(PNP-C₁₀)** covered the whole range of visible spectrum (400-800 nm) (See **Figure 3. 63**), it was envisaged that electrochemical co-polymerization via repetitive cycling or constant potential electrolysis of **PSeP-C₁₀** and **PNP-C₁₀** with a certain monomer feed-ratio might provide an entry into neutral state black polymers.

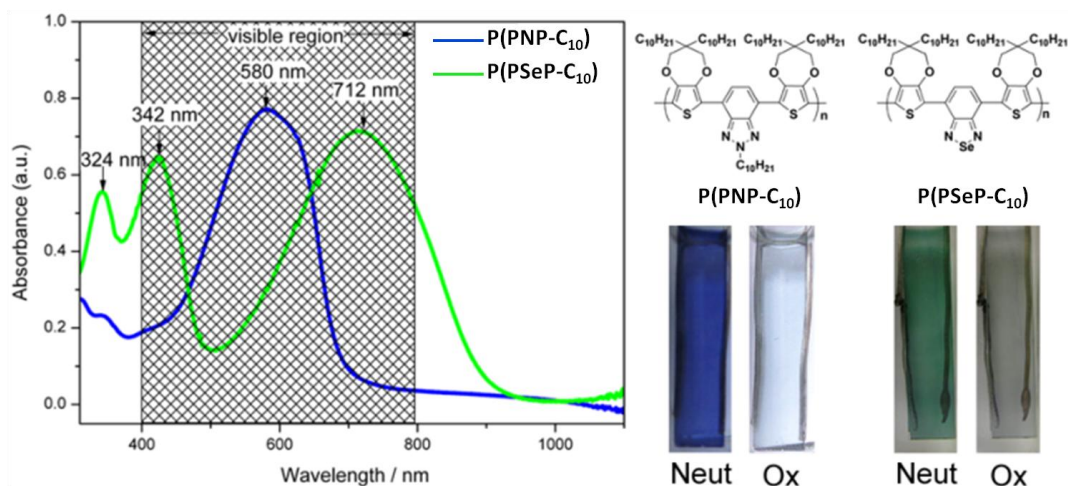


Figure 3.63. Electronic absorption spectra of **P(PSeP-C₁₀)** and **P(PNP-C₁₀)** in their neutral states in 0.1 M TBAH dissolved in ACN and the colors of the polymers in different redox states.

Initially, the redox behavior of a mixture of **PSeP-C₁₀** and **PNP-C₁₀** was investigated by CV. Although both monomers were highly soluble in dichloromethane (DCM), the cyclic voltammograms of the mixture of **PSeP-C₁₀** and **PNP-C₁₀** were recorded in a mixture of DCM and acetonitrile (ACN, as a non-solvent) in order to hinder the solubility of the polymer film, which was formed on the electrode surface, by cosolvent effects. CV of a mixture of **PSeP-C₁₀** and **PNP-C₁₀** with 1:4 monomer feed ratio in 0.1 M TBAH/DCM-ACN (3/2-v/v) exhibits two consecutive oxidation peaks at 0.93 V and 1.01 V indicating that the electrochemical copolymerization of **PSeP-C₁₀** and **PNP-C₁₀** was feasible. Upon successive scans a new reversible redox couple was also noted which indicates the formation of corresponding copolymer (**P(PSeP-C₁₀ -co- PNP-C₁₀)**) film on the electrode surface (**Figure 3. 64**).

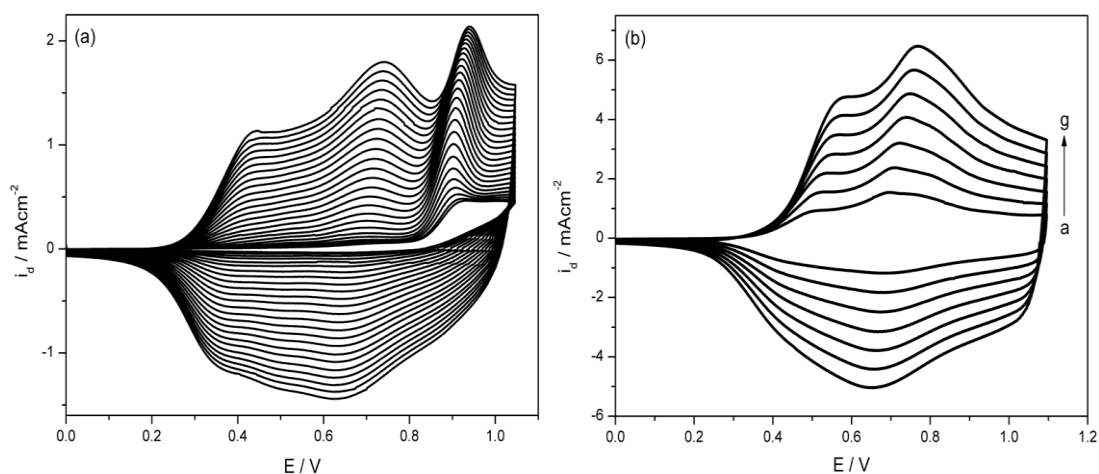


Figure 3.64. CV during the repeated scan electropolymerization of a mixture of **PSeP-C₁₀** and **PNP-C₁₀** with 1:4 monomer feed ratio to give **P(PSeP-C₁₀-co- PNP-C₁₀)** in 0.1 M TBAH/DCM-ACN (3/2-v/v) at a scan rate of 100 mV/s, Pt disk working electrode, and (b) scan rate dependence of the **P(PSeP-C₁₀-co- PNP-C₁₀)** film in 0.1 M TBAH/ACN at different scan rates (mV/s): (a) 50; (b) 75; (c) 100; (d) 125; (e) 150; (f) 175; and (g) 200.

The as-prepared polymer film had black color in the neutral state and it was soluble in common organic solvents (DCM, CHCl₃, *etc.*) and slightly soluble in toluene and diethylether, which clearly suggested that it could easily be processed over surfaces via spin coating, spraying and printing techniques (**Figure 3.65**).

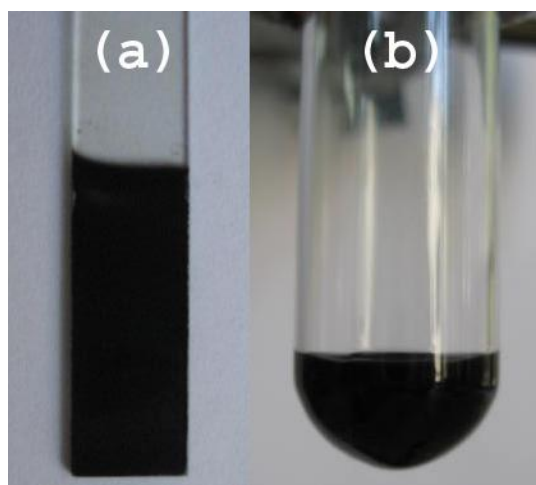


Figure 3.65. **P(PSeP-C₁₀-co- PNP-C₁₀)** film on ITO glass slide and **P(PSeP-C₁₀-co- PNP-C₁₀)** in DCM.

However, it was noteworthy that the peak current versus scan rate curve of the copolymer during p-type doping was linear which brought convincing evidence that the redox process is not diffusion-limited. Interestingly, it was also found that the polymer film has shown almost the same charge/discharge behaviour between the scan rates of 50 mV/s and 200 mV/s. The data suggests that the charge transport takes place rapidly through the coated polymer film and the electroactive sites remain unaltered independent of the externally induced potential. This intriguing feature paves the way for utilizing **P(PSeP-C₁₀-co- PNP-C₁₀)** as p-type material in supercapacitors and/or transistors [106].

The electrochemical stability of **P(PSeP-C₁₀-co- PNP-C₁₀)** was tested by cycling the polymer film between its neutral and oxidized states at a scan rate of 200 mV/s. As shown in **Figure 3.66**, no appreciable change in the electrochemical response of **P(PSeP-C₁₀-co- PNP-C₁₀)** was observed and 90% of the electroactivity was still kept even after four thousands of cycles. It can be safely concluded that **P(PSeP-C₁₀-co- PNP-C₁₀)** exhibits both operational stability and environmental robustness under ambient conditions.

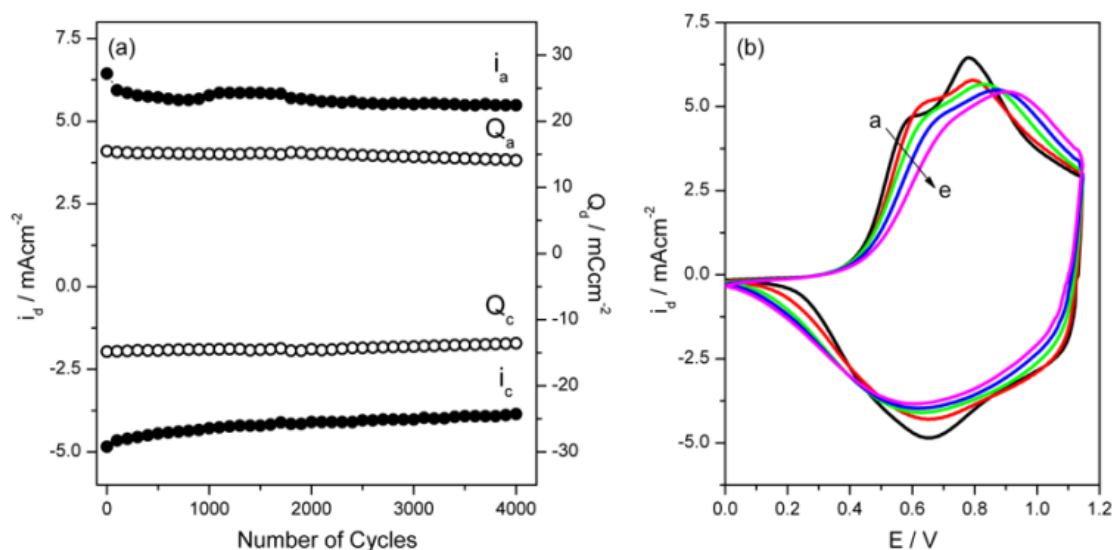


Figure 3.66. (a) Relationship of anodic (i_a), cathodic (i_c) peak currents and the charge (Q_a)/discharge (Q_c) variations of **P(PSeP-C₁₀-co- PNP-C₁₀)** as a function of number of cycles and (b) Cyclic voltammetry stability of **P(PSeP-C₁₀-co- PNP-C₁₀)** film at a scan rates of 200 mV/s between 0.0 V and 1.1 V in 0.1 M TBAH/ACN. Number of cycle: (a) 1; (b) 1000; (c) 2000; (d) 3000; and (e) 4000.

When the spectroelectrochemical behavior of **P(PSeP-C₁₀-co- PNP-C₁₀)** was investigated, in the neutral state, copolymer exhibited a broad absorption band with three shoulders at 422 nm, 522 nm and 660 nm extending virtually over the full visible spectrum (**Figure 3.67**). When compared to the absorption bands of **P(PSeP-C₁₀)** (343 nm, 419 nm and 700 nm) and **P(PNP-C₁₀)** (585 nm) in **Figure 3.7-(c)** and **Figure 3.26-(c)**, respectively; the spectrum of the product confirms the formation of a copolymer since the absorption bands of the claimed copolymer do not exactly match the corresponding homopolymers. **P(PSeP-C₁₀-co- PNP-C₁₀)** had a lower band gap of 1.45 eV, which was calculated from the commencement of the low energy end of the π - π^* transition at 660 nm, than chemically obtained black random copolymer of Reynolds and coworkers [74] ($E_g=1.64$ eV). The intensities of the π - π^* transition bands decreased simultaneously upon p-type doping, which unambiguously

indicated the presence of a homogeneous polymer film rather than bilayer. Furthermore, a new absorption band beyond 900 nm started to intensify due to the formation of charge carriers during doping process (**Figure 3.67**). These absorbance variations occurred around an isosbestic point which appeared at 796 nm (1.56 eV), suggesting that only two phases coexisted. Upon further oxidation, the polaron band reached a maxima while the π - π^* transition band diminished completely.

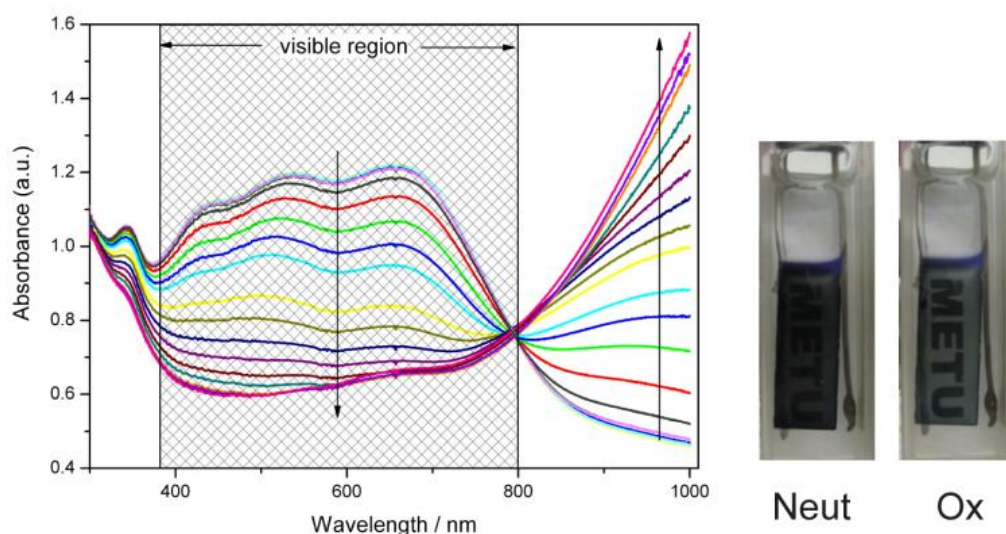


Figure 3.67. Electronic absorption spectra of the **P(PSeP-C₁₀-co- PNP-C₁₀)** film coated on ITO electrode at various applied potentials between 0.0 V and +1.2 V in 0.1 TBAH/ACN, and the colors of the **P(PSeP-C₁₀-co- PNP-C₁₀)** in different redox states.

Finally, these changes in the electronic absorption spectra of **P(PSeP-C₁₀-co- PNP-C₁₀)** film upon doping nicely reflected by a color a change from black ($L=14.3$, $a=0.29$, $b=0.35$) in the neutral state to transmissive grey ($L=39.2$, $a=0.29$, $b=0.33$) in the oxidized state (**Figure 3.67**). The percentage transmittance change ($\Delta\%T$) between the redox states was found to be 15.3 % for 522 nm. The transmittance

changes (optical contrast) was recorded via square-wave potential methods between 0.0 V and 1.2 V with switching times of 10 s, 5 s, 3 s and 2 s. As shown in **Figure 3.68**, **P(PSeP-C₁₀-co- PNP-C₁₀)** film preserved its electro-optical properties with no appreciable changes and the polymer film gave response in a very short time. For example, only 1.1 % optical contrast change was observed when the switching time was decreased to 2 s. These features show the versatility of the polymer film for the construction of high performance displays and electrochromic devices.

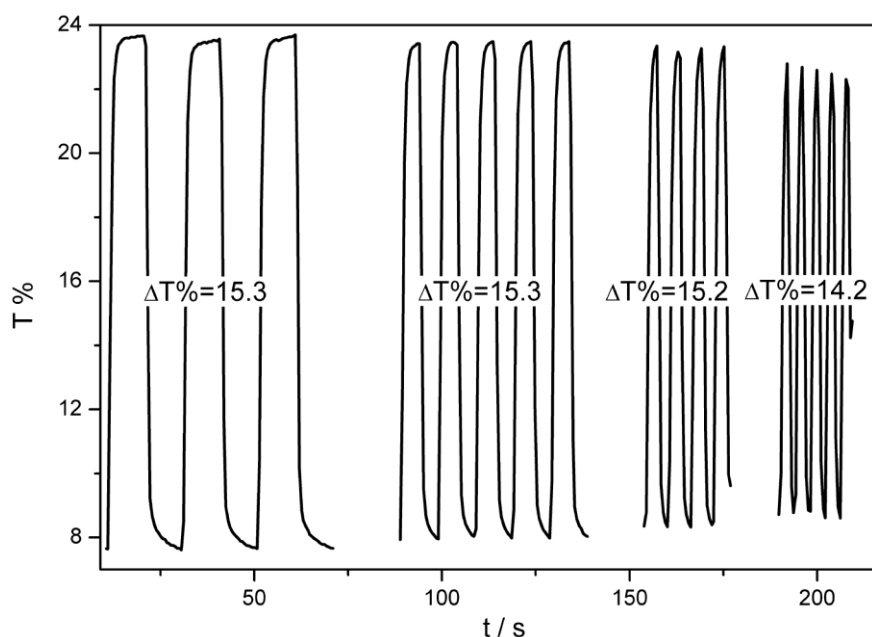


Figure 3.68. Chronoabsorptometry experiment at 522 nm for **P(PSeP-C₁₀-co- PNP-C₁₀)** film on ITO electrode in 0.1 M TBAH/ACN while the polymer was switched between -0.1 V and 1.0 V (vs Ag wire) with a switching time of 10 s, 5 s, 3 s and 2 s.

This copolymer is the first example of electropolymerized materials absorbing nearly the whole visible spectrum (400-800 nm) in the neutral state. Furthermore, **(P(PSeP-C₁₀-co- PNP-C₁₀))** has a low bandgap (1.45 eV) and it exhibits excellent operational and environmental stability. Considering the fact that low bandgap black polymers

hold promise for both solar cells and electronic ink-based applications, **(P(PSeP-C₁₀-co- PNP-C₁₀))** potential candidate for innovative technological applications.

3.2.7. Application of the Obtained Polymers as an Electrochromic Devices

In order to devise an electrochromic device, two polymers were needed. For this aim polymers were coated on the surface of the ITO via constant potential electrolysis. During this coating the most important point is that, the total charge passed during the redox process of the polymers used in the device should be equal in mC/cm^2 units. After coating the polymers on the surface of the ITO (one of them was left in oxidized, the other left in neutral states), they were waited during two hours in order to be dried. Then, ITO electrodes were stucked each other via gel electrolyte from the conductive polymer coated faces. In order to dry it, device was waited during two days, then it was operated (**Figure 3.69**). In order to run an electrochromic device, reference and counter electrodes were shortcuted and attached to the polymer in the oxidized state, and the working electrode was attached to the polymer in neutral state.

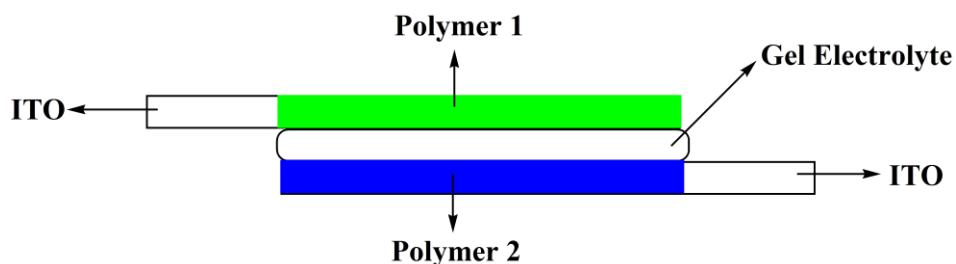


Figure 3.69. Schematic representation of an electrochromic device.

In this study, four different EC devices were devised: **P(PSeP-C₁₀)- P(POP-C₁₀)**, **P(PSeP-C₁₀)-PEDOT**, **P(PSeP-C₁₀)- P(PNP-C₁₀)** and **P(PSP-C₁₀)-PEDOT**.

First of all, in order to determine the working range of the EC devices, CVs of EC devices were employed (**Figure 3.70**). After determining the working range of devices spectroelectrochemical behaviors and switching properties of devices were investigated.

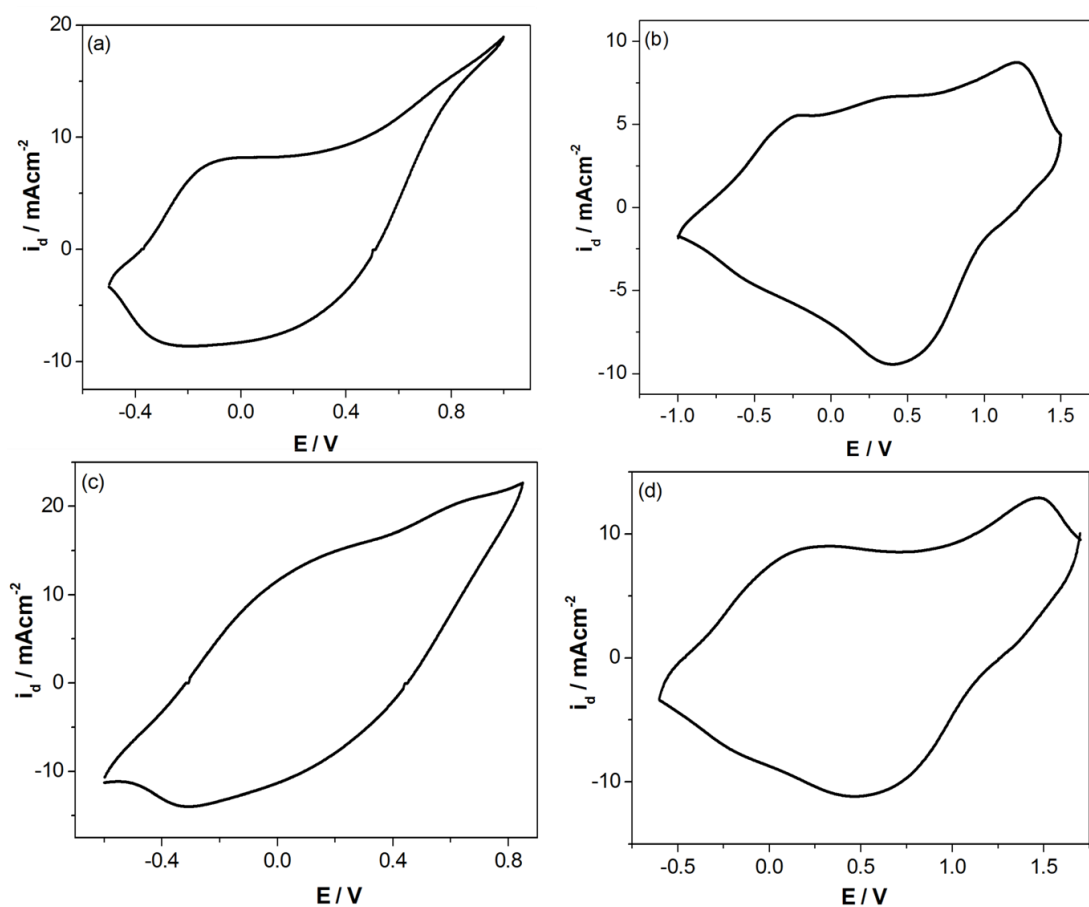


Figure 3.70. CV of (a) P(PSeP-C₁₀)- P(POP-C₁₀) (from -1.0 V to +1.5 V), (b) P(PSeP-C₁₀)-PEDOT (from -0.4 V to +1.0 V), (c) P(PSeP-C₁₀)- P(PNP-C₁₀) (from -0.6 V to +0.9 V) and (d) P(PSP-C₁₀)-PEDOT (from -0.6 V to +1.7 V) devices at 75 mVs⁻¹.

Spectroelectrochemical behaviors of the devices can be seen from the **Figure 3.63**. During the redox process, whereas the color of **P(PSeP-C₁₀)-PEDOT** and **P(PSeP-C₁₀)- P(PNP-C₁₀)** devices was turned from green to blue, the color of **P(PSP-C₁₀)-PEDOT** device was turned from cyan to blue, and the color of **P(PSeP-C₁₀)-P(POP-C₁₀)** device was turned from green to dark cyan (**Figure 3.71**).

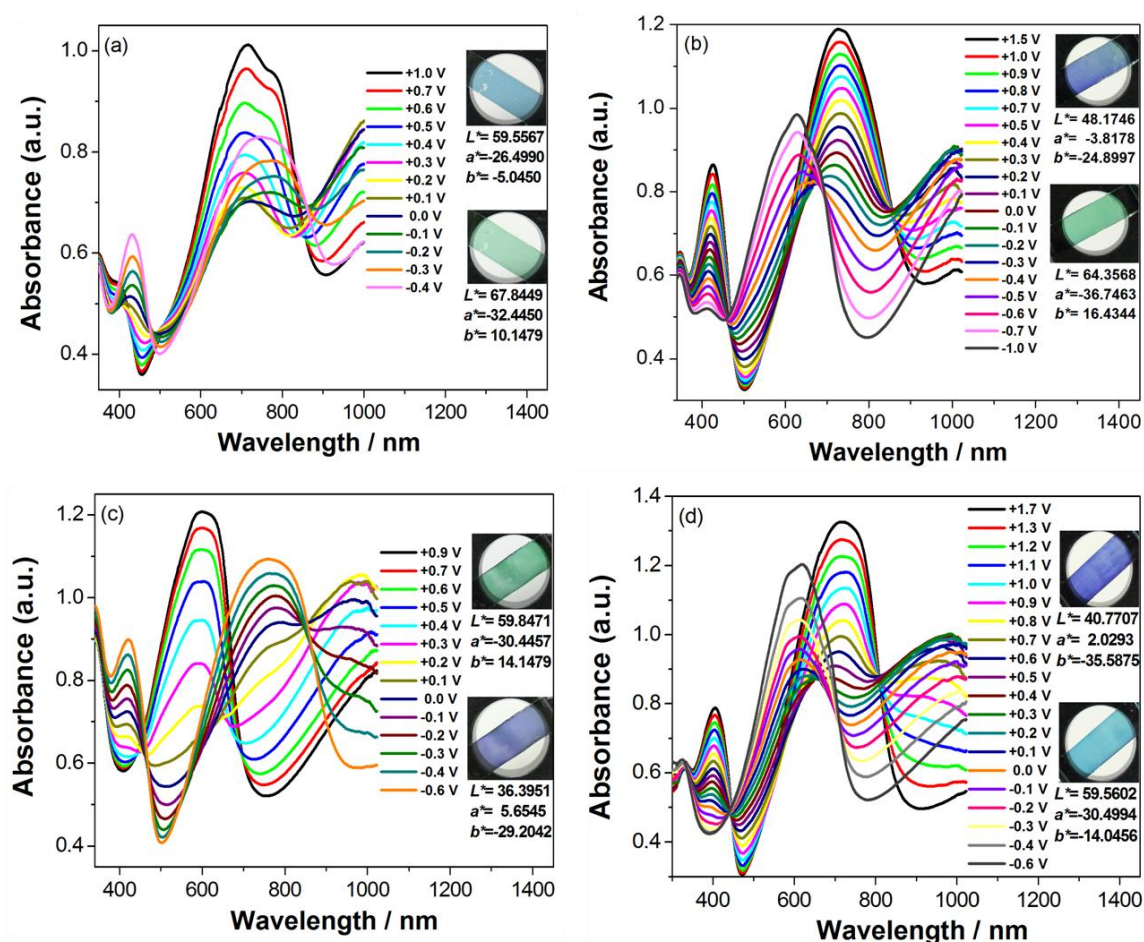


Figure 3.71. Spectroelectrochemical behavior of (a) **P(PSeP-C₁₀)- P(POP-C₁₀)** (from -1.0 V to +1.5 V), (b) **P(PSeP-C₁₀)-PEDOT** (from -0.4 V to +1.0 V), (c) **P(PSeP-C₁₀)- P(PNP-C₁₀)** (from -0.6 V to +0.9 V) and (d) **P(PSP-C₁₀)-PEDOT** (from -0.6 V to +1.7 V) devices. Inset: Pictures of device in two color states and $L^*a^*b^*$ values of these states.

The optical contrast of **P(PSeP-C₁₀)- P(POP-C₁₀)** device was found to be 15 % at 433 nm with a response time of 2 s (95 % of full optical switching), those of **P(PSeP-C₁₀)-PEDOT** device were calculated as 23 % at 427 nm with a response time 5.5 s and 27 % at 737 nm with a response time 6 s. Also, those of **P(PSeP-C₁₀)- P(PNP-C₁₀)** device were found to be 12 % at 612 nm with a response time 1 s and 22 % at 772 nm with a response time 3 s. Lastly, those of **P(PSP-C₁₀)-PEDOT** device were found to be 22 % at 410 nm with a response time 1 s and 15 % at 215 nm with a response time 2 s (**Table 3.12**).

Since these EC devices are the promising candidates as an advanced technological material, optical and electrochemical stabilities of EC devices are important. Therefore, optical and electrochemical stabilities of the EC devices were also determined (see **Table 3.13**). Among all the EC devices, **P(PSeP-C₁₀)- P(PNP-C₁₀)** device had superior properties with high optical and electrochemical stabilities (91 % and 92 %, respectively), and high coloration efficiency (544 cm²/C). However, this CE value is very low when it is compared with that of the SNS-Fluorene based device (25.600 cm²/C) [56].

Table 3.12. Optical and switching time data of **P(PSeP-C₁₀)- P(POP-C₁₀)**, **P(PSeP-C₁₀)-PEDOT**, **P(PSeP-C₁₀)- P(PNP-C₁₀)** and **P(PSP-C₁₀)-PEDOT** devices.

EC Device	Wavelength (λ_{max}, nm)	Contrast %T	CE (cm²/C)	Switching time (t, s)
P(PSeP-C₁₀)- P(POP-C₁₀)	433	15	133	2
P(PSeP-C₁₀)-PEDOT	427	23	293	5.5
	737	27	423	6
P(PSeP-C₁₀)- P(PNP-C₁₀)	612	12	373	1
	772	22	544	3
P(PSP-C₁₀)-PEDOT	410	22	148	1
	720	15	215	2

Table 3.13. Electrochemical and optical stability of **P(PSeP-C₁₀)- P(POP-C₁₀)**, **P(PSeP-C₁₀)-PEDOT**, **P(PSeP-C₁₀)- P(PNP-C₁₀)** and **P(PSP-C₁₀)-PEDOT** devices.

EC Device	Electrochemical Stability Retained (After 5000 Cycles)	Optical Stability Retained (After 5000 Cycles)
P(PSeP-C₁₀)- P(POP-C₁₀)	66 %	88 % (at 433 nm)
P(PSeP-C₁₀)-PEDOT	86 %	79 % (at 427 nm) 61% (at 737 nm)
P(PSeP-C₁₀)- P(PNP-C₁₀)	92 %	86 % (at 612 nm) 91 % (at 772 nm)
P(PSP-C₁₀)-PEDOT	77 %	79 % (at 410 nm) 54 % (at 720 nm)

CHAPTER 4

CONCLUSIONS

In this study, the effect of donor and acceptor groups, and the length of alkyl chains substituted on the donor groups were investigated. During these investigations, three different donor groups were examined: Thiophene, 3,4-ethylenedioxythiophene (EDOT) and dialkyl substituted 3,4-propylenedioxythiophene (ProDOT). It was observed that addition of ProDOT group instead of EDOT and thiophene groups as a donor unit gave some superior properties to the polymers such as higher stability, higher coloration efficiency and processability. Four different acceptor groups were used to determine the effect of acceptor units on the polymer properties: 2-decyl-2H-benzo[d][1,2,3]triazole, benzo[c][1,2,5]oxadiazole, benzo[c][1,2,5]thiadiazole and benzo[c][1,2,5]selenadiazole. Among all these polymers containing these acceptor units, only benzo[c][1,2,5]oxadiazole containing polymer was n-dopable and it was explained with the long alkyl chains in the donor units. That is, because of the steric effect of the long alkyl chain in the ProDOT units hindered n-doping process of the polymers. In order to prove this assumption, different length of alkyl chains were used: Decyl, hexyl and butyl. It was observed that when the alkyl chain was decyl group, polymer was soluble but did not have n-doping property. Replacement of decyl group with butyl group provided n-doping property to the corresponding polymer but the solubility was lost. In this case, it was observed that hexyl chain was the best one among the others, since both solubility and n-doping property could be obtained with hexyl chain at the same time.

It should be also mentioned that the first electrochemically obtained black colored neutral state copolymer with a low band gap (1.45 eV) was synthesized from copolymerization of **PSeP-C₁₀** and **PNP-C₁₀** during this study. Since this copolymer absorbs whole visible spectrum, this is not only a potential candidate for optoelectronic devices, displays (road signs, clocks and shop displays), windows shades along with many flexible and portable art and design applications, but also very valuable for solar cell applications.

It is noteworthy that electropolymerization of these D-A-D systems provided processable and low band gap electrochromes reflecting various hues of blue and green colors in the neutral state. During the investigation of the color tuning, invaluable cyan colored polymers (**P(PSP-C₁₀)**, **P(PSP-C₆)** and **P(POP-C₁₀)**) were obtained. Furthermore, these PEC candidates exhibit high redox stability, high CE, %T and/or contrast ratio, and fast switching time in subsecond scale.

Together with the synthesized polymers, via using color mixing theory, all colors in the RGB and CMY color space were obtained in this study.

EC device applications of these polymers were also investigated. Among all the EC devices, **P(PSeP-C₁₀)**- **P(PNP-C₁₀)** device had superior properties with high optical and electrochemical stabilities (91 % and 92 %, respectively), and high coloration efficiency (544 cm²/C).

It is generally considered that in solar cells the polymer film used as an electron donor part must have at least 0.3-0.4 eV higher LUMO level than that of PCBM used as an electron acceptor part in order to provide an efficient charge separation between these parts [107, 108]. Also, the HOMO level of the low band gap polymer film (lower than 1.8 eV) must have a desired position with respect to the LUMO

level of the acceptor since higher HOMO level will decrease the open circuit voltage and lower HOMO level will reduce the power output [37]. Based on the foregoing findings, all polymers have not only desired LUMO levels with respect to the acceptor but also lower band gaps in order to match of the solar spectrum. Among the all processable polymer films in this study, PPSP-C₁₀ polymer film has the most suitable HOMO and LUMO levels as well as the low band gap with respect to the acceptor, which means that the polymer was a potential candidate for use in organic solar cells.

REFERENCES

- [1] Staudinger, H. *Nobel Lectures, Chemistry 1942-1962*; Elsevier Publishing Company: Amsterdam, 1964.
- [2] Staudinger, H. *Ber. Dtsch. Chem. Ges. B* 1920, 53, 1073.
- [3] Staudinger, H. Fritsch, J. *Helv. Chim. Acta* 1922, 5, 785.
- [4] Chiang, C.K.; Fincher, C.R.; Park, Y.W.; Heeger, A.J.; Shirakawa, H.; Louis, E.J.; Gau, S.C.; MacDiarmid, A.G. *Phys. Rev. Lett.* 1977, 39, 1098.
- [5] Chiang, C.K.; Fincher, C.R.; Park, Y.W.; Heeger, A.J.; Shirakawa, H.; Louis, E.J.; Gau, S.C.; MacDiarmid, A.G. *Phys. Rev. Lett.* 1978, 40, 1472.
- [6] Greenham, N. C.; Moratti, S.; Bradley, D. D. C.; Friend, R. H.; Holmes, A. B. *Nature* 1993, 365, 628.
- [7] Friend, R. H.; Gymer, R. W.; Holmes, A. B.; Burroughes, J. H.; Marks, R. N.; Taliani, C.; Bradley, D. D. C.; Dos Santos, D. A.; Bredas, J. L.; Logdlund, M.; Salaneck, W. R. *Nature* 1999, 397, 121.
- [8] List, E. J. W.; Guentner, R.; De Freitas, P. S.; Scherf, U. *Adv. Mater.* 2002, 14, 374.
- [9] Goel, A.; Dixit, M.; Chaurasia, S.; Kumar, A.; Raghunandan, R.; Maulik, P. R.; Anand, R. S. *Org. Lett.* 2008, 10, 2553.
- [10] Schmidt-Mende, L.; Fechtenkötter, A.; Mullen, K.; Moons, E.; Friend, R. H.; Mackenzie, J. D. *Science* 2001, 293, 1119.
- [11] Liscio, A.; De Luca, G.; Nolde, F.; Palermo, V.; Müllen, K.; Samori, P. *J. Am. Chem. Soc.* 2008, 130, 780.
- [12] Fréchet, J.M.J.; Thompson, B. C. *Angew. Chem., Int. Ed.* 2008, 47, 58.
- [13] Dance, Z. E. X.; Ahrens, M. J.; Vega, A. M.; Ricks, A. B.; McCamant, D. W.; Ratner, M. A.; Wasielewski, M. R. *J. Am. Chem. Soc.* 2008, 130, 830.

- [14] Hagberg, D. P.; Yum, J.-H.; Lee, H.; De Angelis, F.; Marinado, T.; Karlsson, K. M.; Humphry-Baker, R.; Sun, L.; Hagfeldt, A.; Grätzel, M.; Nazeeruddin, Md. K. *J. Am. Chem. Soc.* 2008, 130, 6259.
- [15] Muccini, M. *Nat. Mater.* 2006, 5, 605.
- [16] Gao, P.; Beckmann, D.; Tsao, H. N.; Feng, X.; Enkelmann, V.; Pisula, W.; Müllen, K. *Chem. Commun.* 2008, 1548.
- [17] Usta, H.; Facchetti, A.; Marks, T. J. *J. Am. Chem. Soc.* 2008, 130, 8580.
- [18] Yang, C.; Kim, J. Y.; Cho, S.; Lee, J. K.; Heeger, A. J.; Wudl, F. *J. Am. Chem. Soc.* 2008, 130, 6444.
- [19] Palma, M.; Levin, J.; Lemaur, V.; Liscio, A.; Palermo, V.; Cornil, J.; Geerts, Y.; Lehmann, M.; Samori, P. *Adv. Mater.* 2006, 18, 3313.
- [20] Chen, X.; Jeon, Y.-M.; Jang, J.-W.; Qin, L.; Huo, F.; Wei, W.; Mirkin, C. A. *J. Am. Chem. Soc.* 2008, 130, 8166.
- [21] Coi, T.-L.; Lee, K.-H.; Joo, W.-J.; Lee, S.; Lee, T.-W.; Chae, M. Y. *J. Am. Chem. Soc.* 2007, 129, 9842.
- [22] Skotheim, T. A.; Reynolds, J. R. *Handbook of Conducting Polymers-Conjugated Polymers: Synthesis, Properties and Characterization*; CRC Press: Boca Raton, FL, 2007.
- [23] Forrest, S. R. *Nature* 2004, 428, 911.
- [24] Reese, C.; Roberts, M.; Ling, M.-M.; Bao, Z. *Mater. Today* 2004, 7, 20.
- [25] Schwendeman, I.; Hickman, R.; Sonmez, G.; Schottland, P.; Zong, K.; Welsh, D.; Reynolds, J. R. *Chem. Mater.* 2002, 14, 3118.
- [26] Meng, H.; Tucker, D.; Chaffins, S.; Chen, Y.; Helgeson, R.; Dunn, B.; Wudl, F. *Adv. Mater.* 2003, 15, 146.
- [27] Bange, K.; Gambke, T. *Adv. Mater.* 1990, 2, 10.
- [28] Pennisi, A.; Simone, F.; Barletta, G.; Di Marco, G.; Lanza, L. *Electrochim. Acta* 1999, 44, 3237.
- [29] Rauh, R. *Electrochim. Acta* 1999, 44, 3165.
- [30] Mortimer, R. G. *Chem. Soc. Rev.* 1997, 26, 147.
- [31] Rosseinsky, D. R.; Mortimer, R. J. *Adv. Mater.* 2001, 13, 783.
- [32] Chandrasekhar, P.; Zay, B. J.; Birur, G. C.; Rawal, S.; Pierson, E. A.; Kauder, L.; Swanson, T. *Adv. Funct. Mater.* 2002, 12, 95.

- [33] Beaupré, S.; Breton, A.-C.; Dumas, J.; Leclerc, M. *Chem. Mater.* 2009, 21, 1504.
- [34] Buckley, D. N.; Burke, L. D.; Mukahy, J. K. J. *Chem. Soc., Faraday Trans. 1* 1976, 72, 1896.
- [35] Burke, L. D.; Thomey, T. A. M.; Whelan, D. P. *J. Electroanal. Chem.* 1980, 107, 201.
- [36] Dautremont-Smith, W. C. *Displays* 1982, 3, 3.
- [37] Granqvist, C. G. *Sol. Energy Mater. Sol. Cells* 2000, 60, 201.
- [38] Granqvist, C. G.; Avendano, E.; Azens, A. *Thin Solid Films* 2003, 442, 201.
- [39] Avendano, E.; Berggren, L.; Niklasson, G. A.; Granqvist, C. G.; Azens, A. *Thin Solid Films* 2006, 496, 30]
- [40] Roncali, J. *Chem. Rev.* 1997, 97, 173.
- [41] Cihaner, A.; Algi, F. *Adv. Func. Mater.* 2008, 18, 3583.
- [42] Arbizzani, C.; Mastragostino, M.; Soavi, F. *Electrochim. Acta* 2000, 45, 2273.
- [43] Barbarella, G.; Favaretto, L.; Sotgiu, G.; Zambianchi, M.; Arbizzani, C.; Bongini, A.; Mastragostino, M. *Chem. Mater.* 1999, 11, 2533.
- [44] Bongini, A.; Barbarella, G.; Favaretto, L.; Zambianchi, M.; Mastragostino, M.; Arbizzani, C.; Soavi, F. *Synth. Met.* 1999, 101, 13.
- [45] Suh, M. C.; Jiang, B.; Tilley, T. D. *Angew. Chem. Int. Ed.* 2000, 39, 2870.
- [46] Dubois, C.J., *Donor-Acceptor Methods for Band Gap Control in Conjugated Polymers, Ph.D. Thesis*, 2003, Florida, USA.
- [47] Thomas, C.A., *Donor-Acceptor Methods for Band Gap Reduction in Conjugated Polymers: The Role of Electron-Rich Donor Heterocycles*, Ph.D. Thesis, 2002, Florida, USA.
- [48] Leclerc, M. *Adv. Mater.* 1999, 11, 1491.
- [49] Wise, D. L.; Wnek, G. E.; Trantolo, D. J.; Cooper, T. M.; Gresser, J. D. *Electrical and Optical Polymer Systems: Fundamentals, Methods, and Applications*; Marcel Dekker Press: New York, 1998.
- [50] Dyer, A. L.; Thompson, E. J.; Reynolds, J. R. *Appl. Mater. Interfaces* 2011, DOI: 10.1021/am200040p.
- [51] Beaujuge, P. M.; Reynolds, J. R. *Chem. Rev.* 2010, 110, 268.

- [52] Jones, A. G., *Increasingly Functional Poly(3,4-Alkylenedioxythiophene)s Through Facile Substitution*, Ph.D. Thesis, 2007, Florida, USA.
- [53] Fabretto, M.; Vaithianathan, T.; Hall, C.; Mazurkiewicz, J.; Innis, P. C.; Wallace, G. G.; Murphy, P. *Electrochim. Acta* 2008, 53, 2250.
- [54] Fabretto, M.; Vaithianathan, T.; Hall, C.; Murphy, P.; Innis, P. C.; Mazurkiewicz, J.; Wallace, G. G. *Electrochem. Commun.* 2007, 9, 2032.
- [55] Reeves, B. D.; Grenier, C. R. G.; Argun, A. A.; Cirpan, A.; McCarley, T. D.; Reynolds, J. R. *Macromolecules* 2004, 37, 7559.
- [56] Algi, F.; Cihaner, A. *Tetrahedron Letters* 2008, 49, 3530.
- [57] Beaujuge, P. M.; Ellinger, S.; Reynolds, J. R. *Adv. Mater.* 2008, 20, 2772.
- [58] Chen, R. G.-S.; Patel, A. D. *Water-Soluble Polymers*; ACS Press: Houston, 1986 Chapter 12.
- [59] Inzelt, G. *Conducting Polymers-A New Era in Electrochemistry*; Springer: Germany, 2008.
- [60] Wang, H.-L.; O'Malley, R. M.; Fernanded, J. E. *Macromolecules* 1994, 27, 893.
- [61] İçli, M.; Önal, A. M.; Cihaner, A. *Polym. Int.* 2009, 58, 674.
- [62] Shin, W. S.; Kim, M.; Jin, S.; Shim, Y.; Lee, J.; Lee, J. W.; Gal, Y. *Mol. Cryst. Liq. Cryst.* 2006, 444, 129.
- [63] Furniss, B. S.; Hannaford, A. J.; Smith, P. W. G.; Tatchell, A. R. *Vogel's Text Book of Practical Organic Chemistry*; Dorling Kindersly Press: India, 2006.
- [64] Yasuda, T.; Imase, T.; Yamamoto, T. *Macromolecules* 2005, 38, 7378.
- [65] Zeng, W.; Zhang, Y.; Hou, Q.; Yang, W.; Cao, Y. *Eur. Polym. J.* 2005, 41, 2923.
- [66] Sonmez, G.; Sonmez, H. B.; Shen, C. K. F.; Wudl, F. *Adv. Mater.* 2004, 16, 1905.
- [67] Sonmez, G. *Chem. Commun.* 2005, 42, 5251.
- [68] Sonmez, G.; Shen, C. K. F.; Rubin, Y.; Wudl, F. *Angew. Chem., Int. Ed.* 2004, 43, 1498.
- [69] Havinga, E. E.; Hoeve, W.; Wynberg, H. *Synth. Met.* 1993, 55, 299.
- [70] Xu, X.; Chen, S.; Yu, G.; Di, C.; You, H.; Ma, D.; Liu, Y. *Adv. Mater.* 2007, 19, 1281.
- [71] Zhu, Y.; Kulkarni, A. P.; Jenekhe, S. A. *Chem. Mater.* 2005, 17, 5225.

- [72] Chen, C.-T.; Lin, J.-S.; Moturu, M. V. R. K.; Lin, Y.-W.; Yi, W.; Tao, Y.-T.; Chen, C.-H. *Chem. Commun.* 2005, 16, 3980.
- [73] Heeney, M.; Zhang, W.; Crouch, D. J.; Chabinyc, M. L.; Gordeyev, S.; Hamilton, R.; Higgins, S. J.; McCulloch, I.; Skabara, P. J.; Sparrowe, D.; Tierney, S. *Chem. Commun.* 2007, 18, 5061.
- [74] Beaujuge, P. M.; Ellinger, S.; Reynolds, J. R. *Nat. Mater.* 2008, 7, 795.
- [75] Beaujuge, P. M.; Vasilyeva, S. V.; Ellinger, S.; McCarley, T. D.; Reynolds, J. R. *Macromolecules* 2009, 42, 3694.
- [76] Durmus, A.; Gunbas, G.; Camurlu, P.; Toppare, L. *Chem. Commun.* 2007, 3246.
- [77] Durmus, A.; Gunbas, G.; Toppare, L. *Chem. Mater.* 2007, 19, 6247.
- [78] Durmus, A.; Gunbas, G.; Toppare, L. *Adv. Mater.* 2008, 20, 691.
- [79] Gunbas, G.; Durmus, A.; Toppare, L. *Adv. Funct. Mater.* 2008, 18, 2026.
- [80] Balan, A.; Gunbas, G.; Durmus, A.; Toppare, L. *Chem. Mater.* 2008, 20, 7510.
- [81] Algi, F.; Cihaner, A. *Org. Electron.* 2009, 10, 453.
- [82] Sonmez, G.; Sonmez, H. B.; Shen, C. K. F.; Jost, R. W.; Rubin, Y.; Wudl, F. *Macromolecules* 2005, 38, 669.
- [83] Reese, C.; Roberts, M.; Ling, M.-M.; Bao, Z. *Mater. Today* 2004, 7, 20.
- [84] Monk, P. M. S.; Mortimer, R. J.; Rosseinsky, D. R. *Electrochromism and Electrochromic Devices*; Cambridge University Press: Cambridge, U.K., 2007.
- [85] Argun, A. A.; Aubert, P. H.; Thompson, B. C.; Schwendeman, I.; Gaupp, C. L.; Hwang, J.; Pinto, N. J.; Tanner, D. B.; MacDiarmid, A. G.; Reynolds, J. R. *Chem. Mater.* 2004, 16, 4401.
- [86] Amb, C. M.; Beaujuge, P.; Reynolds, J. R. *Adv. Mater.* 2010, 22, 724.
- [87] İçli-Özkut, M.; Atak, S.; Önal, A. M.; Cihaner, A. *J. Mater. Chem.* 2011, 21, 5268.
- [88] Raimundo, J.-M.; Blanchard, P.; Brisset, H.; Akoudad, S.; Roncali, J. *Chem. Commun.* 2000, 939.
- [89] Sonmez, G.; Meng, H.; Wudl, F. *Chem. Mater.* 2004, 16, 574.
- [90] Gaup, G. L.; Walsh, D. M.; Rauh, R. D.; Reynolds, J. R. *Chem. Mater.* 2002, 14, 3964.

- [91] Shin, W.S.; Kim, S.C.; Lee, S.-J.; Jeon, H.S.; Kim, M.-K.; Naidu, B.V.K.; Jin, S.-H.; Lee, J.-K.; Lee, J.W.; Gal, Y.-S. *J. Polym. Sci. Part A: Polym. Chem.* 2007, 45, 1394.
- [92] Skotheim, T.A.; Reynolds, J.R. *Handbook of conducting polymers-conjugated polymers: processing and applications*: CRC Press Taylor and Francis Group, 2007.
- [93] Kitamura, C.; Tanaka, S.; Yamashita, Y. *Chem. Mater.* 1996, 8, 570.
- [94] Atwani, O.; Baristiran, C.; Erden, A.; Sonmez, G. *Synth. Met.* 2008, 158, 83.
- [95] Balan, A.; Baran, D.; Gunbas, G.; Durmus, A.; Ozyurt, F.; Toppare, L. *Chem. Commun.* 2009, 6768.
- [96] Cetin, G. A.; Balan, A.; Durmus, A.; Gunbas, G.; Toppare, L. *Org. Electron.* 2009, 10, 34.
- [97] İçli, M.; Pamuk, M.; Algi, F.; Önal, A. M.; Cihaner, A. *Chem. Mater.* 2010, 22, 4034.
- [99] Zade, S. S.; Bendikov, M. *Chem. Eur. J.* 2007, 13, 3688.
- [100] Patra, A.; Bendikov, M. *J. Mater. Chem.* 2010, 20, 422.
- [101] Langer, J.J.; Krzyminiwski, R.; Kruczynski, Z.; Gibinski, T.; Czajkowski, I.; Framski, G. *Synth Met.* 2001, 122, 359.
- [102] İçli, M.; Pamuk, M.; Algi, F.; Önal, A. M.; Cihaner, A. *Org. Electron.* 2010, 11, 1255.
- [103] Öktem, G.; Balan, A.; Baran, D.; Toppare, L. *Chem. Commun.* 2011, 47, 3933.
- [104] Krebs, F.C. *Nat. Mater.* 2008, 7, 766.
- [105] Dennler, G.; Scharber, M. C.; Brabec, C. J. *Adv. Mater.* 2009, 21, 1323.
- [106] Sakamoto, Y.; Suzuki, T.; Kobayashi, M.; Gao, Y.; Fukai, Y.; Inoue, Y.; Sato, F.; Tokito, S. *J. Am. Chem. Soc.* 2004, 126, 8138.
- [107] Brabec, C.J.; Sariciftci, N.S.; Hummelen, J.C. *Adv. Func. Mater.* 2001, 11, 15.
- [108] Langer, J.J.; Krzyminiwski, R.; Kruczynski, Z.; Gibinski, T.; Czajkowski, I.; Framski, G. *Synth. Met.* 2001, 122, 359.

APPENDIX A

FTIR SPECTRA OF MONOMERS

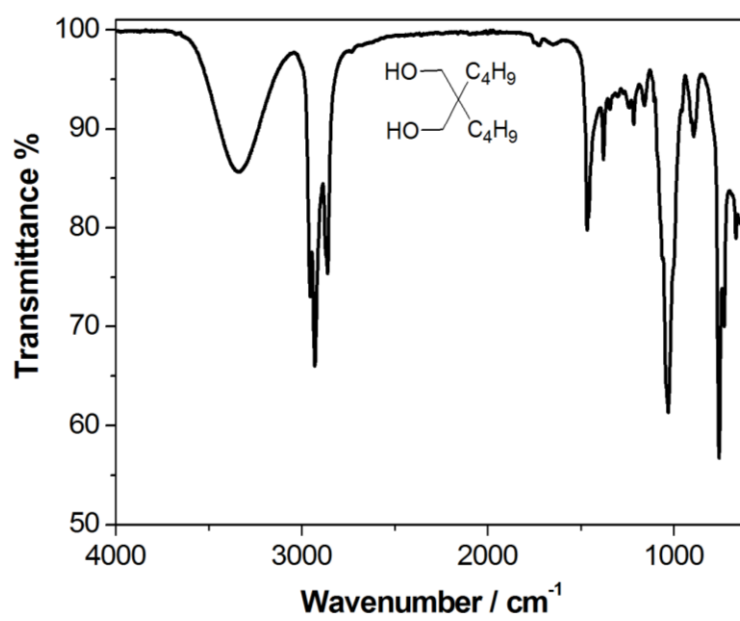


Figure A 1. FTIR spectrum of 4.

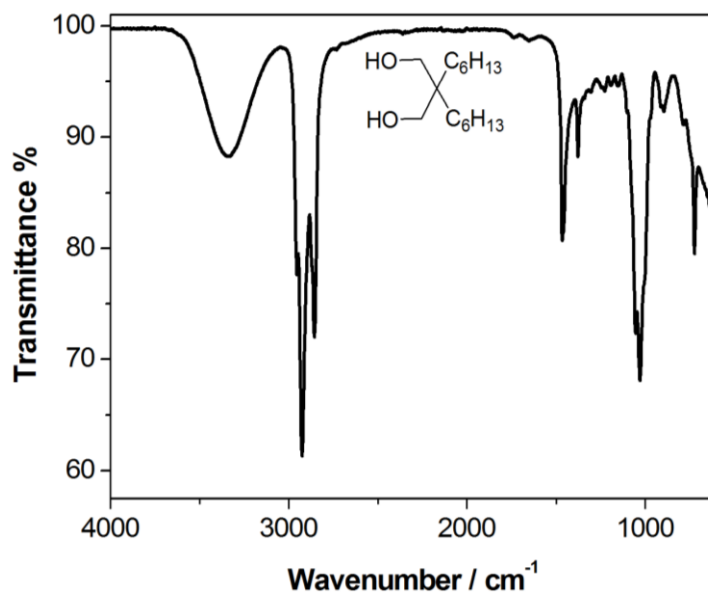


Figure A 2. FTIR spectrum of 5.

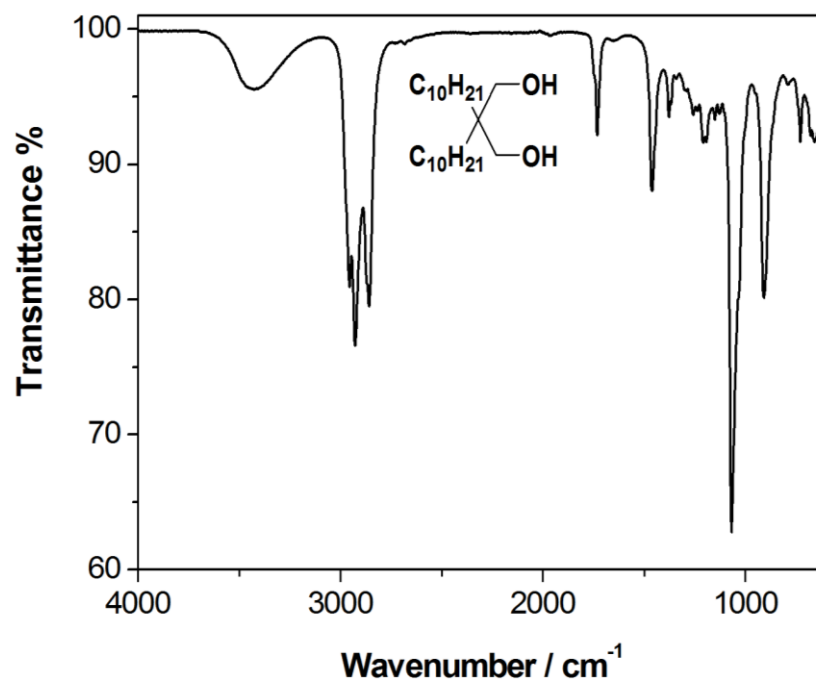


Figure A 3. FTIR spectrum of 6.

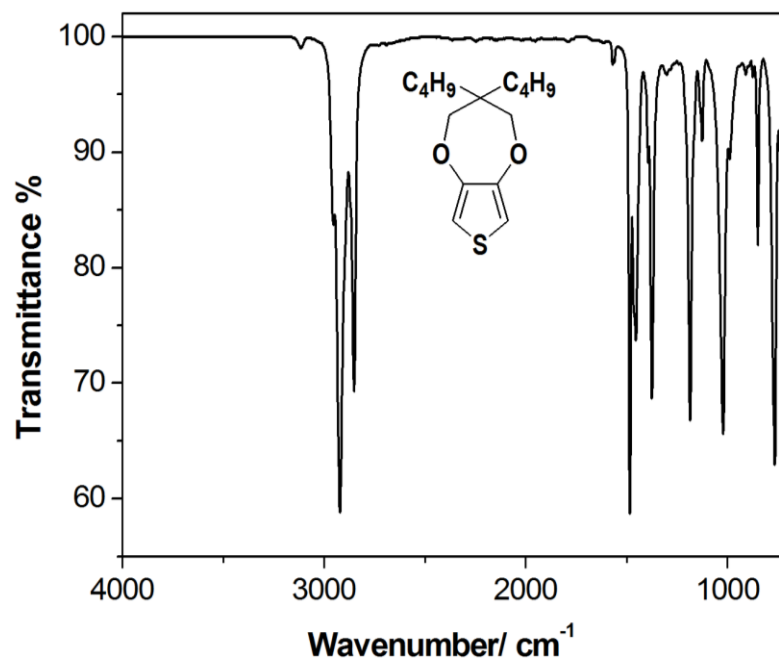


Figure A 4. FTIR spectrum of 7.

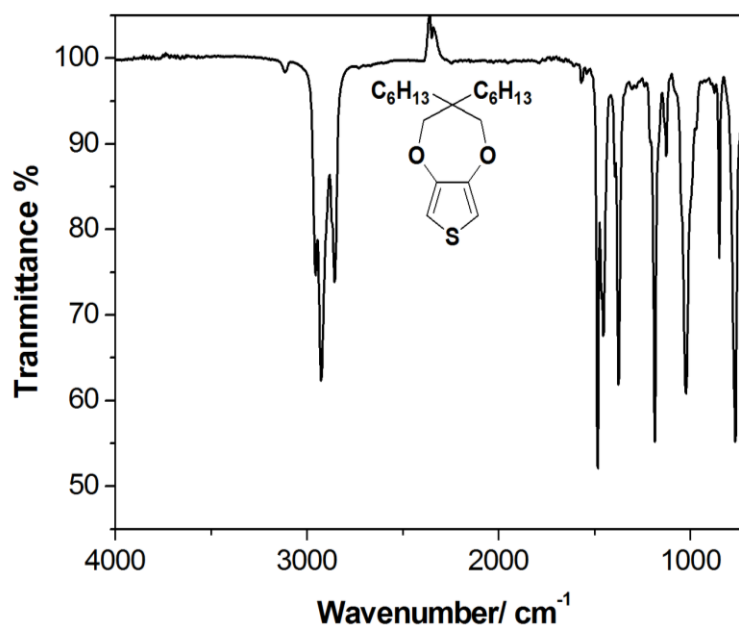


Figure A 5. FTIR spectrum of 8.

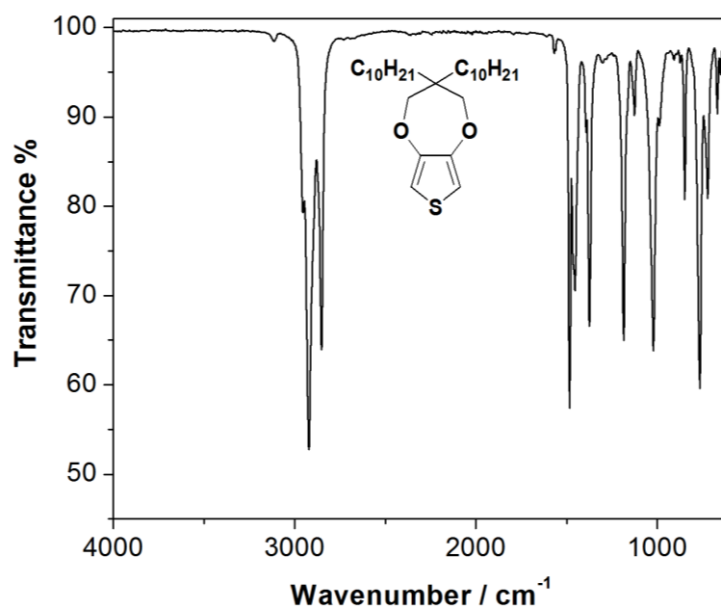


Figure A 6. FTIR spectrum of 9.

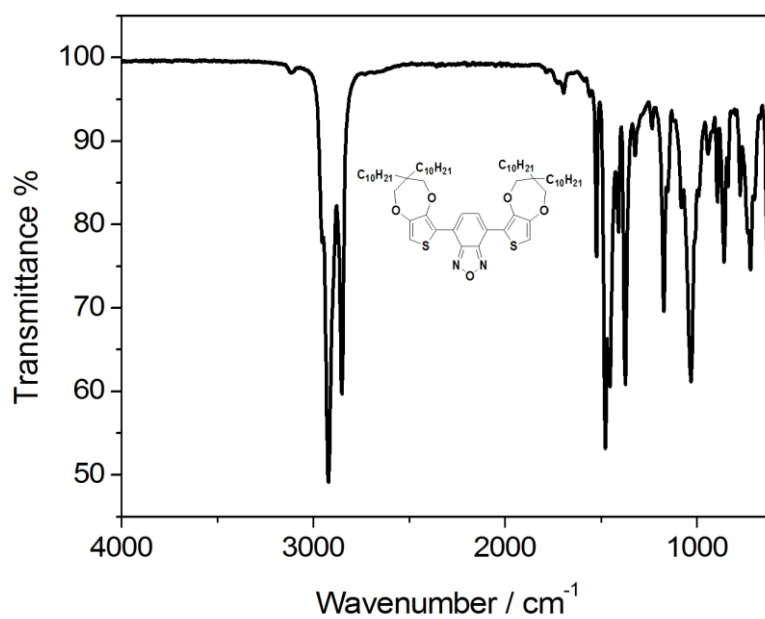


Figure A 7. FTIR spectrum of POP-C₁₀.

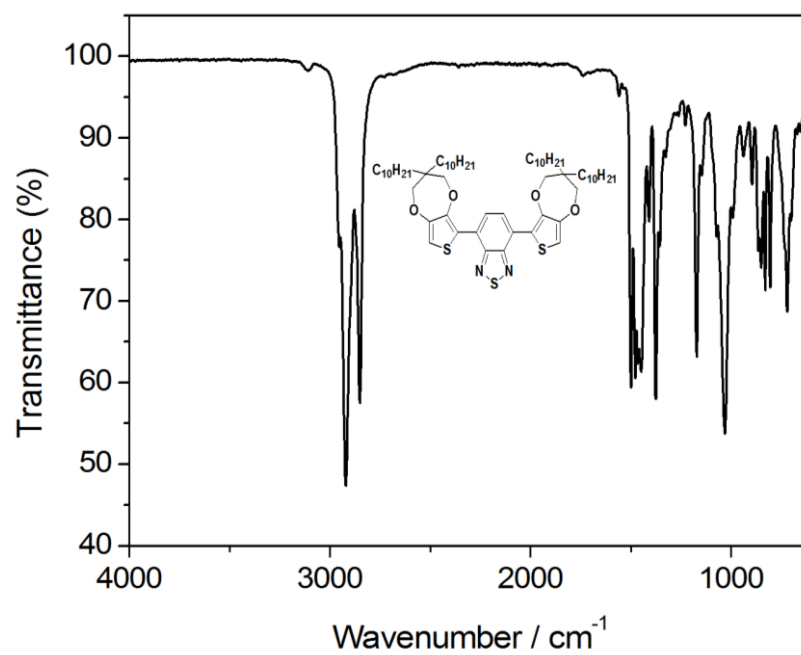


Figure A 8. FTIR spectrum of **PSP-C₁₀**.

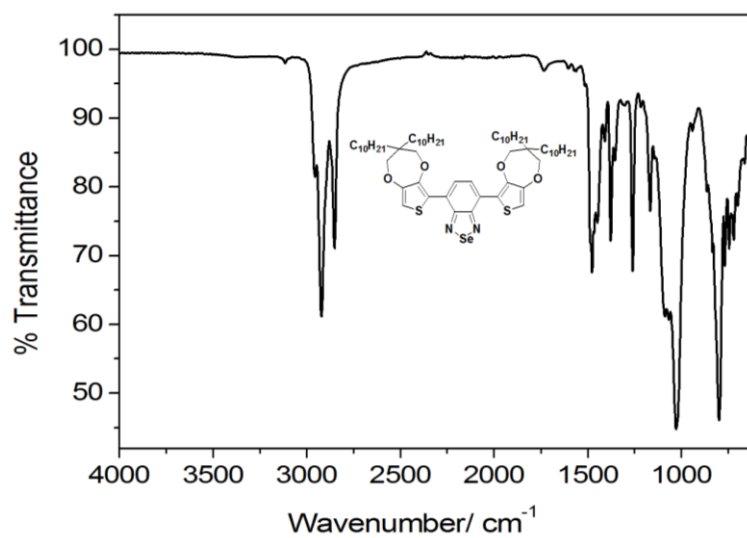


Figure A 9. FTIR spectrum of **PSeP-C₁₀**.

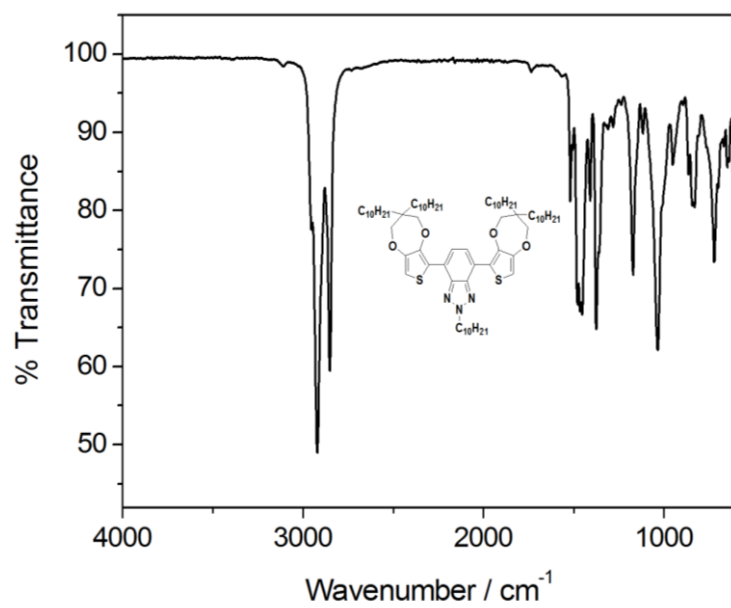


Figure A 10. FTIR spectrum of PNP-C₁₀.

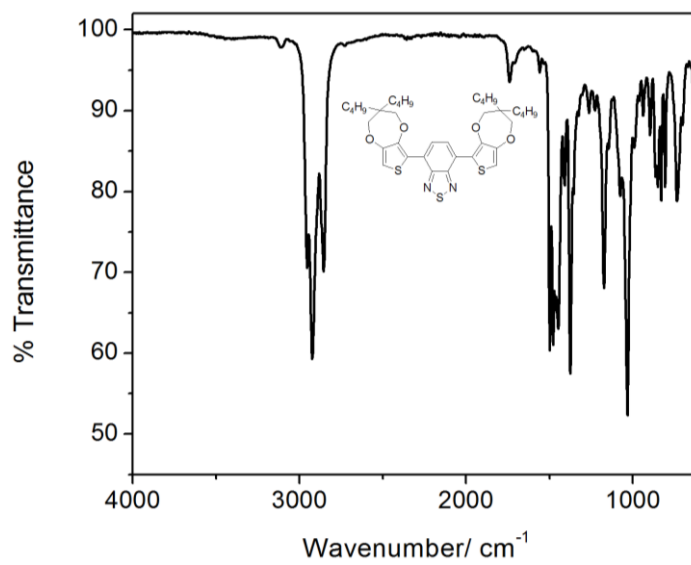


Figure A 11. FTIR spectrum of PSP-C₄.

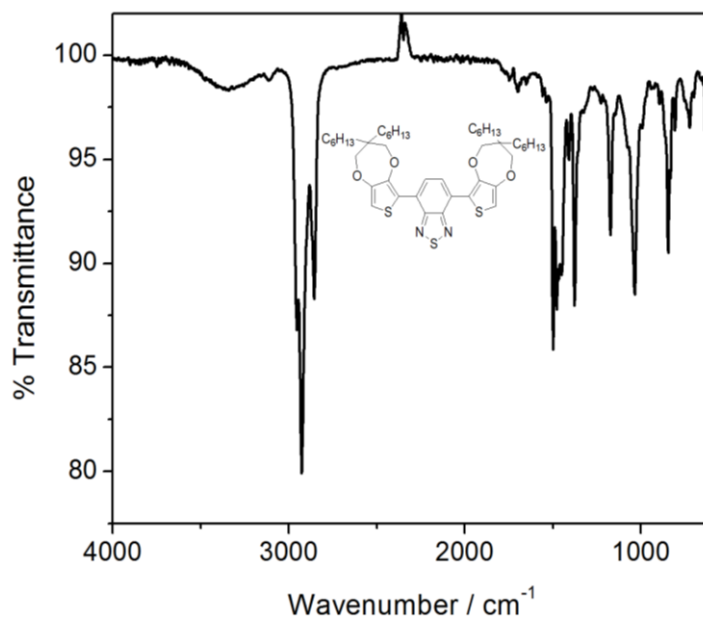


Figure A 12. FTIR spectrum of **PSP-C₆**.

APPENDIX B

NMR SPECTRA OF MONOMERS

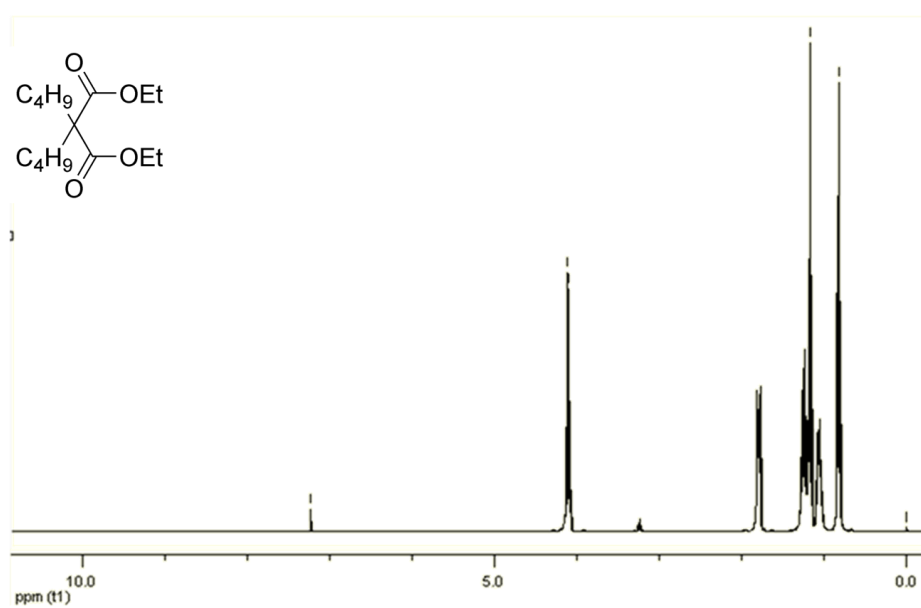


Figure B 1. ^1H NMR spectrum of 1 in CDCl_3 .

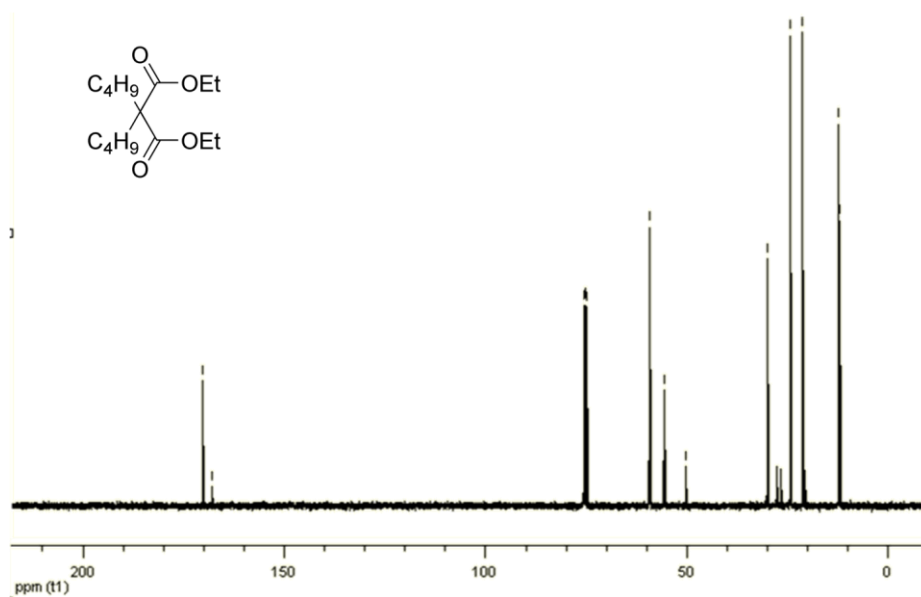


Figure B 2. ^{13}C NMR spectrum of 1 in CDCl_3 .

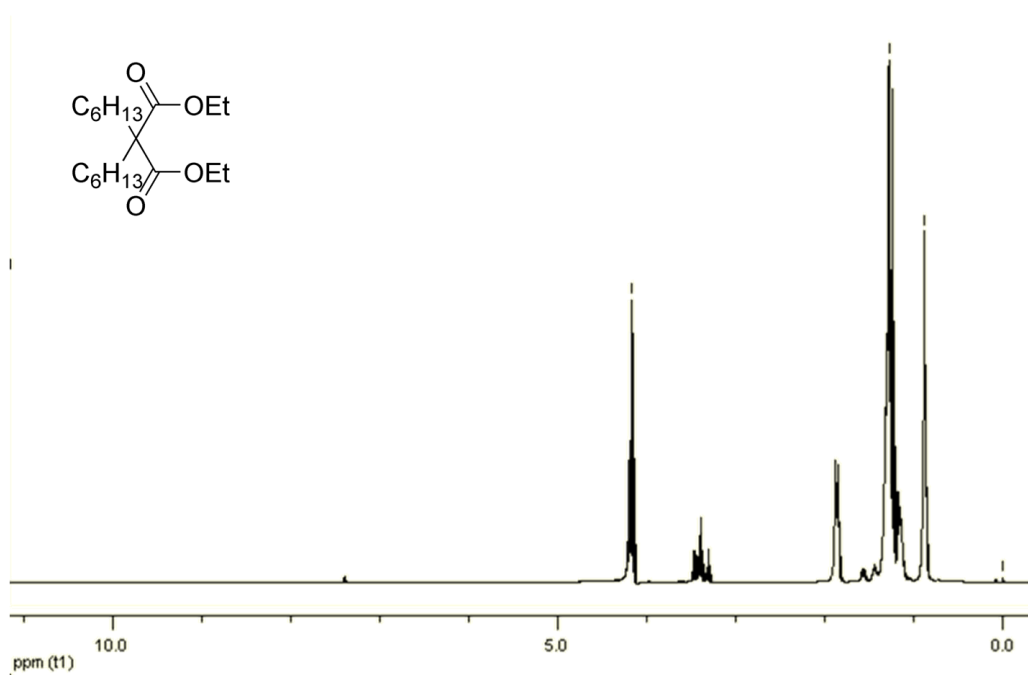


Figure B 3. ¹H NMR spectrum of **2** in CDCl₃.

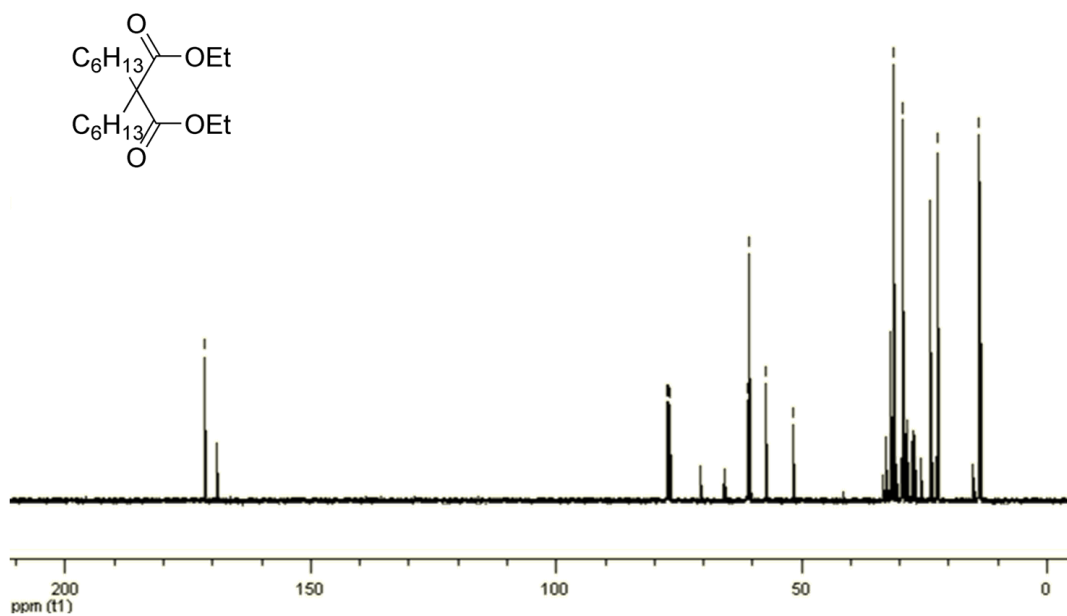


Figure B 4. ¹³C NMR spectrum of **2** in CDCl₃.

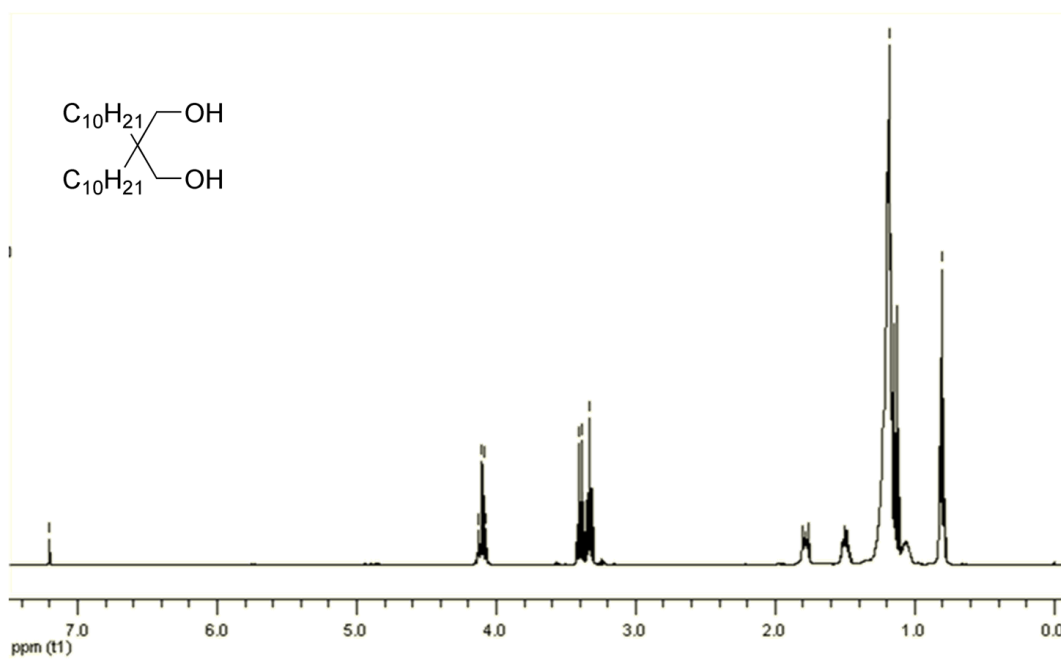


Figure B 5. ^1H NMR spectrum of **6** in CDCl_3 .

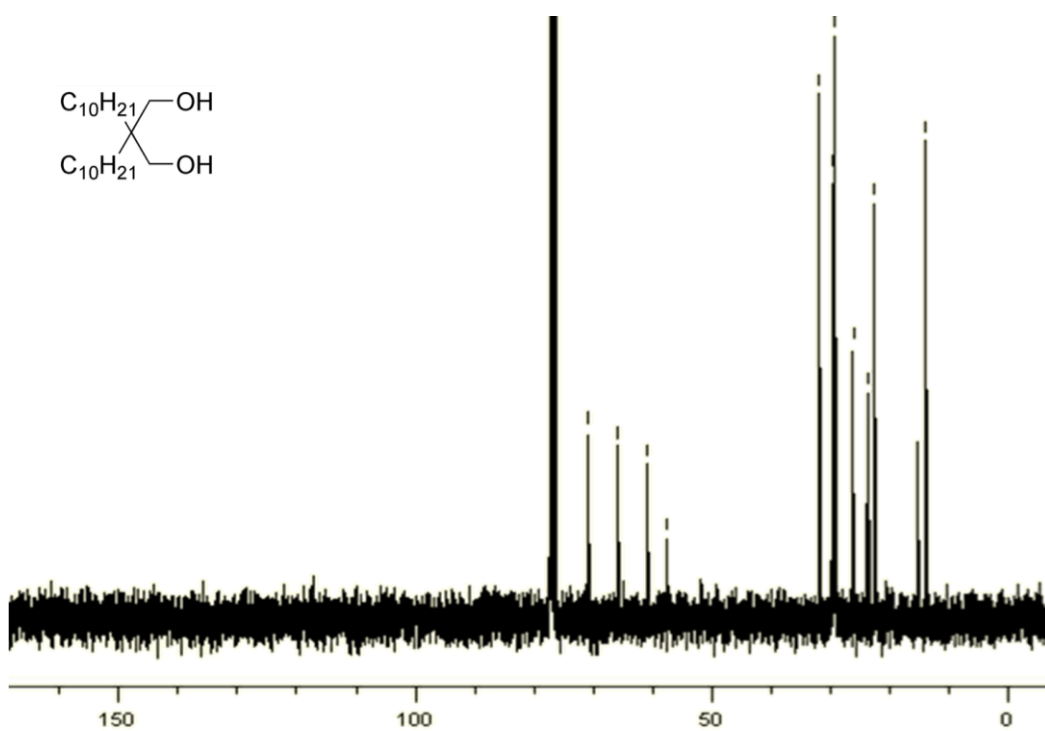


Figure B 6. ^{13}C NMR spectrum of **6** in CDCl_3 .

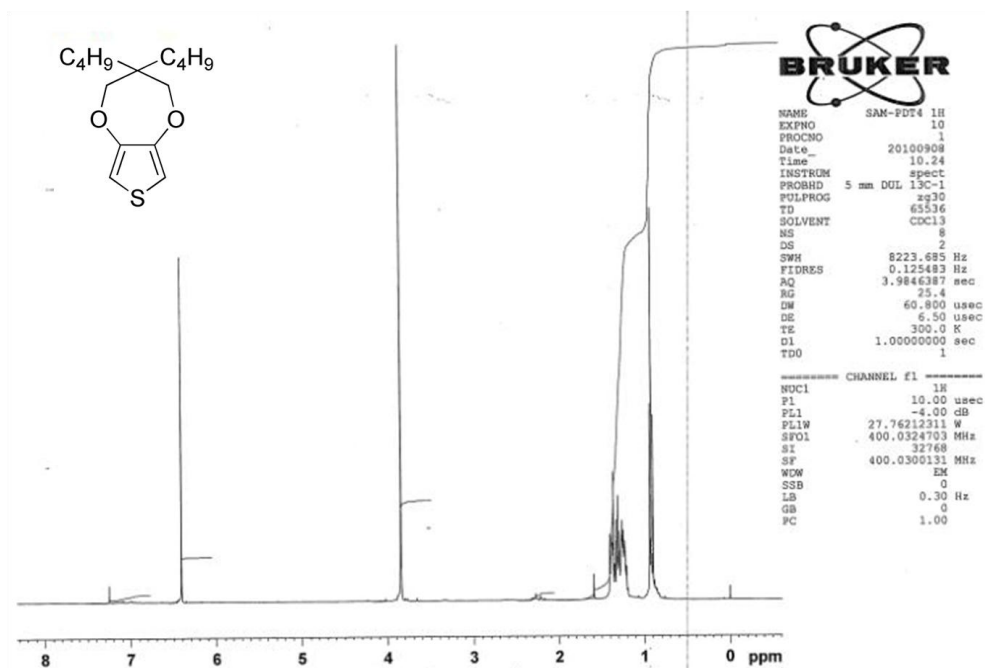


Figure B 7. ^1H NMR spectrum of **7** in CDCl_3 .

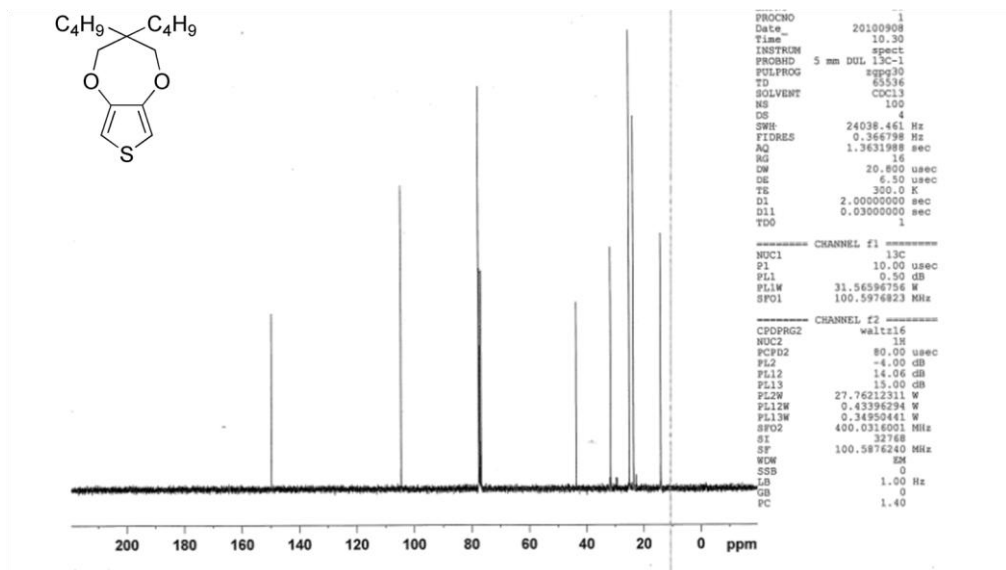


Figure B 8. ^{13}C NMR spectrum of **7** in CDCl_3 .

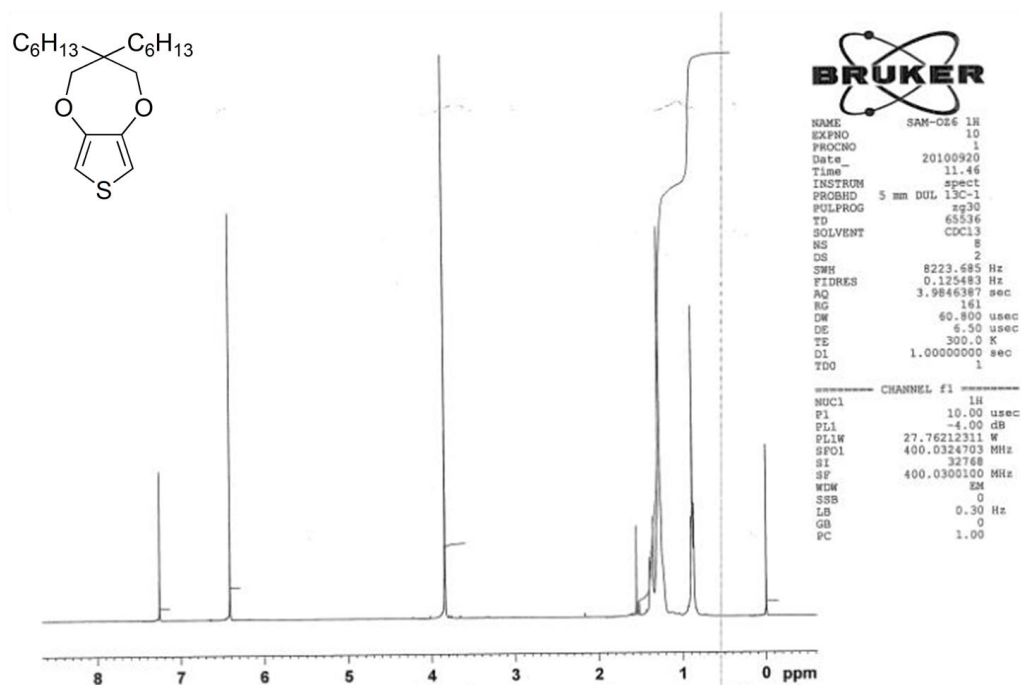


Figure B 9. ^1H NMR spectrum of **8** in CDCl_3 .

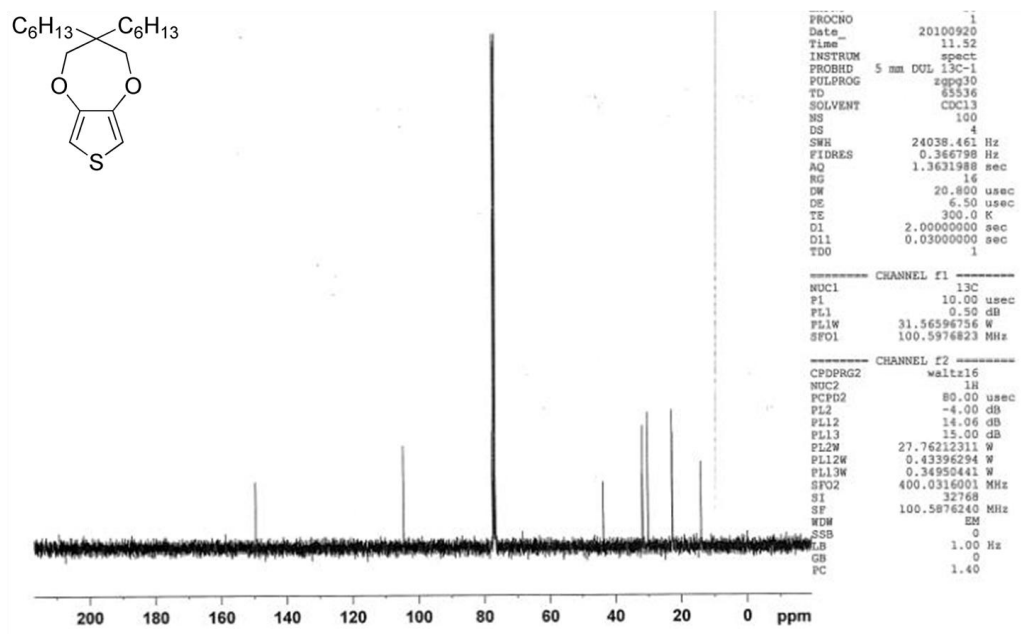


Figure B 10. ^{13}C NMR spectrum of **8** in CDCl_3 .

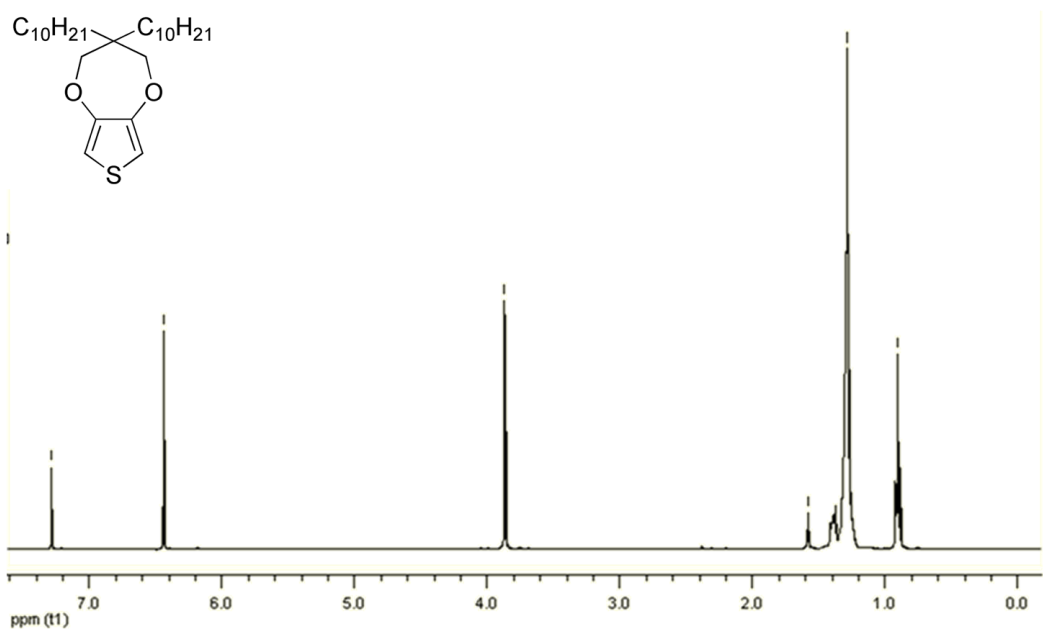


Figure B 11. ^1H NMR spectrum of **9** in CDCl_3 .

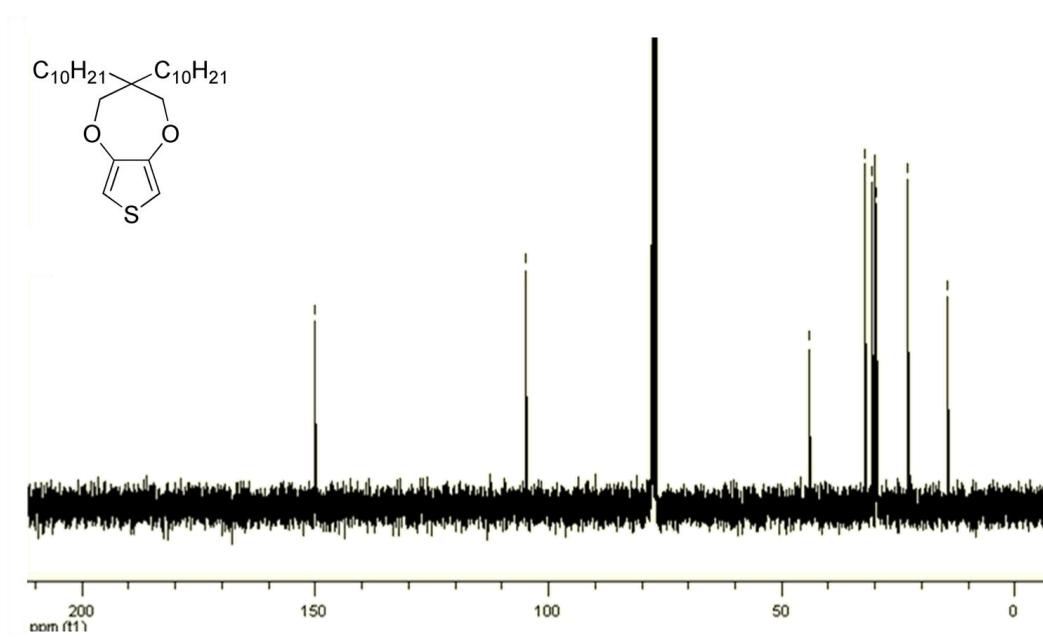


Figure B 12. ^{13}C NMR spectrum of **9** in CDCl_3 .

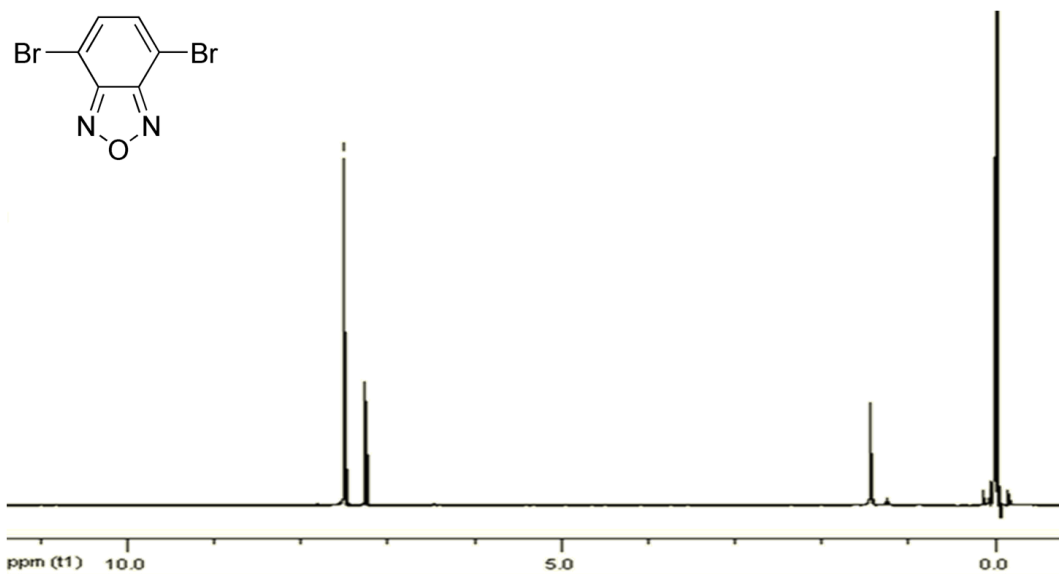


Figure B 13. ^1H NMR spectrum of 10 in CDCl_3 .

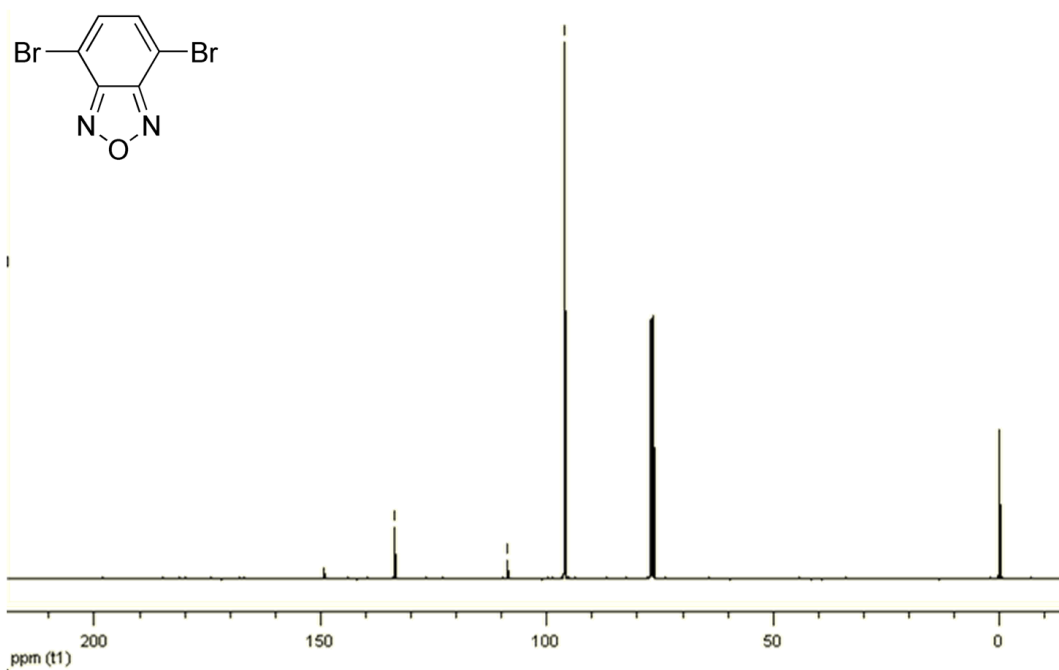


Figure B 14. ^{13}C NMR spectrum of 10 in CDCl_3 .

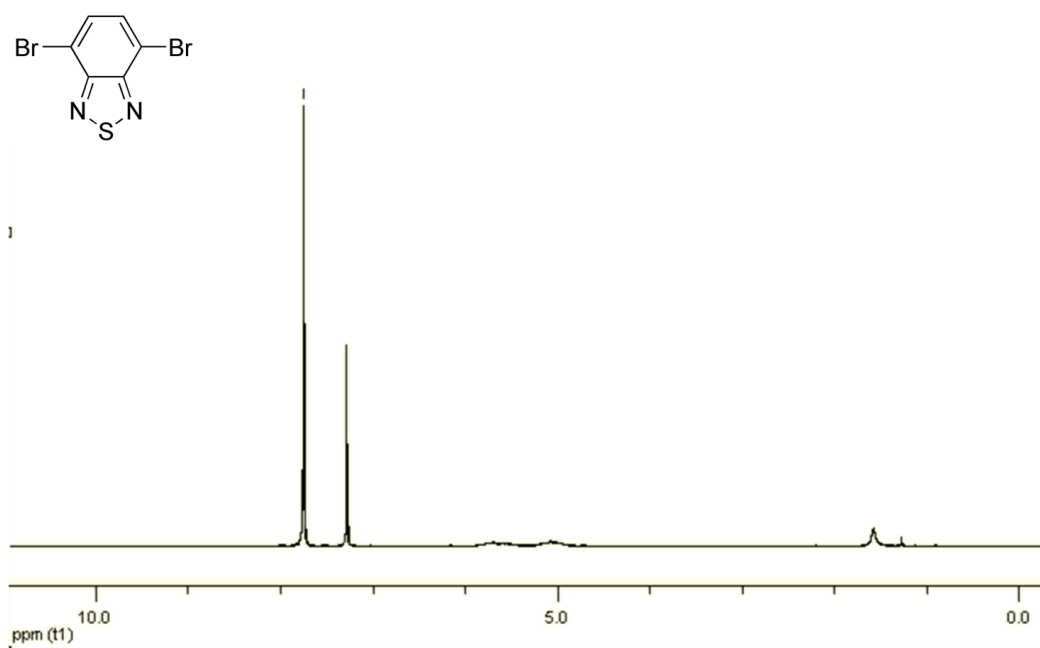


Figure B 15. ¹H NMR spectrum of **11** in CDCl₃.

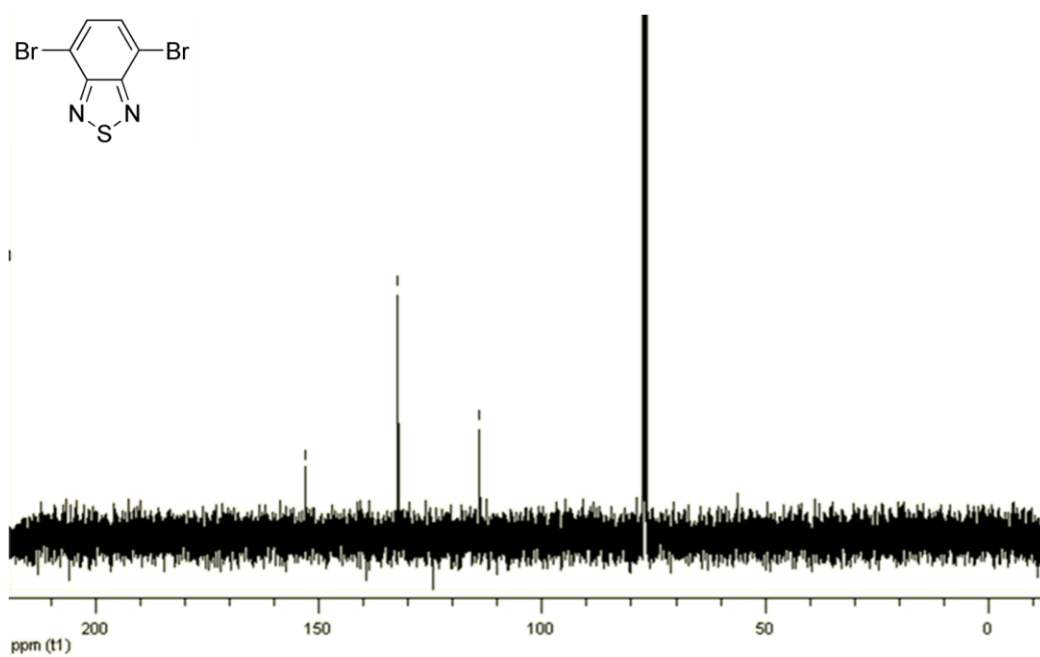


Figure B 16. ¹³C NMR spectrum of **11** in CDCl₃.

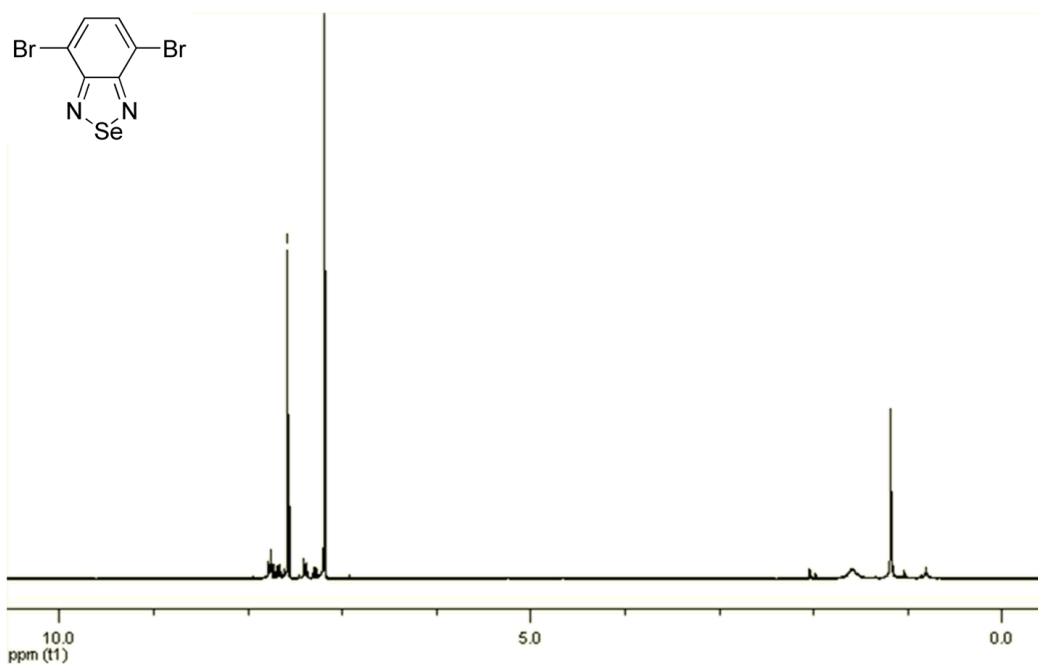


Figure B 17. ^1H NMR spectrum of **12** in CDCl_3 .

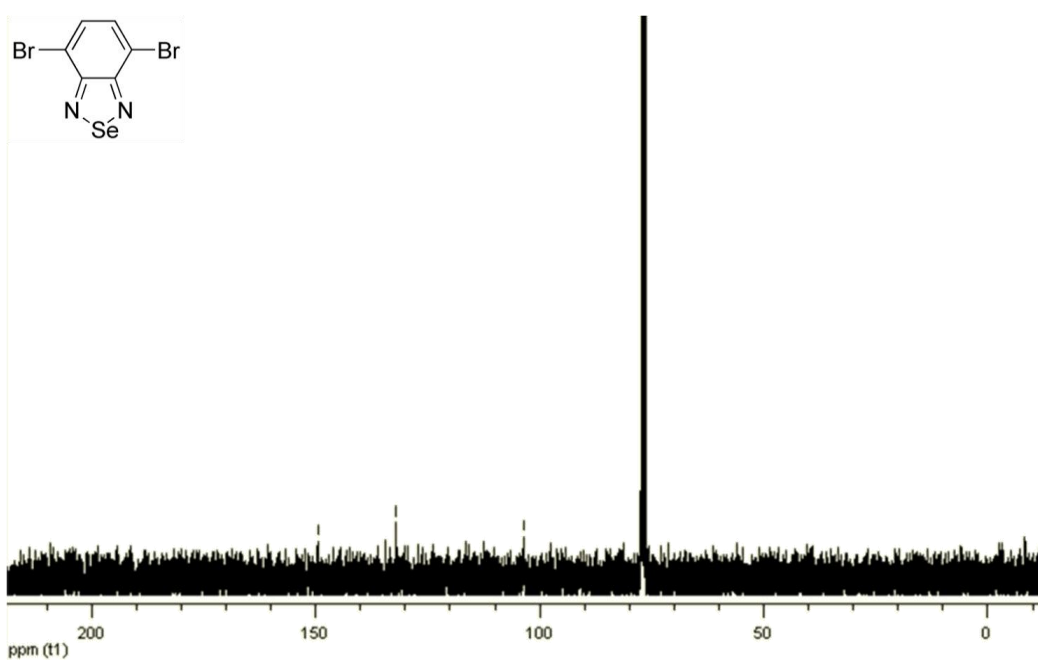


Figure B 18. ^{13}C NMR spectrum of **12** in CDCl_3 .

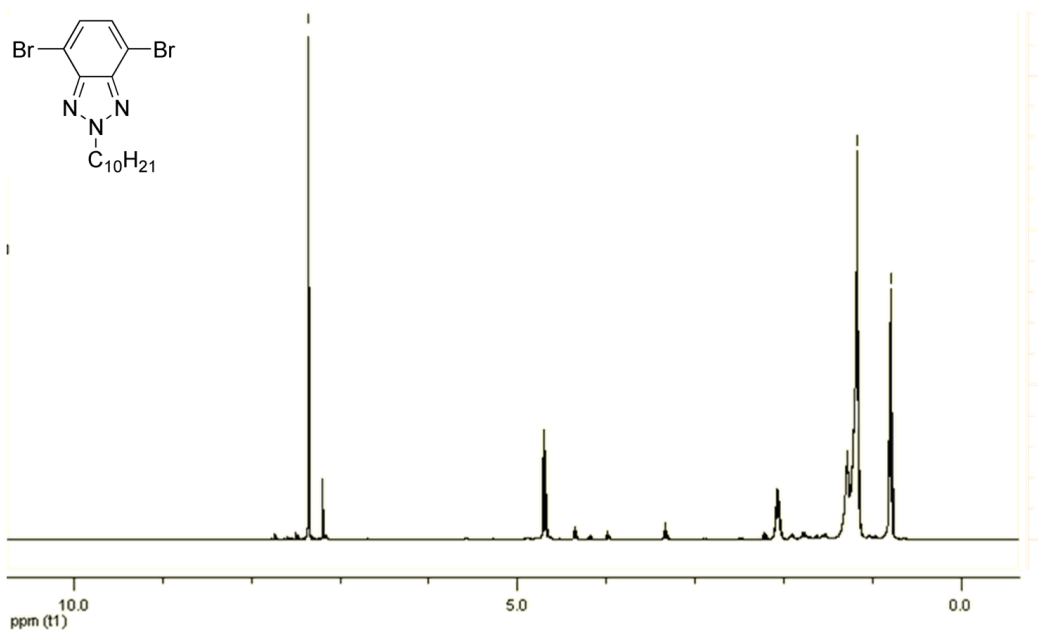


Figure B 19. ^1H NMR spectrum of **13** in CDCl_3 .

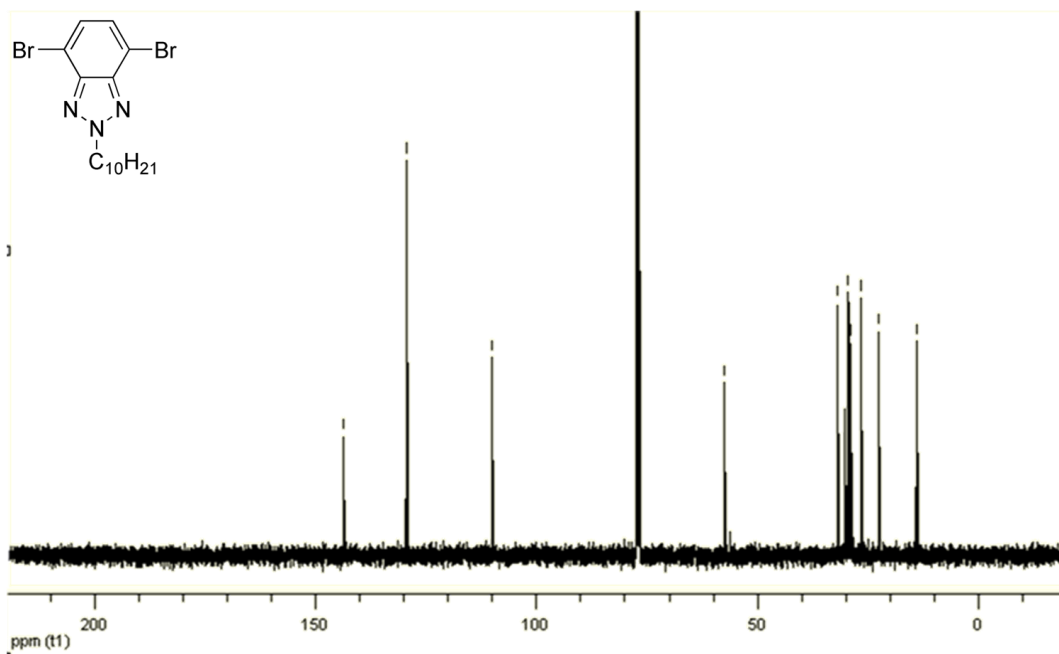


Figure B 20. ^{13}C NMR spectrum of **13** in CDCl_3 .

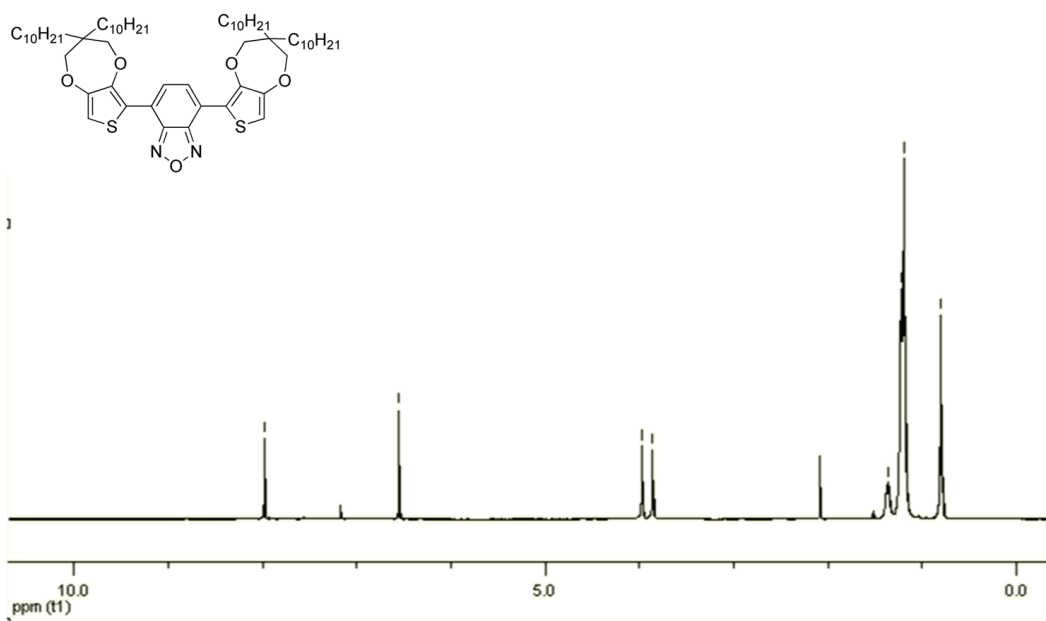


Figure B 21. ^1H NMR spectrum of **POP-C₁₀** in CDCl_3 .

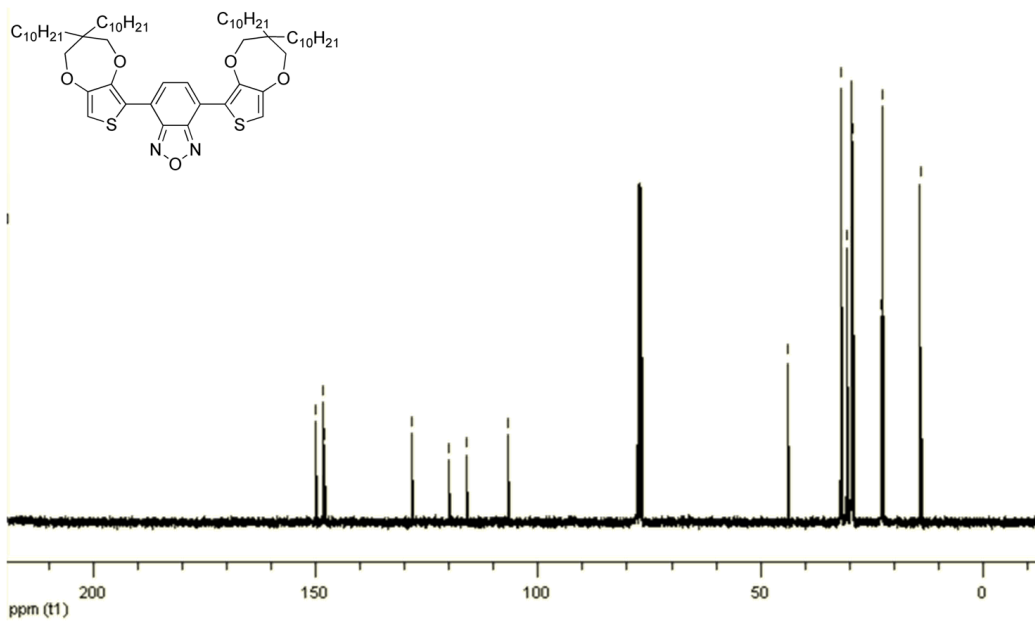


Figure B 22. ^{13}C NMR spectrum of **POP-C₁₀** in CDCl_3 .

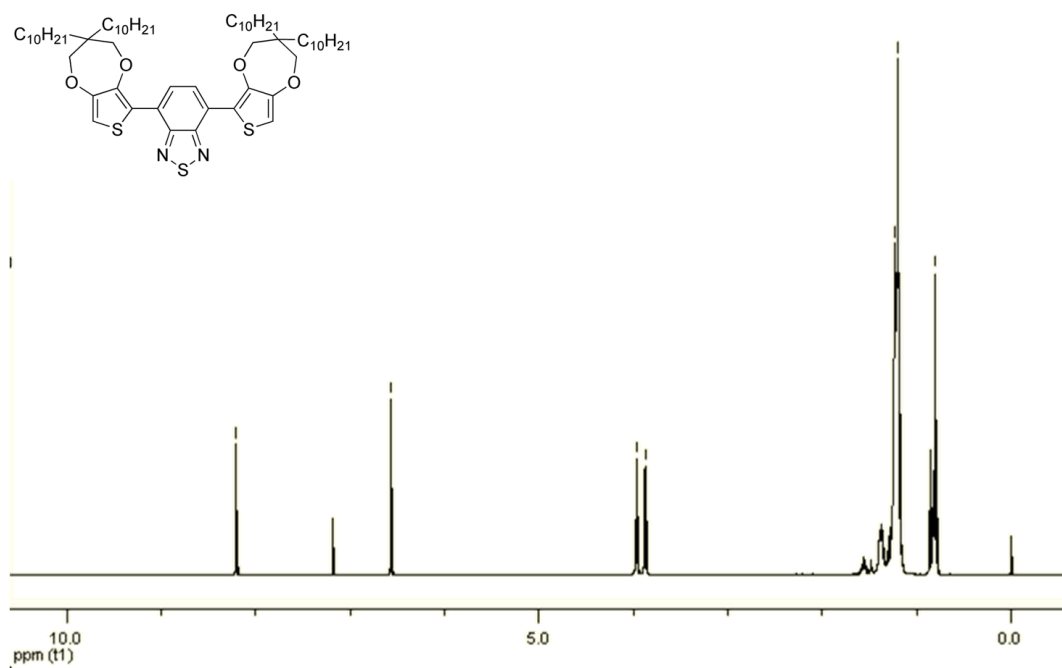


Figure B 23. ^1H NMR spectrum of **PSP-C₁₀** in CDCl_3 .

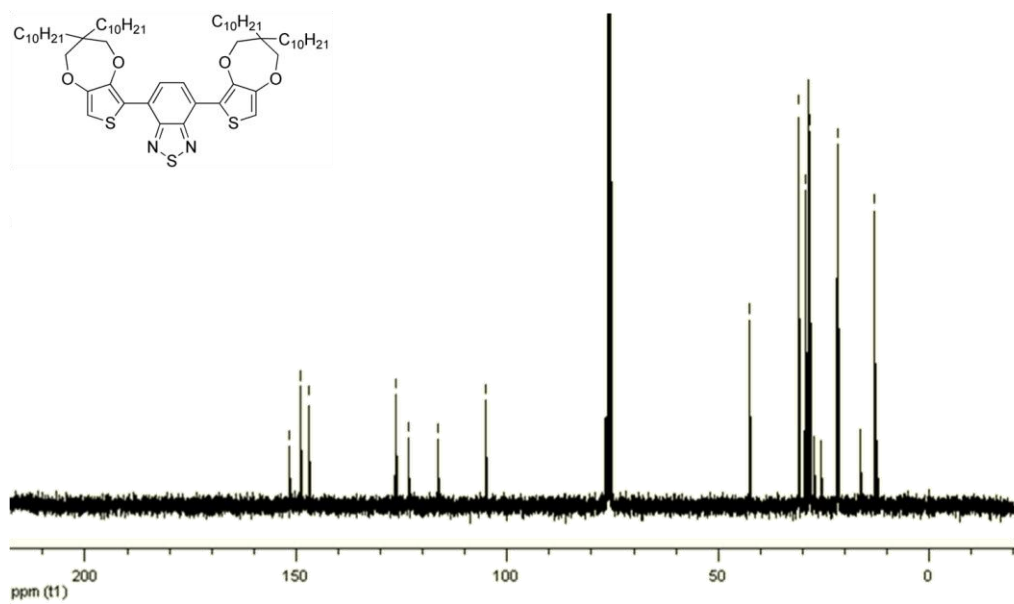


Figure B 24. ^{13}C NMR spectrum of **PSP-C₁₀** in CDCl_3 .

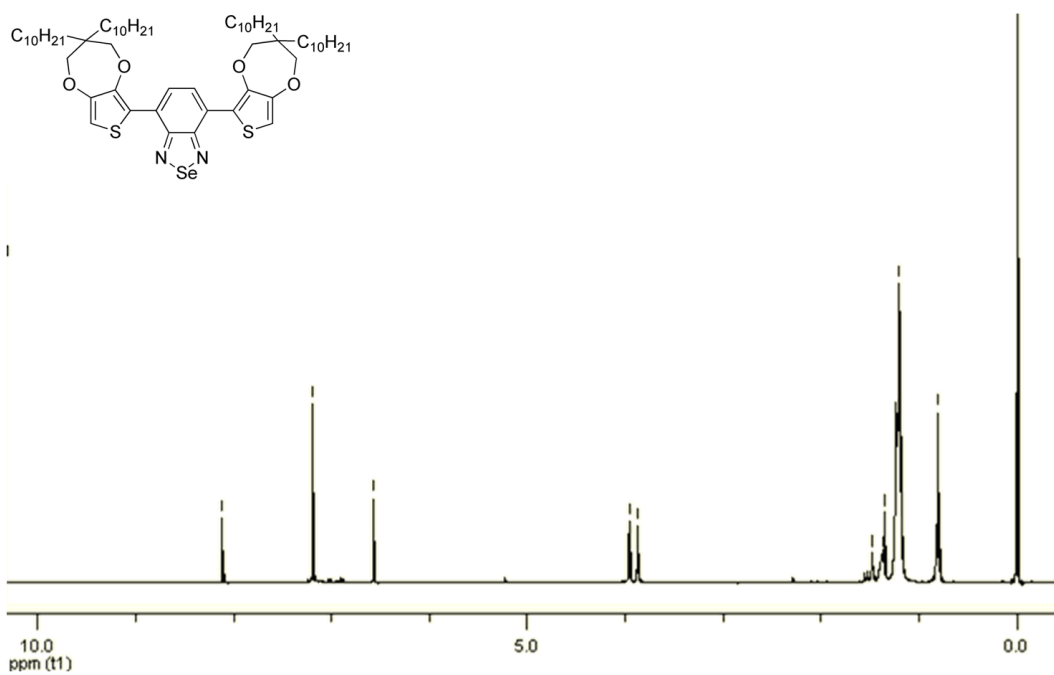


Figure B 25. ^1H NMR spectrum of **PSeP-C₁₀** in CDCl_3 .

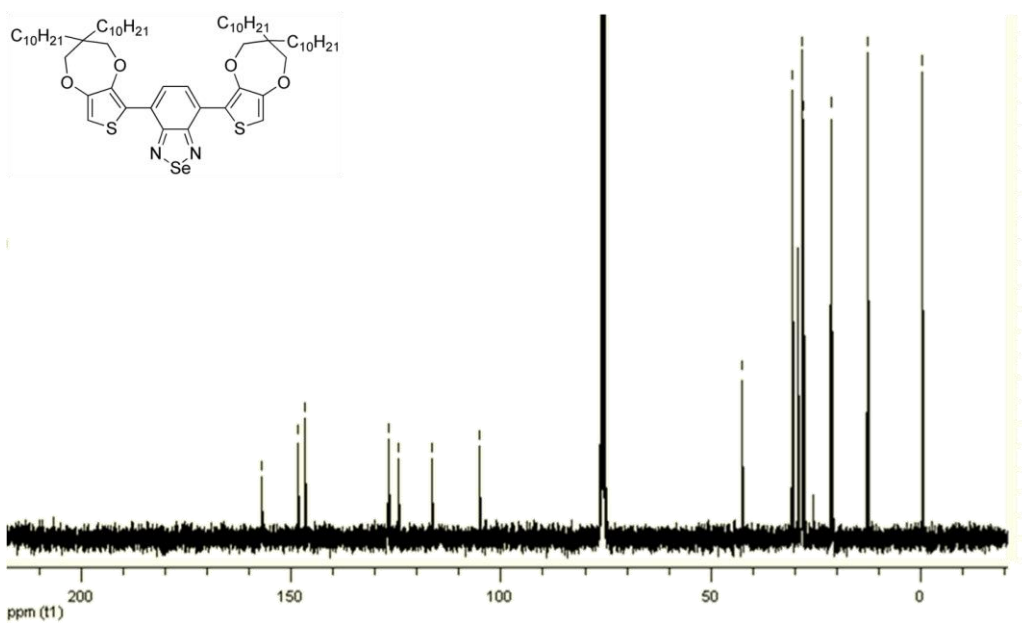


Figure B 26. ^{13}C NMR spectrum of **PSeP-C₁₀** in CDCl_3 .

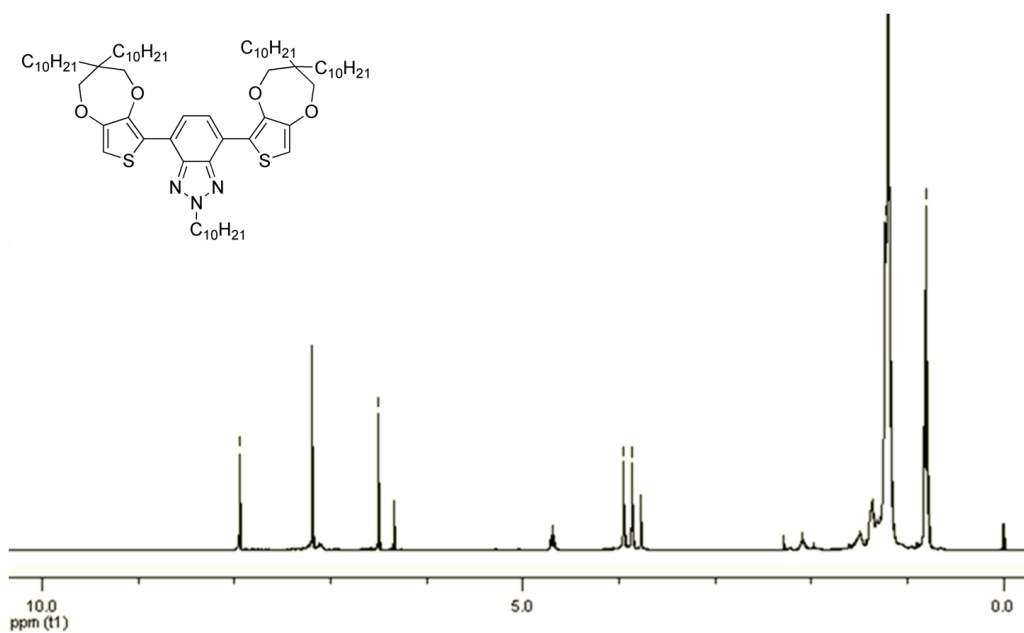


Figure B 27. ^1H NMR spectrum of **PNP-C₁₀** in CDCl_3 .

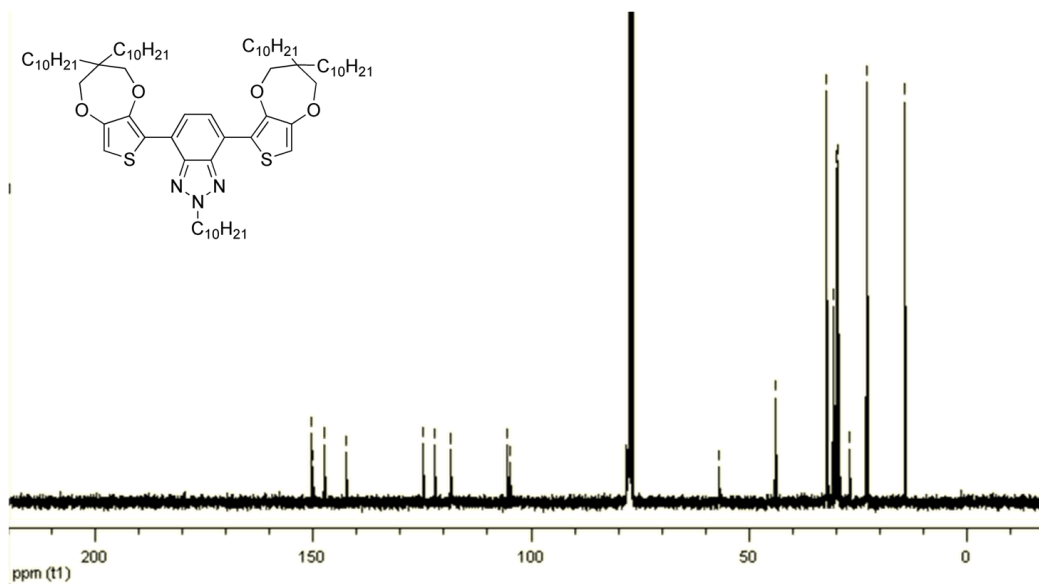


Figure B 28. ^{13}C NMR spectrum of **PNP-C₁₀** in CDCl_3 .

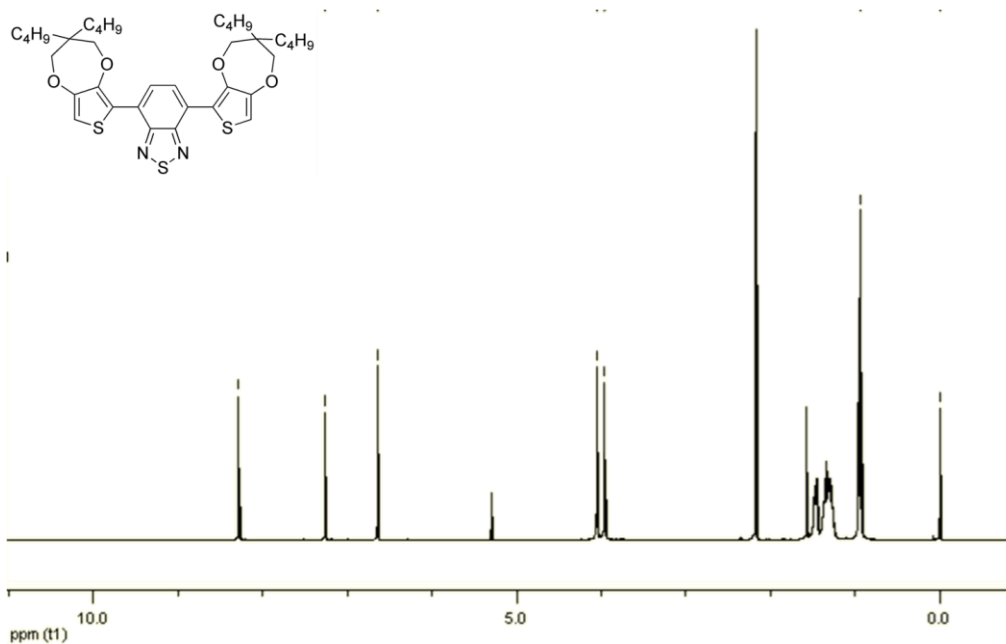


Figure B 29. ¹H NMR spectrum of PSP-C₄ in CDCl₃.

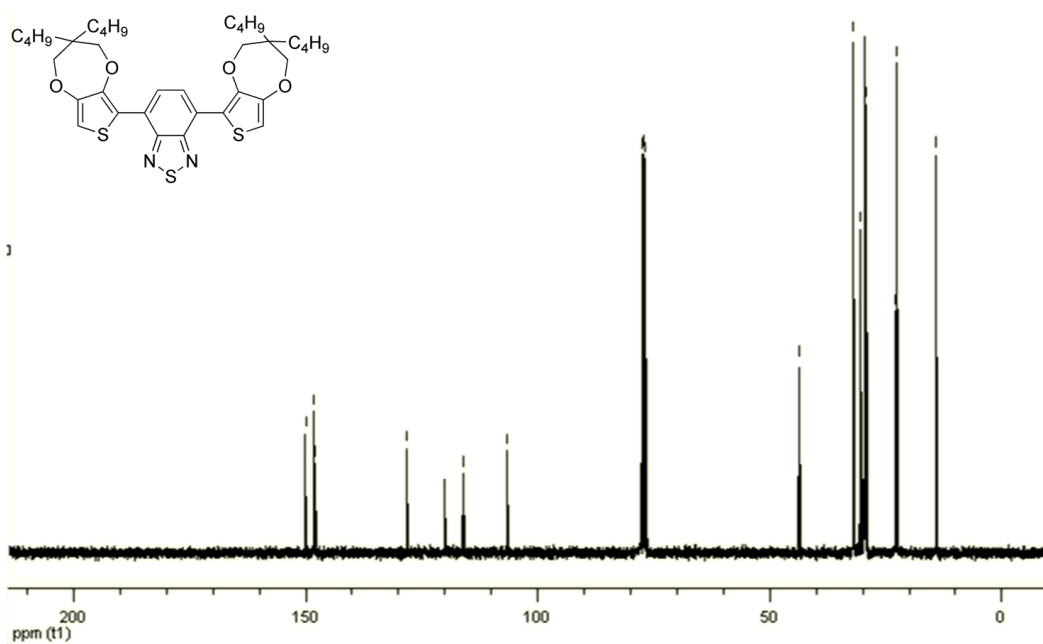


Figure B 30. ¹³C NMR spectrum of PSP-C₄ in CDCl₃.

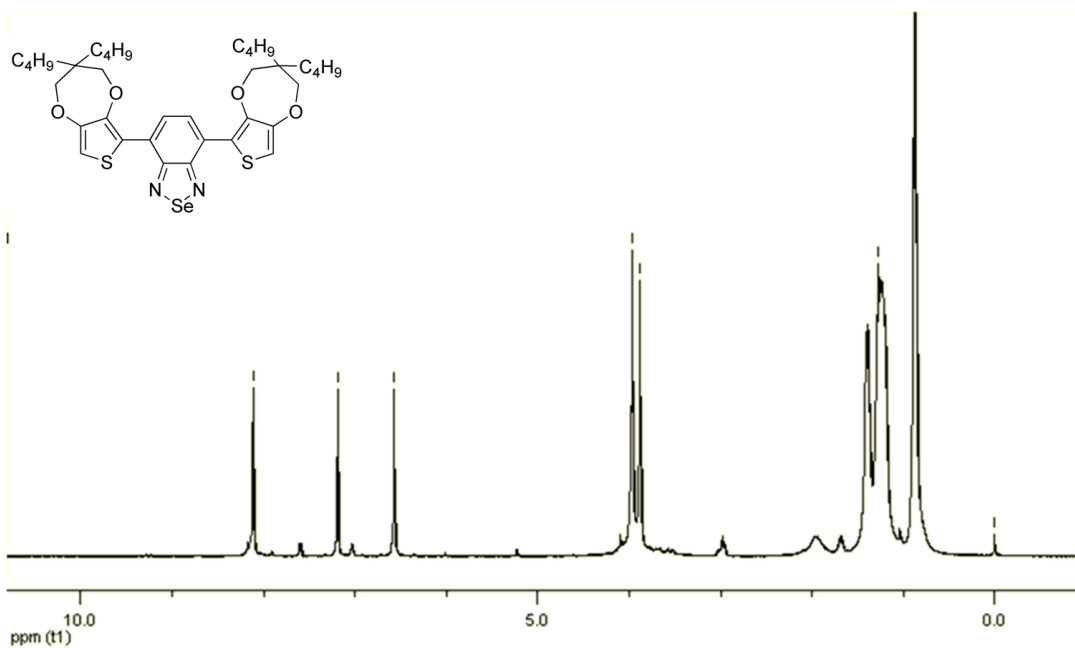


Figure B 31. ¹H NMR spectrum of PSeP-C₄ in CDCl₃.

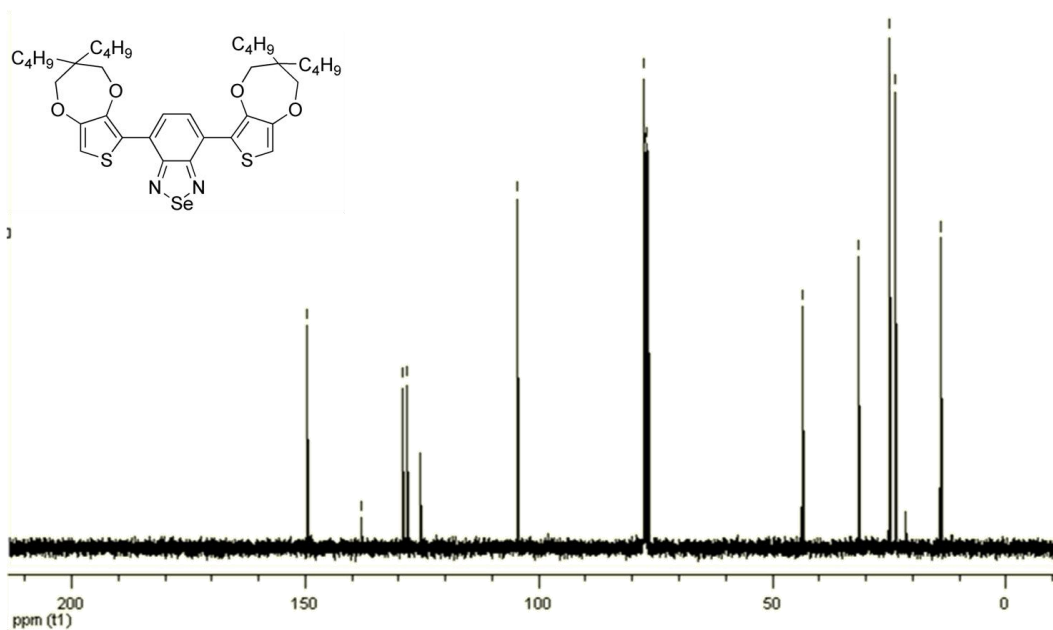


Figure B 32. ¹³C NMR spectrum of PSeP-C₄ in CDCl₃.

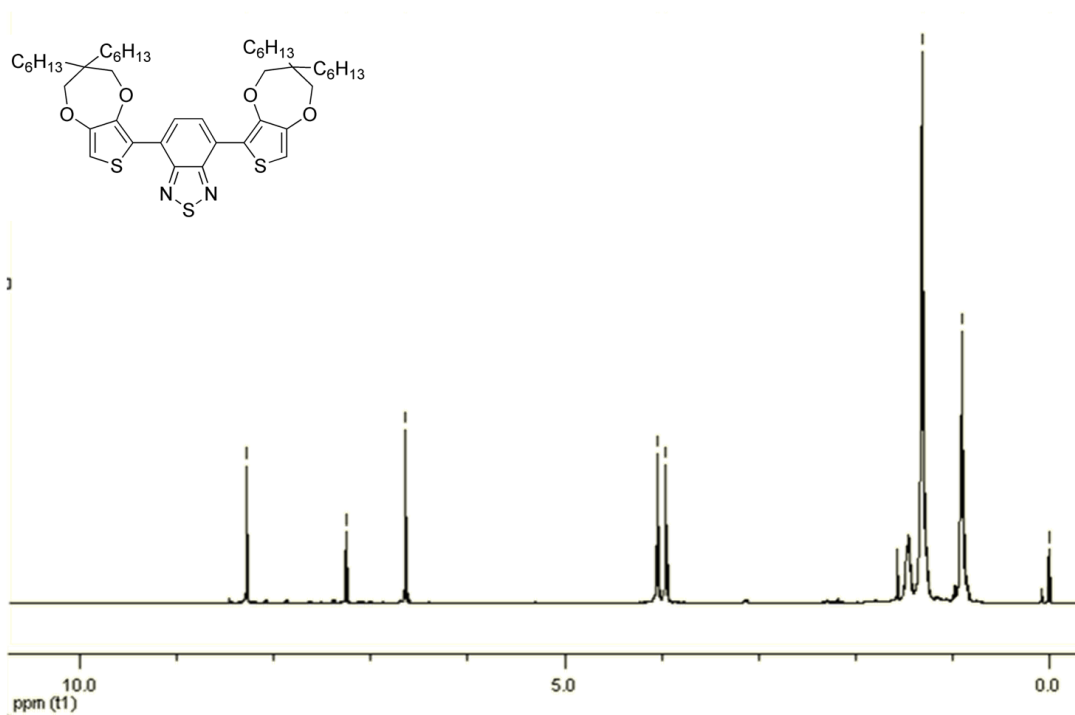


Figure B 33. ^1H NMR spectrum of **PSP-C₆** in CDCl_3 .

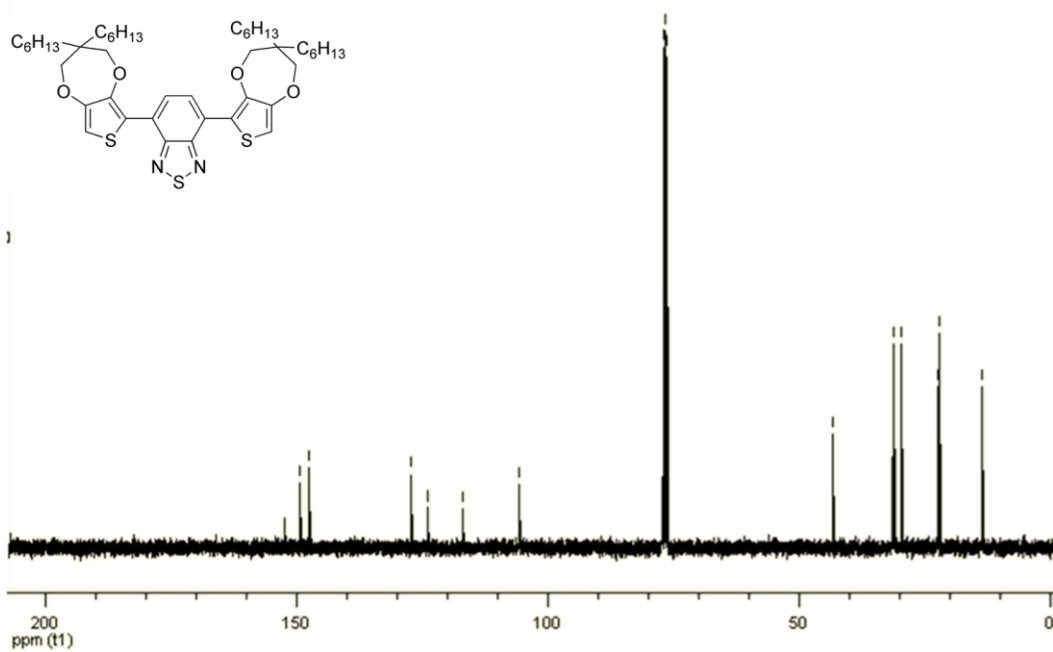


Figure B 34. ^{13}C NMR spectrum of **PSP-C₆** in CDCl_3 .

VITA

PERSONEL INFORMATION

Surname, Name: İçli Özkut, Merve
Nationality: Turkish (TC)
Date and Place of Birth: 29 April 1982, Ankara
Marital Status: Married
Phone: 0506 591 16 38
email: merveicli@gmail.com

EDUCATION

Degree	Institution	Year of Graduation
Ph.D.	METU Chemistry Department	2011
BS	Ankara Univ. Chemistry Department	2004
High School	İncirli Lisesi	2000

WORK EXPERIENCE

Year	Place	Enrollment
2004-Present	METU Department of Chemistry	Research Asistant

FOREIGN LANGUAGES

Advanced English

PUBLICATIONS

1. Atak, S.; İçli Özkut, M.; Önal, A. M.; Cihaner, A. "Soluble Alkyl Substituted Poly(3,4-Propylenedioxy-selenophene)s: A New Platform For Optoelectronic Materials"*J. Poly. Chem. Part A: Poly. Chem.* (2011-DOI: 10.1002/pola.24880).
2. İçli Özkut, M.; Öztaş, Z.; Algi, F. ve Cihaner, A. "A Neutral State Yellow to Navy Polymer Electrochrome with Pyrene Scaffold", *Org. Elec.*, 12, 1505-1511, (2011).
3. İçli Özkut, M.; Atak, S.; Önal, A. M.; Cihaner, A. "Blue to Highly Transmissive Soluble Electrochromic Based on Poly(3,4-propylenedioxy-selenophene) with High Stability and Coloration Efficiency" *J. Mater. Chem.*, **21**, 5268-5272, (2011).
4. İçli, M.; Pamuk, M.; Algi, F., Önal, A. M. and Cihaner, A. "Donor-Acceptor Polymer Electrochromes with Tunable Colors and Performance", *Chem. Mater.*, **22**, 4034-4044, (2010).
5. İçli, M.; Pamuk, M.; Algi, F., Önal, A. M. and Cihaner, A., "A New Soluble Neutral State Black Electrochromic Copolymer Via A Donor-Acceptor Approach", *Org. Electron.*, **11**, 1255-1260, (2010).
6. İçli, M.; Cihaner, A. and Önal, A.M., "Template-Free Micro and Hollow Sphere Formation of Polymethylanilines", *Polym. Inter.*, **58**, 674-679 (2009).
7. İçli, M.; Cihaner, A. ve Önal, A.M., "Anodic polymerization of 2,5-di-(2- thienyl)-furan in ethanol", *Electrochim. Acta*, **52**, 8039-8043 (2007).